

**UCLA**

**UCLA Electronic Theses and Dissertations**

**Title**

Discovery and Mechanistic Insights of Main-Group Catalyzed C-H Functionalization Reactions of Dicoordinate Carbocations

**Permalink**

<https://escholarship.org/uc/item/1jw004mp>

**Author**

Shao, Brian

**Publication Date**

2019

Peer reviewed|Thesis/dissertation

UNIVERSITY OF CALIFORNIA

Los Angeles

Discovery and Mechanistic Insights of Main-Group  
Catalyzed C–H Functionalization Reactions of  
Dicoordinate Carbocations

A dissertation submitted in partial satisfaction of the  
requirements for the degree Doctor of Philosophy  
in Chemistry

by

Brian Shao

2019

© Copyright by

Brian Shao

2019

## ABSTRACT OF THE DISSERTATION

Discovery and Mechanistic Insights of Main-Group  
Catalyzed C–H Functionalization Reactions of  
Dicoordinate Carbocations

by

Brian Shao

Doctor of Philosophy in Chemistry

University of California, Los Angeles, 2019

Professor Hosea M. Nelson, Chair

This dissertation focuses on the discovery and developments of novel carbon–carbon (C–C) bond forming reactions through dicoordinate carbocation intermediates. Chapter one provides a brief introduction into the known reactivity of relevant aryl and vinyl carbocations. In particular, C–C bond forming transformations will be the main focus of this discussion.

Our experimental work begins with the account of serendipitous discovery of intermolecular C–H insertion reactions of an aryl cation intermediate. We detail the reactivity-driven nature of our initial hypothesis and its development into a novel hydrocarbon arylation methodology. It was demonstrated that *ortho*-silylated aryl fluorides can be used as precursors for generating aryl cations capable of C–H insertion. The insertion chemistry exhibits inherent



terminal selectivity in linear alkanes and is capable of activating one of the most challenges C–H bonds in methane.

Subsequently, we followed the reactivity of our aryl cations to other dicoordinate carbocations as in vinyl cations. Utilizing a similar strategy hinged upon the use of silylium–weakly coordinating anion catalysis, vinyl cations were found to also undergo intermolecular insertion into  $sp^3$  C–H bonds. Here, we establish a reductive coupling process between vinyl triflates and various hydrocarbons. Extensive deuterium labeling studies also helped to uncover key features of the dicoordinate carbocation insertion mechanism. A detailed account of our hypotheses in establishing our mechanistic probe experiments is reported.

In efforts to bring our new methodology to a more broadly applicable chemical space, we were determined to further develop our system for heteroatom compatibility. Our progress has culminated in a new mode of generation for vinyl cations under highly basic conditions, and results in the C–H insertion reactions in the presence of a wide variety of heteroatom-containing substrates. In these studies, 3-substitued cyclooctenyl vinyl triflates was a substrate class used to highlight the increased functional group tolerance of our new method. Utilization of lithium–weakly coordinating anions has allowed entry for our dicoordinate carbocation insertion chemistry into applications such as fine chemical syntheses.

The dissertation of Brian Shao is approved.

Neil Kamal Garg

Alexander Michael Spokoyny

Yi Tang

Hosea Martin Nelson, Committee Chair

University of California, Los Angeles

2019

*For my family*

## TABLE OF CONTENTS

ABSTRACT OF THE DISSERTATION.....	ii
COMMITTEE PAGE.....	iv
DEDICATION PAGE.....	v
TABLE OF CONTENTS.....	vi
LIST OF FIGURES.....	xi
LIST OF SCHEMES.....	xxi
LIST OF TABLES.....	xxii
LIST OF ABBREVIATIONS.....	xxiv
ACKNOWLEDGEMENTS.....	xxvii
BIOGRAPHICAL SKETCH.....	xxxii
CHAPTER ONE: Fundamental Reactivity of Dicoordinate Carbocations.....	1
1.1 Abstract.....	1
1.2 Introduction.....	1
1.3 Aryl Cations.....	2
1.3.1 Mascarelli's Phenyl Cation.....	3
1.3.2 Phenyl Cations In Other Dediazoniatio	4
1.3.2 Direct Solvolysis of Aryl Triflates.....	6
1.3.3 Photolytic Generation of Aryl Cations and the Singlet Phenyl Cation.....	7

1.3.4 Aryl Cations Paired With Weakly Coordinating Anions .....	9
1.4 Vinyl Cations.....	11
1.4.1 Vinyl Cation Solvolysis Reactivity .....	12
1.4.2 Friedel-Crafts Alkylation of Vinyl Cations .....	13
1.4.3 Intramolecular C–H Insertion of Vinyl Cations .....	15
1.5 Conclusion .....	16
1.6 Notes and References .....	17
CHAPTER TWO: Arylation of Hydrocarbons Enabled by Organosilicon Reagents and Weakly Coordinating Anions.....	21
2.1 Abstract.....	21
2.2 Introduction .....	21
2.3 Initial Hypothesis and Serendipitous Discovery .....	22
2.4 Development of Intermolecular C–H Insertion Reactions of Aryl Cations .....	25
2.5 Mechanistic Studies on the C–H Insertion of Aryl Cations .....	30
2.6 Conclusion .....	32
2.7 Experimental Section.....	33
2.7.1 Materials and Methods .....	33
2.7.2 Preparation of Aryl Fluoride Substrates .....	34
2.7.3 General Procedure for Yield Calculations by GC .....	38
2.7.4 Optimization Table for Aryl Insertion Reaction.....	38

2.7.5 Initial Investigation of Aryl Fluorides .....	39
2.7.5.1 Fluorobenzene Control .....	39
2.7.5.2 Application of Conditions from Reference 4 .....	40
2.7.5.3 Positional Effects of Silyl Group.....	41
2.7.6 General Procedure for Intermolecular Aryl Insertion Reactions.....	43
2.7.7 Intramolecular Alkane Insertion Reaction.....	53
2.7.8 Optimization Table for Intermolecular Alkane Insertion Reaction.....	54
2.7.9 General Procedure for Intermolecular Alkane Insertion Reactions.....	54
2.7.10 Procedure for D-labeling Experiment in C <sub>6</sub> D <sub>6</sub> .....	62
2.7.11 Procedure for D-labeling Experiment in D <sub>12</sub> -cyclohexane.....	63
2.7.12 Procedure for Deuterium Competition Experiment.....	66
2.7.13 Methan Reaction.....	69
2.8 Spectra Relevant to Chapter Two .....	72
2.9 Notes and References .....	90
 CHAPTER THREE: Teaching an Old Carbocation New Tricks: Intermolecular C–H Insertion Reactions of Vinyl Carbocations .....	 93
3.1 Abstract.....	93
3.2 Introduction .....	93
3.3 Development of Intermolecular C–H Insertion Reactions of Vinyl Cations.....	95
3.4 Deuterium Labeling Studies .....	97

3.5 Reductive Friedel-Crafts Methodology of Vinyl Cations .....	101
3.6 Conclusion .....	102
3.7 Experimental Section.....	103
3.7.1 Materials and Methods .....	103
3.7.2 Synthesis of Vinyl Triflate Substrates .....	104
3.7.3 General Procedure for Yield Calculations by GC .....	109
3.7.4 Optimization for Alkane Alkylation Reactions.....	110
3.7.5 General Procedure for Intermolecular Alkane Insertion Reactions.....	110
3.7.6 General Procedures for Intermolecular Arene Insertion Reactions.....	117
3.7.7 Procedure for Deuterium Competition Experiments .....	125
3.7.8 Procedure for D-labeling Experiments .....	127
3.8 Spectra Relevant to Chapter Three.....	131
3.9 Notes and References .....	164
CHAPTER FOUR: Vinyl Carbocations Generated Under Basic Conditions and Their Intramolecular C–H Insertion Reactions .....	166
4.1 Abstract.....	166
4.2 Introduction .....	166
4.3 Development of Lithium-Mediated Insertion Reactions of Vinyl Cations .....	167
4.4 Incorporating Heteroatom Compatibility and Olefin Selectivity .....	169
4.5 Conclusion .....	172

4.6 Experimental Section.....	172
4.6.1 Materials and Methods .....	172
4.6.2 Synthesis of Cyclooctenyl Substrate Class <b>4.6</b> .....	174
4.6.3 Optimization Table for Cyclooctenyl Triflate .....	181
4.6.4 General Procedure for Transannular C–H Insertion Reactions .....	181
4.6.5 Insertion Reactions of Cyclooctenyl Triflate Derivaties .....	182
4.7 Spectra Relevant to Chapter Four.....	189
4.8 Notes and References .....	206



## LIST OF FIGURES

### CHAPTER ONE

<i>Figure 1.1</i> Proposed Intermediates in the Mascarelli Reaction .....	3
---	---

### CHAPTER TWO

<i>Figure 2.1</i> Reactivity-Driven Methodology .....	22
<i>Figure 2.2</i> Catalytic Aryne Hypothesis .....	23
<i>Figure 2.3</i> Proposed Catalytic Cycle .....	25
<i>Figure 2.4</i> Intermolecular Reactivity and Importance of $\beta$ -Silicon Stabilization .....	26
<i>Figure 2.5</i> Investigation of Aryl Cation Intermediate Through Mechanistic Probe Substrates.....	31
<i>Figure 2.6</i> Deuterium Labeling Studies in Arene Solvent.....	32
<i>Figure 2.7</i> Deuterium Labeling Studies in Alkane Solvent .....	32
<i>Figure 2.8</i> GC Trace for Internal Standard Nonane and Biphenyl in 1:1 Ratio .....	39
<i>Figure 2.9</i> GC Trace for Internal Standard Nonane in Fluorobenzene Control Reaction Showing Formation of Biphenyl in <5% Yield.....	40
<i>Figure 2.10</i> GC Trace for Application of Reference 4 Conditions to Fluorobenzene at 30 °C Showing Formation of Biphenyl in <5% Yield .....	40
<i>Figure 2.11</i> GC Trace for Internal Standard Nonane and Biphenyl in 1:1 Ratio .....	41
<i>Figure 2.12</i> GC Trace for Internal Standard Nonane and <b>2.15</b> After 2 Hour Reaction Time Showing No Formation of Biphenyl.....	42
<i>Figure 2.13</i> GC Trace for Internal Standard Nonane and <b>2.16</b> After 2 Hour Reaction Time Showing No Formation of Biphenyl.....	42

<b>Figure 2.14</b> GC Trace for Internal Standard Nonane and <b>2.1</b> After 2 Hour Reaction Time Showing Formation of Biphenyl in 47% Yield.....	42
<b>Figure 2.15</b> GC Trace for Internal Standard Nonane and <b>2.13</b> in 1:1 Ratio.....	44
<b>Figure 2.16</b> GC Trace for Yield Shown in Figure <b>2.4</b> From Manuscript .....	44
<b>Figure 2.17</b> GC Trace for Internal Standard Nonane and <b>2.17</b> in 1:1 Ratio.....	45
<b>Figure 2.18</b> GC Trace Showing Formation of <b>2.17</b> in 56% Yield.....	45
<b>Figure 2.19</b> GC Trace for Internal Standard Nonane and <b>2.19</b> in 1:1 Ratio.....	46
<b>Figure 2.20</b> GC Trace Showing Formation of <b>2.19</b> in 47% Yield.....	46
<b>Figure 2.21</b> GC Trace for Internal Standard Nonane and <b>2.20</b> in 1:1 Ratio.....	47
<b>Figure 2.22</b> GC Trace Showing Formation of <b>2.20</b> in 52% Yield.....	47
<b>Figure 2.23</b> GC Trace Showing Formation of <b>2.21</b> in 77% Yield.....	48
<b>Figure 2.24</b> GC Trace for Internal Standard Nonane and <b>2.23</b> in 1:1 Ratio.....	49
<b>Figure 2.25</b> GC Trace Showing Formation of <b>2.23</b> in 63% Yield.....	49
<b>Figure 2.26</b> GC Trace for Internal Standard Nonane and <b>2.24</b> in 1:1 Ratio.....	50
<b>Figure 2.27</b> GC Trace Showing Formation of <b>2.24</b> in 36% Yield.....	50
<b>Figure 2.28</b> GC Trace Showing Formation of <b>2.27</b> in 45% Yield.....	51
<b>Figure 2.29</b> GC Trace for Internal Standard Nonane and <b>2.38</b> in 1:1 Ratio.....	53
<b>Figure 2.30</b> GC Trace Showing Formation of <b>2.38</b> in 43% Yield.....	54
<b>Figure 2.31</b> GC Trace for Internal Standard Nonane and <b>2.29</b> in 1:1 Ratio.....	55
<b>Figure 2.32</b> GC Trace Showing Formation of <b>2.29</b> in 41% Yield.....	56
<b>Figure 2.33</b> GC Trace for a 1:1:1 Ratio of Phenylhexane Isomers Showing an Integral Relationship of 1.....	57
<b>Figure 2.34</b> GC Trace for Internal Standard Nonane and 1-phenylhexane in 1:1 Ratio ..	58

<b>Figure 2.35</b> GC Trace Showing the Formation of 1-phenylhexane From <b>2.1</b> in 26% Yield .....	58
<b>Figure 2.36</b> GC Trace for Internal Standard Nonane and 2-phenylhexane in 1:1 Ratio ..	58
<b>Figure 2.37</b> GC Trace Showing the Formation of 2-phenylhexane From <b>2.1</b> in 9% Yield .....	59
<b>Figure 2.38</b> GC Trace for Internal Standard Nonane and 3-phenylhexane in 1:1 Ratio ..	59
<b>Figure 2.39</b> GC Trace Showing the Formation of 3-phenylhexane From <b>2.1</b> . The Error Associated With the 3-phenylhexane Calibration Curve was Shown to be Greater Than the Theoretical Yield .....	59
<b>Figure 2.40</b> GC Trace for a 1:1:1 Ratio of Phenylpentane Isomers .....	60
<b>Figure 2.41</b> GC Trace for Internal Standard Nonane and 1-phenylpentane in 1:1 Ratio .	60
<b>Figure 2.42</b> GC Trace Showing Formation of 1-phenylpentane From <b>2.1</b> in 30% Yield	61
<b>Figure 2.43</b> GC Trace for Internal Standard Nonane and 2-phenylpentane in 1:1 Ratio .	61
<b>Figure 2.44</b> GC Trace Showing Formation of 2-phenylpentane From <b>2.1</b> in 10% Yield	61
<b>Figure 2.45</b> GC Trace for Internal Standard Nonane and 3-phenylpentane in 1:1 Ratio .	62
<b>Figure 2.46</b> GC Trace Showing Formation of 3-phenylpentane From <b>2.1</b> in 2% Yield ..	62
<b>Figure 2.47</b> GCMS Spectrum Showing Deuterium Scrambling of <b>2.41</b> in C <sub>6</sub> D <sub>6</sub> Reaction .....	63
<b>Figure 2.48</b> GCMS Trace for D <sub>12</sub> -phenylcyclohexane (m/z: 172) Showing No Deuterium Scrambling.....	65
<b>Figure 2.49</b> GCMS Spectrum of Competition Experiment Showing No Deuterium Crossover. C <sub>12</sub> H <sub>16</sub> (m/z: 160) and C <sub>12</sub> H <sub>4</sub> D <sub>12</sub> (m/z: 172) are Both Present With No Intermediate Masses .....	67

<b>Figure 2.50</b> GC Trace for a Solution of 4.3 mg of D <sub>12</sub> -phenylcyclohexane and 5.4 mg of Phenylcyclohexane. A Comparison of Molar and Integral Ratios Show a 1:1 Relationship .....	68
<b>Figure 2.51</b> GC Trace for Trial 1 of Deuterium Competition Experiment.....	68
<b>Figure 2.52</b> GC Trace for Trial 2 of Deuterium Competition Experiment.....	68
<b>Figure 2.53</b> GC Trace for Trial 3 of Deuterium Competition Experiment.....	69
<b>Figure 2.54</b> GC Trace for Crude Methane Insertion Reaction Showing Both <b>2.35</b> and the Major Byproduct 1-fluoronaphthalene .....	71
<b>Figure 2.55</b> <sup>1</sup> H NMR (400 MHz, CDCl <sub>3</sub> ) of compound <b>2.1</b> .....	73
<b>Figure 2.56</b> <sup>1</sup> H NMR (400 MHz, CDCl <sub>3</sub> ) of compound <b>2.15</b> .....	73
<b>Figure 2.57</b> <sup>1</sup> H NMR (400 MHz, CDCl <sub>3</sub> ) of compound <b>2.16</b> .....	74
<b>Figure 2.58</b> <sup>1</sup> H NMR (400 MHz, CDCl <sub>3</sub> ) of compound <b>2.34</b> .....	74
<b>Figure 2.59</b> <sup>13</sup> C NMR (100 MHz, CDCl <sub>3</sub> ) of compound <b>2.34</b> .....	75
<b>Figure 2.60</b> <sup>19</sup> F NMR (376 MHz, CDCl <sub>3</sub> ) of compound <b>2.34</b> .....	75
<b>Figure 2.61</b> <sup>1</sup> H NMR (300 MHz, CDCl <sub>3</sub> ) of compound <b>2.37</b> .....	76
<b>Figure 2.62</b> <sup>13</sup> C NMR (100 MHz, CDCl <sub>3</sub> ) of compound <b>2.37</b> .....	76
<b>Figure 2.63</b> <sup>19</sup> F NMR (282 MHz, CDCl <sub>3</sub> ) of compound <b>2.37</b> .....	77
<b>Figure 2.64</b> <sup>1</sup> H NMR (400 MHz, CDCl <sub>3</sub> ) of compound <b>2.39</b> .....	77
<b>Figure 2.65</b> <sup>13</sup> C NMR (100 MHz, CDCl <sub>3</sub> ) of compound <b>2.39</b> .....	78
<b>Figure 2.66</b> <sup>19</sup> F NMR (376 MHz, CDCl <sub>3</sub> ) of compound <b>2.39</b> .....	78
<b>Figure 2.67</b> <sup>1</sup> H NMR (400 MHz, CDCl <sub>3</sub> ) of compound <b>2.7</b> and <b>2.8</b> .....	79
<b>Figure 2.68</b> <sup>1</sup> H NMR (400 MHz, CDCl <sub>3</sub> ) of compound <b>2.13</b> .....	79
<b>Figure 2.69</b> <sup>1</sup> H NMR (400 MHz, CDCl <sub>3</sub> ) of compound <b>2.17</b> .....	80

<i>Figure 2.70</i> $^1\text{H}$ NMR (400 MHz, $\text{CDCl}_3$ ) of compound <b>2.18</b> .....	80
<i>Figure 2.71</i> $^1\text{H}$ NMR (400 MHz, $\text{CDCl}_3$ ) of compound <b>2.19</b> .....	81
<i>Figure 2.72</i> $^1\text{H}$ NMR (400 MHz, $\text{CDCl}_3$ ) of compound <b>2.20, 2.21</b> .....	81
<i>Figure 2.73</i> $^1\text{H}$ NMR (400 MHz, $\text{CDCl}_3$ ) of compound <b>2.22</b> .....	82
<i>Figure 2.74</i> $^1\text{H}$ NMR (400 MHz, $\text{CDCl}_3$ ) of compound <b>2.23</b> .....	82
<i>Figure 2.75</i> $^1\text{H}$ NMR (400 MHz, $\text{CDCl}_3$ ) of compound <b>2.24, 2.27</b> .....	83
<i>Figure 2.76</i> $^1\text{H}$ NMR (400 MHz, $\text{CDCl}_3$ ) of compound <b>2.25</b> .....	83
<i>Figure 2.77</i> $^{13}\text{C}$ NMR (125 MHz, $\text{CDCl}_3$ ) of compound <b>2.25</b> .....	84
<i>Figure 2.78</i> $^1\text{H}$ NMR (400 MHz, $\text{CDCl}_3$ ) of compound <b>2.26</b> .....	84
<i>Figure 2.79</i> $^{13}\text{C}$ NMR (100 MHz, $\text{CDCl}_3$ ) of compound <b>2.26</b> .....	85
<i>Figure 2.80</i> $^1\text{H}$ NMR (400 MHz, $\text{CDCl}_3$ ) of compound <b>2.28</b> .....	85
<i>Figure 2.81</i> $^1\text{H}$ NMR (400 MHz, $\text{CDCl}_3$ ) of compound <b>2.29</b> .....	86
<i>Figure 2.82</i> $^1\text{H}$ NMR (400 MHz, $\text{CDCl}_3$ ) of compound <b>2.30</b> .....	86
<i>Figure 2.83</i> $^1\text{H}$ NMR (400 MHz, $\text{CDCl}_3$ ) of compound <b>2.31</b> .....	87
<i>Figure 2.84</i> $^1\text{H}$ NMR (400 MHz, $\text{CDCl}_3$ ) of compound <b>2.32</b> .....	87
<i>Figure 2.85</i> $^1\text{H}$ NMR (400 MHz, $\text{CDCl}_3$ ) of compound <b>2.33</b> .....	88
<i>Figure 2.86</i> $^1\text{H}$ NMR (500 MHz, $\text{CDCl}_3$ ) of compound <b>2.35</b> .....	88
<i>Figure 2.87</i> $^1\text{H}$ NMR (500 MHz, $\text{CDCl}_3$ ) of compound <b>2.38</b> .....	89
<i>Figure 2.88</i> $^1\text{H}$ NMR (500 MHz, $\text{CDCl}_3$ ) of compound <b>2.43</b> .....	89

### CHAPTER THREE

<i>Figure 3.1</i> Proposed Catalytic Cycle for C–H Insertion of Vinyl Cations .....	95
<i>Figure 3.2</i> GC Trace Showing 1:1 Mixture of Nonane to Bicyclohexyl.....	111

<b>Figure 3.3</b> GC Trace Showing 87% Yield of Bicyclohexyl .....	112
<b>Figure 3.4</b> GC Trace Showing 1:1 Mixture of Nonane to Cyclohexylcycloheptane.....	113
<b>Figure 3.5</b> GC Trace Showing 88% Yield of Cyclohexylcycloheptane .....	113
<b>Figure 3.6</b> GC Traces Showing 1:1 Mixture of Nonane to 3-cyclohexylpentane (Top), Nonane to 2-cyclopentane (Middle), Nonane to 1-cyclopentane (Bottom) .....	114
<b>Figure 3.7</b> GC Trace Showing 11% of 3-cyclopentane, 36% of 2-cyclopentane and 21% of 1-cyclopentane .....	114
<b>Figure 3.8</b> GC Trace Showing ~15:1 d.r. <b>3.12</b> .....	116
<b>Figure 3.9</b> GC Trace Showing 1:1 Mixture of Nonane to Octahydropentalene .....	116
<b>Figure 3.10</b> GC Trace Showing 91% Yield of <b>3.14</b> .....	117
<b>Figure 3.11</b> GC Trace Showing 1:1 Mixture of Nonane to Phenylcyclohexane .....	118
<b>Figure 3.12</b> GC Trace Showing 74% Yield of Phenylcyclohexane .....	119
<b>Figure 3.13</b> GCMS Spectrum of C <sub>6</sub> H <sub>12</sub> /C <sub>6</sub> D <sub>12</sub> Crossover Experiment. A = Cyclohexylcyclohexane- <i>d</i> <sub>12</sub> (m/z = 178); B = Cyclohexylcyclohexane (m/z = 166) .....	126
<b>Figure 3.14</b> GCMS Spectrum of Et <sub>3</sub> SiH/Et <sub>3</sub> SiD Competition Experiment.....	127
<b>Figure 3.15</b> <sup>1</sup> H NMR (400 MHz, CDCl <sub>3</sub> ) of compound <b>3.3</b> .....	132
<b>Figure 3.16</b> <sup>1</sup> H NMR (500 MHz, CDCl <sub>3</sub> ) of compound <b>3.11</b> .....	132
<b>Figure 3.17</b> <sup>1</sup> H NMR (400 MHz, CDCl <sub>3</sub> ) of compound <b>3.13</b> .....	133
<b>Figure 3.18</b> <sup>1</sup> H NMR (400 MHz, CDCl <sub>3</sub> ) of compound <b>3.21</b> .....	133
<b>Figure 3.19</b> <sup>1</sup> H NMR (400 MHz, CDCl <sub>3</sub> ) of compound <b>3.29</b> .....	134
<b>Figure 3.20</b> <sup>13</sup> C NMR (125 MHz, CDCl <sub>3</sub> ) of compound <b>3.29</b> .....	134
<b>Figure 3.21</b> <sup>19</sup> F NMR (376 MHz, CDCl <sub>3</sub> ) of compound <b>3.29</b> .....	135
<b>Figure 3.22</b> <sup>1</sup> H NMR (400 MHz, CDCl <sub>3</sub> ) of compound <b>3.41</b> .....	135

<i>Figure 3.23</i> $^1\text{H}$ NMR (400 MHz, $\text{CDCl}_3$ ) of compound <b>3.42</b> .....	136
<i>Figure 3.24</i> $^1\text{H}$ NMR (400 MHz, $\text{CDCl}_3$ ) of compound <b>3.43</b> .....	136
<i>Figure 3.25</i> $^{13}\text{C}$ NMR (125 MHz, $\text{CDCl}_3$ ) of compound <b>3.43</b> .....	137
<i>Figure 3.26</i> $^{19}\text{F}$ NMR (376 MHz, $\text{CDCl}_3$ ) of compound <b>3.43</b> .....	137
<i>Figure 3.27</i> $^1\text{H}$ NMR (400 MHz, $\text{CDCl}_3$ ) of compound <b>3.8</b> .....	138
<i>Figure 3.28</i> $^1\text{H}$ NMR (400 MHz, $\text{CDCl}_3$ ) of compound <b>3.9</b> .....	138
<i>Figure 3.29</i> $^{13}\text{C}$ NMR (125 MHz, $\text{CDCl}_3$ ) of compound <b>3.9</b> .....	139
<i>Figure 3.30</i> $^1\text{H}$ NMR (400 MHz, $\text{CDCl}_3$ ) of compound <b>3.10</b> .....	139
<i>Figure 3.31</i> $^{13}\text{C}$ NMR (125 MHz, $\text{CDCl}_3$ ) of compound <b>3.10</b> .....	140
<i>Figure 3.32</i> $^1\text{H}$ NMR (500 MHz, $\text{CDCl}_3$ ) of compound <b>3.12</b> .....	140
<i>Figure 3.33</i> $^{13}\text{C}$ NMR (125 MHz, $\text{CDCl}_3$ ) of compound <b>3.12</b> .....	141
<i>Figure 3.34</i> $^1\text{H}$ NMR (400 MHz, $\text{CDCl}_3$ ) of compound <b>3.14</b> .....	141
<i>Figure 3.35</i> $^1\text{H}$ NMR (400 MHz, $\text{CDCl}_3$ ) of compound <b>3.32</b> .....	142
<i>Figure 3.36</i> $^1\text{H}$ NMR (500 MHz, $\text{CDCl}_3$ ) of compound <b>3.33</b> .....	142
<i>Figure 3.37</i> $^{13}\text{C}$ NMR (125 MHz, $\text{CDCl}_3$ ) of compound <b>3.33</b> .....	143
<i>Figure 3.38</i> $^{19}\text{F}$ NMR (376 MHz, $\text{CDCl}_3$ ) of compound <b>3.33</b> .....	143
<i>Figure 3.39</i> $^1\text{H}$ NMR (500 MHz, $\text{CDCl}_3$ ) of compound <b>3.34</b> .....	144
<i>Figure 3.40</i> $^{13}\text{C}$ NMR (125 MHz, $\text{CDCl}_3$ ) of compound <b>3.34</b> .....	144
<i>Figure 3.41</i> 2D HMBC NMR (500 MHz, $\text{CDCl}_3$ ) of compound <b>3.34</b> .....	145
<i>Figure 3.42</i> 2D HSQC NMR (500 MHz, $\text{CDCl}_3$ ) of compound <b>3.34</b> .....	145
<i>Figure 3.43</i> $^1\text{H}$ NMR (500 MHz, $\text{CDCl}_3$ ) of compound <b>3.35</b> .....	146
<i>Figure 3.44</i> $^{13}\text{C}$ NMR (125 MHz, $\text{CDCl}_3$ ) of compound <b>3.35</b> .....	146
<i>Figure 3.45</i> $^1\text{H}$ NMR (500 MHz, $\text{CDCl}_3$ ) of compound <b>3.36</b> .....	147

<i>Figure 3.46</i> $^{13}\text{C}$ NMR (125 MHz, $\text{CDCl}_3$ ) of compound <b>3.36</b> .....	147
<i>Figure 3.47</i> $^{19}\text{F}$ NMR (376 MHz, $\text{CDCl}_3$ ) of compound <b>3.36</b> .....	148
<i>Figure 3.48</i> 2D HSQC NMR (500 MHz, $\text{CDCl}_3$ ) of compound <b>3.36</b> .....	148
<i>Figure 3.49</i> 2D HMBC NMR (500 MHz, $\text{CDCl}_3$ ) of compound <b>3.36</b> .....	149
<i>Figure 3.50</i> $^1\text{H}$ NMR (500 MHz, $\text{CDCl}_3$ ) of compound <b>3.37</b> .....	149
<i>Figure 3.51</i> $^1\text{H}$ NMR (400 MHz, $\text{CDCl}_3$ ) of compound <b>3.38</b> .....	150
<i>Figure 3.52</i> $^1\text{H}$ NMR (400 MHz, $\text{CDCl}_3$ ) of compound <b>3.39</b> .....	150
<i>Figure 3.53</i> $^1\text{H}$ NMR (500 MHz, $\text{CDCl}_3$ ) of compound <b>3.40</b> .....	151
<i>Figure 3.54</i> $^{13}\text{C}$ NMR (125 MHz, $\text{CDCl}_3$ ) of compound <b>3.40</b> .....	151
<i>Figure 3.55</i> 2D HSQC NMR (500 MHz, $\text{CDCl}_3$ ) of compound <b>3.40</b> .....	152
<i>Figure 3.56</i> 2D HMBC NMR (500 MHz, $\text{CDCl}_3$ ) of compound <b>3.40</b> .....	152
<i>Figure 3.57</i> $^1\text{H}$ COSY NMR (500 MHz, $\text{CDCl}_3$ ) of compound <b>3.40</b> .....	153
<i>Figure 3.58</i> $^1\text{H}$ NOESY NMR (500 MHz, $\text{CDCl}_3$ ) of compound <b>3.40</b> .....	153
<i>Figure 3.59</i> $^1\text{H}$ NMR (500 MHz, $\text{CDCl}_3$ ) of compound <b>3.44</b> .....	154
<i>Figure 3.60</i> $^{13}\text{C}$ NMR (125 MHz, $\text{CDCl}_3$ ) of compound <b>3.44</b> .....	154
<i>Figure 3.61</i> $^1\text{H}$ NMR (500 MHz, $\text{C}_6\text{D}_6$ ) of compound <b>3.44</b> .....	155
<i>Figure 3.62</i> $^{13}\text{C}$ NMR (125 MHz, $\text{C}_6\text{D}_6$ ) of compound <b>3.44</b> .....	155
<i>Figure 3.63</i> 2D HSQC NMR (500 MHz, $\text{C}_6\text{D}_6$ ) of compound <b>3.44</b> .....	156
<i>Figure 3.64</i> $^1\text{H}$ NMR (500 MHz, $\text{C}_6\text{D}_6$ ) of compound <b>3.22</b> .....	156
<i>Figure 3.65</i> $^{13}\text{C}$ NMR (125 MHz, $\text{C}_6\text{D}_6$ ) of compound <b>3.22</b> .....	157
<i>Figure 3.66</i> $^{13}\text{C}$ NMR (125 MHz, $\text{C}_6\text{D}_6$ ) of compound <b>3.22</b> .....	157
<i>Figure 3.67</i> 2D HSQC NMR (500 MHz, $\text{C}_6\text{D}_6$ ) of compound <b>3.22</b> .....	158
<i>Figure 3.68</i> 2D HSQC NMR (500 MHz, $\text{C}_6\text{D}_6$ ) of compound <b>3.22</b> .....	158



<b>Figure 3.69</b> $^1\text{H}$ NMR (500 MHz, $\text{CDCl}_3$ ) of compound <b>3.27</b> .....	159
<b>Figure 3.70</b> $^{13}\text{C}$ NMR (125 MHz, $\text{CDCl}_3$ ) of compound <b>3.22</b> .....	159
<b>Figure 3.71</b> $^1\text{H}$ NMR (500 MHz, $\text{CDCl}_3$ ) comparison of compound <b>3.27</b> with <b>3.44</b> .....	160
<b>Figure 3.72</b> $^{13}\text{C}$ NMR (125 MHz, $\text{CDCl}_3$ ) comparison of compound <b>3.27</b> with <b>3.44</b> .....	160
<b>Figure 3.73</b> $^1\text{H}$ NMR (500 MHz, $\text{CDCl}_3$ ) of compound <b>3.30</b> .....	161
<b>Figure 3.74</b> $^{13}\text{C}$ NMR (125 MHz, $\text{CDCl}_3$ ) of compound <b>3.30</b> .....	161
<b>Figure 3.75</b> $^{13}\text{C}$ NMR (125 MHz, $\text{CDCl}_3$ ) of compound <b>3.30</b> .....	162
<b>Figure 3.76</b> $^1\text{H}$ NMR (500 MHz, $\text{C}_6\text{D}_6$ ) of compound <b>3.45</b> .....	162
<b>Figure 3.77</b> $^{13}\text{C}$ NMR (125 MHz, $\text{C}_6\text{D}_6$ ) of compound <b>3.45</b> .....	163
<b>Figure 3.78</b> $^{13}\text{C}$ NMR (125 MHz, $\text{C}_6\text{D}_6$ ) of compound <b>3.45</b> with <b>3.44</b> .....	163

#### CHAPTER FOUR

<b>Figure 4.1</b> Milder Initiators.....	167
<b>Figure 4.2</b> Proposed Catalytic Cycle of Li-mediated C–H Insertion.....	168
<b>Figure 4.3</b> $^1\text{H}$ NMR (500 MHz, $\text{CDCl}_3$ ) of compound <b>4.18</b> .....	190
<b>Figure 4.4</b> $^{13}\text{C}$ NMR (125 MHz, $\text{CDCl}_3$ ) of compound <b>4.18</b> .....	190
<b>Figure 4.5</b> $^{19}\text{F}$ NMR (376 MHz, $\text{CDCl}_3$ ) of compound <b>4.18</b> .....	191
<b>Figure 4.6</b> $^1\text{H}$ NMR (500 MHz, $\text{CDCl}_3$ ) of compound <b>4.19</b> .....	191
<b>Figure 4.7</b> $^{13}\text{C}$ NMR (125 MHz, $\text{CDCl}_3$ ) of compound <b>4.19</b> .....	192
<b>Figure 4.8</b> $^{19}\text{F}$ NMR (376 MHz, $\text{CDCl}_3$ ) of compound <b>4.19</b> .....	192
<b>Figure 4.9</b> $^1\text{H}$ NMR (500 MHz, $\text{CDCl}_3$ ) of compound <b>4.20</b> .....	193
<b>Figure 4.10</b> $^{13}\text{C}$ NMR (125 MHz, $\text{CDCl}_3$ ) of compound <b>4.20</b> .....	193
<b>Figure 4.11</b> $^{19}\text{F}$ NMR (376 MHz, $\text{CDCl}_3$ ) of compound <b>4.20</b> .....	194

<i>Figure 4.12</i>	$^1\text{H}$ NMR (500 MHz, $\text{CDCl}_3$ ) of compound <b>4.21</b> .....	194
<i>Figure 4.13</i>	$^{13}\text{C}$ NMR (125 MHz, $\text{CDCl}_3$ ) of compound <b>4.21</b> .....	195
<i>Figure 4.14</i>	$^{19}\text{F}$ NMR (376 MHz, $\text{CDCl}_3$ ) of compound <b>4.21</b> .....	195
<i>Figure 4.15</i>	$^1\text{H}$ NMR (500 MHz, $\text{CDCl}_3$ ) of compound <b>4.22</b> .....	196
<i>Figure 4.16</i>	$^{13}\text{C}$ NMR (125 MHz, $\text{CDCl}_3$ ) of compound <b>4.22</b> .....	196
<i>Figure 4.17</i>	$^{19}\text{F}$ NMR (376 MHz, $\text{CDCl}_3$ ) of compound <b>4.22</b> .....	197
<i>Figure 4.18</i>	$^1\text{H}$ NMR (500 MHz, $\text{CDCl}_3$ ) of compound <b>4.23</b> .....	197
<i>Figure 4.19</i>	$^{13}\text{C}$ NMR (125 MHz, $\text{CDCl}_3$ ) of compound <b>4.23</b> .....	198
<i>Figure 4.20</i>	$^{19}\text{F}$ NMR (376 MHz, $\text{CDCl}_3$ ) of compound <b>4.23</b> .....	198
<i>Figure 4.21</i>	$^1\text{H}$ NMR (500 MHz, $\text{CDCl}_3$ ) of compound <b>4.10</b> .....	199
<i>Figure 4.22</i>	$^{13}\text{C}$ NMR (125 MHz, $\text{CDCl}_3$ ) of compound <b>4.10</b> .....	199
<i>Figure 4.23</i>	$^1\text{H}$ NMR (500 MHz, $\text{CDCl}_3$ ) of compound <b>4.11</b> .....	200
<i>Figure 4.24</i>	$^{13}\text{C}$ NMR (125 MHz, $\text{CDCl}_3$ ) of compound <b>4.11</b> .....	200
<i>Figure 4.25</i>	$^1\text{H}$ NMR (500 MHz, $\text{CDCl}_3$ ) of compound <b>4.12</b> .....	201
<i>Figure 4.26</i>	$^{13}\text{C}$ NMR (125 MHz, $\text{CDCl}_3$ ) of compound <b>4.12</b> .....	201
<i>Figure 4.27</i>	$^1\text{H}$ NMR (500 MHz, $\text{CDCl}_3$ ) of compound <b>4.13</b> .....	202
<i>Figure 4.28</i>	$^{13}\text{C}$ NMR (125 MHz, $\text{CDCl}_3$ ) of compound <b>4.13</b> .....	202
<i>Figure 4.29</i>	$^1\text{H}$ NMR (500 MHz, $\text{CDCl}_3$ ) of compound <b>4.14</b> .....	203
<i>Figure 4.30</i>	$^{13}\text{C}$ NMR (125 MHz, $\text{CDCl}_3$ ) of compound <b>4.14</b> .....	203
<i>Figure 4.31</i>	$^{19}\text{F}$ NMR (282 MHz, $\text{CDCl}_3$ ) of compound <b>4.14</b> .....	204
<i>Figure 4.32</i>	$^1\text{H}$ NMR (500 MHz, $\text{CDCl}_3$ ) of compound <b>4.15</b> .....	204
<i>Figure 4.33</i>	$^{13}\text{C}$ NMR (125 MHz, $\text{CDCl}_3$ ) of compound <b>4.15</b> .....	205

## LIST OF SCHEMES

### CHAPTER ONE

<i>Scheme 1.1</i> Mascarelli's Fluorene Synthesis .....	3
<i>Scheme 1.2</i> Proposed Mechanism of the Gomberg-Bachmann Reaction .....	5
<i>Scheme 1.3</i> Reactivity of Phenyl Cations From Arenediazonium Ions .....	5
<i>Scheme 1.4</i> Solvolysis of Aryl Triflates .....	6
<i>Scheme 1.5</i> Solvolysis of 2,6-substituted Aryl Triflates .....	7
<i>Scheme 1.6</i> C–H Insertion of Aryl Cation Observed by Albini .....	7
<i>Scheme 1.7</i> Rationalization of C–H Insertion Reactivity .....	8
<i>Scheme 1.8</i> Energetics of Bis-silylated Benzenediazonium in Aryl Cation Formation .....	8
<i>Scheme 1.9</i> Discovery of Phenylated Carborane Salts .....	9
<i>Scheme 1.10</i> Evidence for Phenyl Cation Reactivity .....	10
<i>Scheme 1.11</i> Intramolecular Friedel-Crafts Reaction From an Aryl Cation .....	10
<i>Scheme 1.12</i> Intramolecular C–H Insertion of Aryl Cations .....	11
<i>Scheme 1.13</i> Classic Solvolysis Reactions of Vinyl Cation Precursors .....	12
<i>Scheme 1.14</i> Ring-contraction Rearrangement of Cyclic Vinyl Cations .....	13
<i>Scheme 1.15</i> Ring Fusion via 1,5-hydride Shift From Cyclic Vinyl Cation .....	13
<i>Scheme 1.16</i> Friedel-Crafts Alkylation of Linear Vinyl Triflates .....	14
<i>Scheme 1.17</i> Friedel-Crafts Alkylation of Cyclic Vinyl Triflates .....	14
<i>Scheme 1.18</i> Intramolecular Insertion of a Vinyl Cation .....	15
<i>Scheme 1.19</i> Rearrangement/C–H Insertion Reaction of a Vinyl Cation .....	16

## CHAPTER TWO

**Scheme 2.1** Aryne Generation Probes by [4+2] Cycloaddition .....23

**Scheme 2.2** Serendipitous Discovery of Alkane Arylation.....24

## CHAPTER THREE

**Scheme 3.1** Inspiration for Initial Vinyl Cation Reactivity Studies.....94

**Scheme 3.2** Initial Deuterium Labeling Studies of Triflate **3.3** .....98

**Scheme 3.3** Design of Mechanistic Probe Substrates .....100

**Scheme 3.4** Deuterium Labeling Experiments in Support of 1,1-C–H Insertion Pathway  
.....100

**Scheme 3.5** Reductive Arylation of Vinyl Triflates.....102

## CHAPTER FOUR

**Scheme 4.1** Pitfalls of Silylium-mediated Reactions .....167

**Scheme 4.2** Unselective Products of Model Substrate.....169

**Scheme 4.3** Hypothesis for New Substrate Class.....170

**Scheme 4.4** Benzosuberone-derived Triflates.....172

## LIST OF TABLES

### CHAPTER TWO

**Table 2.1** Arene Scope Table .....27

**Table 2.2** Arylation Scope of Alkanes and Methane.....29

**Table 2.3** Optimization of (2-fluorophenyl)trimethylsilane Substrate in Benzene .....38

<b>Table 2.4</b> Optimization of (2-fluorophenyl)trimethylsilane Substrate in Cyclohexane.....	54
<b>Table 2.5</b> Optimization of (1-fluoronaphthalen-2yl)trimethylsilane for the Insertion Reaction With Methane .....	69

### CHAPTER THREE

<b>Table 3.1</b> Reductive Alkylation Reactions of Vinyl Triflates and Alkanes.....	97
<b>Table 3.2</b> Optimization of Intermolecular Alkylation Reaction.....	110

### CHAPTER FOUR

<b>Table 4.1</b> Scope of Cyclooctenyl Triflates.....	171
<b>Table 4.2</b> Optimization of Intramolecular C–H Insertion Reaction of Cyclooctenyl Triflate (4.1).....	181

## LIST OF ABBREVIATIONS

$\alpha$	alpha
$\beta$	beta
$\gamma$	gamma
$\delta$	delta
$\lambda$	lambda
m/z	mass to charge ratio
$\mu$	micro
aq.	aqueous
Ar	aryl
br	broad
Bu	butyl
<i>n</i> -Bu	butyl (linear)
<i>s</i> -Bu	<i>sec</i> -butyl
<i>t</i> -Bu	<i>tert</i> -butyl
°C	degrees Celsius
ca.	crude approximate
cat.	catalytic
CI	chemical ionization
Conc.	concentration
COSY	correlation spectroscopy
cm	centimeter
d	doublet or deuterium
D ( <i>d</i> )	deuterium
dba	dibenzylideneacetone
dd	doublet of doublet
ddd	doublet of doublet of doublet
d.r.	diastereomeric ratio
DCM	dichloromethane
DFB	difluorobenzene
DMF	<i>N,N</i> -dimethylformamide
DMSO	dimethyl sulfoxide
dppf	1,1'-bis(diphenylphosphino)ferrocene

dt	doublet of triplet
equiv	equivalent
EI-MS	electron ionization mass spectroscopy
Et <sub>3</sub> N	triethylamine
ESI	electrospray ionization
Et	ethyl
FID	flame ionization detection
FTIR	fourier transform infrared
g	gram(s)
GC	gas-phase chromatography
GCMS	gas-phase chromatograph mass spectroscopy
GCT	gas-phase chromatograph time-of-flight
h	hour(s)
H	hydrogen or hydride
HMBC	heteronuclear multiple bond coherence
HMDS	hexamethyldisilazide
HPLC	high pressure liquid chromatography
HRMS	high resolution mass spectroscopy
HSQC	heteronuclear single quantum coherence
Hz	hertz
IR	infrared (spectroscopy)
<i>J</i>	coupling constant
kcal	kilocalorie(s)
KIE	kinetic isotope effect
L	liter
LCMS	liquid-phase chromatograph mass spectroscopy
LCT	liquid-phase chromatograph time-of-flight
LDA	lithium diisopropylamide
LiHMDS	lithium hexamethyldisilazide
LIFDI	liquid injection field desorption ionization
<i>m</i>	meta
m	multiplet or milli
min	minute(s)
mmHg	millimeters of mercury

mol	mole(s)
M	molecular mass or molar
Me	methyl
MeDTBP	methyl-di- <i>tert</i> -butylpyridine
Mes	mesityl
MHz	megahertz
MS	molecular sieves
NMR	nuclear magnetic resonance
<i>n</i>	normal (linear)
NOESY	nuclear overhauser effect spectroscopy
<i>o</i>	ortho
OTf (Tf)	trifluoromethanesulfonate (triflate)
pH	hydrogen ion concentration in aqueous solution
ppm	parts per million
Ph	phenyl
Pr	propyl
<i>i</i> -Pr	isopropyl
q	quartet
quint.	quintet
rt	room temperature
s	singlet
sat.	saturated
sext.	sextet
t	triplet
TBS	<i>tert</i> -butyldimethylsilyl
td	triplet of doublet
Temp.	temperature
TF <sub>2</sub> O	triflic anhydride
TFE	2,2,2-trifluoroethanol
THF	tetrahydrofuran
TLC	thin layer chromatography
TMS	trimethylsilyl
UV	ultraviolet
WCA	weakly coordinating anion



## ACKNOWLEDGEMENTS

To begin, I must thank my advisor, Hosea Nelson, for his guidance and unwavering support over the years. I will never forget the day I first met Hosea during my visitation weekend at UCLA. His charismatic nature and drive for pushing the boundaries of science ended up convincing me to join and help establish the Nelson lab. Still, I always considered myself lucky that with my limited synthetic experience at the time, Hosea still took me in, believing that I had the “hands” to be a good chemist. Having Hosea teach me synthetic techniques first-hand was not only incredibly fun, but has also instilled a great level of confidence in my own abilities today. I can certainly attribute my accelerated growth as a scientist to my exposure to Hosea’s attention to detail and endless creativity. As I’m sad to be leaving, I know the lab will continue to pursue awesome science as I continue to observe the growth of the lab from the outside.

To all of my committee members, thank you. Professors Neil Garg, Alex Spokoyny and Yi Tang have all been wonderful colleagues to the Nelson lab. Our accomplishments could not have been possible without their support. Neil has been our greatest ally since day one and serves as a shining example of success we should all hope to follow in regards to his professionalism and work ethic. Alex is perhaps the only chemistry faculty at UCLA to rival Hosea’s charismatic personality. His contagious humor is matched only by his scientific creativity, and I look forward to seeing the cool chemistry that is sure to come from the Spokoyny lab in the future. Yi Tang, as I learned during my candidacy defense, is a fellow member of the 626. His success will always serve as an example for me in the possibilities of our community.

I would not be where I am today without all the support I’ve received from my previous institutions as well. I thank Ms. Nagaishi for introducing me to the world of chemistry in such an

impactful way. While not directly relating to chemistry, I must also thank my former speech and debate coach, Mr. Tong, for his dedication to students in their interpersonal and professional growth. The public speaking skills I developed during my time on the speech and debate team also proved invaluable over the years, especially in graduate school. In my short stint studying abroad at Academia Sinica, Professor Cheng-Chung Wang and Dr. Chun-Wei Chang, were instrumental in my education. Thank you for showing me the ropes in my first synthetic laboratory experience. In my continued study at UC Davis, Professor Xi Chen helped to cultivate my love for chemistry and provided a truly wonderful research environment in her lab. Special shout out to Dr. Musleh Muthana, Dr. Teri Slack and Dr. Abhishek Santra for all their teachings and the hospitality they offered to me as a naïve undergrad. My decision to pursue a PhD was heavily influenced by my time at the Chen lab.

When I first joined UCLA, I never would have expected to be with a cohort so incredibly brilliant and sociable. There was certainly a period of time where I had an intense case of imposter syndrome given the talents of all my colleagues. However, I think this simply speaks volumes to the compassion of our class, as I was never made to feel inadequate in the face of my fellow peers. The frequent gatherings at Wendell Scott's old apartment was just one of the things that I'm sure kept me, and others of our cohort, sane during our first year of graduate school. Wendell and Prier Panescu's ability to rally people together is a skill that is often underappreciated. Hopefully some day we can revisit the old Vegas gang again. Michael Yamano, Jacob Dander, Robert Susick and the rest of the Garg lab members, thanks for the camaraderie over the years. Andy Smaligo, thanks for being such a source of positivity in our cohort. I will miss your undying kindness to all those around you.

My co-workers in the Nelson lab deserve the upmost praise. Alex “Bags” Bagdasarian, is a colleague that everyone deserves to have on their team. His loyalty knows no bounds, and his intense passion for chemistry is infectious. He’s also pretty athletic when he’s in the water (not so much on land). As one of the first students in Hosea’s lab, we’ve had a truly unique experience. Bags’ unyielding resolve had certainly helped me find the willpower to continue pushing through the hard times in my first quarter in graduate school. I owe a great deal to Bags and all that he’s done for me. More than anything, I’m grateful to be able to call Bags a dear friend. There’s an inexplicable connection that only we can understand at times given our trials and tribulations.

I would be remiss to not mention Dr. Jonny Gordon when thinking back to my first year. He was an invaluable asset to the lab as our first postdoc, boasting a vast knowledge of synthetic skills as well as being an excellent bench chemist. He has a magnetic personality and a great sense of humor that I’ve missed ever since he moved to his industry position.

The second class of students, Sydnee “Syd” Green and Stasik Popov, have come a long way since their debut in the lab. Syd has a way with bringing people together, and I really believe the lab as a whole has become closer since she’s been around. She’s also a good source of free food and drink since she never finishes anything. When talking about Syd, it’s hard to exclude her number one protégé, Hayden “Blo\$\$y” Montgomery-Aytac. During her time in the lab learning under Syd, Hayden has become a great scientist and friend to all of us (kudos to Syd). Even though you’ve been at UCLA for what seems to be a lifetime, I’m sure you’ll do great in your continued stay in the Spokoyny/Maynard groups. Stasik is unique and irreplaceable in many ways. There’s not another human being I know in the world that would eat nothing but pounds of meat for lunch and dinner without any carbs, vegies, or fruits. I’m glad you decided to

join our lab in the end knowing you had many options. I'd like to believe that our musings over professional StarCraft had a lot to do with your decision. In categorizing my acknowledgements by yearly cohorts, I would have to include Roy Pan this section as well, even though his path in our lab has been quite complicated. As an undergrad that bore witness to the Nelson lab's first year of operation, he has been exposed to so much more chemistry than probably most of his contemporaries. I'll always cherish the memories we shared with bags grinding it out in the bullpen; the late nights at the NMR where you discovered the key cyclopropanation reaction toward Vibralactone. Thanks for being such a great co-worker and friend through all of my time here at UCLA. Even though you've since moved on from the Nelson lab, I know you're destined for success in your future endeavors.

Sepand Nistanaki, Benjamin Wigman, Jessica Burch, Lee Joon "LJ" Kim and Christopher Jones, our biggest class yet, deserves their props too. Chris started the microED project not too long ago, and it's already become such a large part of our lab. LJ and Jess are incredibly versatile scientists, starting in synthetic chemistry when they first joined and then switching gears completely to work on microED. On a lighter note, LJ, hopefully one day you find the light to play a superior game in StarCraft; Jess, I hope your "meal (microwave) prepping" continues even when I'm gone as your life coach. Ben has been an incredibly fun colleague to work with over the years and has really made his mark on the lab. Call me up anytime for the next Mac Demarco concert. Sepand is pretty smart when it comes to chemistry. Pop-culture references though...a different story. Nonetheless, I have enjoyed Sepand's company in 3221 greatly, and I have no doubts that he will have a bright future ahead of him—perhaps too bright that he can't see it himself sometimes.

My time with Dr. Matt Asay, Chloé Williams, Wenjing Wei and Woojin Lee has been far too short. Wenjing and Woojin have been especially kind colleagues to work with. Chloé was able to transition into our lab seamlessly with her friendly, outgoing nature. I'm rooting for you all. Matt, now our most tenured postdoc in lab history, has been truly a treat to work with (boom!). His humor, quick wit and inorganic/organometallic prowess have all been greatly appreciated.

Lastly, I need to thank the rest of my family and my girlfriend, Annie, for their continued support throughout my time in grad school. None of this would have been possible without you guys.

## BIOGRAPHICAL SKETCH

### Education:

#### University of California, Los Angeles

Los Angeles, CA

*Department of Chemistry and Biochemistry*

Ph.D. Candidate, Organic Chemistry, expected December 2019

#### University of California, Davis

Davis, CA

*Department of Chemistry*

B.S., Pharmaceutical Chemistry, Highest Honors

### Experience:

#### University of California, Los Angeles

Los Angeles, CA

*Graduate Student, Advisor: Professor Hosea M. Nelson*

- August 2015–November 2019
- Discovered novel C–H insertion reaction of aryl cations
- Spearheaded mechanistic investigations of dicoordinate carbocations
- Experienced in project lead position with demonstrated success working in teams
- Strong background in organic synthesis and methods development
- Interdisciplinary breadth in inorganic synthesis and organometallic chemistry
- Trained in highly collaborative environments to propel projects forward
- Presented research at both academic and industry settings

#### University of California, Davis

Davis, CA

*Undergraduate Researcher, Advisor: Professor Xi Chen*

- June 2014–June 2015
- Utilized chemo-enzymatic synthesis to construct heparin-analogue oligosaccharides
- Trained in analytical instrumentation for purification of complex oligosaccharides
- Presented research at UC Davis LaRock Undergraduate Conference

#### Academia Sinica, Institute of Chemistry

Taipei, Taiwan

*Undergraduate Researcher, Advisor: Professor Cheng-Chung Wang*

- March–June 2014
- Synthesized a variety of carbohydrate intermediates for methods development

### Publications:

1. Shao, B.; Bagdasarian, A. L.; Popov, S.; Nelson, H. M. “Intermolecular C–H Insertion of Aryl Cations.” *Trends Chem.* **2019**, *Just Accepted*, DOI: 10.1016/j.trechm.2019.10.004
2. Wigman, B.; Popov, S.; Bagdasarian, A. L.; **Shao, B.**; Benton, T. R.; Williams, C. G.; Fisher, S. P.; Lavallo, V.; Houk, K. N.; Nelson, H. M. “Vinyl Carbocations Generated Under Basic Conditions and Their Intramolecular C–H Insertion Reactions.” *J. Am. Chem. Soc.* **2019**, *141*, 9140–9144.

3. Popov, S.; **Shao, B.**; Bagdasarian, A. L.; Benton, T. R.; Zou, L.; Zhongyue, Y.; Houk, K. N.; Nelson, H. M. “Teaching an Old Carbocation New Tricks: Intermolecular C–H Insertion Reactions of Vinyl Cations.” *Science* **2018**, *361*, 381–387.
4. **Shao, B.**; Bagdasarian A. L.; Popov, S.; Nelson, H. M. “Arylation of Hydrocarbons Enabled by Organosilicon Reagents and Weakly Coordinating Anions.” *Science* **2017**, *355*, 1403–1407.

#### **Honors and Recognition:**

- **UCLA Dissertation Year Fellowship**

*The fellowship supports select doctoral students with demonstrated success and accomplishments in their last year of studies.*

- **Genentech Graduate Student Symposium in Chemical Research Award**

*The award recognizes promising young scientists with career interests in pharmaceutical research and development.*

- **Link Foundation Energy Fellowship Program – Honorable Mention**

*An honorable mention signifies a deserving proposal in the top percentages of applicants. My proposal aimed to address problems in the societal production and utilization of energy through an innovative catalytic method of methane conversion to liquid fuels.*

- **UC Davis College of Letters and Science**

*Undergraduate Honors Research – Highest Honors  
Citation for Outstanding Graduating Senior  
Dean’s Honor List*

#### **Presentations:**

1. **Genentech Graduate Student Symposium in Chemical Research 2019**

*Formal talk highlighting my research accomplishments as a fourth year graduate student in chemistry at Genentech headquarters*

2. **ACS San Francisco, UCLA Research Showcase 2017**

*Poster presentation of my hydrocarbon arylation chemistry at the annual UCLA showcase in the ACS national meeting*

3. **UC Davis LaRock Undergraduate Conference 2015**

*Formal talk on accomplishments in undergraduate research*

## CHAPTER ONE

### Fundamental Reactivity of Dicoordinate Carbocations

#### 1.1 Abstract

Herein an overview of classically known reactivities of dicoordinate carbocations is discussed. Emphasis is given to C–C bond forming transformations reported in the literature of relevant aryl and vinyl cations. As early as the 1930s, Mascarelli and co-workers disclosed the first C–C bond forming reaction of a putative aryl cation intermediate. Jacob and co-workers presented the first proposal of a vinyl cation intermediate in the 1940s. From these findings, nearly a century of mechanistic studies and methodology developments have been conducted on these dicoordinate carbocations. In modern examples, the groups of Siegel and Reed disclosed the use of weakly coordinating anions (WCAs) to help tame the reactivity of these otherwise promiscuous intermediates.

#### 1.2 Introduction

As synthetic chemists, much of what we understand in organic chemistry and synthesis can be attributed at least in part to developments in carbocation chemistry. The importance of carbocations was recognized through the Nobel Prize, given to Olah in 1994 for his work in studying these reactive intermediates.<sup>1</sup> Olah's work, in combination with developments built upon the seminal works of those involved in the field such as Meerwin, Ingold, Hughes, Bartlett, Schleyer and others, helped to shape our understanding of carbocations as retrons in classic transformations such as nucleophilic substitution and elimination reactions.<sup>2–7</sup> It would be remiss not to also mention the independent studies performed by Norris, Kehrmann and Baeyer on the



formation of the triphenylmethyl cation in 1901.<sup>8-10</sup> These examples in carbocation chemistry share the resonance and/or hyperconjugation stabilization present in more traditional tricoordinate carbocations. However, in the case of dicoordinate carbocations, the lack of these types of stabilization effects has limited methodological and conceptual advancements with respect to their trivalent counterparts.<sup>11,12</sup> This is especially true for the highly reactive phenyl and vinyl cations.

As a reactivity-driven catalysis group, we were intrigued with the prospect of investigating reactive intermediates as a starting point in our search for new discoveries. We were particularly inspired by the classic reactivity studies conducted on aryl and vinyl cations. Given that developments in this area were quite rare, a clear path for a unique research program began to present itself through the application of these fundamental studies towards novel catalytic methodologies. Herein, a close examination into the documented reactivity profiles of these dicoordinate cations will shed light on the design and approach of the Nelson lab to carbocation chemistry. Moreover, this chapter will do more to both focus on both C–C bond forming reactions of dicoordinate carbocations, and to help highlight the contrast of developments from the Nelson lab in the ensuing chapters.

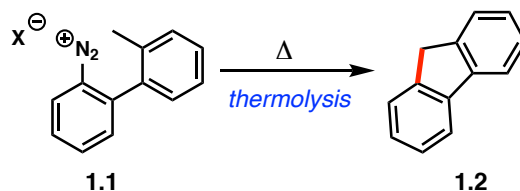
### **1.3 Aryl Cations**

Phenyl cations have been the subject of nearly a century of theoretical and experimental studies. Due to their high-energy profiles and promiscuous reactivity, many early studies of the phenyl cation were conducted on simple solvolysis and decomposition product experiments

involving aryl diazonium salts. Contemporary C–C bond forming developments employing the use of phenyl cations will also be discussed.

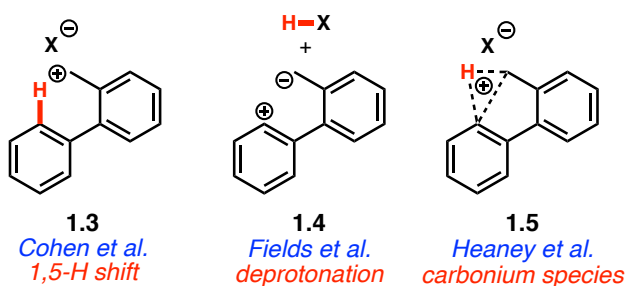
### 1.3.1 Mascarelli's Phenyl Cation

**Scheme 1.1** Mascarelli's Fluorene Synthesis



One of the earliest examples implicating the intermediacy of a phenyl cation able to engage in a C–C bond forming transformation can be traced back to Mascarelli (Scheme 1.1). In 1936, Mascarelli described the thermolysis reaction of an aryl diazonium salt **1.1** that led to formation of fluorene **1.2**.<sup>13</sup> This report spawned a decades-long debate as to the mechanism at play for this unusual reaction.<sup>14</sup> While numerous proposals were offered over the years, the most pervasive mechanistic proposals are shown in Figure 1.1.<sup>15–17</sup>

**Figure 1.1** Proposed Intermediates in the Mascarelli Reaction



Following loss of nitrogen at elevated temperatures, Cohen and co-workers proposed an intramolecular 1,5-hydride shift leading to generation of intermediate **1.3**.<sup>15</sup> Fields and co-workers very quickly offered a rebuttal to the initial mechanistic proposal. In Fields' proposed

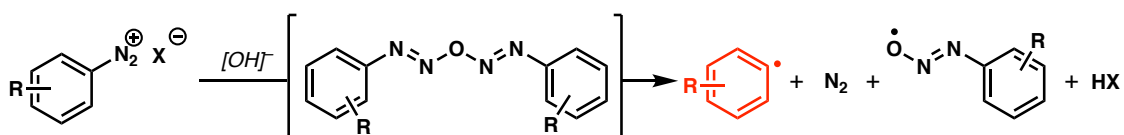
mechanism, generation of a putative phenyl cation would polarize the pendant benzylic C–H bond to yield a zwitterionic intermediate **1.4** upon deprotonation.<sup>16</sup> This intermediate is then believed to furnish the final fluorene product. It would not be until a decade later that Heaney and co-workers would offer new speculations on this reaction pathway. Following the exquisite carbocation studies conducted by Olah and the great classical vs. nonclassical cation debate of the 20<sup>th</sup> century, Heaney proposed the intermediacy of a nonclassical pentacoordinate carbonium species (**1.5**) to explain the transformation reported by Mascarelli.<sup>17</sup> While this result received little attention in its initial application towards novel synthetic methods, these studies served as invaluable inspiration to more recent aryl cation studies, including our own, as will be discussed later in this document.

### 1.3.2 Phenyl Cations In Other Dediazoniating Reactions

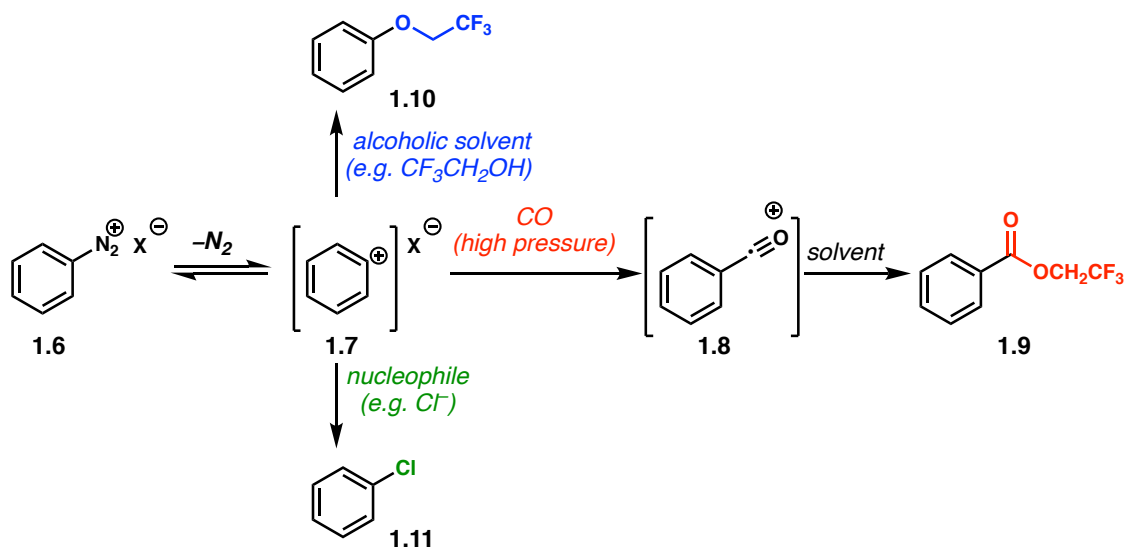
While the Mascarelli reaction was certainly an important early advancement in the field of aryl cation study, many developments in the reactivity of arenediazonium ions have been made since this seminal report. As an arylating agent, diazonium salts have also been used in heterolytic biaryl synthesis since the late 1800s.<sup>18</sup> The Gomberg-Bachmann reaction was a large advance in this realm, but the mechanism of this classic transformation has been widely outlined to proceed through an aryl radical pathway (Scheme **1.2**).<sup>19</sup> On the other hand, conditions reported by several groups utilizing certain benzenediazonium salts demonstrate a heterolytic substitution mechanism when biaryl products were not observed.<sup>20–22</sup> With increasing evidence being presented in 1970s, phenyl cations became an increasingly accepted intermediate in the community for dediazoniating reactions. Lead investigators including Zollinger, Swain, and

Lewis were among many of the pioneers during this time.<sup>20–22</sup> It was found that benzenediazonium precursors (**1.6**) undergo a unimolecular process of N<sub>2</sub> loss to generate a phenyl cation (**1.7**) with highly indiscriminate reactivity (Scheme 1.3).

**Scheme 1.2** Proposed Mechanism of the Gomberg-Bachmann Reaction



**Scheme 1.3** Reactivity of Phenyl Cations From Arenediazonium Ions

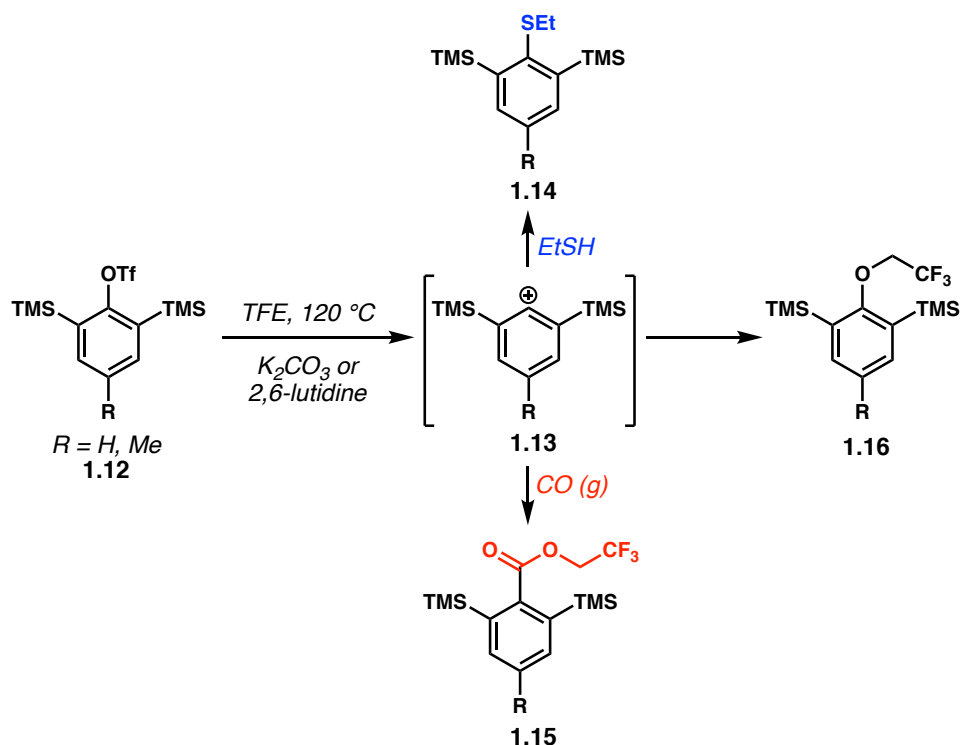


In the presence of various alcohol solvents, oxides, weak nucleophiles and carbon monoxide, generated phenyl cations were shown to react with rates ranging from  $10^2$  to  $10^7$  s<sup>-1</sup>.<sup>22</sup> Various aryl products (**1.9** to **1.11**) have been reported in analogous dediazoniaion reactions. A notable example in the context of C–C bond formation was a report by Zollinger and co-workers, detailing the reversibility of phenyl cation generation and its ability to give acyl ion **1.8** under high pressures of carbon monoxide.<sup>20</sup> The acyl ion is then converted to benzoate **1.9** in the presence of 2,2,2-trifluoroethanol (TFE) solvent conditions.

### 1.3.2 Direct Solvolysis of Aryl Triflates

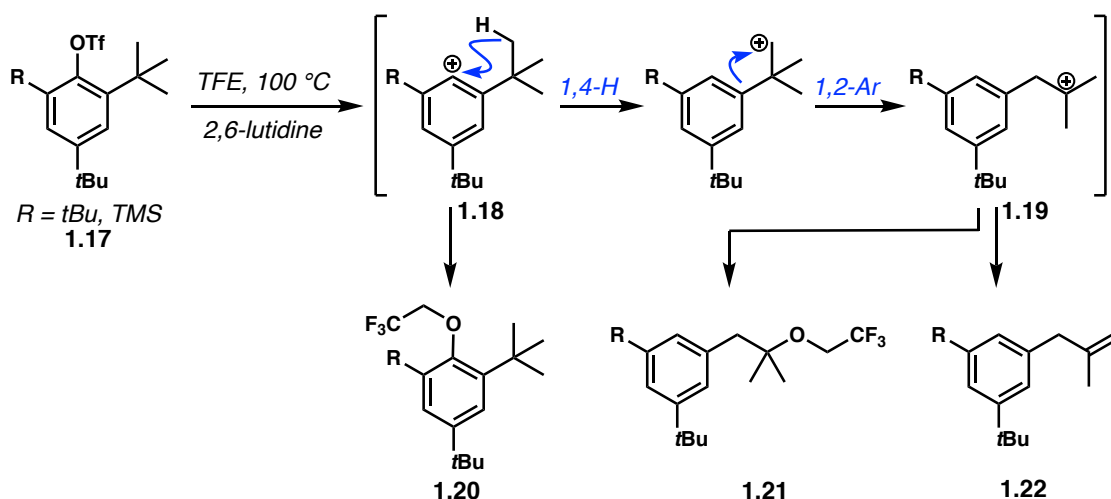
While the early mode of generation for aryl cations were performed on diazonium salts, substrates with other highly reactive leaving groups were also explored. Aryl triflates were among the most successful precursors beside diazonium salts for the study of phenyl cations under solvolysis conditions. Although initial triflate derivatives failed to yield productive evidence for phenyl cation generation, Sonoda and co-workers were able to utilize the  $\beta$ -silicon effect to great success in their phenyl cation studies (Scheme 1.4).<sup>23</sup> Taking into account the elegant theoretical investigation of Apeloig and Arad, trimethylsilylated aryl triflate derivatives were reacted in TFE solutions to study aryl cation reactivity.<sup>24,25</sup> Here, 2,6-substituted silyl triflates **1.12** were shown to undergo an  $S_N1$  mechanism to yield various ethers (**1.16**), thioethers (**1.14**) and benzoates (**1.15**) aligned with the results of previous dediazonation reactions.<sup>20</sup>

Scheme 1.4 Solvolysis of Aryl Triflates



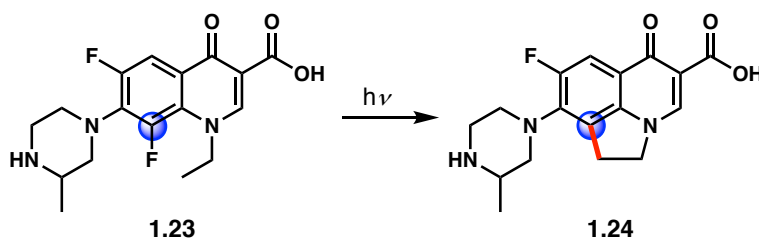
The report by Sonoda also examined ortho *tert*-butyl derivatives (**1.17**) in aryl triflate solvolysis reactions (Scheme 1.5). In this system, the observed products **1.20** to **1.22** suggests the possibility of a 1,4-hydride shift occurring after formation of phenyl cation **1.18**, followed by a 1,2-aryl shift to cation **1.19**.<sup>20</sup> The authors note that two factors are crucial for effective solvolysis of aryl triflates: (1) stabilization via hyperconjugative effects and (2) relief of steric strain by release of the triflate group.<sup>20</sup>

**Scheme 1.5** Solvolysis of 2,6-substituted Aryl Triflates



### 1.3.3 Photolytic Generation of Aryl Cations and the Singlet Phenyl Cation

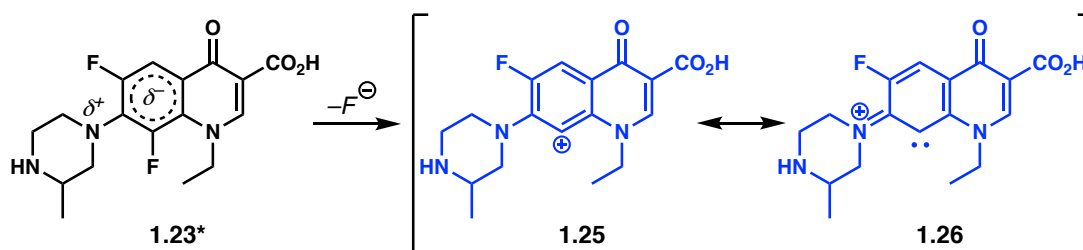
**Scheme 1.6** C–H Insertion of Aryl Cation Observed by Albini



Near the turn of the 20<sup>th</sup> century, a new renaissance of aryl cation reactivity studies was initiated through reported works by Albini, Fagnoni, Olah and others.<sup>26–28</sup> Albini and co-workers

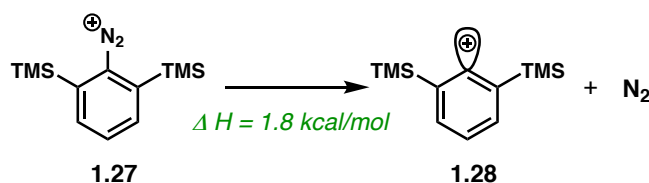
discovered a unique mode of phenyl cation generation through photolytic methods.<sup>26</sup> Irradiating ( $\lambda > 310\text{nm}$ ) aryl fluoride derivative **1.23** yielded a surprising cyclization product **1.24** in minor amounts (Scheme **1.6**). The proposed mechanism of this transformation begins with heterolytic loss of  $\text{F}^-$  after initial excitation to **1.23\***. Here, the aryl cation **1.25** is believed to exist also in a carbene resonance form (**1.26**), a proposed rationale for the observed C–H insertion reactivity (Scheme **1.7**).<sup>26</sup>

**Scheme 1.7** Rationalization of C–H Insertion Reactivity



In the years following Albini's report of photogenerated singlet phenyl cations, insightful computational reports have also helped to validate and expand on the findings of this initial study. Harvey and Aschi elaborated on calculated stable spin states of a number of para substituted aryl cations to be the singlet state.<sup>29</sup> Olah and co-workers found that ortho silylation of parent benzene diazonium species can lower the overall energetics of aryl cation formation by almost 14 kcal/mol for each ortho substitution.<sup>27</sup> From this trend, the authors suggest that loss of  $\text{N}_2$  from 2,6-bis(trimethylsilyl)benzene diazonium species **1.27** could be spontaneous to yield singlet aryl cation **1.28** (Scheme **1.8**).

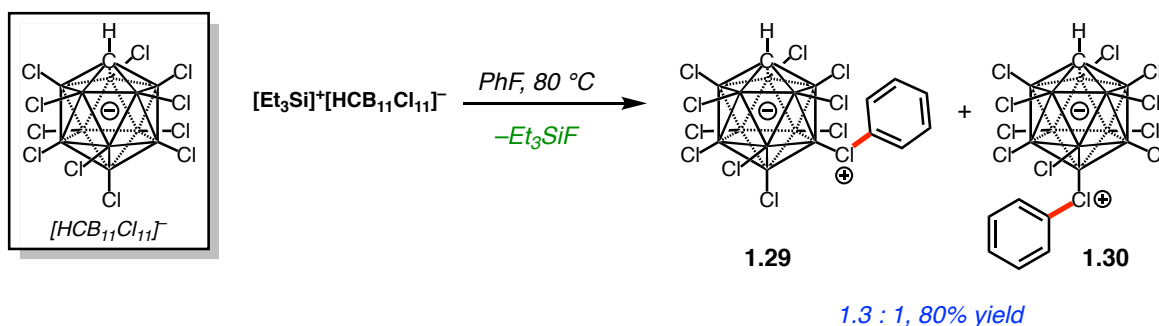
**Scheme 1.8** Energetics of Bis-silylated Benzenediazonium in Aryl Cation Formation



### 1.3.4 Aryl Cations Paired With Weakly Coordinating Anions

Recent advancements in phenyl cation chemistry involve the ionic pairing of weakly coordinating anions (WCAs). While not discussed in this document, there are numerous sources available for comprehensive reviews on relevant WCAs.<sup>30</sup> A key discovery by Reed and Siegel showed that reacting highly Lewis acidic and fluorophilic silylium-carborane salts with fluorobenzene yields isolable salts **1.29** and **1.30** (Scheme 1.9).<sup>31</sup> Essential to the C–F bond activation step is the enhanced Lewis acidity of silylium imparted by the exceptionally weakly coordinating nature of the  $[\text{HCB}_{11}\text{Cl}_{11}]^-$  anion. This allows for kinetically viable aryl fluoride abstraction and is thermodynamically driven through the formation of a Si–F bond.

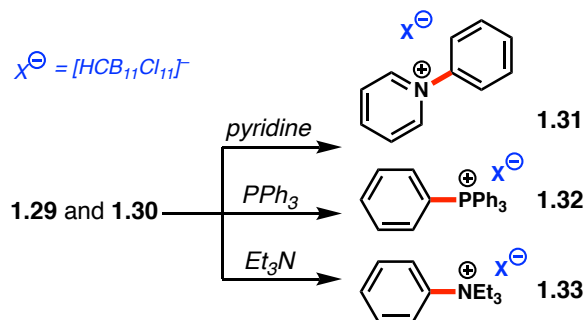
**Scheme 1.9** Discovery of Phenylated Carborane Salts



Upon isolation, chloronium salts **1.X** and **1.X** could then be subjected to a variety of nucleophiles such as  $\text{Et}_3\text{N}$ ,  $\text{PPh}_3$  and pyridine to generate phenylated products (**1.31** to **1.33**, Scheme 1.10).<sup>31</sup> In contrast to many of the previously reported studies on aryl cations involving solvolysis in polar protic solvents, the ability to generate incipient phenyl cations in such nonpolar media offered a new means to study these reactive intermediates in solution.

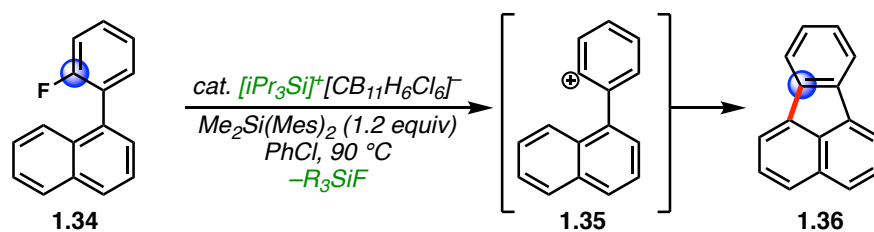


### Scheme 1.10 Evidence for Phenyl Cation Reactivity



Subsequent to their collaborative work with Reed, Siegel and co-workers disclosed an innovative catalytic method for C–C bond formation through aryl cation intermediates (**1.35**).<sup>32</sup> Here, intramolecular Friedel-Crafts reactions of fluoroarenes (**1.34**) allow for high yielding generation of polyaromatic compounds (**1.36**), initiated by catalytic proton or silylium paired WCAs and fueled by stoichiometric silane (Scheme **1.11**). Moreover, this arene–arene bond formation stands in stark contrast with the classical Gomberg-Bachmann or Pschorr cyclization reactions as it represents the first phenyl cation-based example.<sup>18,33</sup>

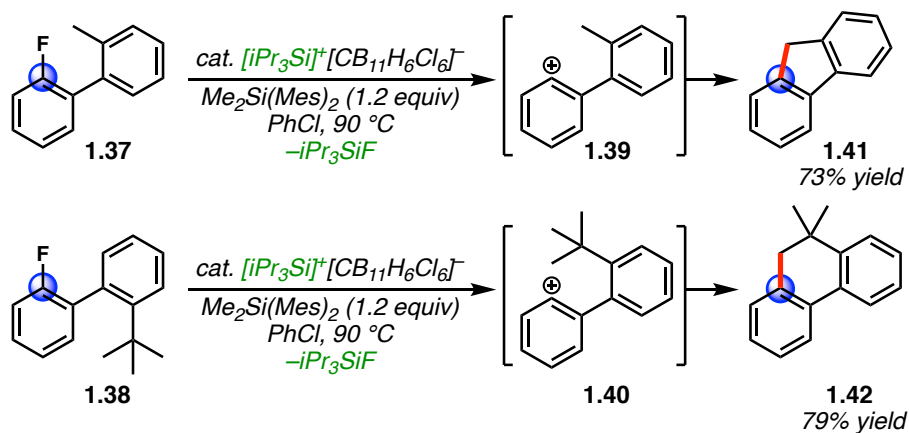
### Scheme 1.11 Intramolecular Friedel-Crafts Reactivity From an Aryl Cation



From the lessons learned in the silylium-mediated formation of aryl cations, Siegel and co-workers also described a catalytic intramolecular reaction analogous to Mascarelli's fluorene synthesis.<sup>34</sup> In taking fluorinated biphenyl compounds **1.37** and **1.38**, the aryl cations generated (**1.39** and **1.40**) undergo a C–H insertion reaction with the proximal methyl group to produce cyclized products **1.41** and **1.42**, respectively. The combination of experimental and computational analysis in this work helps to unify many of the themes previously discussed on

aryl cation reactivity. Revisiting the Mascarelli reaction, there is now credible evidence for a C–H insertion event being at play for phenyl cations.<sup>13</sup> Furthermore this is in alignment with the work of Albini and Fagnoni, as singlet aryl cations with reminiscent carbene reactivity are shown to undergo intramolecular C–H insertion.<sup>26</sup>

**Scheme 1.12** Intramolecular C–H Insertion of Aryl Cations



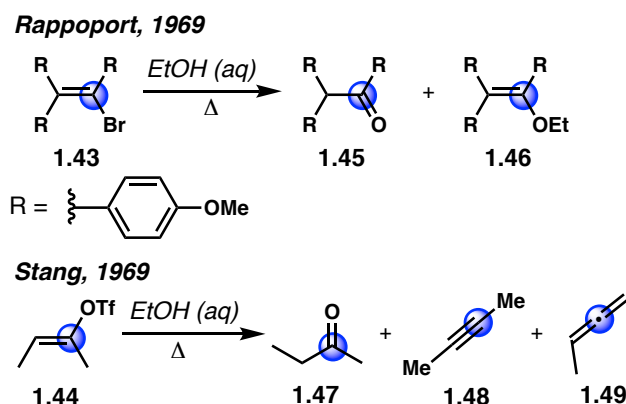
## 1.4 Vinyl Cations

In the field of dicoordinate carbocations, vinyl cations are perhaps the most well studied class of reactive intermediates.<sup>35</sup> While Jacobs and Searles first proposed the existence of vinyl cations in 1944, it was not until the 1960s that these intermediates were widely accepted in the chemical community.<sup>36,37</sup> In parallel with the phenyl cation, many of the early investigations of vinyl cations revolved around solvolysis in polar aqueous media. With the emphasis of C–C bond forming reactions in mind, modern examples of vinyl cation-based transformations will also be highlighted.

### 1.4.1 Vinyl Cation Solvolysis Reactivity

Major contributors in the development of vinyl cation chemistry include the works of Grob, Hanack, Rappoport, Schleyer, Stang and others.<sup>37-41</sup> Given the volume of studies conducted on vinyl cation solvolysis over the past five decades, an abbreviated survey of classical reactivity will be highlighted. Rappoport and Gal reported the solvolysis of aryl substituted vinyl halides (**1.43**) and their utility as competent vinyl cation precursors (Scheme 1.13).<sup>38</sup> Stang and co-workers described the preparation and solvolysis of vinyl triflates (**1.44**).<sup>39</sup> Representative to most studies from this era in vinyl cation development, the product distribution of these two reports is comprised largely of nucleophilic attack from heteroatom-containing solvent molecules (**1.45** to **1.47**) to the cation and elimination when possible (e.g **1.48** and **1.49**).<sup>38,39</sup>

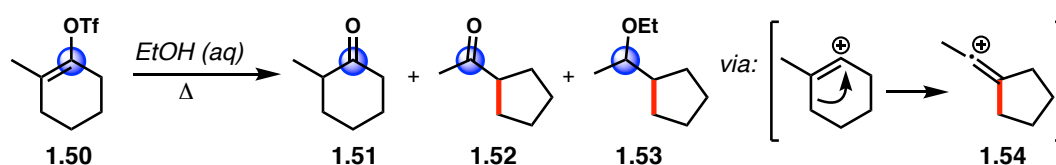
**Scheme 1.13** Classic Solvolysis Reactions of Vinyl Cation Precursors



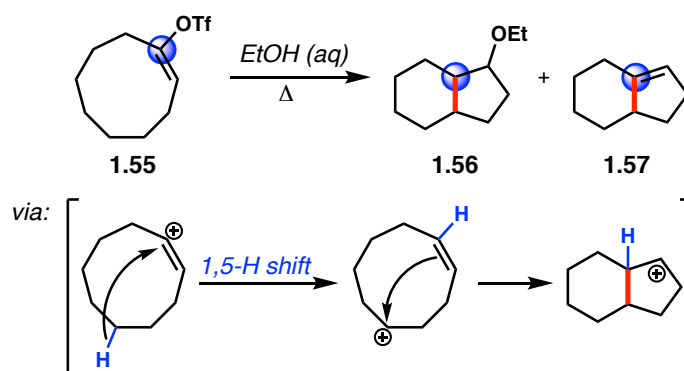
Following the use of vinyl triflates and the discovery of their ability to react orders of magnitude faster than traditional halide leaving groups, much of subsequent vinyl cation chemistry revolved around these triflate substrates. Here, some interesting developments in the field were made through the use of cyclic vinyl triflates. Schleyer and co-workers described the ring-contraction products **1.51** to **1.53** from 2-substituted cyclic vinyl triflate **1.50** (Scheme

**1.14).**<sup>40</sup> This rearrangement is rationalized to occur due to the favorable adoption of a linear sp-hybridized vinyl cation (**1.54**). Furthermore, Hanack and co-workers observed ring-fused products (**1.56** and **1.57**) upon solvolysis of medium-sized carbocycle substrate **1.55** (Scheme **1.15**).<sup>41</sup> In addition to the independent studies by Olah and Caple, this unusual C–C bond forming process is hypothesized to proceed through a rebound mechanism depicted in Scheme **1.15**.<sup>42,43</sup>

**Scheme 1.14** Ring-contraction Rearrangement of Cyclic Vinyl Cations



**Scheme 1.15** Ring Fusion via 1,5-hydride Shift From Cyclic Vinyl Cation

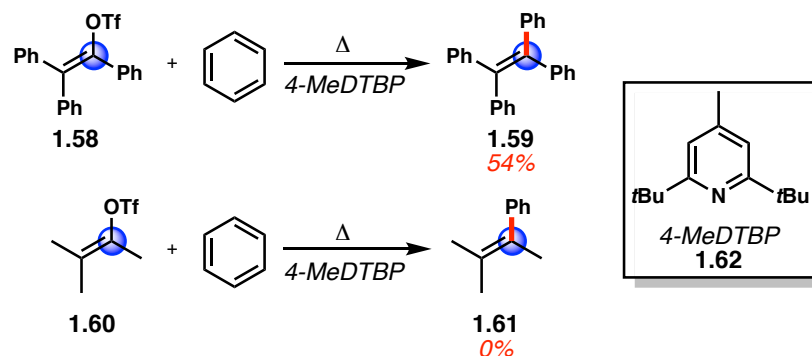


## 1.4.2 Friedel-Crafts Alkenylation of Vinyl Cations

While aromatic alkylations reactions with unsaturated precursors have been reported as early as the 19<sup>th</sup> century, the involvement of vinyl cation intermediates in these transformations was not extensively investigated until the 1970s.<sup>44,45</sup> Stang and co-workers disclosed the first mechanistic study to postulate vinyl cations as reactive intermediates in Friedel-Crafts alkylation reactions of linear and cyclic vinyl triflates (Scheme **1.16** and **1.17**).<sup>45</sup> Interestingly, some distinct

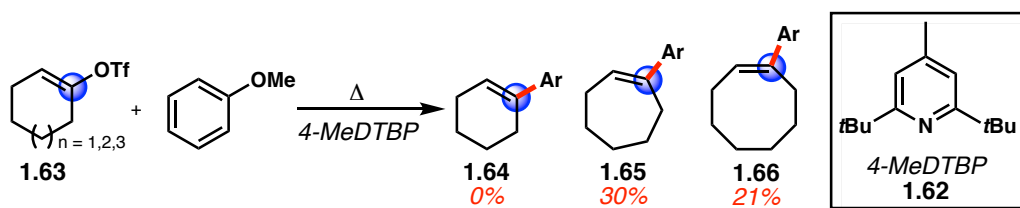
reactivity profiles were observed between linear and cyclic vinyl cations in the context of electrophilic aromatic substitution.

**Scheme 1.16** Friedel-Crafts Alkylation of Linear Vinyl Triflates



Linear substrates, in the absence of  $\beta$ -hydrogens and/or incapable of  $\beta$ -elimination (e.g **1.58**), undergo smooth aromatic coupling with arenes such as benzene (**1.59**). Alkylation was not observed in substrates with  $\beta$ -hydrogens present (e.g **1.60**). Moreover, triflate **1.60** produced only tar at higher temperatures, which the authors attribute to  $\beta$ -elimination and allene oligomerization.<sup>45</sup>

**Scheme 1.17** Friedel-Crafts Alkylation of Cyclic Vinyl Triflates



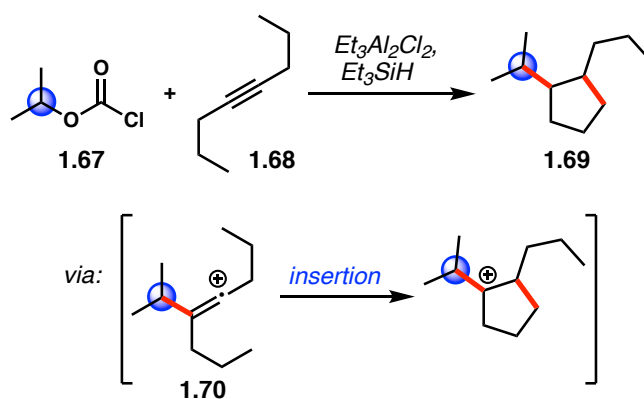
Cyclic vinyl cation precursors **1.63** exhibited similar reactivity in relation to previous studies on solvolysis reactions in aqueous ethanol. However, alkylation of anisole is uniquely linked to ring size of the starting vinyl triflate substrates (Scheme **1.17**). The reaction conditions required in yielding **1.65** were much more demanding in comparison to **1.66**; No alkylation was observed in the case of cyclohexenyl triflate (**1.64**). The observed trend is hypothesized to be the

result of increasing ring strain energy of the bent vinyl cation involved in these aromatic substitution reactions.<sup>45</sup>

### 1.4.3 Intramolecular C–H Insertion of Vinyl Cations

In more contemporary developments in vinyl cation chemistry, Metzger and Brewer independently proposed the C–H insertion reactivity of vinyl cations in intramolecular systems.<sup>46,47</sup> Metzger and co-workers utilized alkyl chloroformates and alkynes to generate vinyl cations that are able to cyclize upon insertion into a pendant  $sp^3$  C–H bond (Scheme 1.18).<sup>46</sup> Lewis acid-mediated decarboxylation of chloroformate **1.67** generates an isopropyl cation that produces vinyl cation **1.70** in the presence of an alkyne (e.g. **1.68**). The unexpected formation of cyclopentane **1.69** introduces a new mode of reactivity for vinyl cations. In corroboration with computational studies, this C–H insertion of vinyl cations parallel the singlet carbene reactivity found in related phenyl cations.<sup>26</sup>

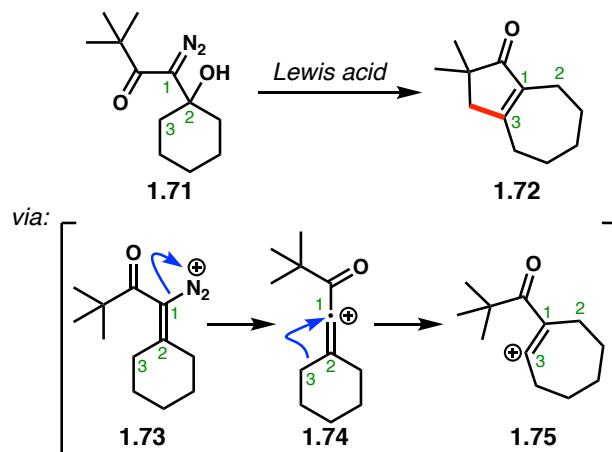
**Scheme 1.18** Intramolecular Insertion of Vinyl Cation



Brewer and co-workers reported a similar transformation involving a C–H insertion reaction in the intramolecular cyclization reaction of  $\beta$ -hydroxy- $\alpha$ -diazo ketones (**1.71**) to cyclopentanones (Scheme 1.19).<sup>47</sup> Lewis acid-mediated elimination of the  $\beta$ -hydroxy group

yields diazonium **1.73**. Loss of  $N_2$  generates an initial vinyl cation **1.74** that rapidly performs a ring-expansion due to the destabilizing withdrawing effect of the carbonyl group. C–H insertion of the cycloheptenyl vinyl cation **1.75** into the pendant methyl group then leads to the final product **1.72**.

**Scheme 1.19** Rearrangement/C–H Insertion Reaction of a Vinyl Cation



## 1.5 Conclusion

In summary, dicoordinate carbocations have played an integral part to the understanding of modern synthetic organic chemistry. Beginning with the use of aryl diazonium salts in the late 1800s, it would not be until a century later when phenyl cations would be implicated as plausible reactive intermediates. A similar account is exemplified in literature reports involving vinyl cations. While solvolysis and intramolecular reactions predominated the studies of these two classes of divalent carbocations, the lessons learned from the exquisite mechanistic studies of these intermediates are invaluable to the chemical sciences. Furthermore, recent advancements in both phenyl and vinyl cation chemistry regarding C–H insertion reactivity reveal an intriguing new application of carbocations in synthetic methodology.

## 1.6 Notes and References

- (1) Olah, G. A. *Angew. Chem. Int. Ed.* **1995**, *34*, 1393–1405.
- (2) Olah, G. A. *J. Org. Chem.* **2001**, *66*, 5943–5957.
- (3) Meerwein, H.; van Emster, K. *Chem. Ber.* **1922**, *55*, 2500–2528.
- (4) Ingold, C. K. *Structure and Mechanism in Organic Chemistry*; Cornell University Press: Ithaca, NY, 1953; and references therein.
- (5) Charman, H. B.; Hughes, E. D.; Ingold, C. K.; Volger, H. C. *J. Chem. Soc.* **1961**, 1142–1151.
- (6) (a) Bartlett, P. D.; Rice, M. R. *J. Org. Chem.* **1963**, *28*, 3351–3353. (b) Bartlett, P. D.; Sargent, G. D. *J. Am. Chem. Soc.* **1965**, *87*, 1297–1308. (c) Bartlett, P. D.; Bank, S.; Crawford, R. J.; Schmid, G. H. *J. Am. Chem. Soc.* **1965**, *87*, 1288–1308. (d) Bartlett, P. D.; Closson, W. D.; Cogdell, T. J. *J. Am. Chem. Soc.* **1965**, *87*, 1308–1314. (e) Bartlett, P. D.; Trahanovsky, W. S.; Bolon, D. A.; Schmid, G. H. *J. Am. Chem. Soc.* **1965**, *87*, 1314–1319.
- (7) (a) Saunders, M.; Schleyer, P. v. R.; Olah, G. A. *J. Am. Chem. Soc.* **1964**, *86*, 5680–5681. (b) Olah, G. A.; Schleyer, P. v. R., Eds. *Carbonium Ions*; Wiley-Interscience: New York, 1968–76.
- (8) Norris, J. F. *Am. Chem. J.* **1901**, *25*, 117–122.
- (9) Kehrman, F.; Wentzel, F. *Ber. Dtsch. Chem. Ges.* **1901**, *34*, 3815–3819.
- (10) Baeyer, A. *Ber. Dtsch. Chem. Ges.* **1902**, *35*, 1189–1201.
- (11) Olah, G. A.; Schlosberg, R. H. *J. Am. Chem. Soc.* **1968**, *90*, 272–2727.
- (12) (a) Pellicciari, R., et al. *J. Am. Chem. Soc.* **1996**, *118*, 1–12. (b) Zhang, F., et al. *J. Am. Chem. Soc.* **2014**, *136*, 8851–8854.
- (13) Mascarelli, L. *Gazz. Chim. Ital.* **1936**, *66*, 843–850.



- (14) Stumpe, R. W. *Tetrahedron Lett.* **1980**, *21*, 4891–4892.
- (15) (a) Cohen, T.; Lipowitz, J. *J. Am. Chem. Soc.* **1964**, *86*, 2514–2515. The first hypothesis of a phenyl cation insertion in the Mascarelli reaction was actually reported by Cohen; see: (b) Cohen, T.; Lipowitz, J. *J. Am. Chem. Soc.* **1964**, *86*, 2515–2516.
- (16) Puskas, I.; Fields, E. K. *J. Org. Chem.* **1968**, *33*, 4237–4242.
- (17) Daudpota, A. S.; Heaney, H. *Tetrahedron Lett.* **1978**, *19*, 3471–3474.
- (18) For early examples of diazonium salts used near the turn of the 19<sup>th</sup> century, see: (a) Culmann, C.; Gasiorowski, K. *J. Prakt. Chem.* **1889**, *40*, 97–120. (b) Gatterman, L.; Erhart, R. *Ber. Dtsch. Chem. Ges.* **1890**, *23*, 1226. (c) Hirsch, R. *Ber. Dtsch. Chem. Ges.* **1890**, *23*, 3705–3710. (d) Bamberger, E. *Ber. Dtsch. Chem. Ges.* **1895**, *28*, 403–407. (e) Bamberger, E. *Ber. Dtsch. Chem.* **1896**, *29*, 446. (f) Niementowski, S. V. *Ber. Dtsch. Chem. Ges.* **1901**, *34*, 3325–3337. (g) Gomberg, M.; Bachmann, W. E. *J. Am. Chem. Soc.* **1924**, *46*, 2339–2343.
- (19) Rüchardt, C.; Merz, E. *Tetrahedron Lett.* **1964**, *5*, 2431–2436. For a comprehensive review of hemolytic aromatic arylation, see: (b) Augood, D. R.; Williams, G. H. *Chem. Rev.* **1957**, *57*, 123–190.
- (20) (a) Kaul B. L.; Zollinger, H. *Helv. Chim. Acta* **1968**, *51*, 2132–2134. (b) Gloor, B.; Kaul, B. L.; Zollinger, H. *Helv. Chim. Acta*, **1972**, *55*, 1596–1610. (c) Burri, P.; Zollinger, H. *Helv. Chim. Acta* **1973**, *56*, 2204–2216. (d) Burri, P.; Loewenschuss, H.; Zollinger, H.; Zwolinski, G. K. *Helv. Chim. Acta* **1974**, *57*, 395–402. (d) Bergstrom, R. G.; Landells, R. G. M.; Wahl, G. H.; Zollinger, H. *Tetrahedron Lett.* **1974**, 2975–2978. (e) Bergstrom, R. G.; Landells, R. G. M.; Wahl, G. H.; Zollinger, H. *J. Am. Chem. Soc.* **1976**, *98*, 3301–3305.

- (21) (a) Swain, C. G., et al. *Tetrahedron Lett.* **1974**, 2973. (b) Swain, C. G.; Scheats, J. E.; Harbison, K. G. *J. Am. Chem. Soc.* **1975**, *97*, 783–790. (c) Swain, C. G.; Scheats, J. E.; Harbison, K. G. *J. Am. Chem. Soc.* **1975**, *97*, 791–795. (d) Swain, C. G.; Scheats, J. E.; Harbison, K. G. *J. Am. Chem. Soc.* **1975**, *97*, 796–798.
- (22) (a) Lewis, E. S. *J. Am. Chem. Soc.* **1958**, *80*, 1371–1373. (b) Lewis, E. S.; Insole, J. M. *J. Am. Chem. Soc.* **1962**, *84*, 3847–3852. (c) Lewis, E. S.; Insole, J. M. *J. Am. Chem. Soc.* **1964**, *86*, 32–34.
- (23) Himeshima, Y.; Kobayashi, H.; Sonoda, T. *J. Am. Chem. Soc.* **1985**, *107*, 5286–5288.
- (24) Apeloig, Y.; Arad, D. *J. Am. Chem. Soc.* **1985**, *107*, 5285–5286.
- (25) For a review on the  $\beta$ -silicon effect, see: Lambert, J. B. *Tetrahedron* **1990**, *46*, 2677–2689.
- (26) Fasani, M., et al. *Chem. Commun.* **1997**, 1329–1330.
- (27) Laali, K. K.; Rasul, G.; Prakash, S. G. K.; Olah, G. A. *J. Org. Chem.* **2002**, *67*, 2913–2918.
- (28) Dichiarante, V., et al. *J. Am. Chem. Soc.* **2007**, *129*, 15919–15926.
- (29) Aschi, M.; Harvey, J. N. *J. Chem. Soc., Perkin Trans. 2* **1999**, 1059–1061.
- (30) For reviews on the monocarborane clusters, see: (a) Körbe, S.; Schreiber, P. J.; Michl, J. *Chem. Rev.* **2006**, *106*, 5208–5249. (b) Reed, C. A. *Acc. Chem. Res.* **2009**, *43*, 121–128.
- (31) Duttwyler, S., et al. *Angew. Chem.* **2010**, *122*, 7681–7684.
- (32) Allemann, O., et al. *Science* **2011**, *332*, 574–577.
- (33) Pschorr, R. *Ber. Dtsch. Chem. Ges.* **1896**, *29*, 496–501.
- (34) Allemann, O. Baldrige, K. K.; Siegel, J. S. *Org. Chem. Front.* **2015**, *2*, 1018–1021.
- (35) For a comprehensive reviews of vinyl cations, see: (a) Stang, P. J.; Rappoport, Z.; Hanack, M.; Subramanian, L. R. *Vinyl Cations*; Academic Press: New York, NY, 1979. (b) Rappoport, Z.; Stang P. J., Eds. *Dicoordinated Carbocations*; John Wiley & Sons: New

- York, NY, 1997. (c) Hanack, M. *Angew. Chem. Int. Ed.* **1978**, *17*, 333–341. (d) Byrne, P. A., et al. *J. Am. Chem. Soc.* **2017**, *139*, 1499–1511.
- (36) Jacobs, T. L.; Searles Jr., S. *J. Am. Chem. Soc.* **1944**, *66*, 686–689.
- (37) Grob, C. A.; Csapilla, J.; Cseh, G. *Helv. Chim. Acta* **1964**, *47*, 1590–1602.
- (38) (a) Rappoport, Z.; Gal, A. *J. Am. Chem. Soc.* **1969**, *91*, 5246–5254. (b) Rappoport, Z. *Acc. Chem. Rem. Res.* **1976**, *9*, 265–273.
- (39) (a) Stang, P. J.; Summerville, R. H. *J. Am. Chem. Soc.* **1969**, *91*, 4600–4601. (b) Stang, P. *J. Acc. Chem. Res.* **1978**, *11*, 107–114.
- (40) Pfeifer, W. D.; Bahn, C. A.; Schleyer, P. v. R. *J. Am. Chem. Soc.* **1971**, *93*, 1513–1516.
- (41) Lamparter, E.; Hanack, M. *Eur. J. Inorg. Chem.* **1972**, *105*, 3789–3793.
- (42) Olah, G. A.; Mayr, H. *J. Am. Chem. Soc.* **1976**, *98*, 7333–7340.
- (43) Kanishchev, M. I., et al. *J. Am. Chem. Soc.* **1979**, *101*, 5660–5671.
- (44) For early examples of aromatic alkylations of unsaturated reaction partners, see: (a) Demole, E. *Ber. Dtsch. Chem. Ges.* **1879**, *12*, 2245–2247. (b) Anshütz, R. *Justus Liebigs Ann. Chem.* **1886**, *235*, 150–229. (c) Schmerling, L.; West, J. P.; Welch, R. W. *J. Am. Chem. Soc.* **1958**, *80*, 576–579. (d) Roberts, R. M.; Abdel-Baset, M. B. *J. Org. Chem.* **1976**, *41*, 1698–1701.
- (45) Stang, P. J.; Anderson, A. G. *J. Am. Chem. Soc.* **1978**, *100*, 1520–1525.
- (46) Biermann, U.; Koch, R.; Metzger, J. O. *Angew. Chem. Int. Ed.* **2006**, *45*, 3076–3079.
- (47) Cleary, S. E.; Hensinger, M. J.; Brewer, M. *Chem. Sci.* **2017**, *8*, 6810–6814.

## CHAPTER TWO

### Arylation of Hydrocarbons Enabled by Organosilicon Reagents and Weakly Coordinating Anions

Adapted from: Brian Shao<sup>†</sup>, Alex L. Bagdasarian<sup>†</sup>, Stasik Popov, and Hosea M. Nelson

*Science*, **2017**, 355, 1403–1407.

#### 2.1 Abstract

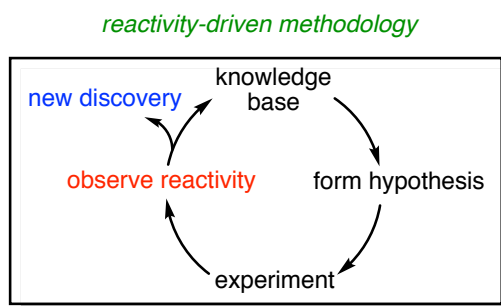
For nearly a century, phenyl cation intermediates have been implicated in a variety of C–H arylation reactions. Due to their high-energy and promiscuous reactivity profiles, selective applications of these cations have received little attention in organic methodology. Herein, we disclose our laboratory’s account in the serendipitous discovery of an intermolecular coupling process through aryl cations. Specifically, we find that  $\beta$ -silicon-stabilized aryl cation equivalents, generated via silylium-mediated fluoride activation, undergo insertion into  $sp^3$  and  $sp^2$  C–H bonds. This reaction manifold provides a framework for the catalytic arylation of hydrocarbons, including simple alkanes such as methane. This process uses low loadings of Earth-abundant initiators (1–5 mol%) and occurs under mild conditions (30 to 100 °C).

#### 2.2 Introduction

As a reactivity-driven group, the Nelson lab adopts a specific approach to research (Figure 2.1). Starting from a foundation of chemical knowledge, we form initial hypotheses that we can probe through experimentation. Here, the key to our success is in careful observations of the reactivity presented to us. As one might surmise, we allow the reactivity we observe to help

guide us in our next experiments and hypotheses. Through this iterative cycle, we in turn expand our knowledge base and cultivate new discoveries as an occasional product.

**Figure 2.1** Reactivity-Driven Methodology



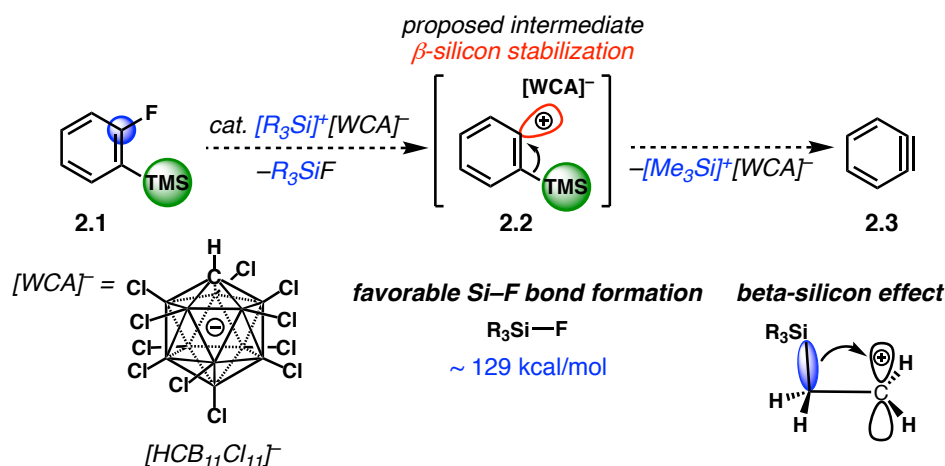
We looked favorably to the field of reactive intermediates as a productive starting point for developing new chemistries. In our exploratory stage, the inorganic community heavily influenced our studies given their expertise in isolation and characterization of reactive intermediates.<sup>1,2</sup> We were especially drawn to the chemistry of weakly coordinating monocarborane clusters in their incredible ability to stabilize otherwise reactive carbocations.<sup>3</sup> Moreover, our initial hypotheses were greatly inspired by the exquisite phenyl cation-based methodologies based on the use of these weakly coordinating anions (WCAs) reported by Reed and Siegel.<sup>2,4</sup>

### 2.3 Initial Hypothesis and Serendipitous Discovery

We initially sought to discover a catalytic method for the generation of arynes. Our original hypothesis draws on the substantial works of Lambert, Reed and Siegel (refer to chapter one) in silylium-mediated phenyl cation generation.<sup>3-5</sup> Here, we envisioned that  $\beta$ -silicon stabilization of aryl fluoride **2.1** would lower the barrier for fluoride abstraction and temper the  $\sigma$ -electrophilicity of the resulting phenyl cation. Furthermore, we anticipated that the  $\beta$ -silicon

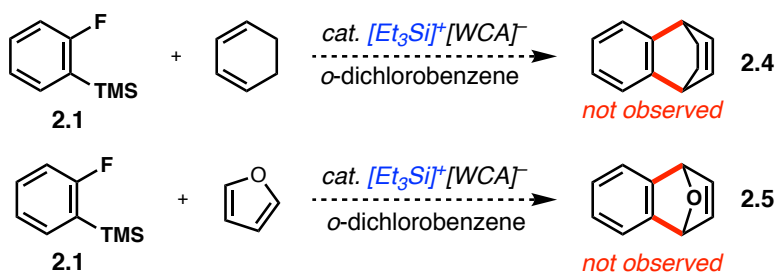
group in phenyl cation intermediate **2.2** would undergo an elimination event to yield our desired aryne **2.3**.

**Figure 2.2** Catalytic Aryne Hypothesis



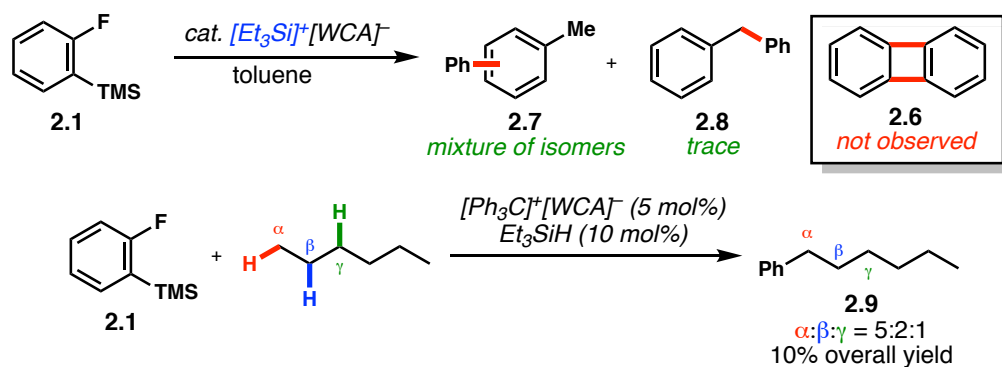
In testing our hypothesis, we subjected a variety of dienes to our reaction conditions in attempts to trap and take advantage of the well-known [4+2] reactivity of arynes.<sup>6</sup> To our disappointment, we were never able to detect any signs of cycloaddition products (**2.4**, **2.5**). Notably, in the absence of any added trapping agents, peculiar products were observed. While we were initially probing for biphenylene (**2.6**) formation via [2+2] dimerization of benzyne,<sup>6</sup> we instead isolated arylated solvent molecules (e.g toluene, **2.7**). To our surprise, we were also able to identify trace amounts of diphenylmethane **2.8**.<sup>7</sup>

**Scheme 2.1** Aryne Generation Probes by [4+2] Cycloaddition



Although we could not confidently explain the formation of **2.8**, we were adamant in our pursuit of aryne chemistry. Given the reactivity with arene solvent, we hypothesized that moving to more inert alkane solvent conditions would aid in our detection of arynes. Remarkably, in hexanes solvent we now observed alkane arylation products with catalytic turnover and selectivity for terminal  $sp^3$  C–H (5:2:1 ratio, Scheme **2.9**). Astonished by our discovery, we quickly searched for literature precedent of similar reactivity. In analogous reports by Mascarelli, Albini and Siegel, intramolecular C–H insertion of putative aryl cation intermediates is proposed.<sup>8–10</sup>

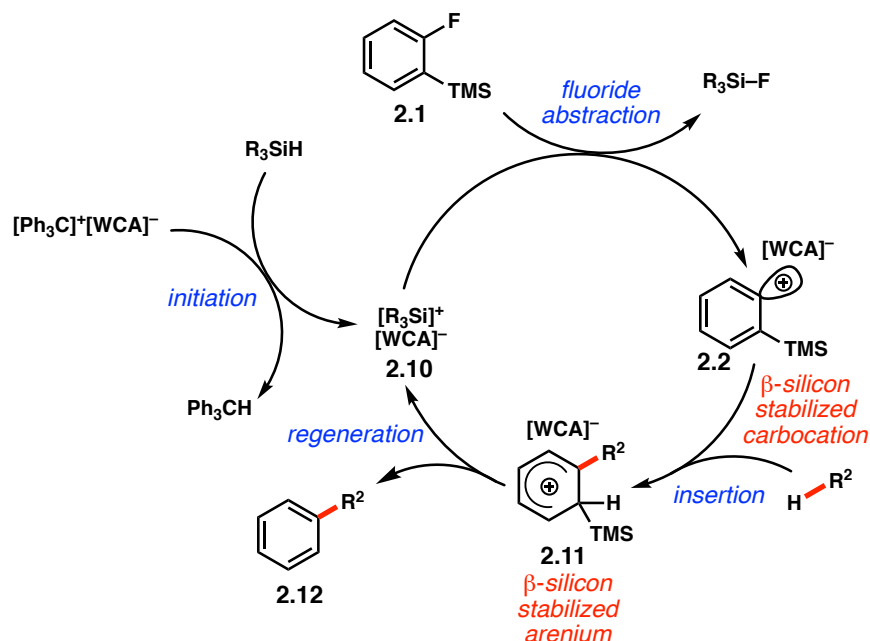
**Scheme 2.2** Serendipitous Discovery of Alkane Arylation



Taking into account also the mechanistic underpinnings of singlet phenyl cations and the frontier molecular orbital analogy with carbene species, we pursued application of these dicoordinate carbocations in catalytic, intermolecular C–H functionalization reactions.<sup>11</sup> Reevaluating our initial reaction design concepts, we now believe that in addition to lowering the barrier of fluoride abstraction, (1)  $\beta$ -silicon substitution can also enhance the nucleophilicity of the arene  $\pi$ -system, perhaps improving the insertion reactivity of phenyl cation intermediate; and (2) elimination of the  $\beta$ -silicon group occurs after arenium (**2.10**, Figure **2.3**) formation to regenerate the key reactive silicon species.<sup>5</sup>

A proposed catalytic cycle involving a cationic chain process is depicted in Figure 2.3. Here, a substoichiometric silylium-carborane initiator **2.10**,<sup>12</sup> generated via Bartlett-Condon-Schneider hydride transfer, could abstract a fluoride from fluoroarene **2.1** to generate aryl cation equivalent **2.2**.<sup>13</sup> Subsequent insertion into the hydrocarbon C–H bond would yield  $\beta$ -silicon-stabilized Wheland intermediate **2.11**. Elimination of trimethylsilylium would then afford C–H arylation product **2.12**. This elementary step would generate the active trimethylsilylium-carborane salt that proceeds through the catalytic cycle.

**Figure 2.3** Proposed Catalytic Cycle



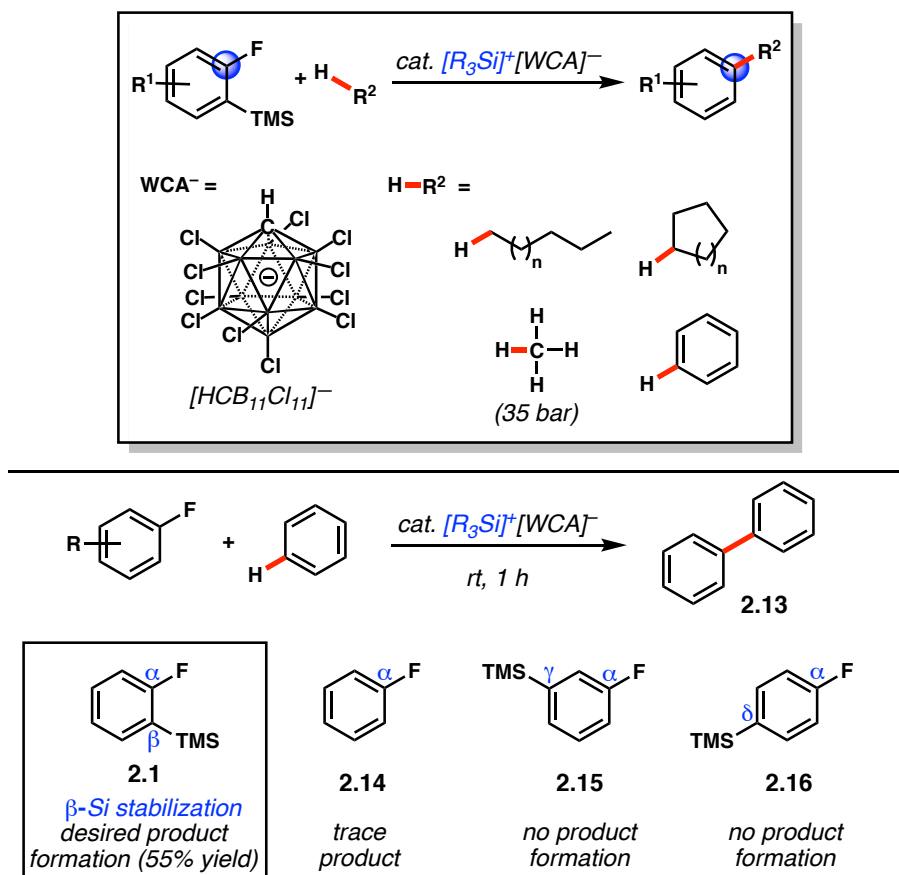
## 2.4 Development of Intermolecular C–H insertion Reactions of Aryl Cations

We report the successful execution of this methodological hypothesis, wherein a broad scope of  $\beta$ -silylated aryl fluorides are shown to be competent reagents for the arylation of unactivated  $\text{sp}^3$  and  $\text{sp}^2$  C–H bonds, including the characteristically inert bonds in methane



(Figure 2.4).<sup>14</sup> After a short examination of reaction conditions (29), we found that exposure of fluoride **2.1** to 1 mol% of  $[\text{Ph}_3\text{C}]^+[\text{HCB}_{11}\text{Cl}_{11}]^-$  and 2 mol% of triethylsilane in benzene solvent resulted in the facile formation of biphenyl (**2.13**) in 55% yield, at 30 °C in 1 hour.<sup>15</sup> It is worthy to note that application of Siegel's intramolecular reaction conditions to fluorobenzene (**2.14**) only resulted in trace product (**2.13**), while use of *meta*- and *para*-silylated aryl fluorides **2.15** and **2.16** did not result in product formation.<sup>4</sup>

**Figure 2.4** Intermolecular Reactivity and Importance of  $\beta$ -Silicon Stabilization



With this initial finding in hand, we investigated the scope of this arylation reaction. We were pleased to observe selective C-F functionalization in the presence of weaker carbon-halogen (C-X) bonds, similar to previous reports from Ozerov and co-workers.<sup>16</sup> Specifically,

entries 1 to 4 (**2.17** to **2.20**) in Table **2.1** highlight the fluorophilicity of the silylium-carborane catalyst. In these cases, weaker C–X bonds that have less steric encumbrance than the C–F bond do not undergo ionization. This selectivity stands in stark contrast to many traditional reactions of aryl halides, where reactivity is often inversely proportional to bond dissociation energy.<sup>17</sup> To further investigate this unusual selectivity and to separate  $\beta$ -silicon effects from fluorophilicity, we exposed (2-bromo-6-fluorophenyl)trimethylsilane (Table **2.1**, entry 5) to our reaction conditions. Remarkably, *m*-bromobiphenyl (**2.21**) was formed in good yield, supporting our claim of halide selectivity. In general, halide substitution was well tolerated.

**Table 2.1** Arene Scope Table<sup>a</sup>

Reaction scheme:  $\text{R}^1\text{-C}_6\text{H}_4\text{-F-TMS} + \text{H-Ar} \xrightarrow[30-70\text{ }^\circ\text{C, 0.2-48 h}]{[\text{Ph}_3\text{C}]^+[\text{HCB}_{11}\text{Cl}_{11}]^- (2\text{ mol}\%), \text{Et}_3\text{SiH} (4\text{ mol}\%)}$   $\text{R}^1\text{-C}_6\text{H}_4\text{-Ar}$

Entry 1	Entry 2	Entry 3	Entry 4	Entry 5	Entry 6
<b>2.17</b> 56% yield <sup>a</sup>	<b>2.18</b> 71% yield <sup>b</sup>	<b>2.19</b> 47% yield <sup>a</sup>	<b>2.20</b> 52% yield <sup>a</sup>	<b>2.21</b> 77% yield <sup>a</sup>	<b>2.22</b> 49% yield <sup>c</sup>
Entry 7	Entry 8	Entry 9	Entry 10	Entry 11	Entry 12
<b>2.23</b> 63% yield <sup>a</sup>	<b>2.24</b> 45% yield <sup>a</sup>	<b>2.25</b> 47% yield <sup>c</sup>	<b>2.26</b> 99% yield <sup>b</sup>	<b>2.27</b> 36% yield <sup>a</sup>	<b>2.28</b> 29% yield <sup>c</sup> (from OTBS)

<sup>a</sup>Reactions performed at 0.1 M fluoroarene in benzene solvent. <sup>b</sup>Yield determined by gas chromatography–flame ionization detector (GC-FID) using nonane as an internal standard. <sup>c</sup>Yield determined by NMR using an internal standard. <sup>d</sup>Isolated yield.

Polycyclic aromatic fluorides (Table **2.1**, entry 6) were competent under the reaction conditions, as demonstrated by the formation of 1-phenylnaphthalene (**2.22**) in 49% yield. Additionally, aryl and alkyl substitution (**2.23–2.26**) were tolerated under the reaction conditions,

providing phenylated aromatics in moderate to excellent yields (45 to 99%). Consecutive arylation of difluorides was also possible, as demonstrated by the formation of *o*-terphenyl (**2.27**), albeit in a diminished 36% yield. Finally, the presence of heteroatom donor substituents, typically incompatible with silylium catalysis, provides 29% yield of the desired phenol derivative (**2.28**). In cases where the yields were moderate, we observed several byproducts, including fluoroarenes resulting from protodesilylation of the starting material (presumably from highly acidic arenium intermediates) as well as products resulting from a second arylation event.

Throughout our scope studies, some general reactivity trends were apparent. Positional selectivity was preserved in all cases, including those with lower yields. Halide substituents required higher reaction temperatures, whereas alkyl and aryl substituents allowed faster, lower temperature arylation. These observations are consistent with the intermediacy of a cationic aryl species.

Bolstered by these results, we began our investigation into the arylation of alkanes. After optimization of reaction conditions,<sup>18</sup> we found that cyclohexane could be phenylated by aryl fluoride **2.1** in 41% yield (**2.29**). We were surprised to find that this alkane arylation reaction proceeded at 60 °C in two hours. Likewise, cyclopentane underwent smooth arylation under similar conditions in 54% yield (**2.30**). Cycloheptane could also be arylated in 40% yield (**2.31**). With these results in hand, we set out to investigate reactivity with acyclic alkanes. We were pleased to find that *n*-hexane undergoes arylation to yield all three phenylhexane isomers in 40% overall yield (**2.32**). Notably, this C–H arylation reaction displays terminal selectivity, with an  $\alpha:\beta:\gamma$  ratio of 5:2:1. In a similar fashion, *n*-pentane also undergoes terminal selective arylation to yield phenylpentane isomers in 42% yield with a 10:3:1 ratio (**2.33**). In an earlier report, direct

and terminal-selective arylation of saturated hydrocarbons required zeolite catalysts at >200 °C and delivered <5% yield.<sup>19</sup>

**Table 2.2** Arylation Scope of Alkanes<sup>a</sup> and Methane<sup>b</sup>

Entry	Alkane	Temp. (°C)	Time (hr)	Product	Yield (%)
1		60	2		41 <sup>c</sup>
2		70	1		54 <sup>d</sup>
3		100	9		40 <sup>d,e</sup>
4		60	8		40 <sup>c</sup> α:β:γ 26:9:5
5		60	8		42 <sup>c</sup> α:β:γ 30:10:2

---

<sup>a</sup>Reactions performed at 0.05 M fluoroarene in alkane solvent. <sup>b</sup>Reactions performed at 0.1 M fluoroarene in C<sub>6</sub>F<sub>6</sub> solvent. <sup>c</sup>Yield determined by GC-FID using nonane as an internal standard. <sup>d</sup>Yield determined by NMR using an internal standard. <sup>e</sup>Reaction was performed in the absence of *o*-dichlorobenzene.

The terminal C–H bonds of alkanes, although kinetically more accessible, have higher bond dissociation energies (98 kcal/mol) than their internal counterparts (93 to 95 kcal/mol).<sup>20</sup>

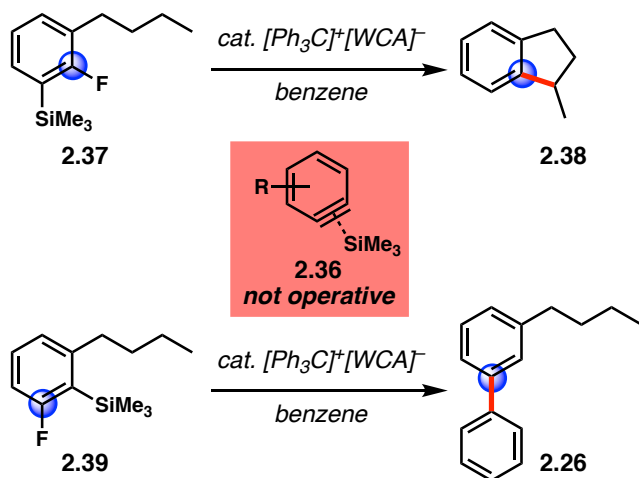
Given our ability to arylate the strongest of C–H bonds (Table 2.2, entries 4 and 5), and the longstanding interest in hydrocarbon gas functionalization, we became intrigued by the prospect of arylating methane gas (C–H bond dissociation energy ~105 kcal/mol).<sup>17,21</sup> Initial experiments were thwarted by deleterious arylation of solvent. After optimization, we found that use of C<sub>6</sub>F<sub>6</sub> solvent allowed for the arylation of methane in 32% yield at low temperatures (60 °C) and synthetically relevant pressures (35 bar).<sup>22</sup> The conversion of naphthalene **2.34** to 1-methylnaphthalene (**2.35**) serves as a rare example of methane gas functionalization using main group catalysis.<sup>23</sup>

## 2.5 Mechanistic Studies on the C–H Insertion of Aryl Cations

Several experiments were performed to probe the nature of the reactive intermediate. Arynes, as well as their transition metal complexes, have been shown to undergo C–H insertion reactions,<sup>24</sup> however, intermolecular insertion into sp<sup>3</sup> C–H bonds has not been reported.<sup>25</sup> The different products observed in certain Table 2.1, entries 1 vs. 2, which would presumably go through an identical aryne intermediate (**2.36**), suggest that an aryne intermediate is not active. Instead, these entries suggest that an electrophilic site is localized to the C–F bond carbon. As a further means of investigation, we prepared butyl derivative **2.37**. The intermediacy of aryne **2.36** (R = butyl) would lead to the formation of biaryl **2.26** from both fluorides **2.37** and **2.39**. However, unlike the arylation reactivity observed in Table 2.1, 3-butyl-biphenyl (**2.26**) was not observed in the reaction of butyl derivative **2.37** (Figure 2.5). Instead, we observed rapid intramolecular C–H insertion to form 1-methylindane (**2.38**) in 35% yield. These observations do not rule out an unsymmetrical silylium-dicarbene species analogous to the silver complex

proposed by Lee and coworkers.<sup>24</sup> However, it is clear that the reactive intermediate is not an aryne, as C–C bond formation occurs at the C–F carbon exclusively.

**Figure 2.5** Investigation of Aryl Cation Intermediate Through Mechanistic Probe Substrates



To investigate the nature of the key C–H insertion event, we carried out isotopic labeling studies. Our first experiments involved the use of benzene- $\text{d}_6$  in hopes to track the movement of deuterium in our products. As seen in Figure 2.6, our reactions performed in deuterated arene solvent provided an intractable mixture of  $\text{D}_0$  to  $\text{D}_{12}$  biphenyl products (**2.41**). We believe that the high concentration of acidic arenium **2.42** in arene solvent prevents quantitative assessment of our isotopic labeling studies. To circumvent this issue, we moved to our alkane arylation conditions. Using cyclohexane- $\text{d}_{12}$ , we observed formation of phenylcyclohexane- $\text{d}_{12}$  (**2.43**) with an overall D-incorporation of 80% (Figure 2.7). While deuterium was incorporated primarily at the *ortho*-position, enrichment of the *meta*- and *para*-positions was also observed. Here, we attribute the mixture of  $\text{D}_{12}$  isomers to rapid hydride shifts of Wheland intermediate **2.11** (Figure 2.3).<sup>26</sup> However, the lack of apparent deuterium crossover (i.e. presence of  $\text{D}_{12\pm n}$  products), supports a concerted C–H insertion process. Furthermore, a competition experiment using a 1:1

mixture of  $C_6D_{12}$  and  $C_6H_{12}$  provided a kinetic isotope effect (KIE) of 1.08 (Figure 2.7). This intermolecular competition experiment rules out C–H insertion as the rate determining step.<sup>27</sup>

**Figure 2.6** Deuterium Labeling Studies in Arene Solvent

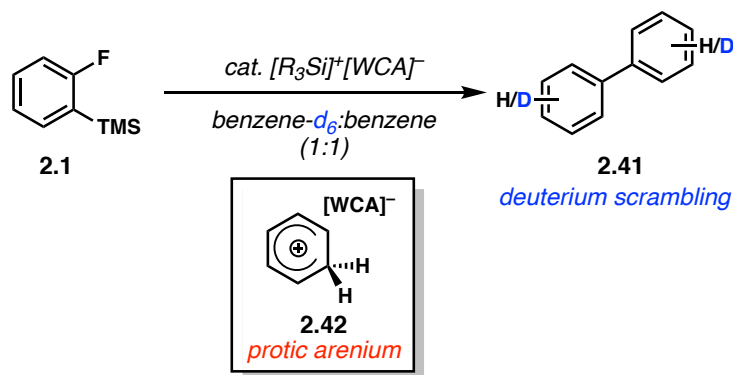
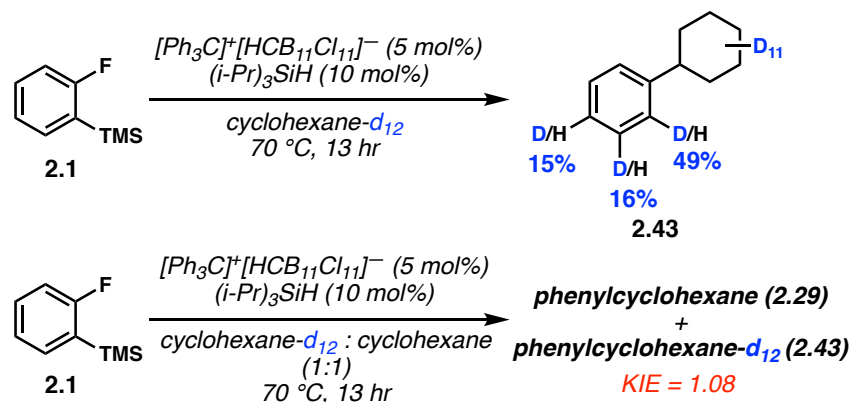


**Figure 2.7** Deuterium Labeling Studies in Alkane Solvent



## 2.6 Conclusion

In closing, we have developed methodology to generate aryl cation equivalents that engage in the catalytic, intermolecular C–H arylation of arenes and alkanes using main group catalysis. This development is enabled through reagent design, wherein  $\beta$ -silicon substitution allows for facile C–F bond activation and catalyst turnover. Furthermore, the hyper-fluorophilicity of the silylium catalyst mediates selective functionalization of C–F bonds in the presence of weaker C–X bonds. This selectivity trend is complementary to transition metal-

catalyzed cross-coupling reactions and traditional nucleophilic substitution reactions. More fundamentally, this work represents an exciting paradigm in catalysis, where strong bonds (C–F and C–H) are directly engaged in C–C bond forming cross-coupling reactions.

## 2.7 Experimental Section

### 2.7.1 Materials and Methods

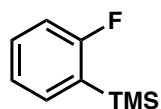
Unless otherwise stated, all reactions were performed in an MBraun glovebox under nitrogen atmosphere with < 0.5 ppm O<sub>2</sub> levels. All glassware and stir-bars were dried in a 160 °C oven for at least 12 hours and allowed to cool *in vacuo* before use. All liquid substrates were either dried over CaH<sub>2</sub> or filtered through dry neutral aluminum oxide. Solid substrates were dried over P<sub>2</sub>O<sub>5</sub>. All solvents were rigorously dried before use. Benzene, *o*-dichlorobenzene, and toluene were degassed and dried in a JC Meyer solvent system and stored inside a glovebox. Cyclohexane (Sigma-Aldrich), fluorobenzene (Sigma-Aldrich), and *n*-hexane (Oakwood) were distilled over potassium. Chlorobenzene (Fisher Scientific), cycloheptane (Alfa Aesar) and *o*-difluorobenzene (Oakwood) were distilled over sodium. Cyclopentane (Matheson Cole and Bell) was filtered through dry neutral aluminum oxide. Pentane (Sigma-Aldrich) was distilled over sodium-potassium alloy. Hexafluorobenzene (Oakwood) was dried over CaH<sub>2</sub> and stored in a glovebox. All solvents were stored over 4 Å molecular sieves. Triethylsilane (Oakwood) and triisopropylsilane (AK Scientific) were dried over CaH<sub>2</sub> and stored inside a glovebox over 4 Å molecular sieves. *Closo*-carborane, [Ph<sub>3</sub>C]<sup>+</sup>[HCB<sub>11</sub>Cl<sub>11</sub>]<sup>-</sup>, were prepared according to literature procedure.<sup>3</sup> Preparatory thin layer chromatography (TLC) was performed using Millipore silica gel 60 F<sub>254</sub> pre-coated plates (0.25 mm) and visualized by UV fluorescence quenching. SiliaFlash P60 silica gel (230–400 mesh) was used for flash chromatography. NMR spectra were recorded



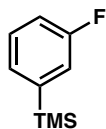
on a Bruker AV-300 ( $^1\text{H}$ ,  $^{19}\text{F}$ ), Bruker AV-400 ( $^1\text{H}$ ,  $^{13}\text{C}$ ,  $^{19}\text{F}$ ), Bruker DRX-500 ( $^1\text{H}$ ), and Bruker AV-500 ( $^1\text{H}$ ,  $^{13}\text{C}$ ).  $^1\text{H}$  NMR spectra are reported relative to  $\text{CDCl}_3$  (7.26 ppm) and  $\text{CD}_2\text{Cl}_2$  (5.32 ppm). Data for  $^1\text{H}$  NMR spectra are as follows: chemical shift (ppm), multiplicity, coupling constant (Hz), integration. Multiplicities are as follows: s = singlet, d = doublet, t = triplet, dd = doublet of doublet, dt = doublet of triplet, ddd = doublet of doublet of doublet, td = triplet of doublet, m = multiplet.  $^{13}\text{C}$  NMR spectra are reported relative to  $\text{CDCl}_3$  (77.0 ppm). GC spectra were recorded on an Agilent 6850 series GC using an Agilent HP-1 (50 m, 0.32 mm ID, 0.25 mm DF) column. GCMS spectra were recorded on a Shimadzu GCMS-QP2010 using a Restek XTI-5 (50 m, 0.25 mm ID, 0.25 mm DF) column. Reactions incorporating methane gas were conducted using a Parr Model 5000 Multiple Reactor system. The system was operated *via* a 4871 process controller and SpecView version 2.5 software. All pressures were reported from the SpecView interface at room temperature. IR Spectra were recorded on a Perkin Elmer 100 spectrometer and are reported in terms of absorption frequency ( $\text{cm}^{-1}$ ). High-resolution mass spectra (HR-MS) were recorded on a Waters (Micromass) GCT Premier spectrometer and are reported as follows: m/z (% relative intensity).

### 2.7.2 Preparation of Aryl Fluoride Substrates

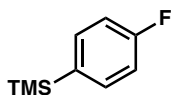
*Note: Experimental information for substrates found in Table 2.1*



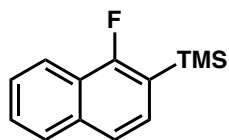
**(2-fluorophenyl)trimethylsilane (2.1)**. Synthesized from fluorobenzene according to reported literature. NMR spectra match those reported in literature.<sup>28</sup>



**(3-fluorophenyl)trimethylsilane (2.15).** Synthesized from 1-bromo-3-fluorobenzene according to reported literature. NMR spectra match those reported in literature.<sup>29</sup>



**(4-fluorophenyl)trimethylsilane (2.16).** Synthesized from 1-bromo-4-fluorobenzene according to reported literature. NMR spectra match those reported in literature.<sup>30</sup>



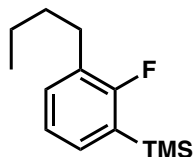
**(1-fluoronaphthalen-2-yl)trimethylsilane (2.34).** To a  $-70$  °C solution of 1.32 M *s*-BuLi in cyclohexane (11.7 mL, 15.5 mmol), hexanes (12 mL), and THF (30 mL), was added 1-fluoronaphthalene (2.26 g, 15.5 mmol). After 2 hours, TMSCl (1.96 mL, 15.5 mmol) was added to the solution and allowed to warm up to room temperature overnight. The reaction mixture was quenched with saturated aqueous ammonium chloride (50 mL) and the aqueous layer extracted with Et<sub>2</sub>O (3 x 50 mL). Combined organics were dried over MgSO<sub>4</sub> and concentrated by rotary evaporation. Crude product was purified by flash column chromatography (pentane) to yield 2.45 g (73%) of colorless oil.

<sup>1</sup>H NMR (400 MHz, CDCl<sub>3</sub>)  $\delta$  8.25–8.20 (m, 1H), 7.91 (ddd,  $J = 4.9, 3.6, 2.0$  Hz, 1H), 7.70 (dd,  $J = 8.2, 0.8$  Hz, 1H), 7.64–7.58 (m, 2H), 7.55 (dd,  $J = 8.2, 5.3$  Hz, 1H), 0.54 (d,  $J = 1.1$  Hz, 9H);  
<sup>13</sup>C NMR (100 MHz, CDCl<sub>3</sub>)  $\delta$  163.4 (d,  $^1J_{C-F} = 246.7$  Hz), 135.8 (d,  $^4J_{C-F} = 5.0$  Hz), 130.0 (d,  $^3J_{C-F} = 12.7$  Hz), 127.3 (d,  $^4J_{C-F} = 3.4$  Hz), 127.0, 126.1 (d,  $^4J_{C-F} = 1.7$  Hz), 123.3 (d,  $^3J_{C-F} = 20.6$

Hz), 123.1 (d,  $^4J_{C-F} = 3.7$  Hz), 120.7 (d,  $^3J_{C-F} = 5.4$  Hz), 119.3 (d,  $^2J_{C-F} = 29.8$  Hz),  $-0.8$  (d,  $^4J_{C-F} = 1.8$  Hz);  $^{19}\text{F}\{^1\text{H}\}$  NMR (376 MHz,  $\text{CDCl}_3$ )  $\delta -109.82$ .

FTIR (Neat Film NaCl): 3054, 2956, 2899, 1633, 1497, 1356, 1339, 1249, 1057, 863, 828, 809,  $756\text{ cm}^{-1}$ .

HR-MS (GC-Cl): Calculated for  $\text{C}_{13}\text{H}_{15}\text{FSi}$ : 218.0927; measured: 218.0920.

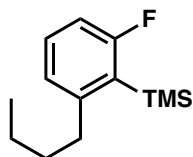


**(3-butyl-2-fluorophenyl)trimethylsilane (2.37).** To a flame dried 500 mL Schlenk flask was added *n*-butylboronic acid (6.60 g, 64.7 mmol), potassium carbonate (13.4 g, 97.1 mmol), and [1,1'-Bis(diphenylphosphino)ferrocene]palladium(II) dichloride (1.50 g, 2.05 mmol). The system was evacuated and back-filled with nitrogen three times before addition of 1,4-dioxane (degassed, 320 mL) and (3-bromo-2-fluorophenyl)trimethylsilane (8.00 g, 32.4 mmol). The reaction was sealed with a glass stopper and heated to  $110\text{ }^\circ\text{C}$  for 48 hours. After cooling to room temperature, the reaction was diluted with 300 mL of water and extracted with  $\text{Et}_2\text{O}$  (3 x 300 mL). Combined organics were dried over  $\text{MgSO}_4$  and concentrated by rotary evaporation. Crude product was purified by flash column chromatography (hexanes) to yield 711 mg (10%) of colorless oil.

$^1\text{H}$  NMR (300 MHz,  $\text{CDCl}_3$ )  $\delta$  7.25–7.15 (m, 2H), 7.04 (t,  $J = 7.3$  Hz, 1H), 2.66–2.58 (m, 2H), 1.66–1.55 (m, 2H), 1.46–1.30 (m, 2H), 0.94 (t,  $J = 7.3$  Hz, 3H), 0.31 (d,  $J = 1.0$  Hz, 9H);  $^{13}\text{C}$  NMR (100 MHz,  $\text{CDCl}_3$ )  $\delta$  165.6 (d,  $^1J_{C-F} = 239.8$  Hz), 132.5 (d,  $^3J_{C-F} = 11.8$  Hz), 131.9 (d,  $^3J_{C-F} = 5.7$  Hz), 128.8 (d,  $^2J_{C-F} = 20.1$  Hz), 125.7 (d,  $^2J_{C-F} = 32.1$  Hz), 123.6 (d,  $^4J_{C-F} = 3.3$  Hz), 32.4, 28.9 (d,  $^3J_{C-F} = 2.4$  Hz), 22.6, 13.9,  $-0.9$  (d,  $^4J_{C-F} = 1.6$  Hz);  $^{19}\text{F}\{^1\text{H}\}$  NMR (282 MHz,  $\text{CDCl}_3$ )  $\delta -106.47$ .

FTIR (Neat Film NaCl): 3058, 2957, 2932, 2882, 1605, 1571, 1423, 1249, 837, 759  $\text{cm}^{-1}$ .

HR-MS (GC-CI): Calculated for  $\text{C}_{13}\text{H}_{21}\text{FSi}$ : 224.1397; measured: 224.1395.



**(2-butyl-6-fluorophenyl)trimethylsilane (2.39).** To a flame dried 100 mL schlenk flask was added *n*-butylboronic acid (697 mg, 6.84 mmol), potassium carbonate (1.42 g, 10.3 mmol), and [1,1'-Bis(diphenylphosphino)ferrocene]palladium(II) dichloride (250 mg, 0.342 mmol). The system was evacuated and back-filled with nitrogen three times before addition of 1,4-dioxane (degassed, 32 mL) and (2-bromo-6-fluorophenyl)trimethylsilane (845 mg, 3.42 mmol). The reaction was sealed with a glass stopper and heated to 110 °C for 48 hours. After cooling to room temperature, the reaction was diluted with 30 mL of water and extracted with  $\text{Et}_2\text{O}$  (3 x 50 mL). Combined organics were dried over  $\text{MgSO}_4$  and concentrated by rotary evaporation. Crude product was purified by flash column chromatography (hexanes) to yield 526 mg (69%) of colorless oil after heating *in vacuo* (0.2 Torr) at 35 °C.

$^1\text{H}$  NMR (400 MHz,  $\text{CDCl}_3$ )  $\delta$  7.30–7.21 (m, 1H), 6.98 (dd,  $J = 7.5, 1.1$  Hz, 1H), 6.82 (ddd,  $J = 9.5, 8.2, 1.1$  Hz, 1H), 2.75–2.69 (m, 3H), 1.62–1.51 (m, 2H), 1.48–1.37 (m, 2H), 0.97 (t,  $J = 7.3$  Hz, 3H), 0.41 (d,  $J = 2.3$  Hz, 9H);  $^{13}\text{C}$  NMR (100 MHz,  $\text{CDCl}_3$ )  $\delta$  167.8 (d,  $^1J_{\text{C-F}} = 239.6$  Hz), 150.9 (d,  $^3J_{\text{C-F}} = 9.6$  Hz), 130.6 (d,  $^3J_{\text{C-F}} = 9.9$  Hz), 125.1 (d,  $^4J_{\text{C-F}} = 2.4$  Hz), 124.0 (d,  $^2J_{\text{C-F}} = 26.5$  Hz), 112.2 (d,  $^2J_{\text{C-F}} = 28.1$  Hz), 36.0, 35.4, 22.7, 14.1, 1.8 (d,  $^4J_{\text{C-F}} = 4.3$  Hz);  $^{19}\text{F}\{^1\text{H}\}$  NMR (376 MHz,  $\text{CDCl}_3$ )  $\delta$  -96.20.

FTIR (Neat Film NaCl): 3059, 2957, 2931, 2873, 1602, 1559, 1449, 1223, 839  $\text{cm}^{-1}$ .

HR-MS (GC-CI): Calculated for  $\text{C}_{13}\text{H}_{21}\text{FSi}$ : 224.1397; measured: 224.1399.

### 2.7.3 General Procedure for Yield Calculations by GC

*Outlined below is our general procedure for the calculation of product yields by GC–FID.*

Calibration curves were made by first preparing 5:1, 3:1, 1:1, 1:3, and 1:5 molar ratio solutions of nonane to product. GC analysis of the chromatogram integrations was plotted on Microsoft Excel to form a linear calibration curve line. All curves were tested to be within  $\leq 7\%$  error. For analysis of reactions, nonane (1 equiv) was added to the reaction mixture after completion. Aliquots were then diluted in hexanes, quenched with a saturated aqueous sodium bicarbonate solution, and the organic layer was filtered through a kimwipe. Yields were then calculated by comparing the integration ratios of nonane to the product against their respective calibration curves.

### 2.7.4 Optimization Table for Aryl Insertion Reaction

In our studies, we optimized our reaction conditions for anion, silane, concentration, and temperature using aryl fluoride **2.1** in benzene. Herein, we summarize our key observations.

**Table 2.3** Optimization of (2-fluorophenyl)trimethylsilane Substrate in Benzene.

Anion	% Cat. Loading	Conc.	Silane	Temperature	Yield
[HCB <sub>11</sub> H <sub>5</sub> Cl <sub>6</sub> ]	5 mol%	0.1 M	iPr <sub>3</sub> SiH (10 mol%)	70 °C	41%
[HCB <sub>11</sub> H <sub>5</sub> Br <sub>6</sub> ]	5 mol%	0.1 M	Et <sub>3</sub> SiH (10 mol%)	70 °C	0%
[HCB <sub>11</sub> Me <sub>5</sub> Br <sub>6</sub> ]	5 mol%	0.1 M	Et <sub>3</sub> SiH (10 mol%)	70 °C	0%
[HCB <sub>11</sub> Cl <sub>11</sub> ]	1 mol%	0.02 M	Et <sub>3</sub> SiH (2 mol%)	30 °C	55%
[HCB <sub>11</sub> Cl <sub>11</sub> ]	2 mol%	0.1 M	Et <sub>3</sub> SiH (4 mol%)	30 °C	49%
[HCB <sub>11</sub> Br <sub>11</sub> ]	5 mol%	0.1 M	Et <sub>3</sub> SiH (10 mol%)	30 °C	31%
[(C <sub>6</sub> F <sub>5</sub> ) <sub>4</sub> B]	5 mol%	0.1 M	Et <sub>3</sub> SiH (10 mol%)	30 °C	27%

## 2.7.5 Initial Investigation of Aryl Fluorides

Outlined below are our initial experiments evaluating the reactivity of aryl fluorides in both the presence and absence of the trimethylsilyl group. We also conducted control experiments using a previously reported silylium-catalyzed C–F functionalization method.<sup>4</sup> Our experiments below support the need for an *ortho*-trimethylsilyl group for our catalytic system.

### 2.7.5.1 Fluorobenzene Control

*Described below is the application of fluorobenzene using our optimized conditions.*

$[\text{Ph}_3\text{C}]^+[\text{HCB}_{11}\text{Cl}_{11}]^-$  (0.8 mg, 1.1  $\mu\text{mol}$ , 0.02 equiv) and triethylsilane (0.5  $\mu\text{L}$ , 2.2  $\mu\text{mol}$ , 0.04 equiv) were stirred in benzene (3 mL) to form a colorless solution (0.02 M) before the addition of fluorobenzene (9.5  $\mu\text{L}$ , 0.054 mmol, 1 equiv). Reaction was stirred at 30 °C. After 5 days, GC-FID showed formation of biphenyl. Addition of nonane (9.7  $\mu\text{L}$ , 0.054 mmol, 1 equiv) as an internal standard showed < 5% yield of biphenyl (Figure 2.9).

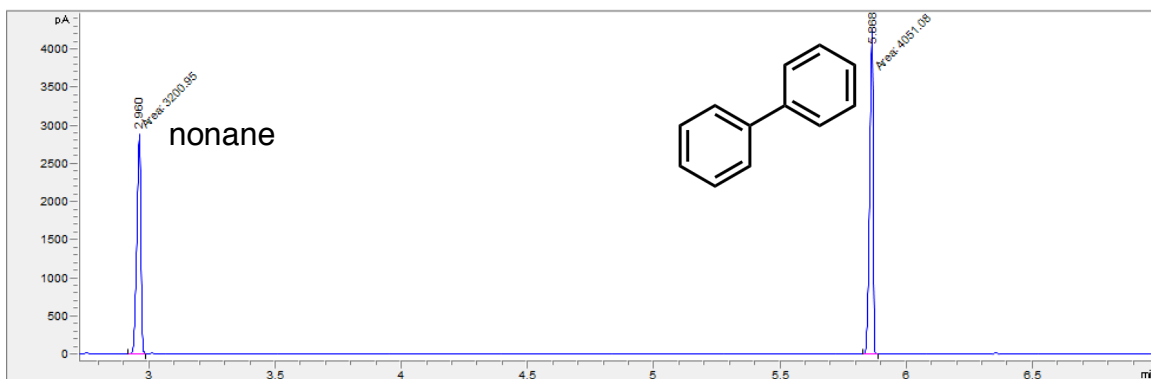


**Figure 2.8** GC Trace for Internal Standard *Nonane* and Biphenyl in 1:1 Ratio.

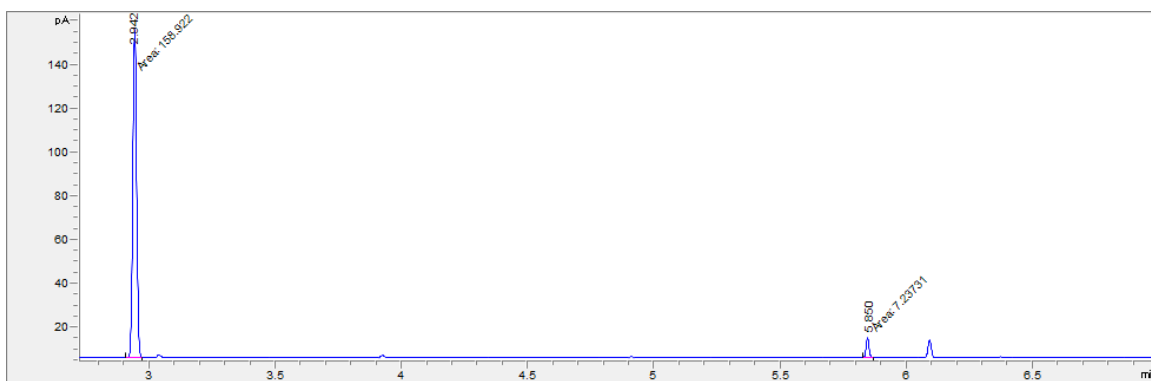


**Figure 2.9** GC Trace for Internal Standard *Nonane* in Fluorobenzene Control Reaction Showing Formation of Biphenyl in < 5% Yield.

### 2.7.5.2 Application of Conditions from Reference 4

*Described below is the application of fluorobenzene with a previously reported silylium-catalyzed C–F functionalization for the intermolecular formation of biphenyl.*

Fluorobenzene (9.5  $\mu$ L, 0.1 mmol, 1 equiv), dimethyldimesitylsilane (25.6 mg, 0.09 mmol, 0.9 equiv) and  $[i\text{Pr}_3\text{Si}]^+[\text{HCB}_{11}\text{H}_5\text{Cl}_6]^-$  (5.3 mg, 0.01 mmol, 0.1 equiv) were dissolved in benzene (1 mL). The reaction was then stirred at 30  $^\circ\text{C}$ . After 13 hours, GC-FID spectra showed formation of biphenyl in < 5% yield (Figure 2.10).

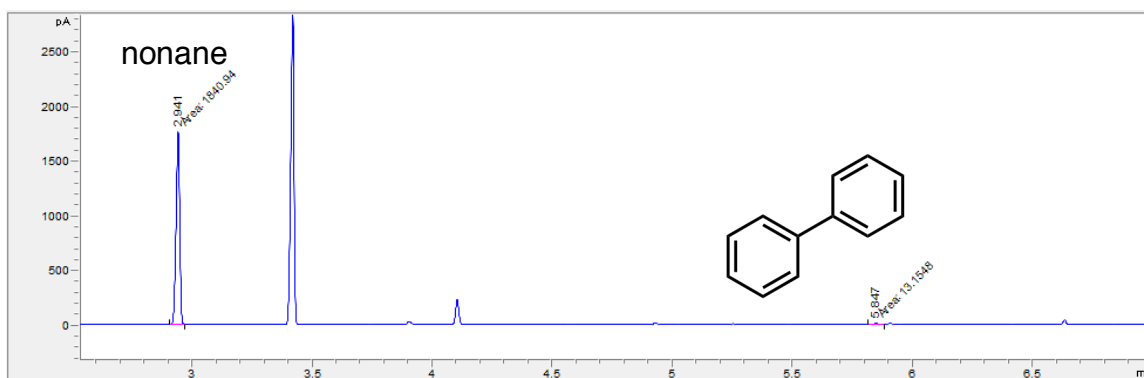


**Figure 2.10** GC Trace for Application of Reference 4 Conditions to Fluorobenzene at 30  $^\circ\text{C}$  Showing Formation of Biphenyl in < 5% Yield.

### 2.7.5.3 Positional Effects of the Silyl Group

Outlined below are a series of experiments probing the reactivity of our substrate in varying the position of the trimethylsilyl group relative to the aryl C–F carbon. The experiments below support the need for a trimethylsilyl group *ortho* to the aryl C–F carbon to generate the desired product in catalytic fashion.

$[\text{Ph}_3\text{C}]^+[\text{HCB}_{11}\text{Cl}_{11}]^-$  (2.5 mg, 3.3  $\mu\text{mol}$ ) and triethylsilane (1  $\mu\text{L}$ , 6.6  $\mu\text{mol}$ ,) were stirred in benzene (1.5 mL) to form a colorless solution. This solution was partitioned equally into three separate vials before aryl fluorides **2.1**, **2.15**, and **2.16** (0.054 mmol) were added in their respective reactions. Reactions were then stirred at 30 °C for 2 hours before addition of nonane (9.7  $\mu\text{L}$ , 0.054 mmol, 1 equiv) as an internal standard. As shown below, no formation of biphenyl was observed when using *meta*- or *para*- trimethylsilyl aryl fluorides (Figure **2.12** and **2.13**). The *ortho*-trimethylsilyl aryl fluoride was the only positional isomer that afforded of biphenyl in 47% yield (Figure **2.14**).

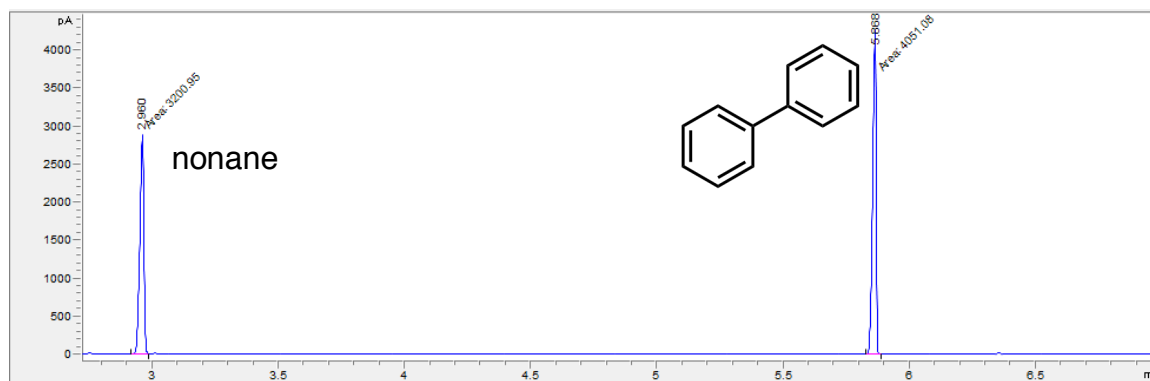


**Figure 2.11** GC Trace for Internal Standard *Nonane* and Biphenyl in 1:1 Ratio.



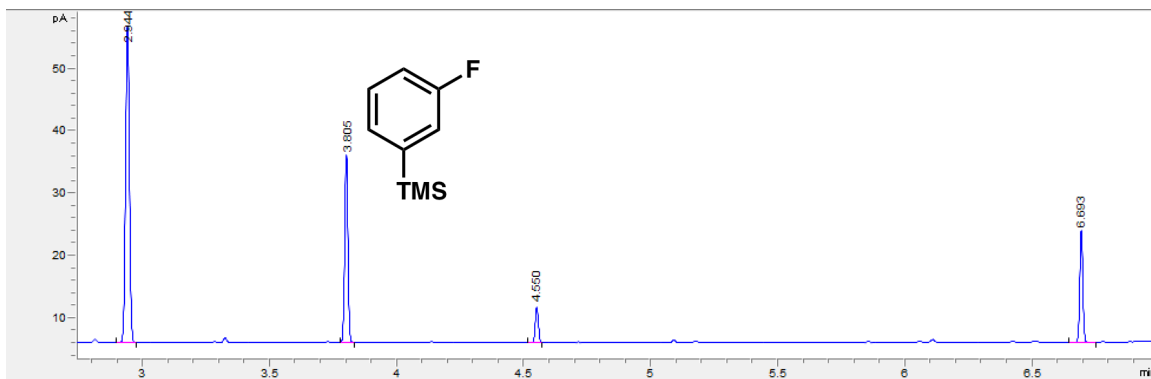


**Figure 2.12** GC Trace for Internal Standard *Nonane* and **2.15** After 2 Hour Reaction Time  
Showing No Formation of Biphenyl.

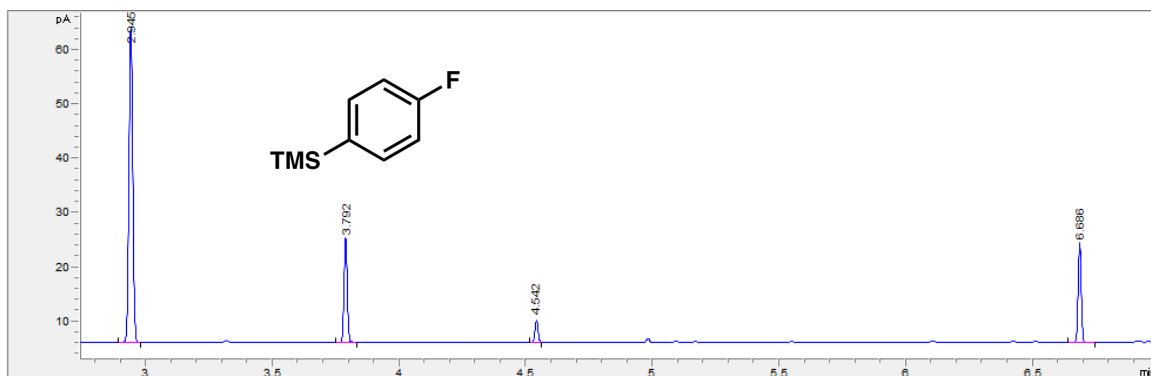


**Figure 2.13** GC Trace for Internal Standard *Nonane* and **2.16** After 2 Hour Reaction Time  
Showing No Formation of Biphenyl.

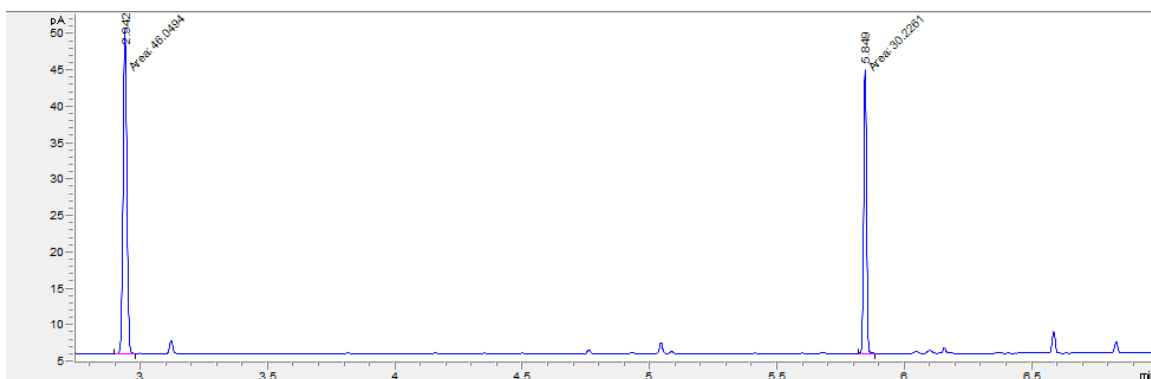
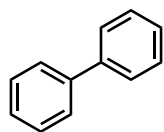


**Figure 2.14** GC Trace for Internal Standard *Nonane* and **2.1** After 2 Hour Reaction Time  
Showing Formation of Biphenyl in 47% Yield

### 2.7.6 General Procedure for Intermolecular Aryl Insertion Reactions

*Described below is the general procedure for the arylation of substituted o-trimethylsilyl aryl fluorides.*

$[\text{Ph}_3\text{C}]^+[\text{HCB}_{11}\text{Cl}_{11}]^-$  (0.8 mg, 1.1  $\mu\text{mol}$ , 0.02 equiv) and triethylsilane (0.5  $\mu\text{L}$ , 2.2  $\mu\text{mol}$ , 0.04 equiv) were stirred in benzene (0.5 mL) to form a colorless solution (0.1 M) before the addition of aryl fluoride substrate (0.054 mmol, 1 equiv). Substrates were stirred between 30–70  $^\circ\text{C}$  for 0.2–9 hours (see individual substrates for reaction conditions). Reactions were monitored by GC-FID spectra. If previously heated, reactions were cooled to room temperature before volatiles were rotary evaporated and purified by flash column or preparatory thin layer chromatography.



**Biphenyl (2.13).** Synthesized according to general procedure 2.6.6 with a modified 1 mol% catalyst loading and 0.02 M concentration. Catalyst loading was achieved by taking 0.55 mL from a freshly prepared stock solution of  $[\text{Ph}_3\text{C}]^+[\text{HCB}_{11}\text{Cl}_{11}]^-$  (1.5 mg) and triethylsilane (0.5  $\mu\text{L}$ ) in benzene (2 mL). Additional benzene was added to reach a total volume of 3 mL before corresponding aryl fluoride (9.1 mg, 0.054 mmol, 1 equiv) was added to the colorless solution of  $[\text{Ph}_3\text{C}]^+[\text{HCB}_{11}\text{Cl}_{11}]^-$  (0.54  $\mu\text{mol}$ , 0.01 equiv) and triethylsilane (1.1  $\mu\text{mol}$ , 0.02 equiv) in benzene. Reaction was stirred at 30  $^\circ\text{C}$  for 1 hour to afford **2.13** in 55% yield (GC) as shown in Figure 2.15.

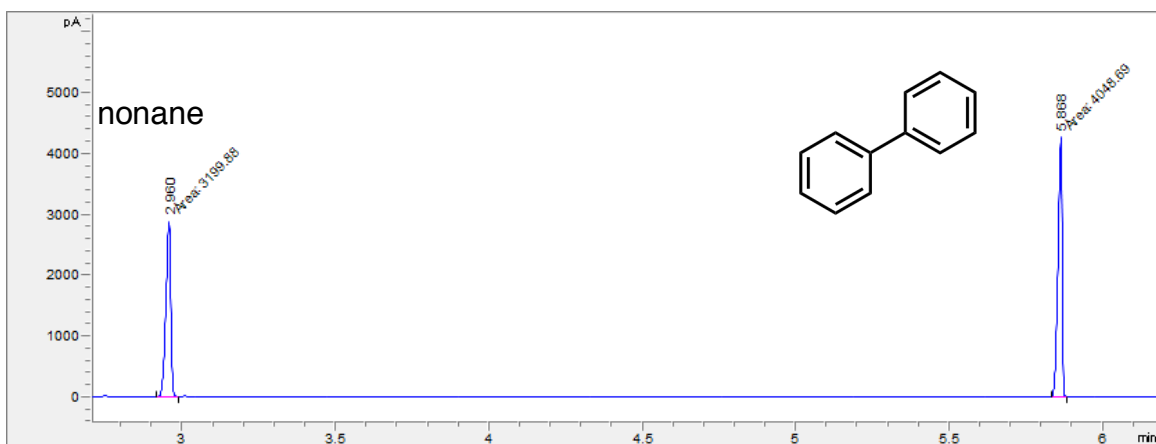


**Figure 2.15** GC Trace for Internal Standard *Nonane* and **2.13** in 1:1 Ratio.

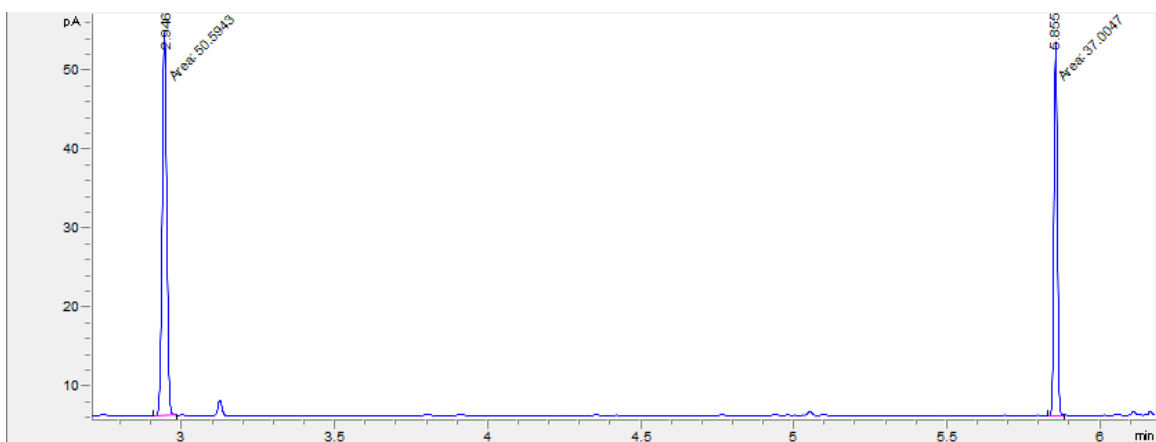
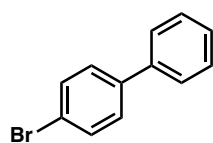


**Figure 2.16** GC Trace for Yield Shown in Figure 2.4 from Manuscript.



**4-bromobiphenyl (2.17)**. Synthesized according to general procedure 2.6.6. Corresponding aryl fluoride (13.4 mg, 0.054 mmol) was added to a colorless solution of  $[\text{Ph}_3\text{C}]^+[\text{HCB}_{11}\text{Cl}_{11}]^-$  (1.1  $\mu\text{mol}$ , 0.02 equiv) and triethylsilane (2.2  $\mu\text{mol}$ , 0.04 equiv), and was stirred at 60 °C for 1 hour to give **2.17** in 56% yield (GC) as shown in Figure 2.18. Crude product was purified by flash column chromatography (hexanes) to give **2.17** as a white solid (5.8 mg, 46%). NMR Spectra match those reported in literature.<sup>31</sup>

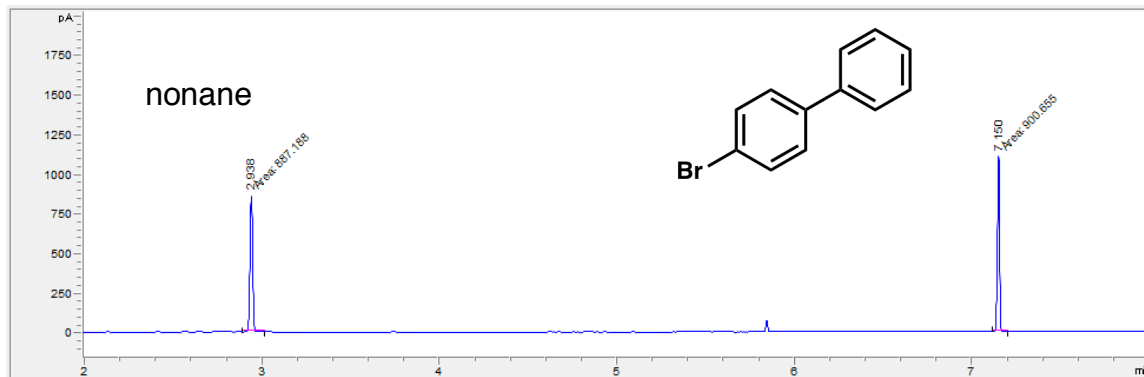


**Figure 2.17** GC Trace for Internal Standard *Nonane* and **2.17** in 1:1 Ratio.

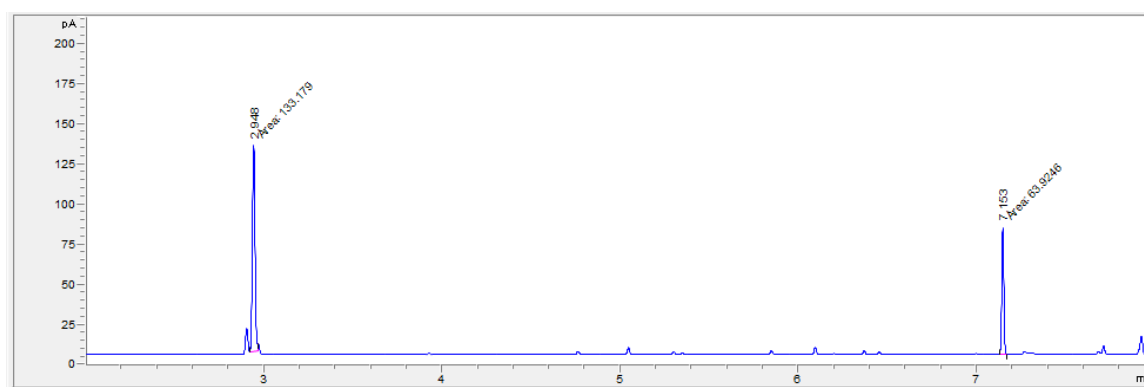
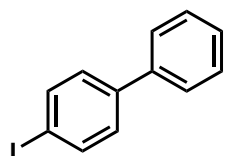
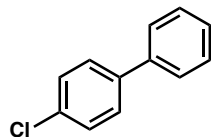


**Figure 2.18** GC Trace Showing Formation of **2.17** in 56% Yield.



**4-iodobiphenyl (2.18)**. Synthesized according to general procedure 2.6.6 Corresponding aryl fluoride (15.9 mg, 0.054 mmol) was added to a colorless solution of  $[\text{Ph}_3\text{C}]^+[\text{HCB}_{11}\text{Cl}_{11}]^-$  (1.1  $\mu\text{mol}$ , 0.02 equiv) and triethylsilane (2.2  $\mu\text{mol}$ , 0.04 equiv) and was stirred at 70 °C for 1 hour to give **2.18** in 71% yield (NMR). Crude product was purified by preparatory thin layer chromatography (hexanes) to give **2.18** as a white solid (7.8 mg, 52%). NMR Spectra match those reported in literature.<sup>32</sup>



**4-chlorobiphenyl (2.19).** Synthesized according to general procedure 2.6.6. Corresponding aryl fluoride (11.0 mg, 0.054 mmol) was added to a colorless solution of  $[\text{Ph}_3\text{C}]^+[\text{HCB}_{11}\text{Cl}_{11}]^-$  (1.1  $\mu\text{mol}$ , 0.02 equiv) and triethylsilane (2.2  $\mu\text{mol}$ , 0.04 equiv), and was stirred at 70 °C for 9 hours to give **2.19** in 47% yield (GC) as shown in Figure 2.20. Crude product was purified by column chromatography (hexanes) to give **2.19** as a white solid (4.1 mg, 40 %). NMR Spectra match those reported in literature.<sup>33</sup>

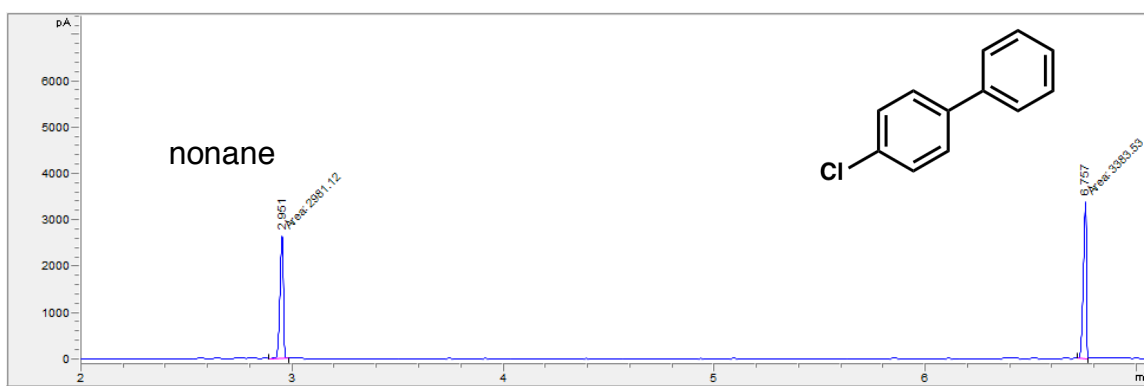


**Figure 2.19** GC Trace for Internal Standard *Nonane* and **2.19** in 1:1 Ratio.

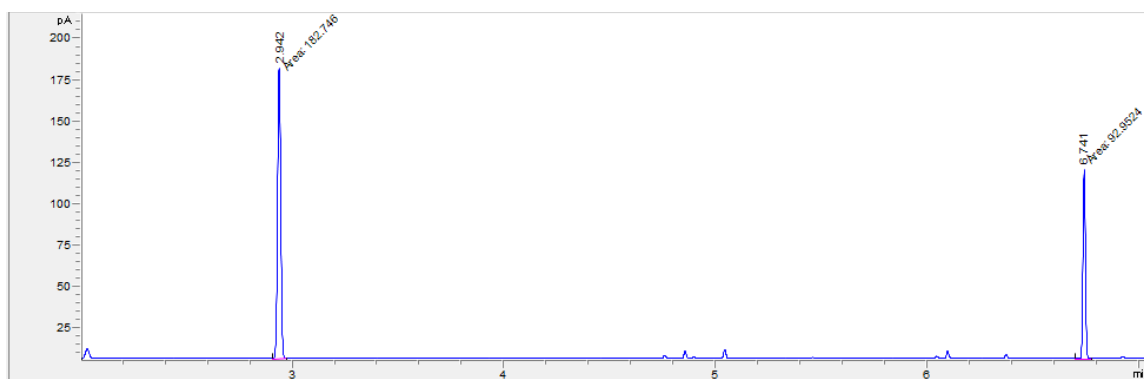
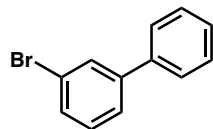


**Figure 2.20** GC Trace Showing Formation of **2.19** in 47% Yield.



**3-bromobiphenyl (2.20 and 2.21).** 3-bromobiphenyl was synthesized from two different substrates according to general procedure 2.6.6.

For Entry 4 in Table **2.1**, corresponding aryl fluoride (13.4 mg, 0.054 mmol) was added to a colorless solution of  $[\text{Ph}_3\text{C}]^+[\text{HCB}_{11}\text{Cl}_{11}]^-$  (1.1  $\mu\text{mol}$ , 0.02 equiv) and triethylsilane (2.2  $\mu\text{mol}$ , 0.04 equiv), and was stirred at 60 °C for 1 hour to give **2.20** in 52% yield (GC) as shown in Figure **2.22**.

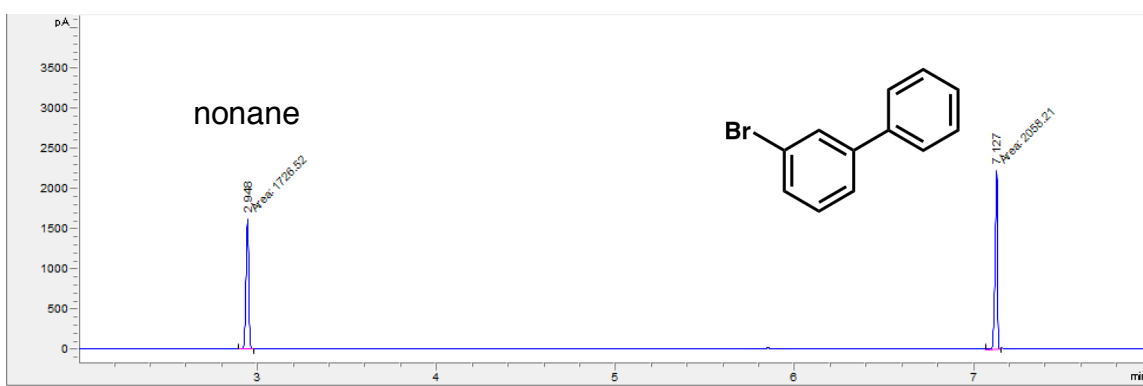


**Figure 2.21** GC Trace for Internal Standard *Nonane* and **2.20** in 1:1 Ratio.

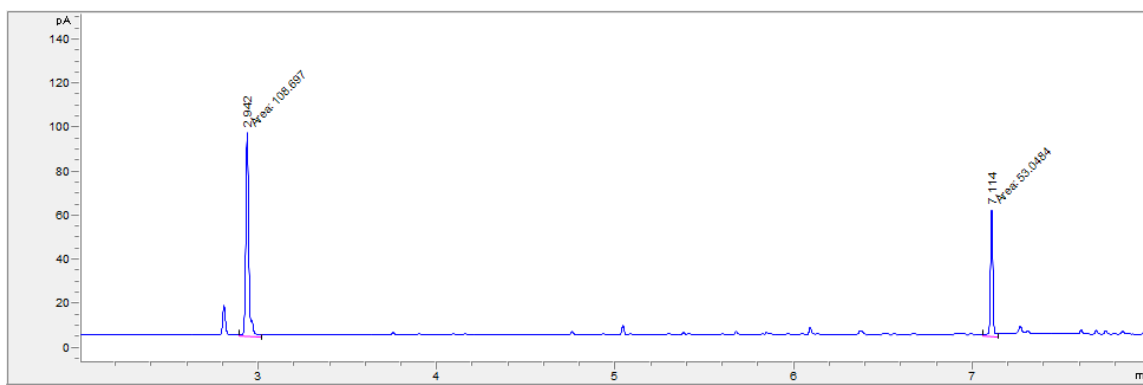


**Figure 2.22** GC Trace Showing Formation of **2.20** in 52% Yield.

For entry 5, Table **2.1**, corresponding aryl fluoride (13.4 mg, 0.054 mmol) was added to a colorless solution of  $[\text{Ph}_3\text{C}]^+[\text{HCB}_{11}\text{Cl}_{11}]^-$  (1.1  $\mu\text{mol}$ , 0.02 equiv) and triethylsilane (2.2  $\mu\text{mol}$ , 0.04 equiv) and was stirred at 60 °C for 1 hour to give **2.21** in 77% yield (GC) as shown in Figure **2.23**. Crude product was purified by preparatory thin layer chromatography (hexanes) to give **2.21** as a white solid (7.4 mg, 59%). NMR Spectra match those reported in literature.<sup>34</sup>

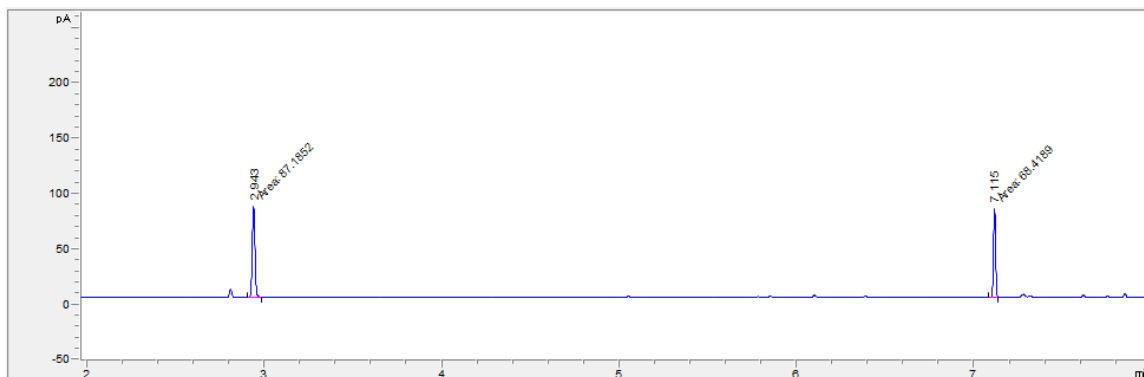
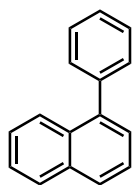
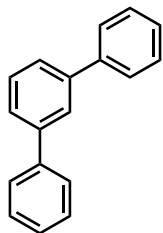


**Figure 2.23** GC Trace Showing Formation of **2.21** in 77% Yield.



**1-phenylnaphthalene (2.22)**. Synthesized according to general procedure 2.6.6. Corresponding aryl fluoride (11.8 mg, 0.054 mmol) was added to a colorless solution of  $[\text{Ph}_3\text{C}]^+[\text{HCB}_{11}\text{Cl}_{11}]^-$  (1.1  $\mu\text{mol}$ , 0.02 equiv) and triethylsilane (2.2  $\mu\text{mol}$ , 0.04 equiv), and was stirred at 30 °C for 1 hour. Crude product was purified by preparatory thin layer chromatography (hexanes) to give **2.22** as a colorless oil (5.4 mg, 49%). NMR Spectra match those reported in literature.<sup>35</sup>



***m*-terphenyl (2.23)**. Synthesized according to general procedure 2.6.6. Corresponding aryl fluoride (13.2 mg, 0.054 mmol) was added to a colorless solution of  $[\text{Ph}_3\text{C}]^+[\text{HCB}_{11}\text{Cl}_{11}]^-$  (1.1  $\mu\text{mol}$ , 0.02 equiv) and triethylsilane (2.2  $\mu\text{mol}$ , 0.04 equiv), and was stirred at 30 °C for 1 hour to give **2.23** in 63% yield (GC) as shown in Figure 2.25. Crude product was purified by flash column chromatography (hexanes) to give **2.23** as a white solid (7.0 mg, 56%). NMR Spectra match those reported in literature.<sup>36</sup>

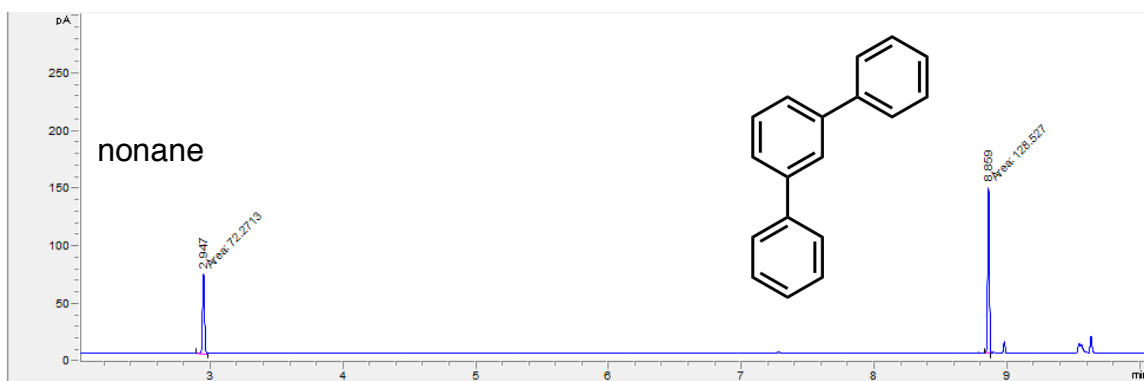


**Figure 2.24** GC Trace for Internal Standard *Nonane* and **2.23** in 1:1 Ratio.

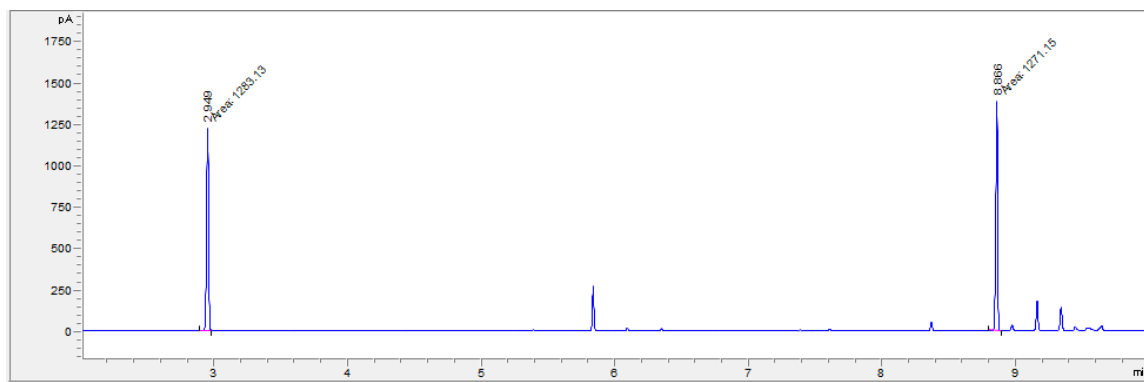
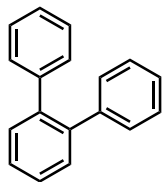


**Figure 2.25** GC Trace Showing Formation of **2.23** in 63% Yield.





***o*-terphenyl (2.24 and 2.27).** *o*-terphenyl was synthesized from two different substrates using general procedure 2.6.6.

For entry 8 in Table 2.1, corresponding aryl fluoride (14.0 mg, 0.054 mmol, 1 equiv) was added to a colorless solution of  $[\text{Ph}_3\text{C}]^+[\text{HCB}_{11}\text{Cl}_{11}]^-$  (1.1  $\mu\text{mol}$ , 0.02 equiv) and triethylsilane (2.2  $\mu\text{mol}$ , 0.04 equiv), and was stirred at 60 °C for 36 hours to give **2.24** in 36% yield (GC) as shown in Figure 2.27.

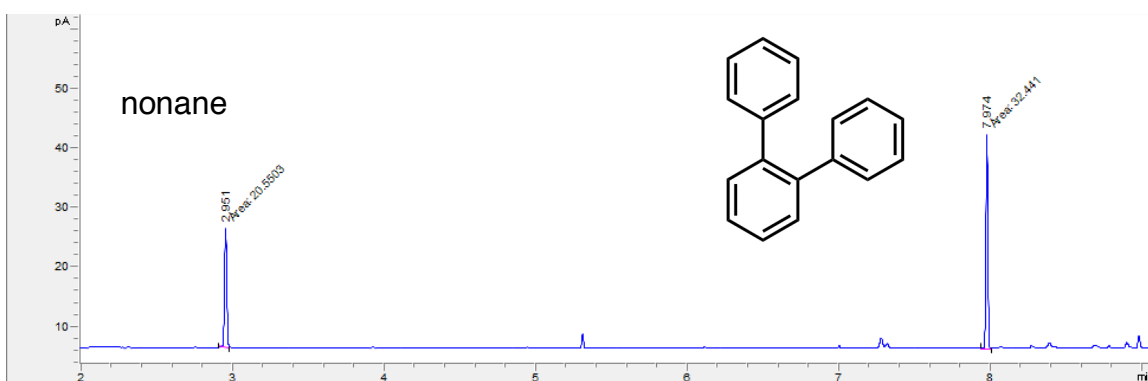


**Figure 2.26** GC Trace for Internal Standard *Nonane* and **2.24** in 1:1 Ratio.

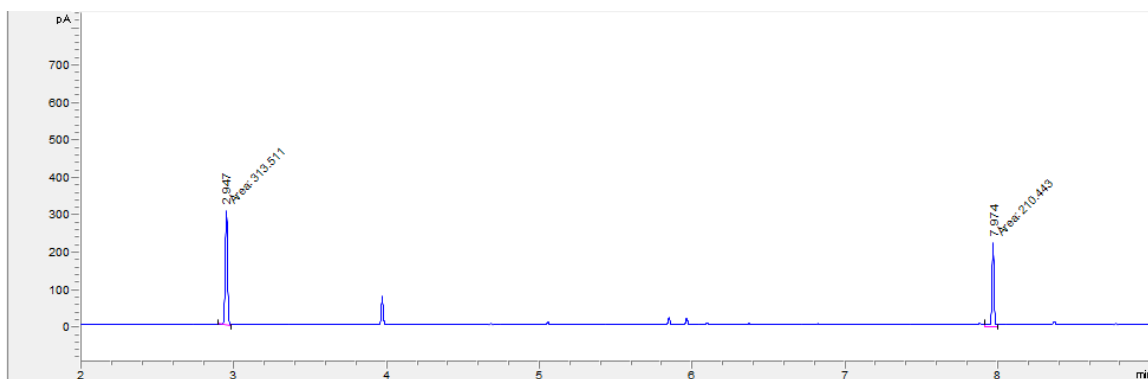


**Figure 2.27** GC Trace Showing Formation of **2.24** in 36% Yield.

For entry 11 in Table 2.1, corresponding aryl fluoride (13.2 mg, 0.054 mmol, 1 equiv) was added to a colorless solution of  $[\text{Ph}_3\text{C}]^+[\text{HCB}_{11}\text{Cl}_{11}]^-$  (1.1  $\mu\text{mol}$ , 0.02 equiv) and triethylsilane (2.2  $\mu\text{mol}$ , 0.04 equiv), and was stirred at 70 °C for 36 hours to give **2.27** in 45% yield (GC) as shown in Figure 2.28. Crude product was purified by flash column chromatography (hexanes) to give **2.27** as a white solid (4.4 mg, 35%). NMR Spectra match those reported in literature.<sup>37</sup>

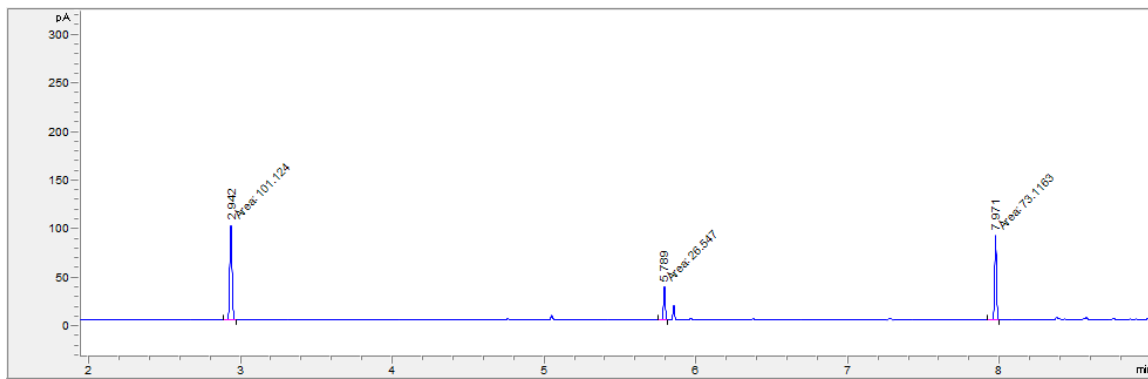
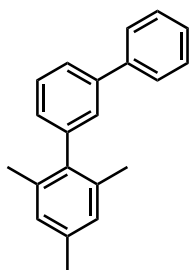


**Figure 2.28** GC Trace Showing Formation of **2.27** in 45% Yield.



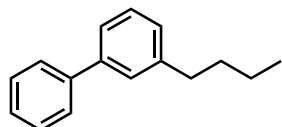
**3-mesitylbiphenyl (2.25).** Synthesized according to general procedure 2.6.6. Corresponding aryl fluoride (15.5 mg, 0.054 mmol) was added to a colorless solution of  $[\text{Ph}_3\text{C}]^+[\text{HCB}_{11}\text{Cl}_{11}]^-$  (1.1  $\mu\text{mol}$ , 0.02 equiv) and triethylsilane (2.2  $\mu\text{mol}$ , 0.04 equiv), and was stirred at 30 °C for 1 hour. Crude product was purified by flash column chromatography (9:1 pentane:dichloromethane) to give **2.25** as a colorless oil (6.9 mg, 47%).

$^1\text{H}$  NMR (400 MHz,  $\text{CDCl}_3$ )  $\delta$  7.66–7.62 (m, 2H), 7.59 (ddd,  $J = 7.8, 1.9, 1.2$  Hz, 1H), 7.52–7.41 (m, 4H), 7.38–7.31 (m, 1H), 7.14 (dt,  $J = 7.5, 1.5$  Hz, 1H), 6.98 (s, 2H), 2.36 (s, 3H), 2.07 (s,

6H);  $^{13}\text{C}$  NMR (125 MHz,  $\text{CDCl}_3$ )  $\delta$  141.5, 141.1, 141.0, 138.9, 136.6, 136.0, 128.8, 128.7, 128.2, 128.1, 128.0, 127.3, 127.1, 125.2, 21.0, 20.8.

FTIR (Neat Film NaCl): 3059, 3030, 2952, 2919, 2867, 1946, 1880, 1803, 1730, 1471, 850, 757  $\text{cm}^{-1}$ .

HR-MS (GC-Cl): Calculated for  $\text{C}_{21}\text{H}_{20}$ : 272.1565; measured: 272.1575.

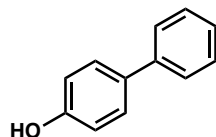


**3-butylbiphenyl (2.26).** Synthesized according to general procedure 2.6.6. Corresponding aryl fluoride (12.1 mg, 0.054 mmol) was added to a colorless solution of  $[\text{Ph}_3\text{C}]^+[\text{HCB}_{11}\text{Cl}_{11}]^-$  (1.1  $\mu\text{mol}$ , 0.02 equiv) and triethylsilane (2.2  $\mu\text{mol}$ , 0.04 equiv), and was stirred at 30  $^\circ\text{C}$  for 0.2 hours to give **2.26** in 99% yield (NMR). Crude product was purified by flash column chromatography (hexanes) to give **2.26** as a colorless oil (10.6 mg, 93%).

$^1\text{H}$  NMR (400 MHz,  $\text{CDCl}_3$ )  $\delta$  7.67–7.60 (m, 2H), 7.51–7.41 (m, 4H), 7.38 (td,  $J = 7.4, 5.2$  Hz, 2H), 7.21 (d,  $J = 7.5$  Hz, 1H), 2.72 (t,  $J = 7.7$  Hz, 2H), 1.74–1.65 (m, 2H), 1.49–1.38 (m, 2H), 0.99 (t,  $J = 7.4$  Hz, 3H);  $^{13}\text{C}$  NMR (100 MHz,  $\text{CDCl}_3$ )  $\delta$  143.3, 141.5, 141.2, 128.7, 128.6, 127.4, 127.3, 127.2, 127.1, 124.5, 35.8, 33.7, 22.4, 14.0.

FTIR (Neat Film NaCl): 3059, 3029 2956, 2928, 2857, 1889, 1873, 1799, 1600, 1479, 754, 697  $\text{cm}^{-1}$ .

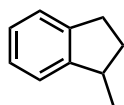
HR-MS (GC-Cl): Calculated for  $\text{C}_{16}\text{H}_{18}$ : 210.1409; measured: 210.1404.



**4-hydroxybiphenyl (2.28).** Synthesized according to general procedure 2.6.6 with a modified work-up procedure. Corresponding aryl fluoride (16.1 mg, 0.054 mmol) was added to a colorless

solution of  $[\text{Ph}_3\text{C}]^+[\text{HCB}_{11}\text{Cl}_{11}]^-$  (1.1  $\mu\text{mol}$ , 0.02 equiv) and triethylsilane (2.2  $\mu\text{mol}$ , 0.04 equiv) and was stirred at 60 °C for 48 hours. After cooling to room temperature, the reaction was quenched with a saturated aqueous sodium bicarbonate solution. The aqueous layer was extracted with  $\text{Et}_2\text{O}$  (3 x 1 mL) and combined organic layers were rotary evaporated. Crude product was purified by flash column chromatography (4:1 hexanes:ethyl acetate) to give **2.28** as a white solid (2.3 mg, 29%). NMR Spectra match those reported in literature.<sup>37</sup>

### 2.7.7 Intramolecular Alkane Insertion Reaction



**1-methylindane (2.38).**  $[\text{Ph}_3\text{C}]^+[\text{HCB}_{11}\text{Cl}_{11}]^-$  (4 mg, 5  $\mu\text{mol}$ , 0.04 equiv) and triethylsilane (1.8  $\mu\text{L}$ , 11  $\mu\text{mol}$ , 0.09 equiv) were dissolved in fluorobenzene (1 mL) to give a colorless solution before addition of aryl fluoride **2.37** (27.5 mg, 0.12 mmol, 1 equiv). Reaction was stirred at 30 °C for 2 hours to give **2.38** in 43% yield (GC) as shown in Figure. After volatiles were rotary evaporated, the crude product was purified by **2.30** flash column chromatography (pentane) to give **2.38** as a colorless oil (5.8 mg, 36%). NMR Spectra match those reported in literature.<sup>38</sup>

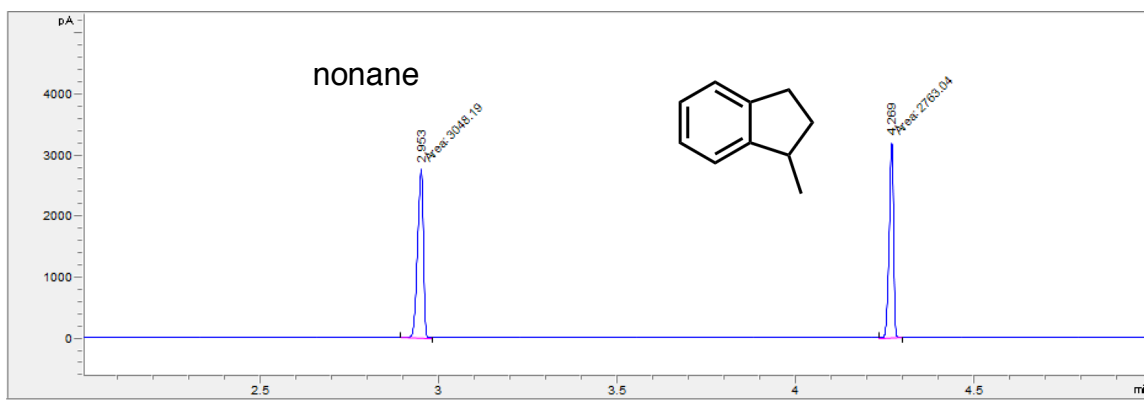


**Figure 2.29** GC Trace for Internal Standard *Nonane* and **2.38** in 1:1 Ratio.

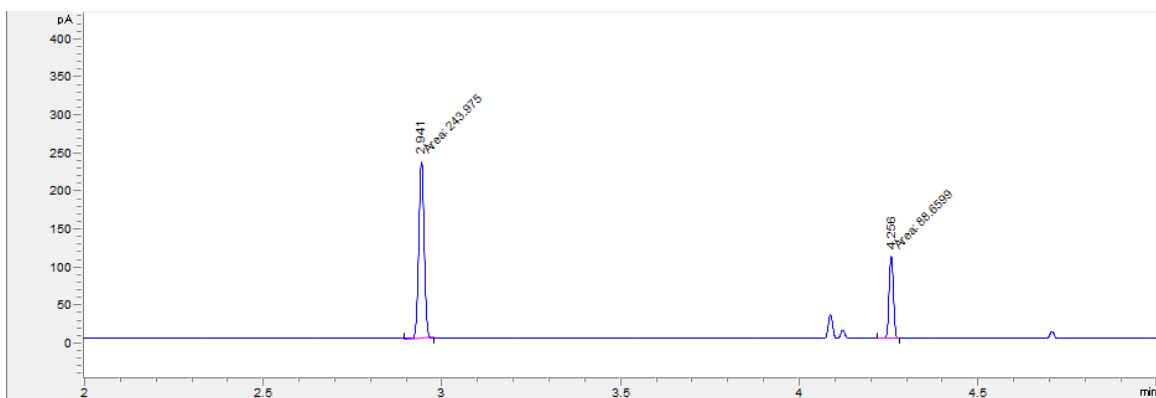


**Figure 2.30** GC Trace Showing Formation of **2.38** in 43% Yield.

### 2.7.8 Optimization Table for Intermolecular Alkane Insertion Reaction

In our studies, we optimized our reaction conditions for anion, silane, and additive using **2.1** in cyclohexane. Below in Table 2.4 we summarize our key observations.

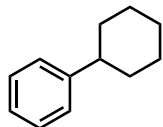
**Table 2.4** Optimization of (2-fluorophenyl)trimethylsilane Substrate in Cyclohexane.

Anion (5 mol%)	Silane (10 mol%)	Additive	Time	Yield
[HCB <sub>11</sub> H <sub>5</sub> Cl <sub>6</sub> ]	iPr <sub>3</sub> SiH	<i>o</i> -C <sub>6</sub> H <sub>4</sub> Cl <sub>2</sub> (10 equiv)	120 hr	32%
[HCB <sub>11</sub> Cl <sub>11</sub> ]	Et <sub>3</sub> SiH	<i>o</i> -C <sub>6</sub> H <sub>4</sub> Cl <sub>2</sub> (10 equiv)	8 hr	24%
[HCB <sub>11</sub> Cl <sub>11</sub> ]	iPr <sub>3</sub> SiH	<i>o</i> -C <sub>6</sub> H <sub>4</sub> Cl <sub>2</sub> (10 equiv)	2 hr	41%
[HCB <sub>11</sub> Cl <sub>11</sub> ]	iPr <sub>3</sub> SiH	Me <sub>2</sub> (Mes) <sub>2</sub> Si (1 equiv)	9 hr	37%
[HCB <sub>11</sub> Cl <sub>11</sub> ]	iPr <sub>3</sub> SiH	<i>o</i> -C <sub>6</sub> H <sub>4</sub> F <sub>2</sub> (10 equiv)	2 hr	27%
[HCB <sub>11</sub> Cl <sub>11</sub> ]	iPr <sub>3</sub> SiH	none	22 hr	38%
[(C <sub>6</sub> F <sub>5</sub> ) <sub>4</sub> B]	iPr <sub>3</sub> SiH	none	36 hr	18%

### 2.7.9 General Procedure for Intermolecular Alkane Insertion Reactions

[Ph<sub>3</sub>C]<sup>+</sup>[HCB<sub>11</sub>Cl<sub>11</sub>]<sup>-</sup> (2.0 mg, 2.7 μmol, 0.05 equiv) and triisopropylsilane (1.1 μL, 5.4 μmol, 0.1 equiv) were stirred in *o*-dichlorobenzene (60 μL, 0.54 mmol, 10 equiv) to give a colorless solution. Alkane solvent (1 mL), followed by aryl fluoride **2.1** (0.054 mmol, 1 equiv), were

added respectively to give a 0.05 M solution. The reaction was then heated between 60–100 °C for 1–9 hours (see individual substrates for reaction conditions). Reaction was monitored by GC-FID. After cooling to room temperature, the reaction mixture was quenched with saturated aqueous sodium bicarbonate and the organic layers were concentrated *via* rotary evaporation and purified by flash column chromatography (hexanes or pentane).



**Phenylcyclohexane (2.29).** Synthesized according to general procedure 2.6.8. **2.1** (9.1 mg, 0.054 mmol) was added to a solution of  $[\text{Ph}_3\text{C}]^+[\text{HCB}_{11}\text{Cl}_{11}]^-$  (2.0 mg, 2.7  $\mu\text{mol}$ , 0.05 equiv), triisopropylsilane (1.1  $\mu\text{L}$ , 5.4  $\mu\text{mol}$ , 0.1 equiv), *o*-dichlorobenzene (60  $\mu\text{L}$ , 0.54 mmol, 10 equiv), and cyclohexane (1 mL). Reaction was stirred at 60 °C for 2 hours to give **2.29** in 41% yield (GC) as shown in Figure 2.32 Crude product was purified by flash column chromatography (pentane) to give **2.29** as a colorless oil. NMR Spectra match those reported in literature.<sup>39</sup>

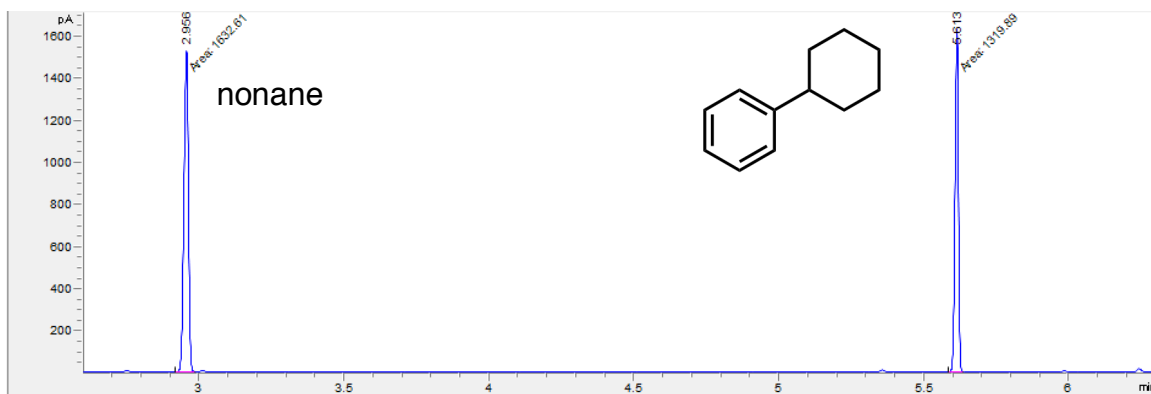


**Figure 2.31** GC Trace for Internal Standard *Nonane* and **2.29** in 1:1 Ratio.

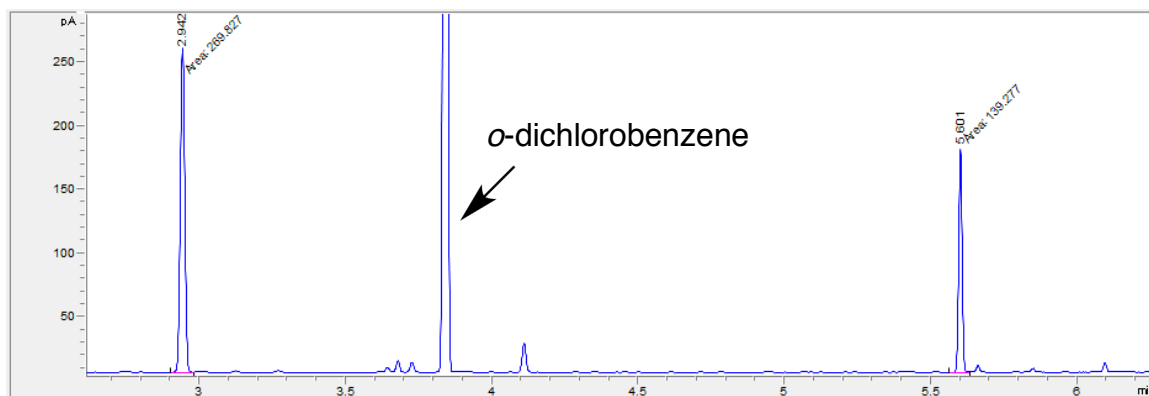
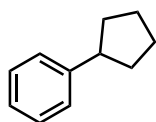
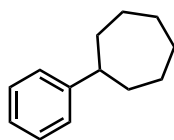


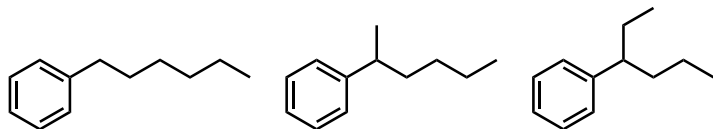
**Figure 2.32** GC Trace Showing Formation of **2.29** in 41% Yield.



**Phenylcyclopentane (2.30).** Synthesized according to general procedure 2.6.8. **2.1** (0.054 mmol, 9.1 mg) was added to a solution of  $[\text{Ph}_3\text{C}]^+[\text{HCB}_{11}\text{Cl}_{11}]^-$  (2.0 mg, 2.7  $\mu\text{mol}$ , 0.05 equiv), triisopropylsilane (1.1  $\mu\text{L}$ , 5.4  $\mu\text{mol}$ , 0.1 equiv), *o*-dichlorobenzene (60  $\mu\text{L}$ , 0.54 mmol, 10 equiv), and cyclopentane (1 mL). Reaction was stirred at 70  $^\circ\text{C}$  for 1 hour to give **2.30** in 54% yield (NMR). Crude product was purified by flash column chromatography (pentane) to give **2.30** as a colorless oil. NMR Spectra match those reported in literature.<sup>40</sup>



**Phenylcycloheptane (2.31).** Synthesized according to general procedure 2.6.8 excluding *o*-dichlorobenzene. **2.1** (0.054 mmol, 9.1 mg) was added to a solution of  $[\text{Ph}_3\text{C}]^+[\text{HCB}_{11}\text{Cl}_{11}]^-$  (2.0 mg, 2.7  $\mu\text{mol}$ , 0.05 equiv), triisopropylsilane (1.1  $\mu\text{L}$ , 5.4  $\mu\text{mol}$ , 0.1 equiv), and cycloheptane (1 mL). Reaction was heated at 100  $^\circ\text{C}$  for 9 hours to give **2.31** in 40% yield (NMR). Crude product was purified by flash column chromatography (hexanes) to give **2.31** as a colorless oil (3.4 mg, 36%). NMR Spectra match those reported in literature.<sup>40</sup>



**Phenylhexane isomers (2.32).** Synthesized according to general procedure 2.6.8. **2.1** (0.054 mmol, 9.1 mg) was added to a solution  $[\text{Ph}_3\text{C}]^+[\text{HCB}_{11}\text{Cl}_{11}]^-$  (2.0 mg, 2.7  $\mu\text{mol}$ , 0.05 equiv), triisopropylsilane (1.1  $\mu\text{L}$ , 5.4  $\mu\text{mol}$ , 0.1 equiv), *o*-dichlorobenzene (60  $\mu\text{L}$ , 0.54 mmol, 10 equiv), and *n*-hexane (1 mL). Reaction was heated at 60 °C for 8 hours to give **2.32** in 40% overall yield (GC). Crude product was purified by flash column chromatography (hexanes) to give **2.32** as a colorless oil. The error associated with the 3-phenylhexane calibration curve was shown to be greater than the theoretical yield. Yield of 3-phenylhexane was then calculated by using 1-phenylhexane and 2-phenylhexane as reference, taking into account the integral ratio of 1 for all isomers shown in Figure 2.33. Calculated yields were: 1-phenylhexane (26%) shown in Figure 2.35, 2-phenylhexane (9%) shown in Figure 2.37, 3-phenylhexane (5%) shown in Figure 2.39 NMR Spectra match those reported in literature.<sup>41</sup>

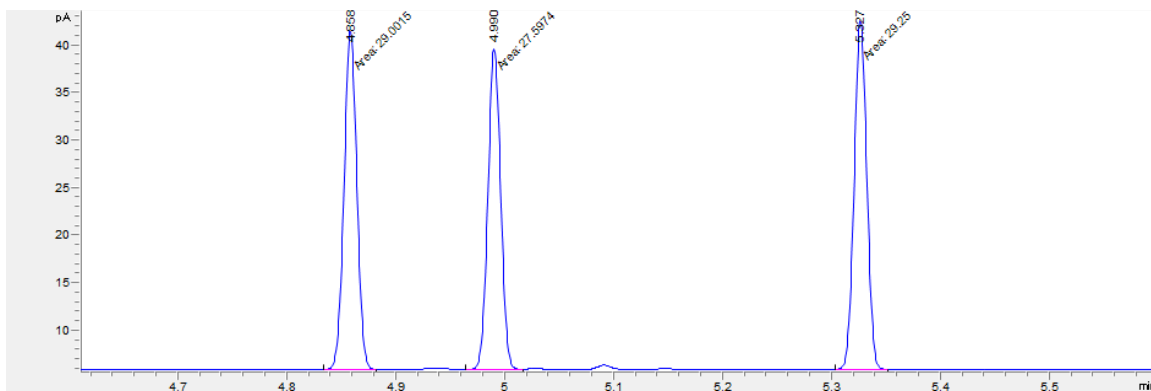


**Figure 2.33** GC Trace for a 1:1:1 Ratio of Phenylhexane Isomers Showing an Integral Relationship of 1.



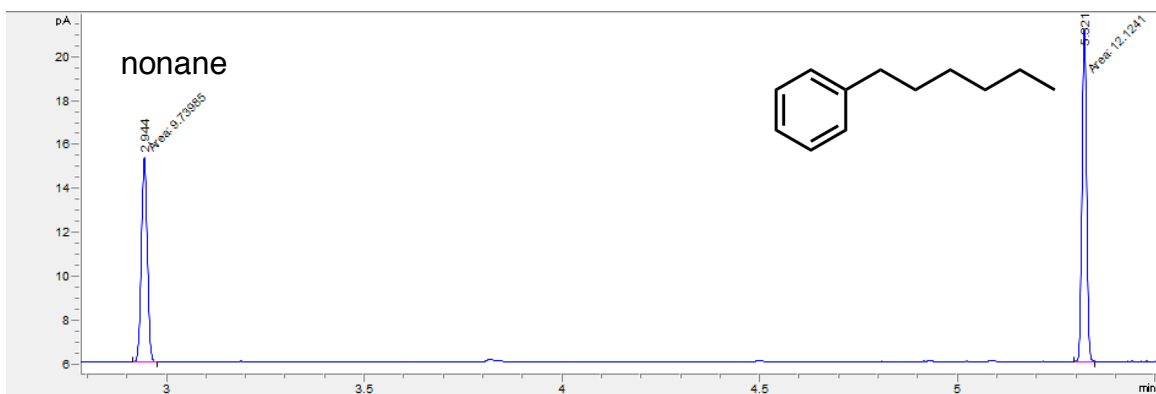


**Figure 2.34** GC Trace for Internal Standard *Nonane* and 1-phenylhexane in 1:1 Ratio.

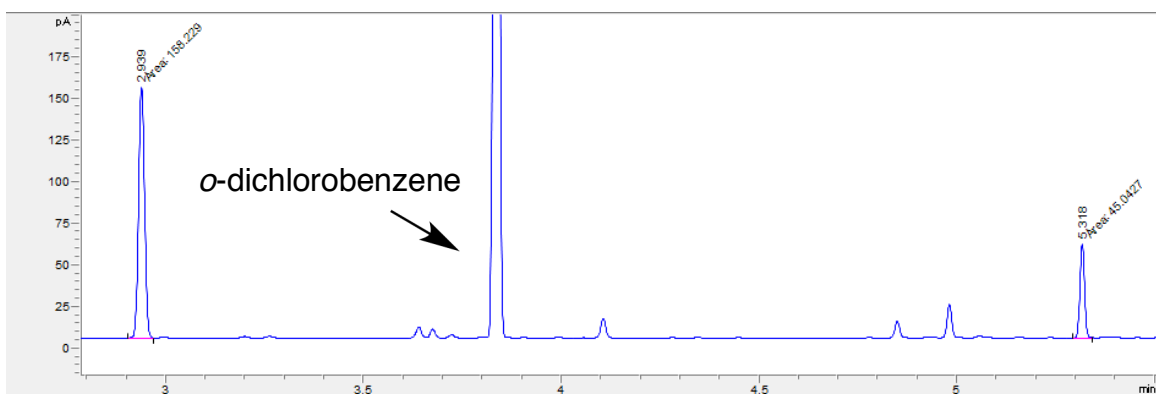


**Figure 2.35** GC Trace Showing the Formation of 1-phenylhexane From **2.1** in 26% Yield.

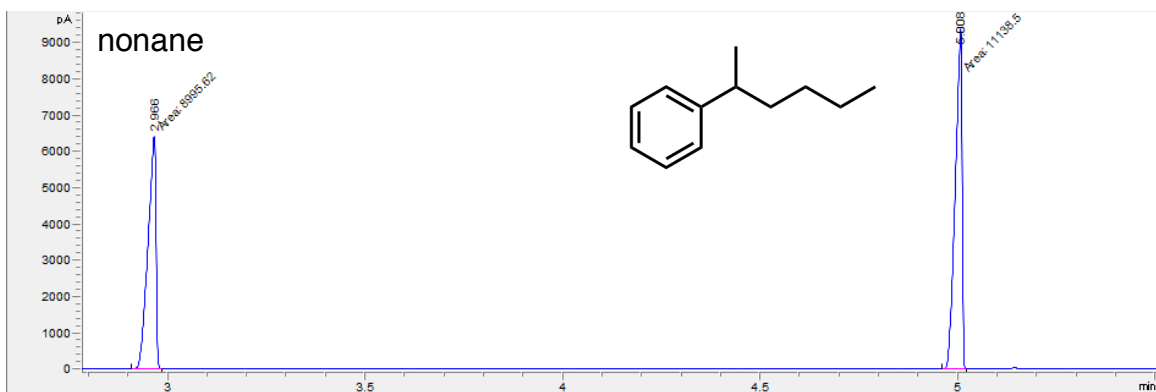


**Figure 2.36** GC Trace for Internal Standard *Nonane* and 2-phenylhexane in 1:1 Ratio.

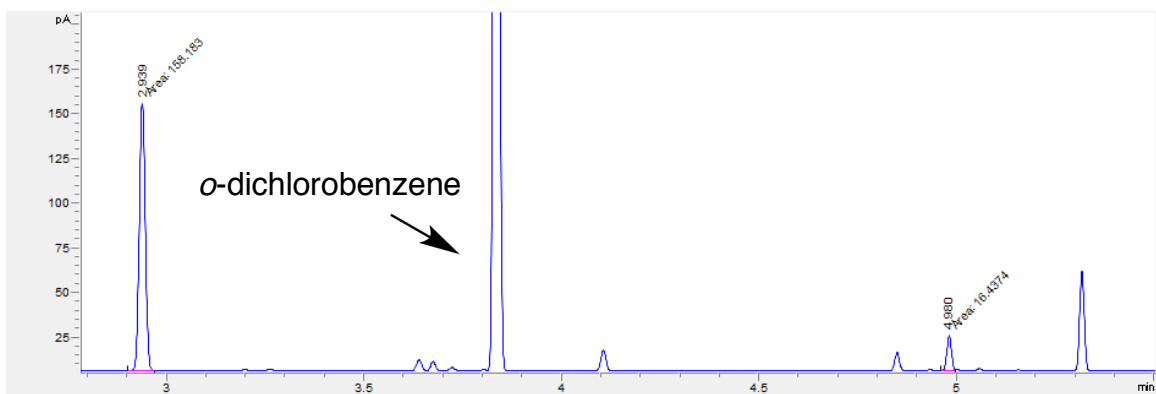


**Figure 2.37** GC Trace Showing the Formation of 2-phenylhexane From **2.1** in 9% Yield.

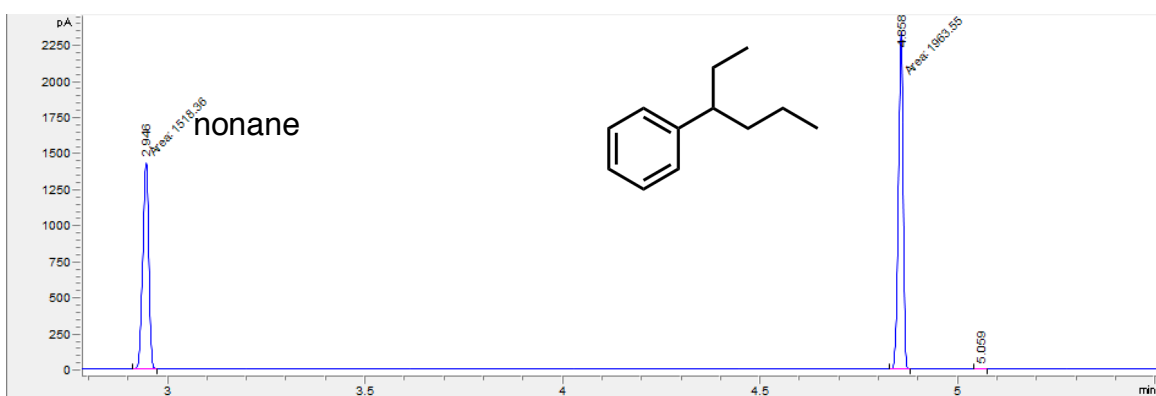


**Figure 2.38** GC Trace for Internal Standard *Nonane* and 3-phenylhexane in 1:1 Ratio.

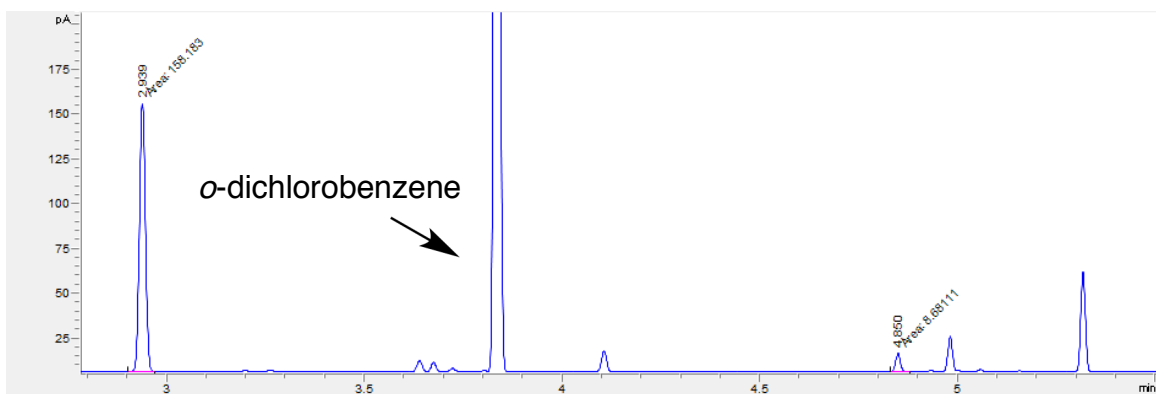
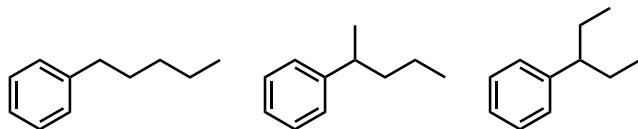


**Figure 2.39** GC Trace Showing Formation of 3-phenylhexane From **2.1**. The Error Associated With the 3-phenylhexane Calibration Curve was Shown to be Greater Than the Theoretical Yield.



**Phenylpentane isomers (2.33).** Synthesized according to general procedure 2.6.8. **2.1** (0.054 mmol, 9.1 mg) was added to a solution of  $[\text{Ph}_3\text{C}]^+[\text{HCB}_{11}\text{Cl}_{11}]^-$  (2.0 mg, 2.7  $\mu\text{mol}$ , 0.05 equiv), triisopropylsilane (1.1  $\mu\text{L}$ , 5.4  $\mu\text{mol}$ , 0.1 equiv), *o*-dichlorobenzene (60  $\mu\text{L}$ , 0.54 mmol, 10 equiv), and *n*-pentane (1 mL). Reaction was heated at 60  $^\circ\text{C}$  for 8 hours to give **2.33** in 42% overall yield (GC). Crude product was purified by flash column chromatography (hexanes) to give **2.33** as a colorless oil. Calculated GC yields were: 1-phenylpentane (30%) shown in Figure 2.41, 2-phenylpentane (10%) shown in Figure 2.44, 3-phenylpentane (2%) shown in Figure 2.46. NMR Spectra match those reported in literature.<sup>42</sup>

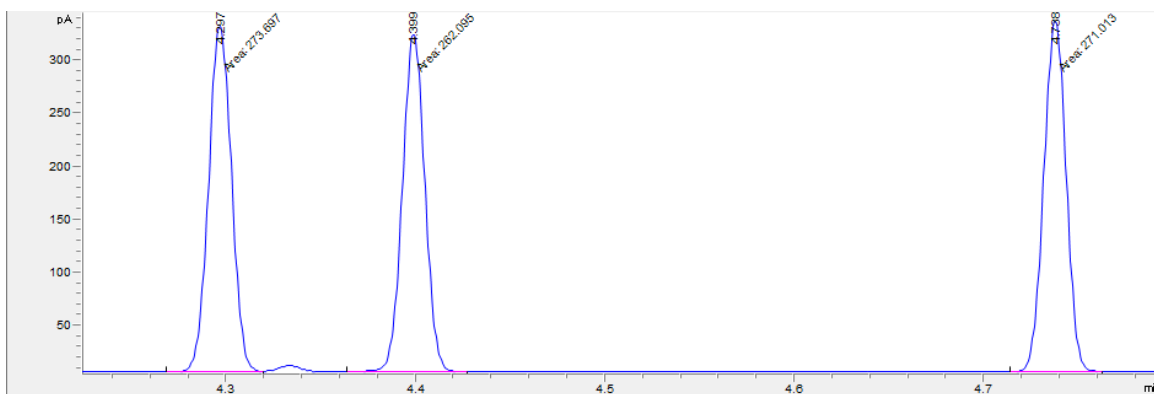


**Figure 2.40** GC Trace for a 1:1:1 Ratio of Phenylpentane Isomers.

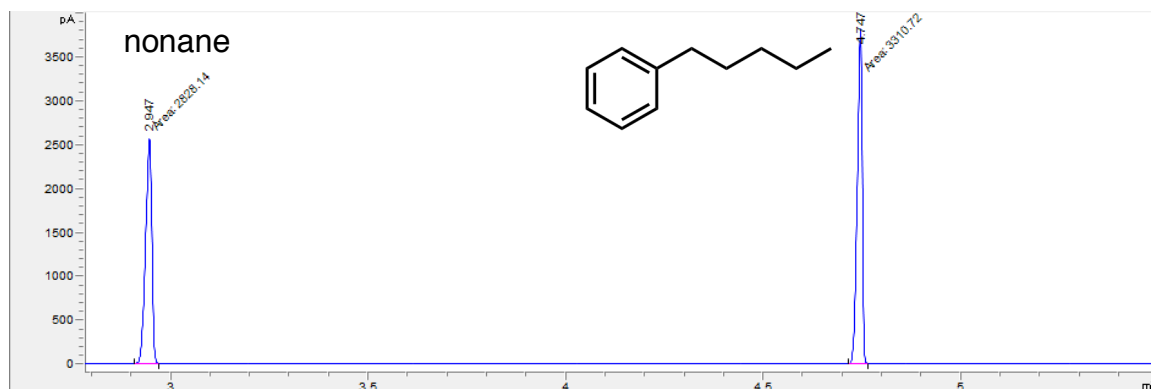


**Figure 2.41** GC Trace for Internal Standard *Nonane* and 1-phenylpentane in 1:1 Ratio.

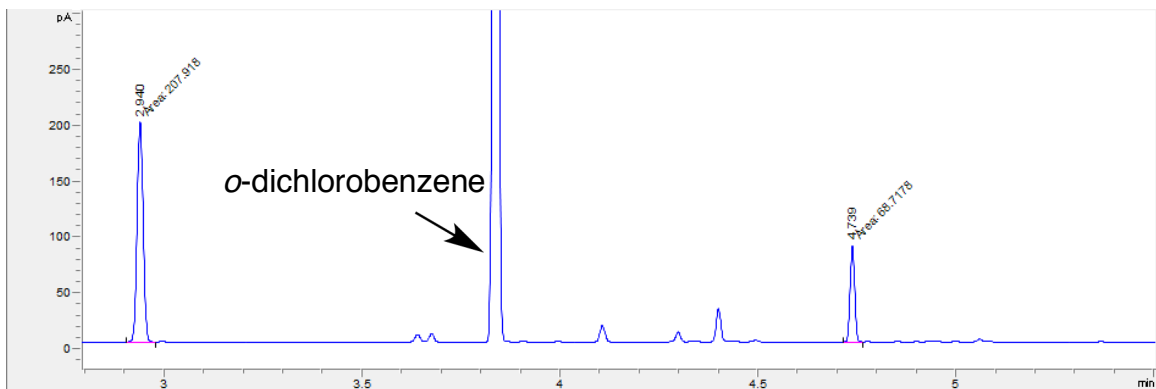


**Figure 2.42** GC Trace Showing Formation of 1-phenylpentane From **2.1** in 30% Yield.

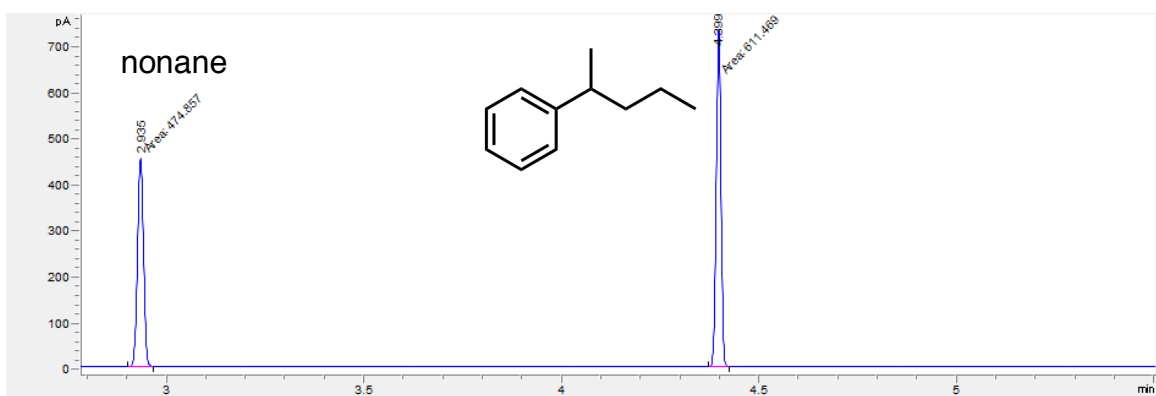


**Figure 2.43** GC Trace for Internal Standard *Nonane* and 2-phenylpentane in 1:1 Ratio.

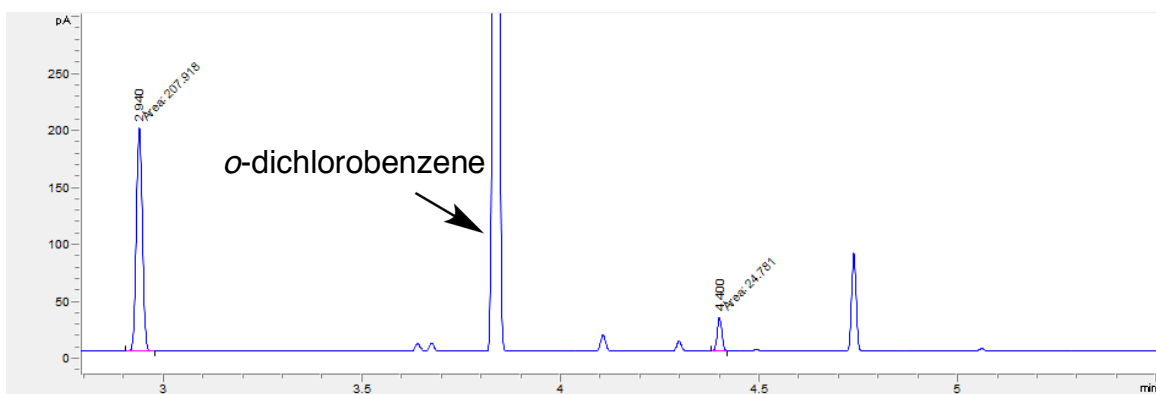


**Figure 2.44** GC Trace Showing Formation of 2-phenylpentane From **2.1** in 10% Yield.

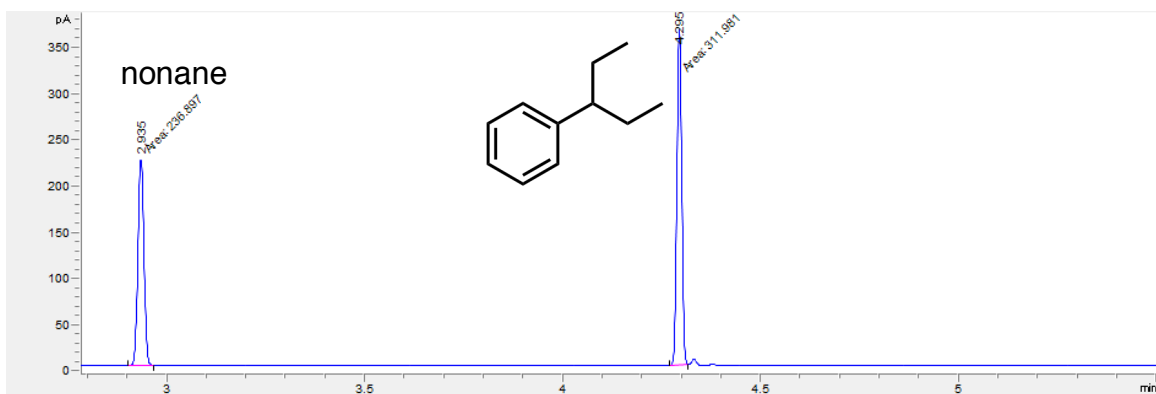


**Figure 2.45** GC Trace for Internal Standard *Nonane* and 3-phenylpentane in 1:1 Ratio.

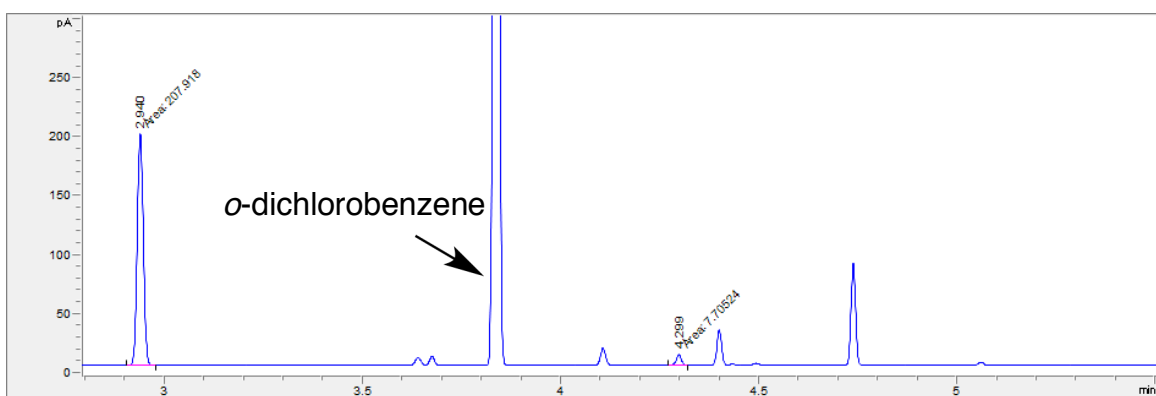
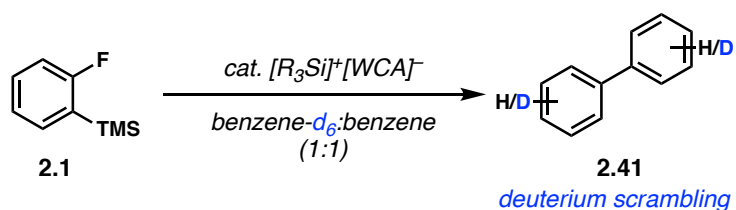


**Figure 2.46** GC Trace Showing Formation of 3-phenylpentane From **2.1** in 2% Yield.

### 2.7.10 Procedure for D-labeling Experiment in $C_6D_6$



The reaction is analogous to that described in general procedure 2.6.6, using  $C_6D_6$  in place of benzene. As shown below, masses ranging from  $C_{12}H_{10}D_0$  ( $m/z$ : 154) to  $C_{12}H_0D_{10}$  ( $m/z$ : 164) are present. This suggests that H/D crossover occurs from the Wheland intermediate (**2.11**) shown in Figure 2.3 from the manuscript.

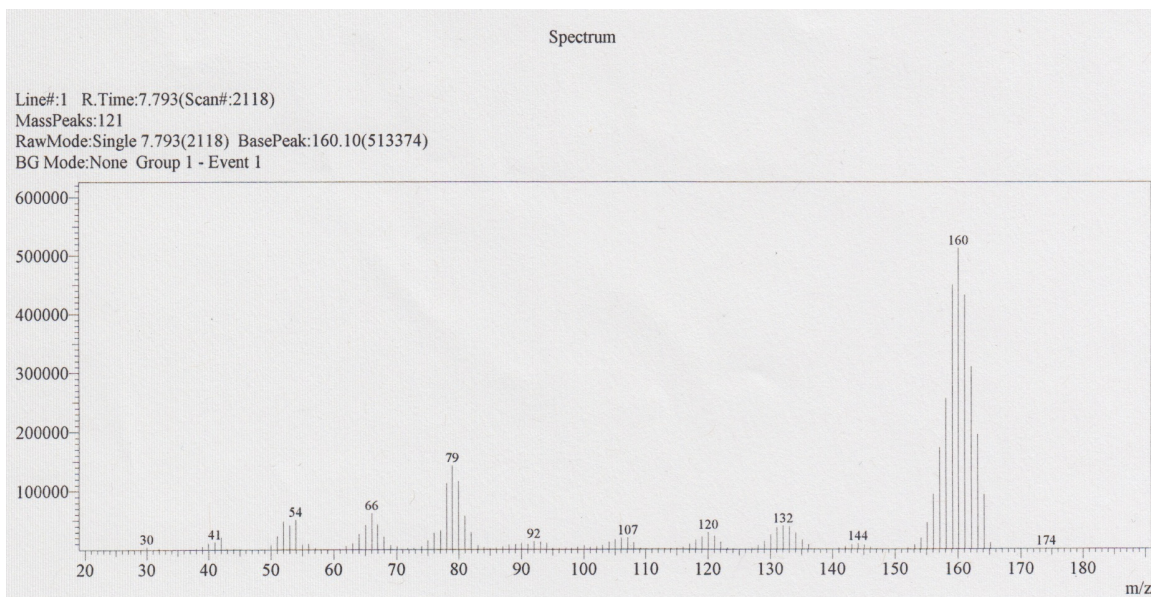


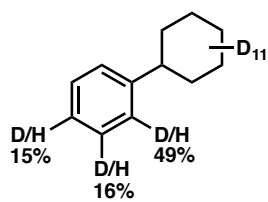
**Figure 2.47** GCMS Spectrum Showing Deuterium Scrambling of **2.41** in  $C_6D_6$  Reaction.

### 2.7.11 Procedure for D-labeling Experiment in $D_{12}$ -cyclohexane

In order to probe the mechanism of the alkane C–H insertion event, we used a modified procedure from general procedure 2.6.8 using  $C_6D_{12}$  in place of cyclohexane and excluding *o*-dichlorobenzene. The  $^1H$  NMR in section 4.7 suggests a 1,2-insertion process. We attribute the *meta*- and *para*- deuterium incorporation due to the rapid hydride shifts of Wheland intermediate **2.11** from the manuscript (Figure **2.3**). Outlined below is the procedure for synthesizing  $D_{12}$ -phenylcyclohexane and determining deuterium incorporation.

$[Ph_3C]^+[HCB_{11}Cl_{11}]^-$  (6.0 mg, 7.8  $\mu$ mol, 0.05 equiv) and triisopropylsilane (3.3  $\mu$ L, 16.1  $\mu$ mol, 0.1 equiv) were stirred in  $D_{12}$ -cyclohexane (3 mL) for 10 minutes to give a heterogeneous yellow suspension before adding aryl fluoride **2.1** (27.3 mg, 0.16 mmol, 1 equiv). The reaction mixture was heated at 70  $^\circ$ C for 13 hours. After cooling to room temperature, volatiles were evaporated by rotary evaporation, and crude product was purified by flash column chromatography (hexanes) and Kugelrohr distillation (0.2 Torr, rt). GC-MS analysis confirmed the formation of

only D<sub>12</sub>-phenylcyclohexane as shown in Figure 2.48. <sup>1</sup>H NMR was normalized against the *para*-position proton to have an integration value of 1. A second <sup>1</sup>H NMR was taken with an internal standard to calculate the deuterium enrichment at the *para*-position, and subsequently the total distribution of deuterium incorporation. The <sup>1</sup>H NMR data is shown in section 4.7.



**$D_{12}$ -phenylcyclohexane (2.43).** Synthesized according to procedure 2.6.10.

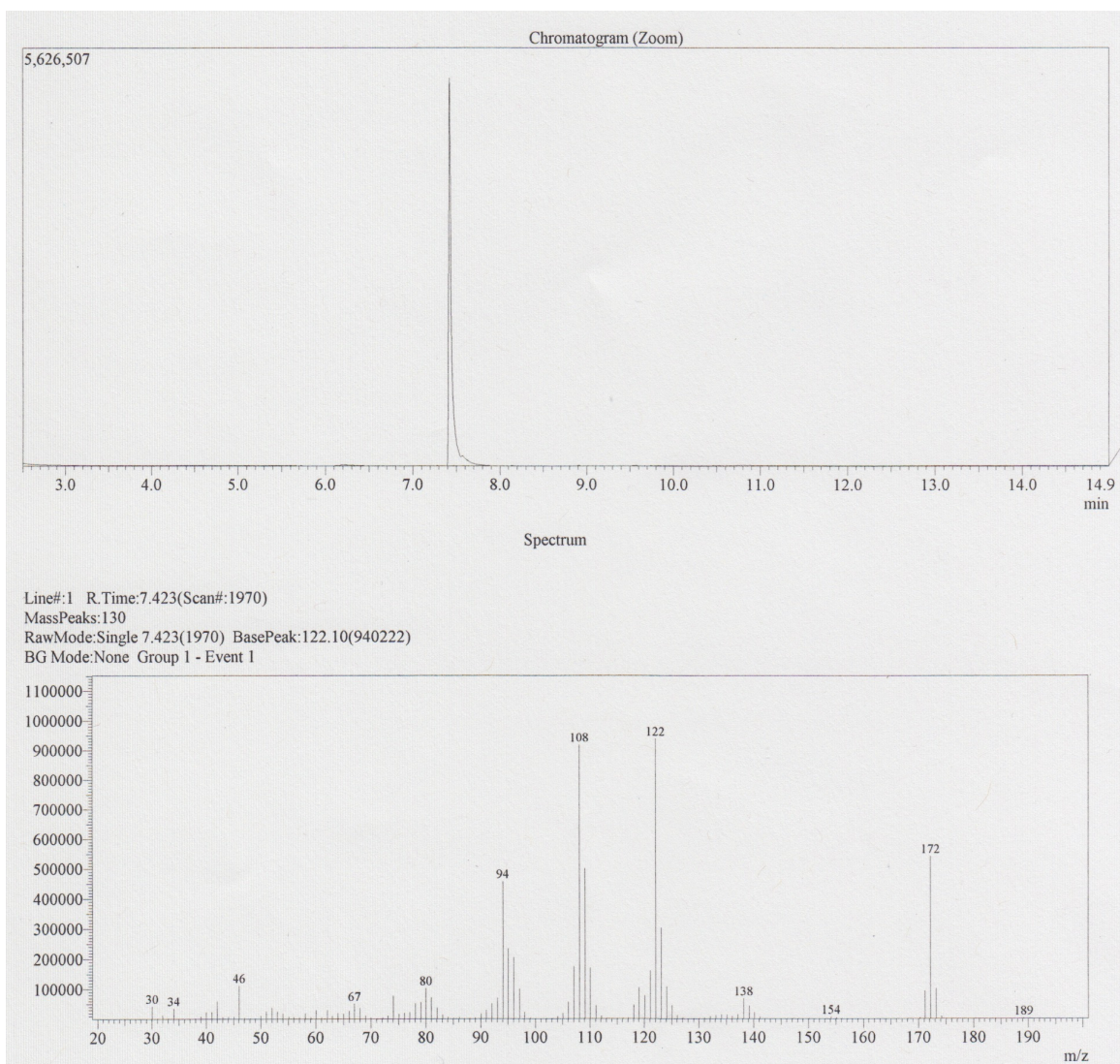


**Figure 2.48** GCMS Trace for  $D_{12}$ -phenylcyclohexane (m/z: 172) Showing No Deuterium Scrambling.



### 2.7.12 Procedure for Deuterium Competition Experiment

In order to probe the kinetics of our reaction, we subjected **2.1** to a competition experiment with 1:1 C<sub>6</sub>H<sub>12</sub>:C<sub>6</sub>D<sub>12</sub>. Lack of deuterium crossover (Figure **2.49**) and a kinetic isotope effect (KIE) of 1.08 suggest that the C–H insertion step is not rate-determining. Outlined below is the procedure for conducting our competition experiment.

[Ph<sub>3</sub>C]<sup>+</sup>[HCB<sub>11</sub>Cl<sub>11</sub>]<sup>-</sup> (2.0 mg, 2.6 μmol, 0.05 equiv) and triisopropylsilane (1.1 μL, 5.4 μmol, 0.1 equiv) were stirred in a 1:1 mixture of D<sub>12</sub>-cyclohexane (0.5 mL) and cyclohexane (0.5 mL) for 10 minutes to give a heterogeneous yellow suspension before addition of aryl fluoride **2.1** (9.1 mg, 0.054 mmol, 1 equiv). The reaction mixture was heated at 70 °C and stirred for 13 hours. Product ratios were analyzed by GC-FID using the coefficient calculated from Figure **2.50**. Over three trials (Figure **2.51**, **2.52**, and **2.53**),  $K_H/K_D = 1.08 \pm 0.01$ .

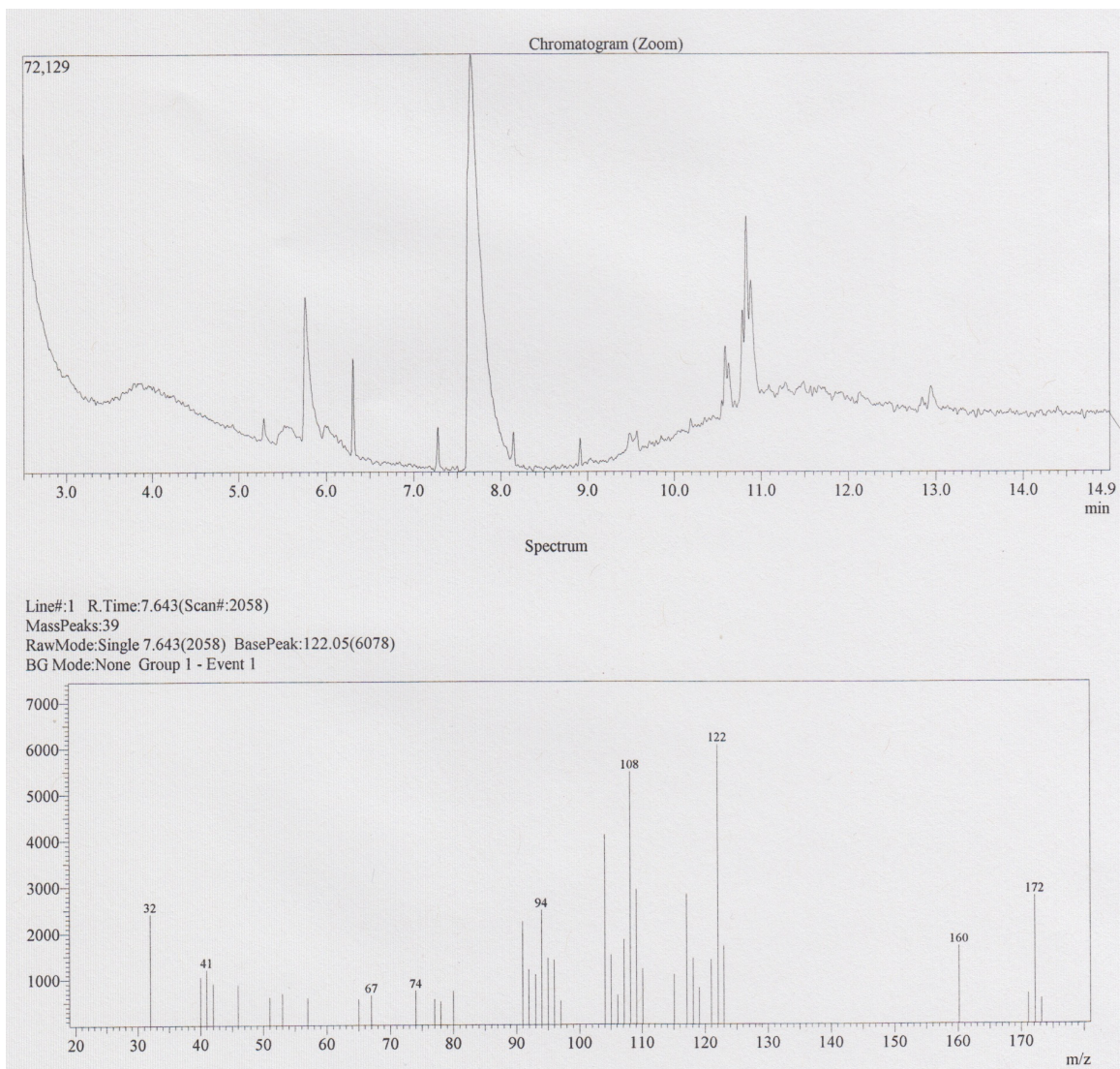


**Figure 2.49** GCMS Spectrum of Competition Experiment Showing No Deuterium Crossover.

$C_{12}H_{16}$  (m/z: 160) and  $C_{12}H_4D_{12}$  (m/z: 172) are Both Present With No Intermediate Masses.

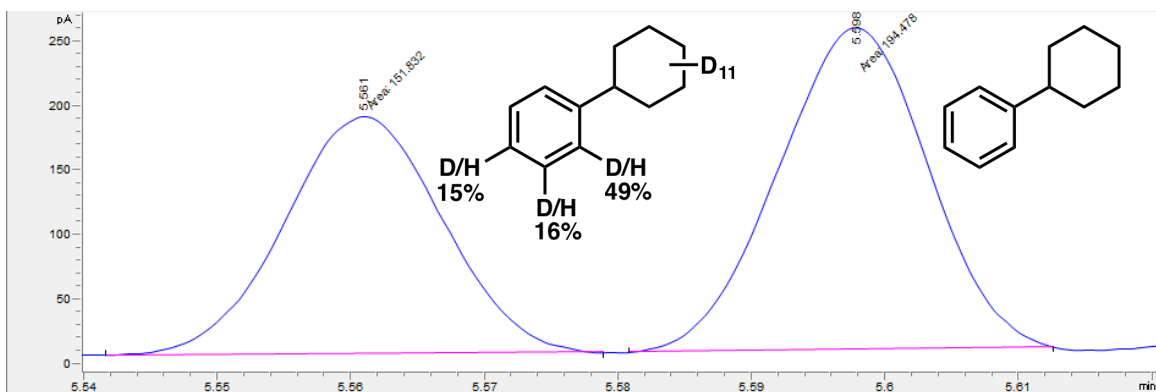


**Figure 2.50** GC Trace for a Solution of 4.3 mg of  $D_{12}$ -phenylcyclohexane and 5.4 mg of Phenylcyclohexane. A Comparison of Molar and Integral Ratios Show a 1:1 Relationship.

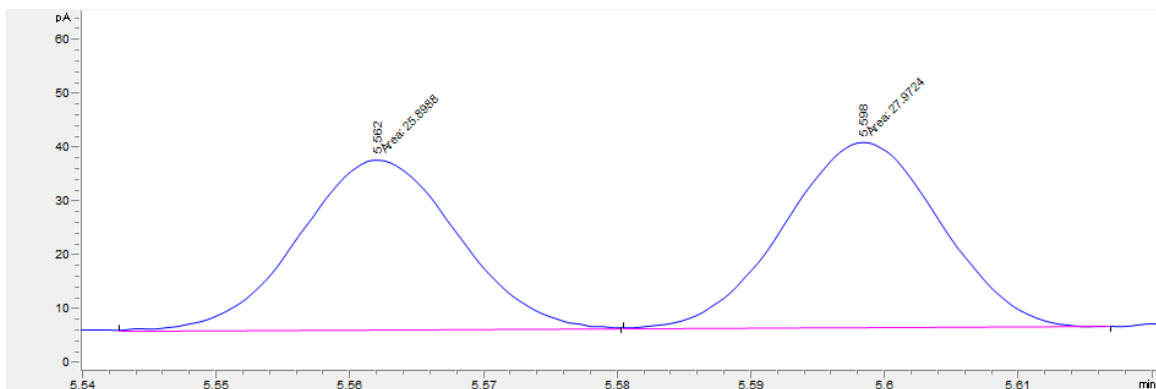


**Figure 2.51** GC Trace for Trial 1 of Deuterium Competition Experiment.

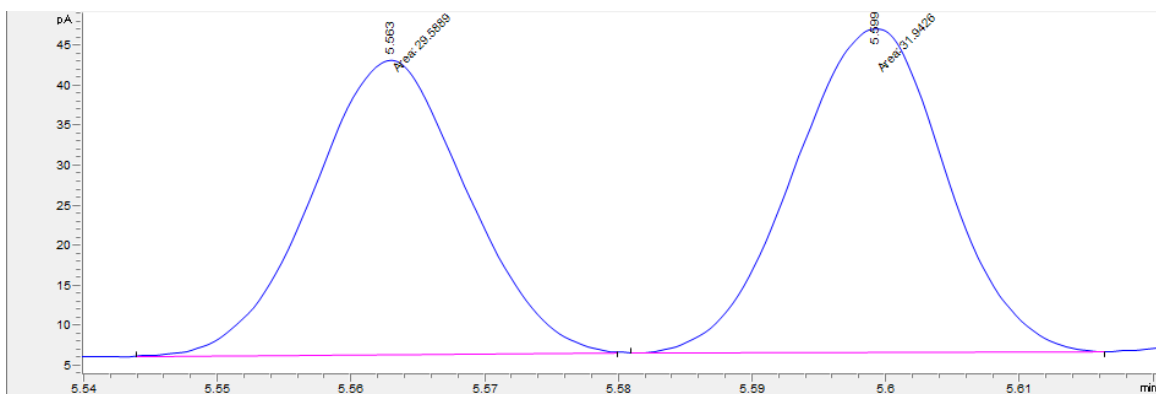


**Figure 2.52** GC Trace for Trial 2 of Deuterium Competition Experiment.

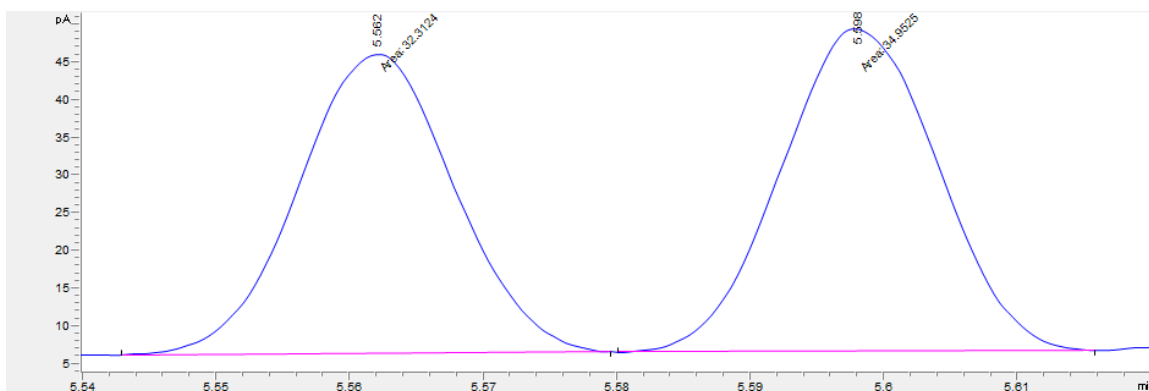


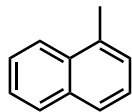
**Figure 2.53** GC Trace for Trial 3 of Deuterium Competition Experiment.

### 2.7.13 Methane Reaction

**Table 2.5** Optimization of (1-fluoronaphthalen-2-yl)trimethylsilane for the Insertion Reaction

With Methane. \*3.6 mol% Catalyst Loading.

Catalyst (5 mol%)	Solvent	Silane (10 mol%)	Yield
[Ph <sub>3</sub> C][HCB <sub>11</sub> Cl <sub>11</sub> ]	<i>o</i> -C <sub>6</sub> H <sub>4</sub> Cl <sub>2</sub>	<i>i</i> Pr <sub>3</sub> SiH	0%
[Et <sub>3</sub> Si][HCB <sub>11</sub> Cl <sub>11</sub> ]*	C <sub>6</sub> F <sub>6</sub>	none	32%
[Ph <sub>3</sub> C][HCB <sub>11</sub> Cl <sub>11</sub> ]	C <sub>6</sub> H <sub>5</sub> Cl	<i>i</i> Pr <sub>3</sub> SiH	0%
[Ph <sub>3</sub> C][HCB <sub>11</sub> Cl <sub>11</sub> ]	<i>o</i> -C <sub>6</sub> H <sub>4</sub> F <sub>2</sub>	<i>i</i> Pr <sub>3</sub> SiH	0%
[Ph <sub>3</sub> C][HCB <sub>11</sub> Cl <sub>11</sub> ]	C <sub>6</sub> F <sub>6</sub>	<i>i</i> Pr <sub>3</sub> SiH	22%
[Ph <sub>3</sub> C][HCB <sub>11</sub> Cl <sub>11</sub> ]	C <sub>6</sub> H <sub>5</sub> F	<i>i</i> Pr <sub>3</sub> SiH	0%



**1-methylnaphthalene (2.35).** Prior to the reaction, the reactor was purged with argon three times at room temperature and heated to 160 °C. After reaching 160 °C, the reactor was purged with argon three times and heated at this temperature for 12 hours. The vessel was then cooled to 25 °C and purged with argon three times.

Inside a glovebox,  $[\text{Et}_3\text{Si}]^+[\text{HCB}_{11}\text{Cl}_{11}]^-$  (2.5 mg, 3.92 mmol, 0.036 equiv) was dissolved in *o*-dichlorobenzene (0.12 mL, 1.08 mmol, 10 equiv). Hexafluorobenzene (1 mL), followed by aryl fluoride **2.34** (23.6 mg, 0.108 mmol, 1 equiv), were added respectively to give a 0.1 M suspension. The reaction was sealed and brought out to assemble in the reactor. Pressure vessel was assembled under a stream of argon as fast as possible to avoid exposure to air (<1 minute). Once sealed, the vessel was purged with argon three times, flushed with methane, then purged with methane three times. The reactor was then pressurized with methane to 35 bar and heated to 60 °C for 24 hours. After cooling to room temperature, the reaction mixture was diluted in hexanes, concentrated by rotary evaporation and purified by flash column chromatography (pentane) to give **2.35** as a colorless oil (4.9 mg, 32%). NMR Spectra match those reported in literature.<sup>43</sup>

Low yields are attributed to protodesilylation of **2.34** during the reaction as shown in Figure **2.54**. This is likely due to adventitious water introduced upon assembly of the reactor.

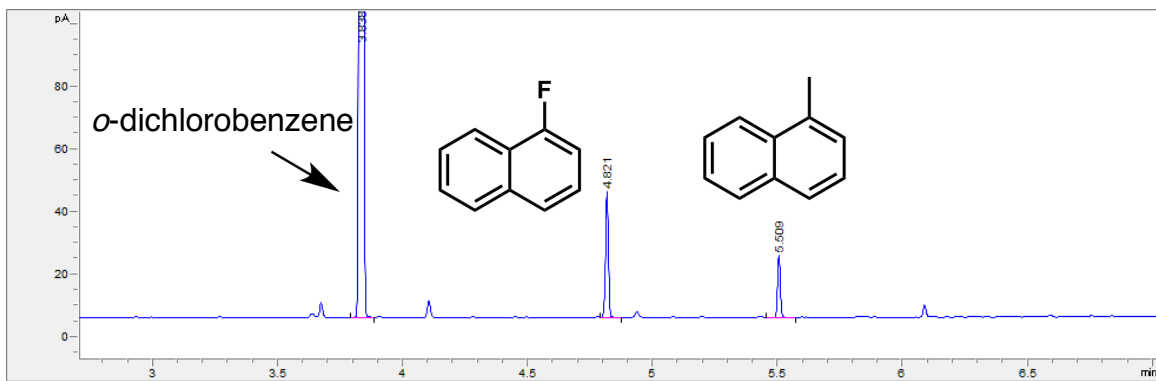


**Figure 2.54** GC Trace for Crude Methane Insertion Reaction Showing Both **2.35** and the Major Byproduct 1-fluoronaphthalene.

## 2.8 Spectra Relevant to Chapter Two:

### **Arylation of Hydrocarbons Enabled by Organosilicon Reagents and Weakly Coordinating Anions**

Adapted from: Brian Shao<sup>†</sup>, Alex L. Bagdasarian<sup>†</sup>, Stasik Popov, and Hosea M. Nelson

*Science*, **2017**, 355, 1403–1407.

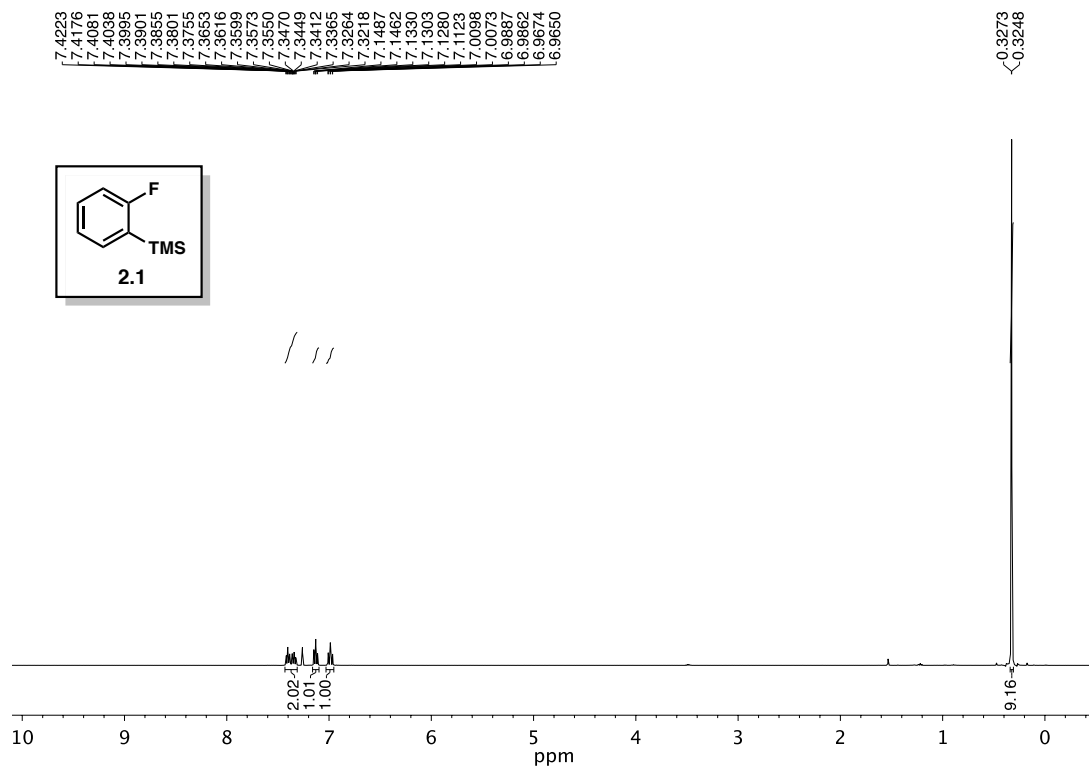


Figure 2.55  $^1\text{H}$  NMR (400 MHz,  $\text{CDCl}_3$ ) of compound 2.1.

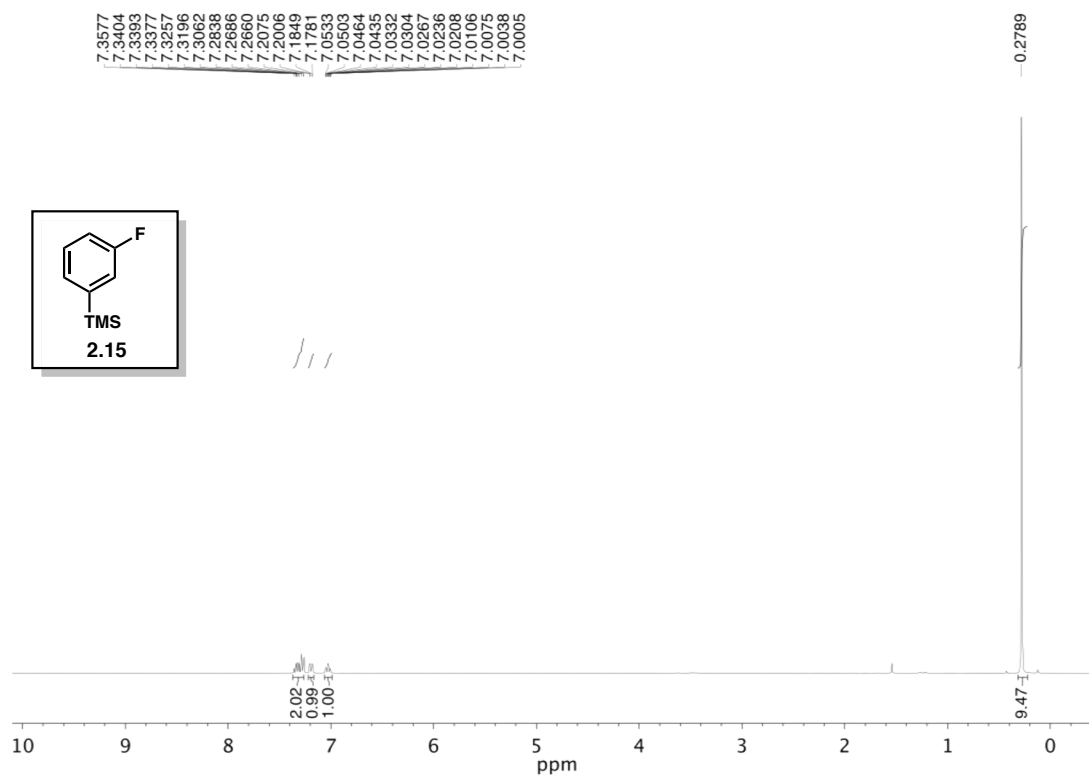


Figure 2.56  $^1\text{H}$  NMR (400 MHz,  $\text{CDCl}_3$ ) of compound 2.15.



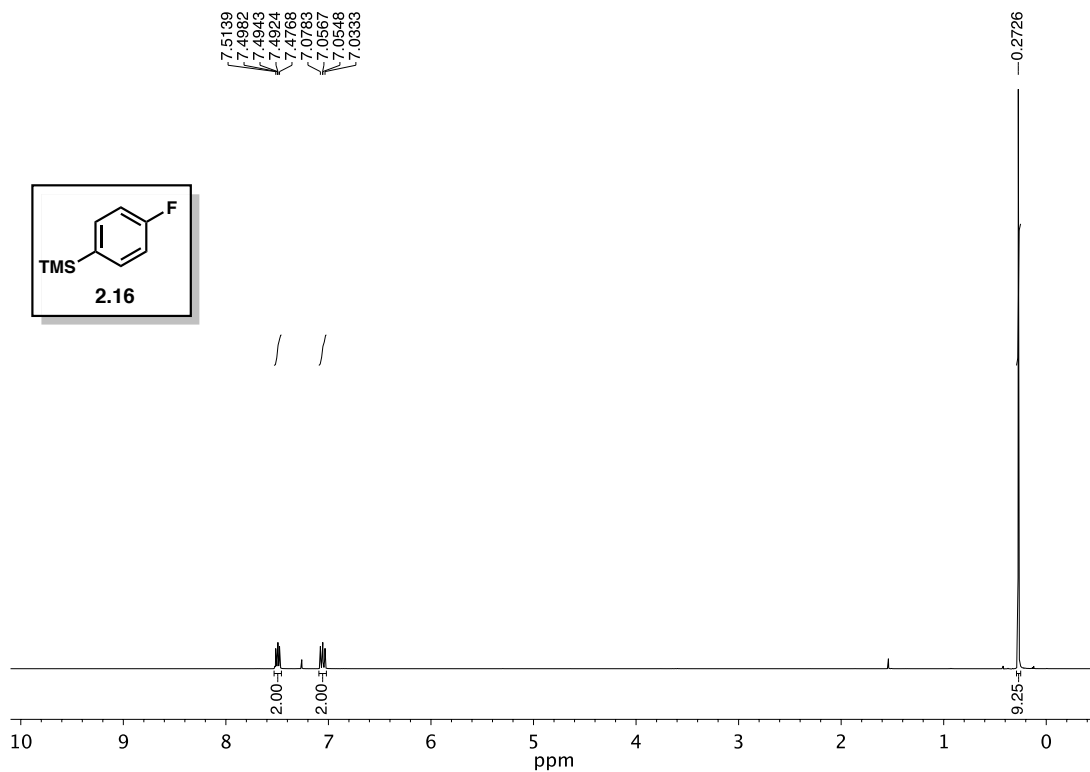


Figure 2.57  $^1\text{H}$  NMR (400 MHz,  $\text{CDCl}_3$ ) of compound 2.16.

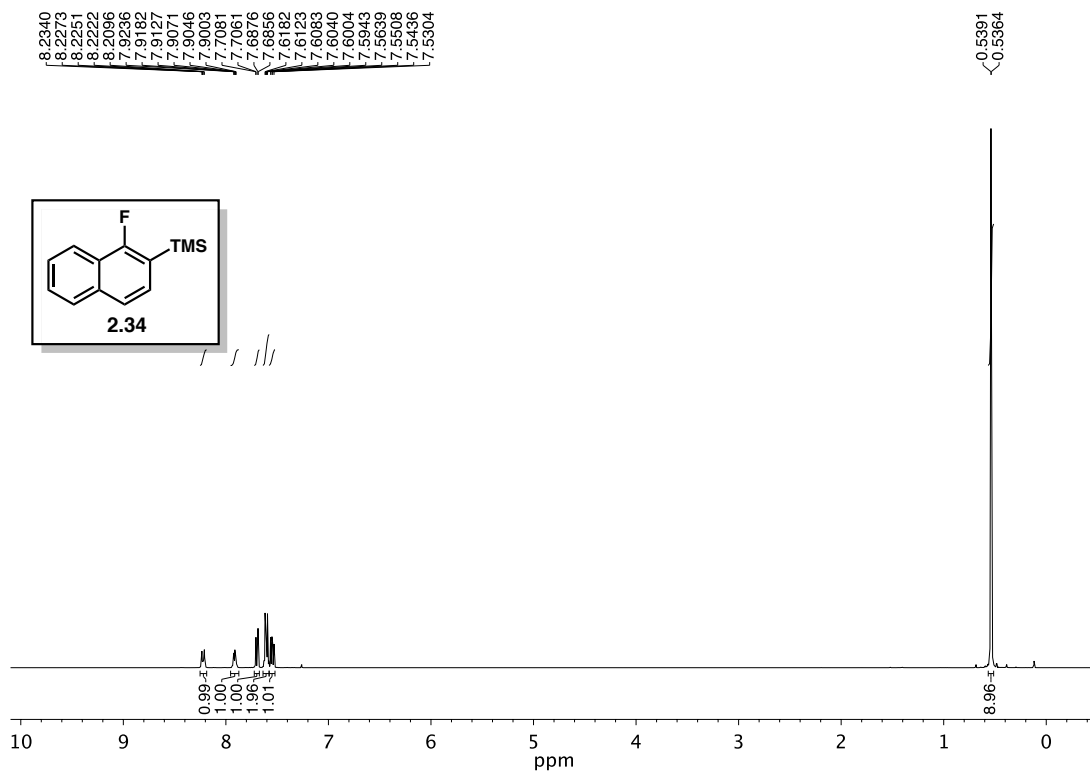
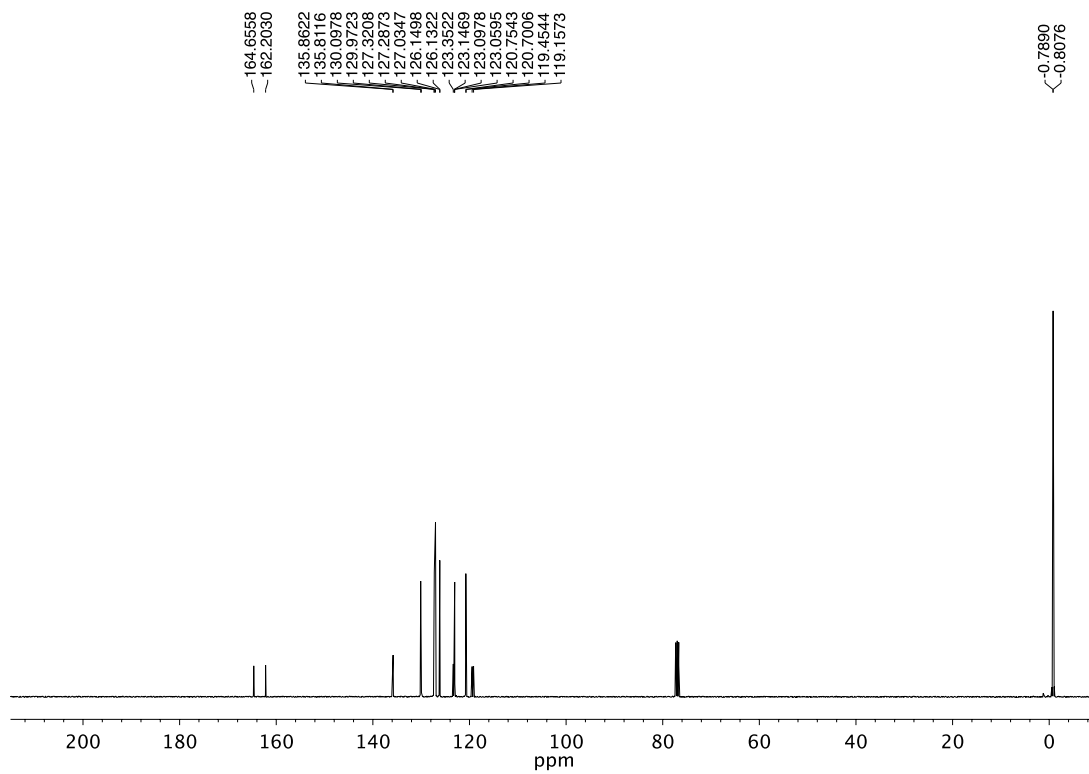
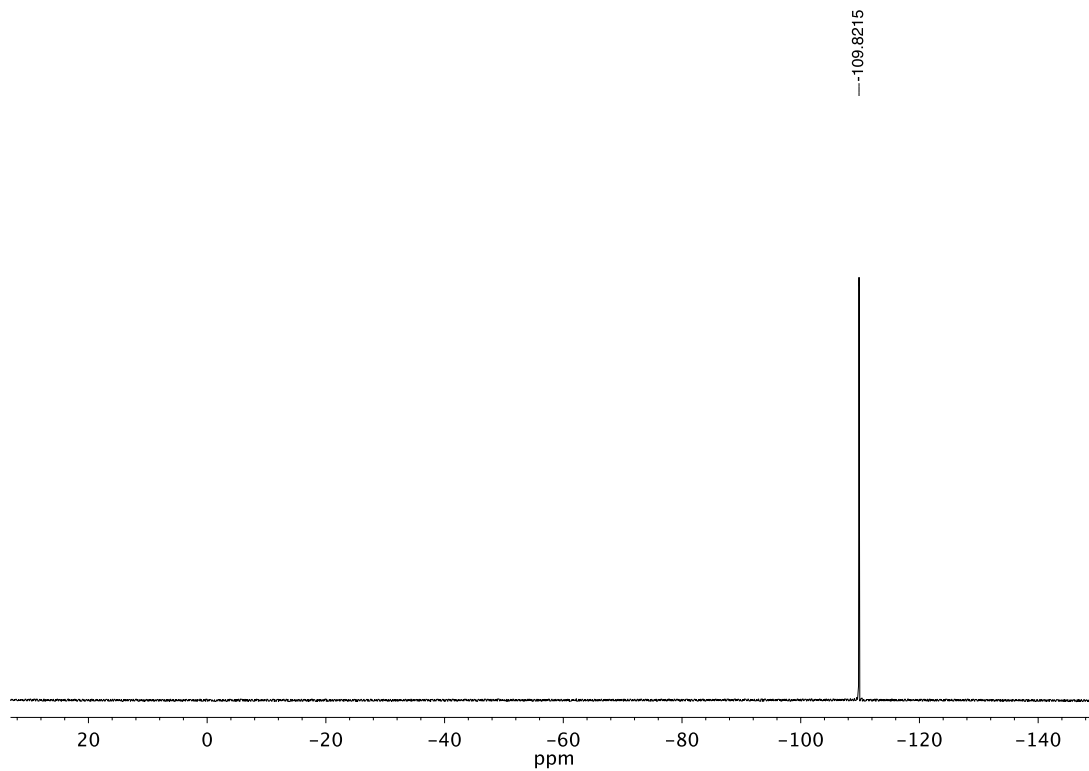


Figure 2.58  $^1\text{H}$  NMR (400 MHz,  $\text{CDCl}_3$ ) of compound 2.34.



**Figure 2.59**  $^{13}\text{C}$  NMR (100 MHz,  $\text{CDCl}_3$ ) of compound **2.34**.



**Figure 2.60**  $^{19}\text{F}$  NMR (376 MHz,  $\text{CDCl}_3$ ) of compound **2.34**.

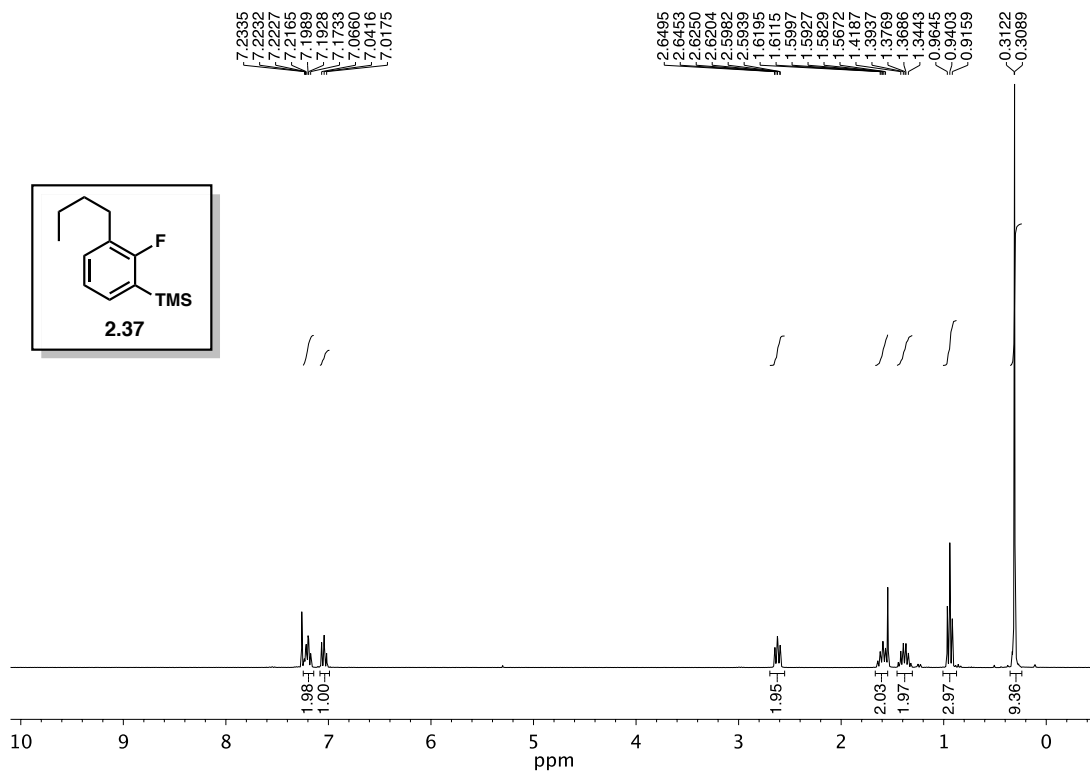


Figure 2.61 <sup>1</sup>H NMR (300 MHz, CDCl<sub>3</sub>) of compound 2.37.

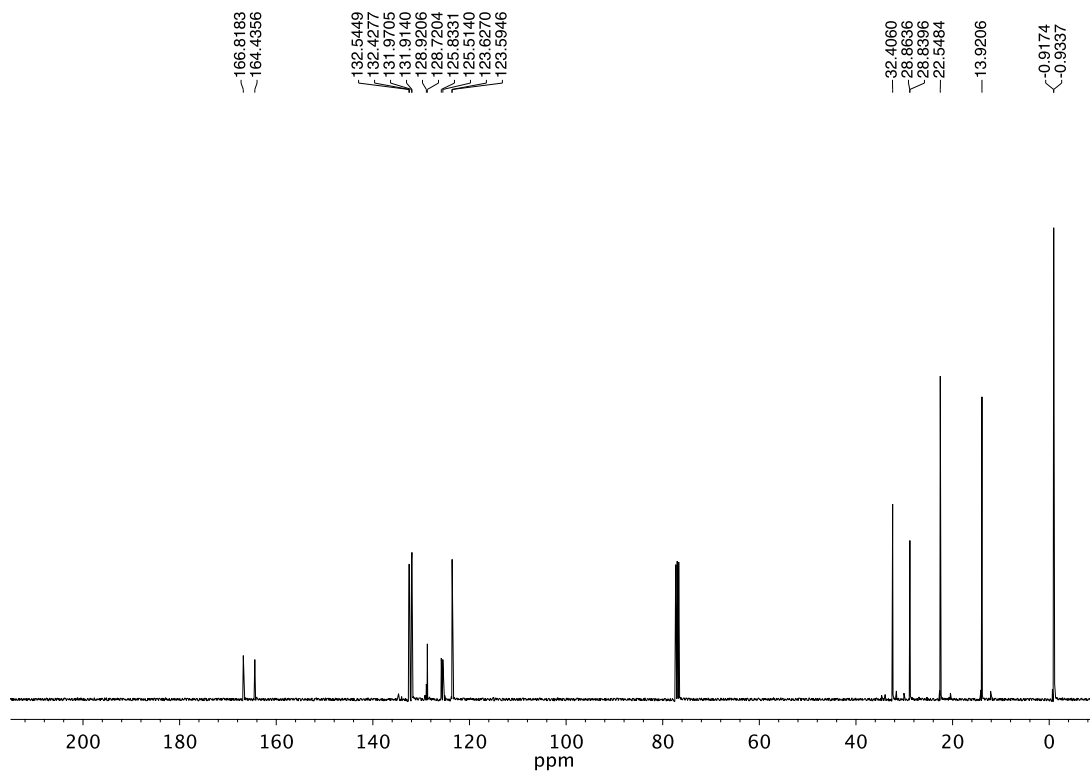


Figure 2.62 <sup>13</sup>C NMR (100 MHz, CDCl<sub>3</sub>) of compound 2.37.

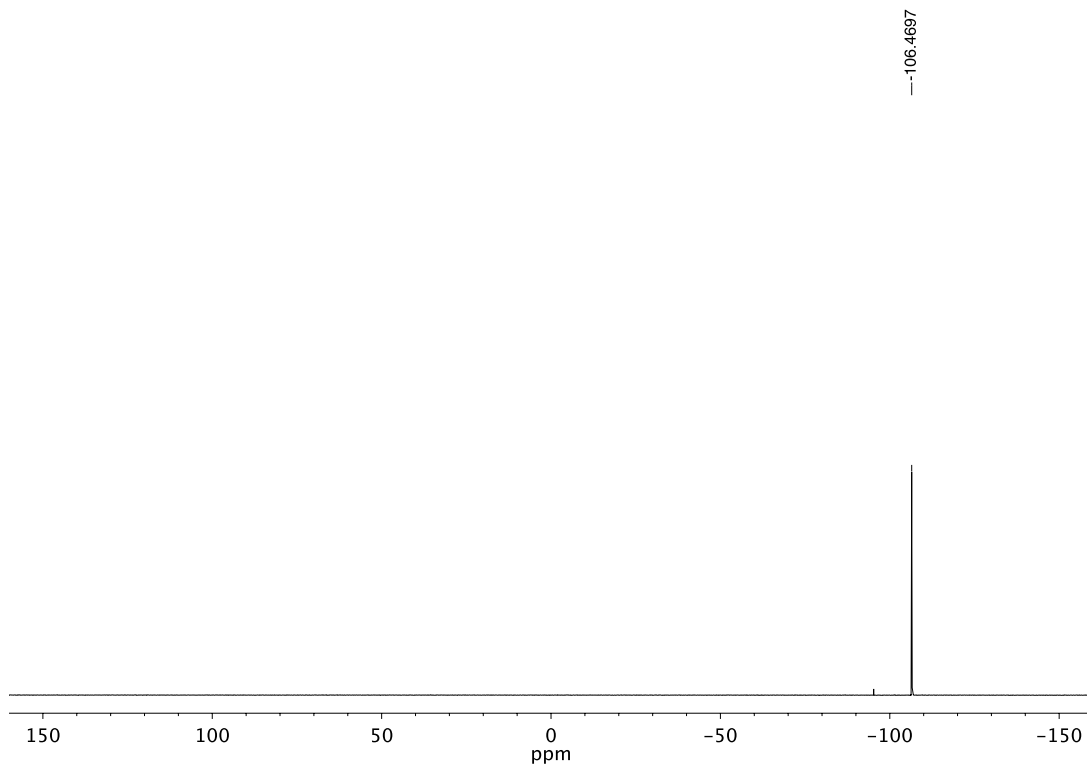


Figure 2.63  $^{19}\text{F}$  NMR (282 MHz,  $\text{CDCl}_3$ ) of compound 2.37.

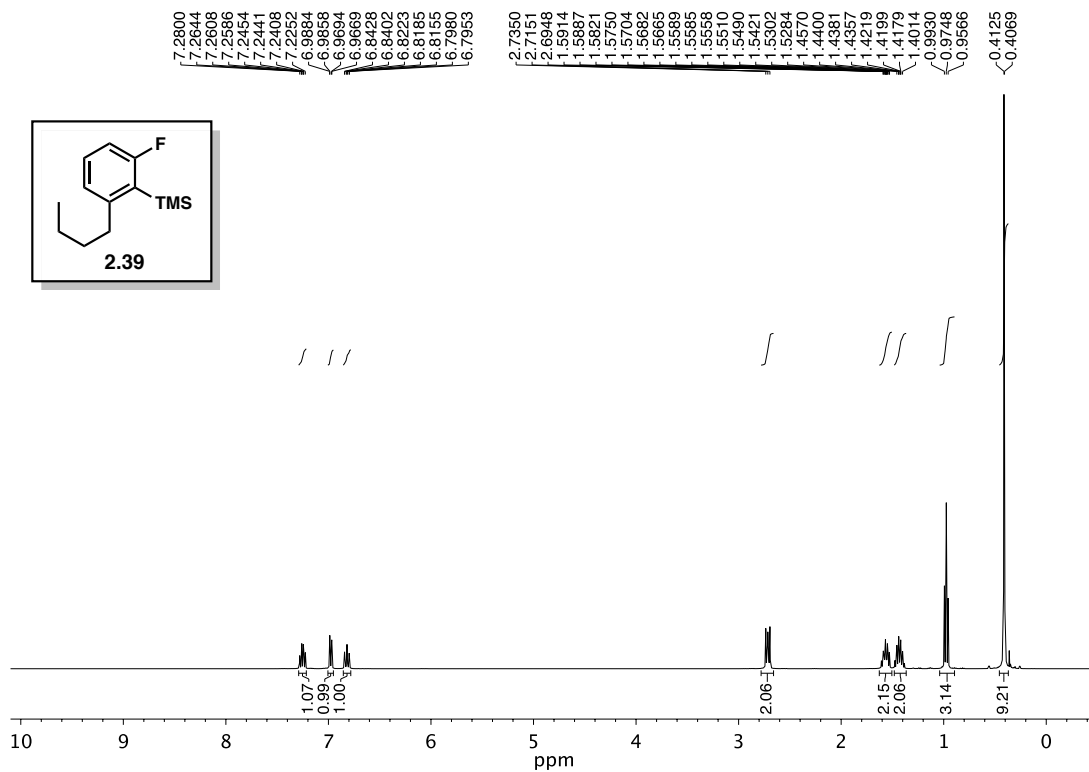
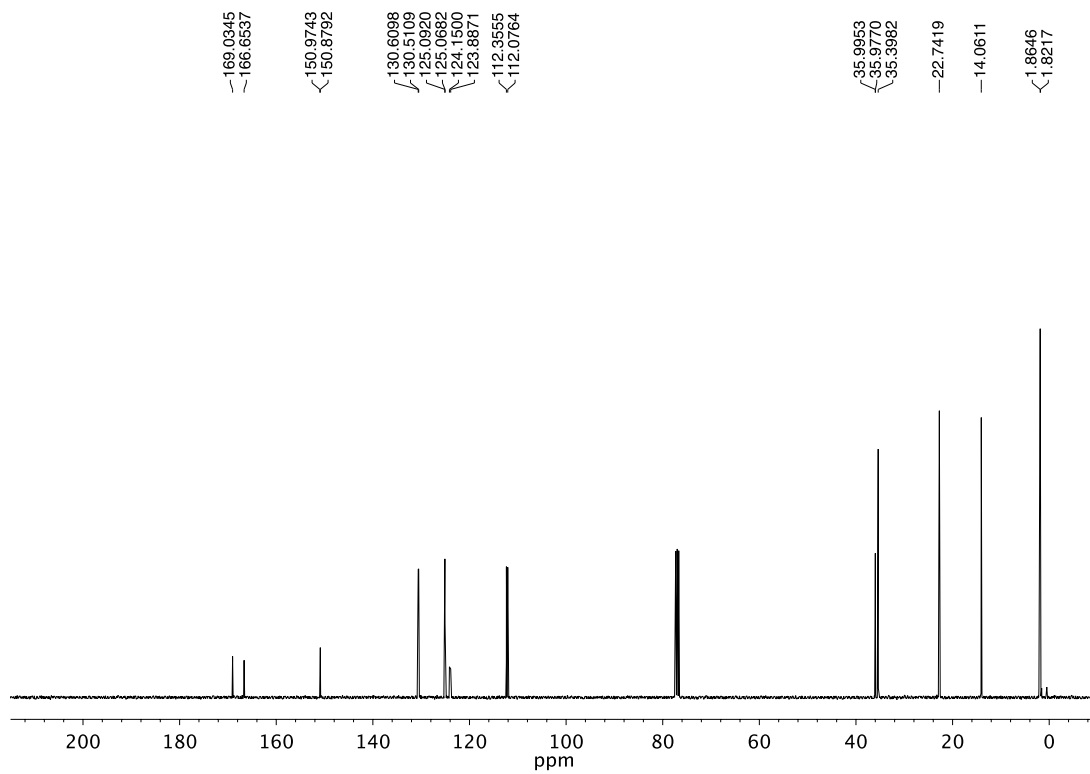
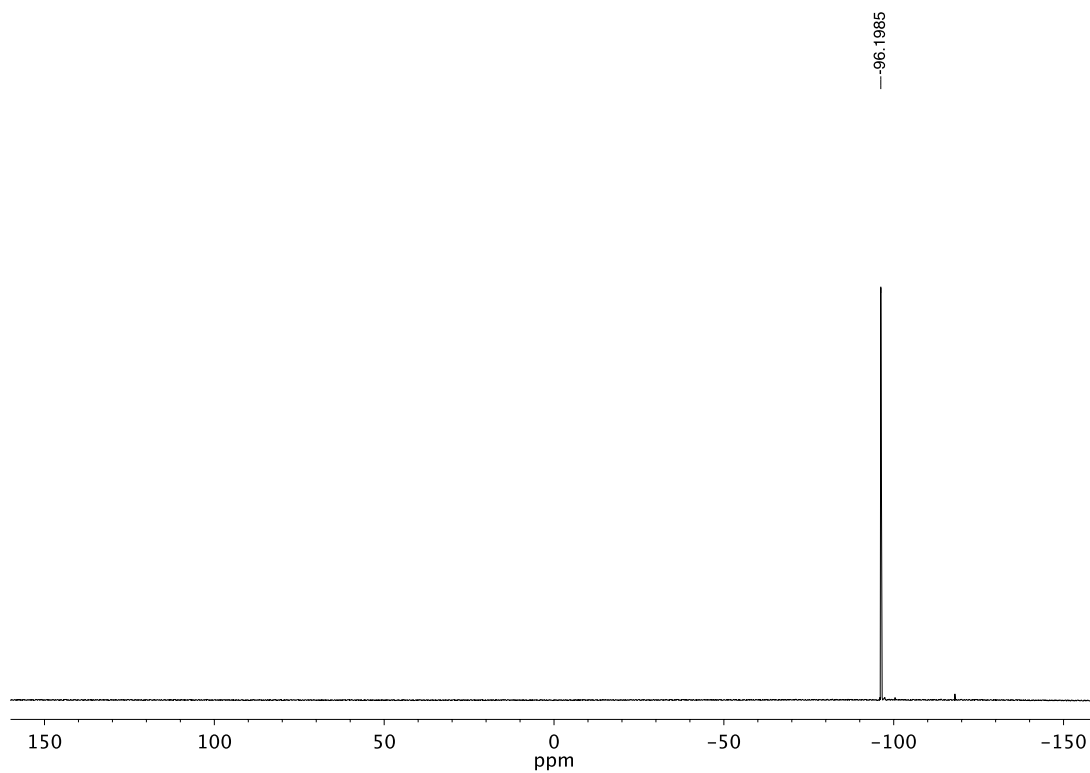


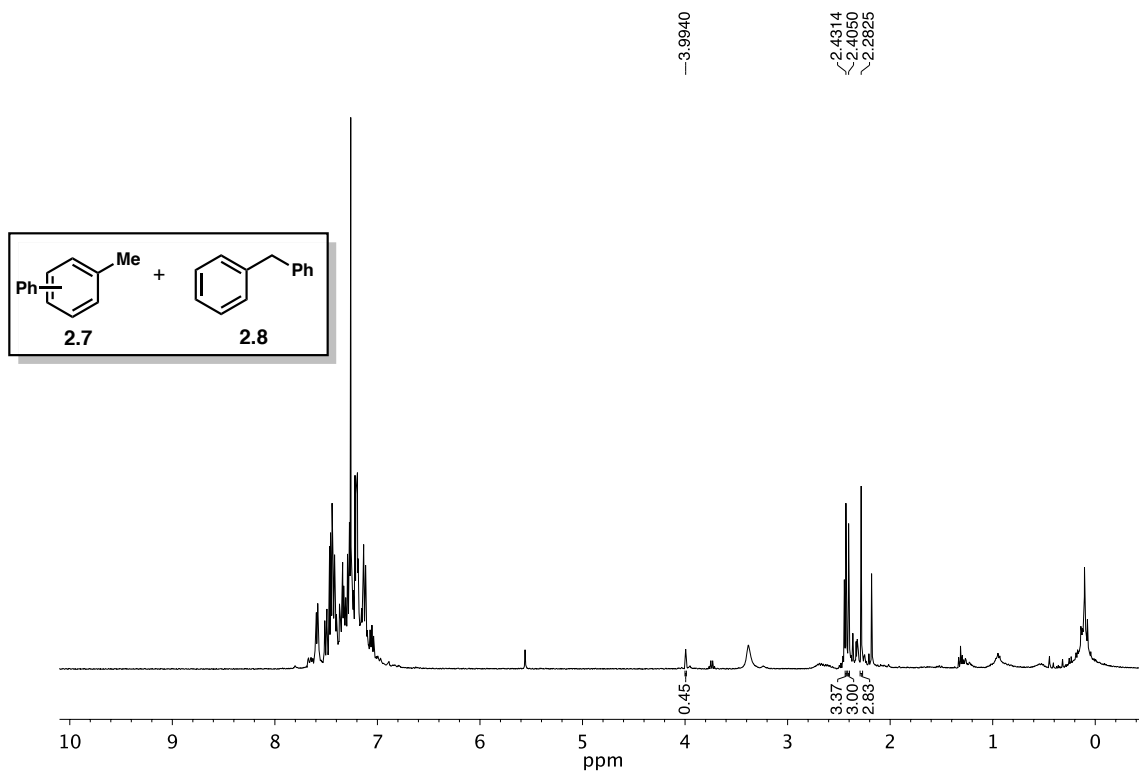
Figure 2.64  $^1\text{H}$  NMR (400 MHz,  $\text{CDCl}_3$ ) of compound 2.39.



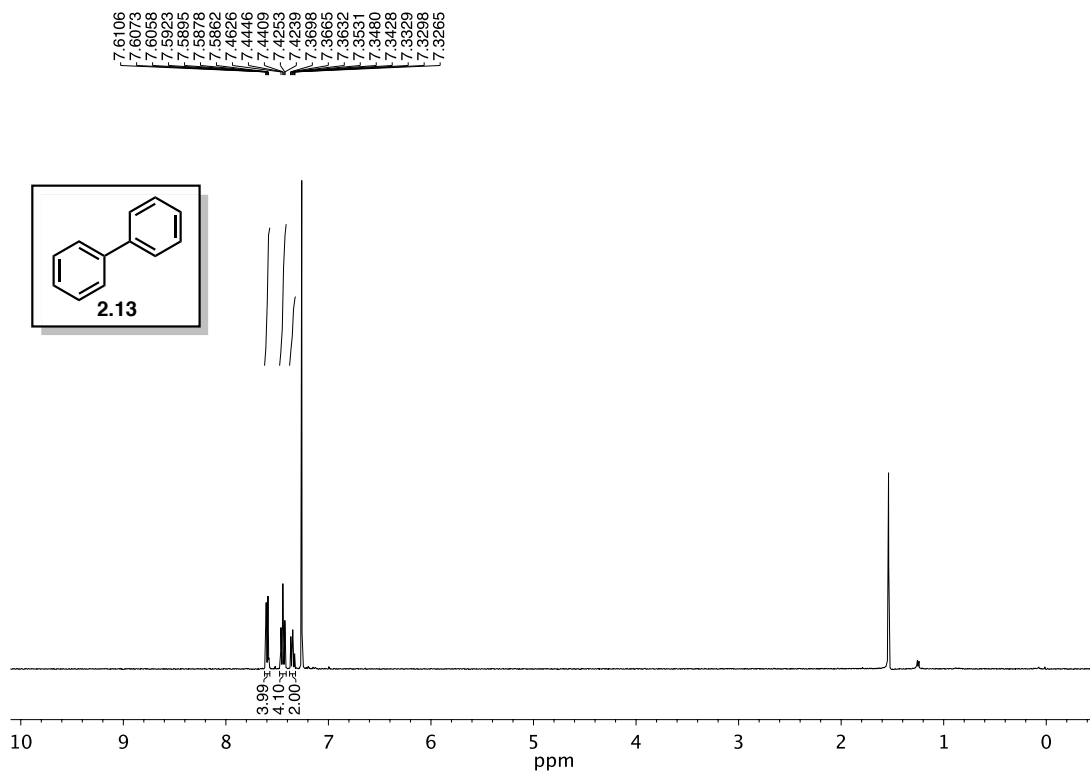
**Figure 2.65**  $^{13}\text{C}$  NMR (100 MHz,  $\text{CDCl}_3$ ) of compound **2.39**.



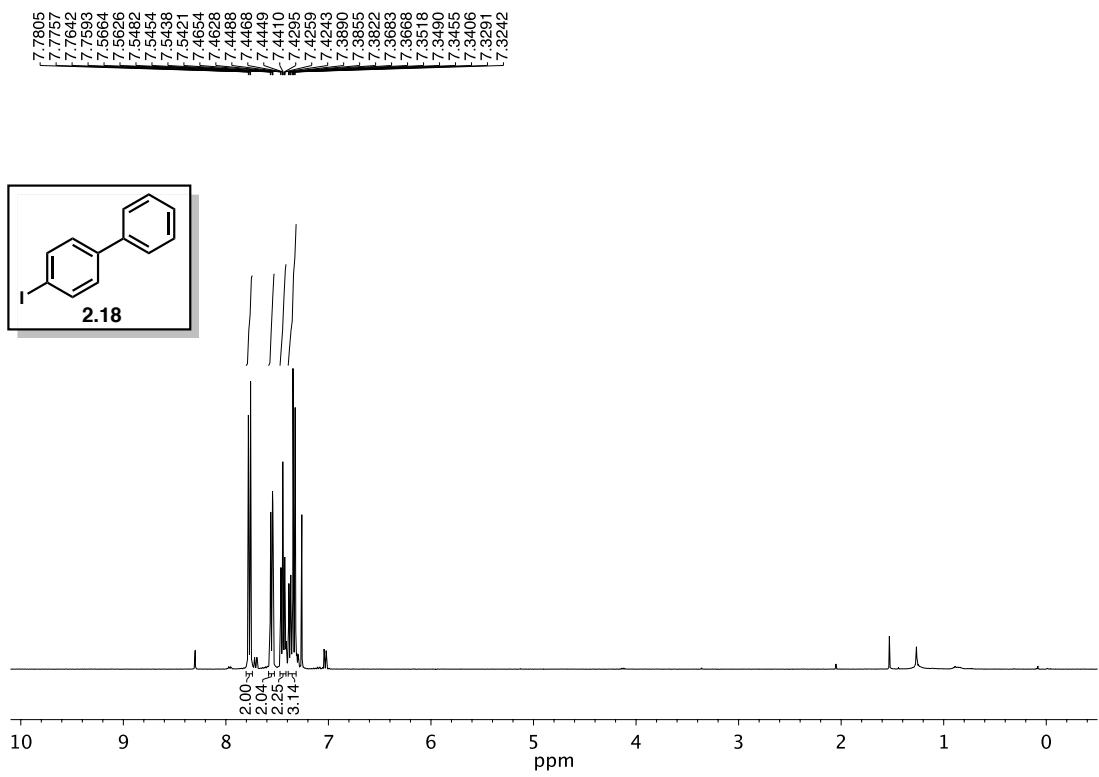
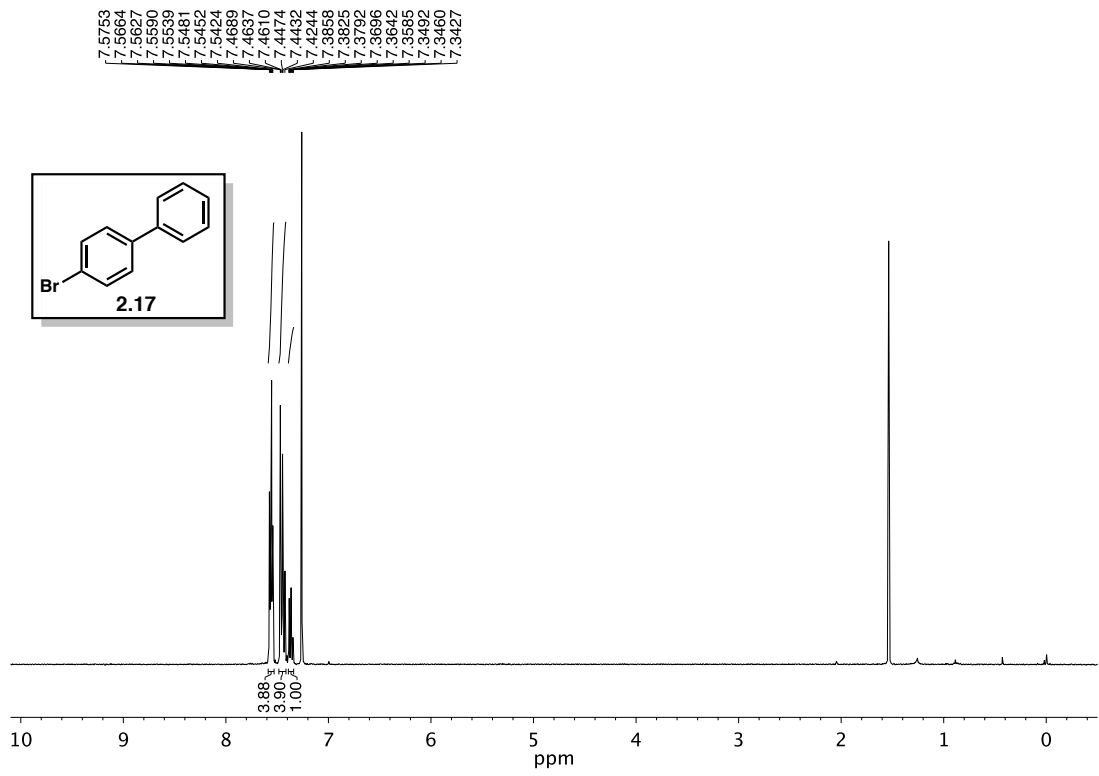
**Figure 2.66**  $^{19}\text{F}$  NMR (376 MHz,  $\text{CDCl}_3$ ) of compound **2.39**.



**Figure 2.67**  $^1\text{H}$  NMR (400 MHz,  $\text{CDCl}_3$ ) of compound **2.7** and **2.8**.



**Figure 2.68**  $^1\text{H}$  NMR (400 MHz,  $\text{CDCl}_3$ ) of compound **2.13**.



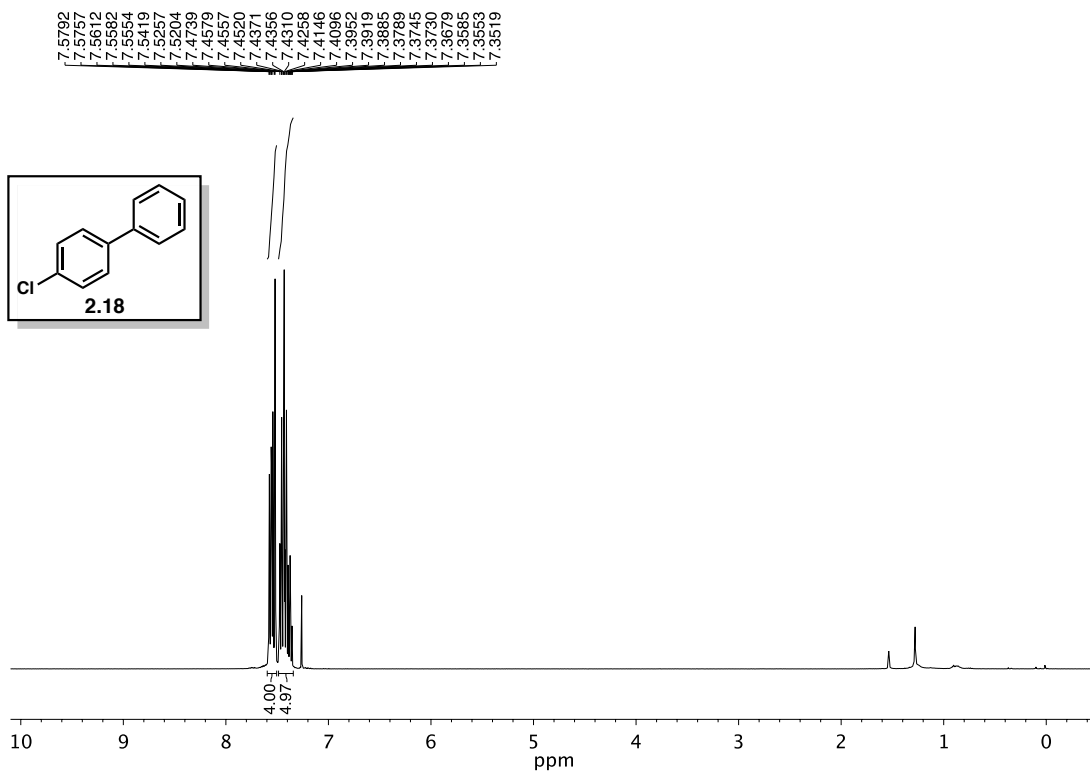


Figure 2.71  $^1\text{H}$  NMR (400 MHz,  $\text{CDCl}_3$ ) of compound 2.19.

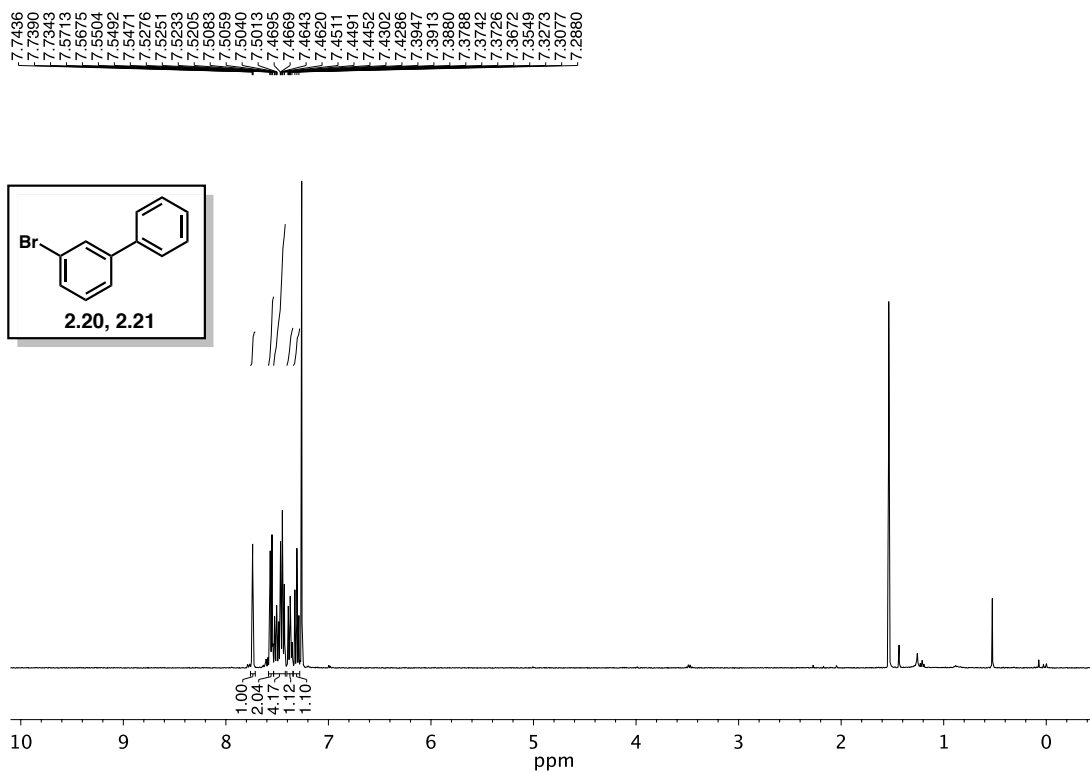
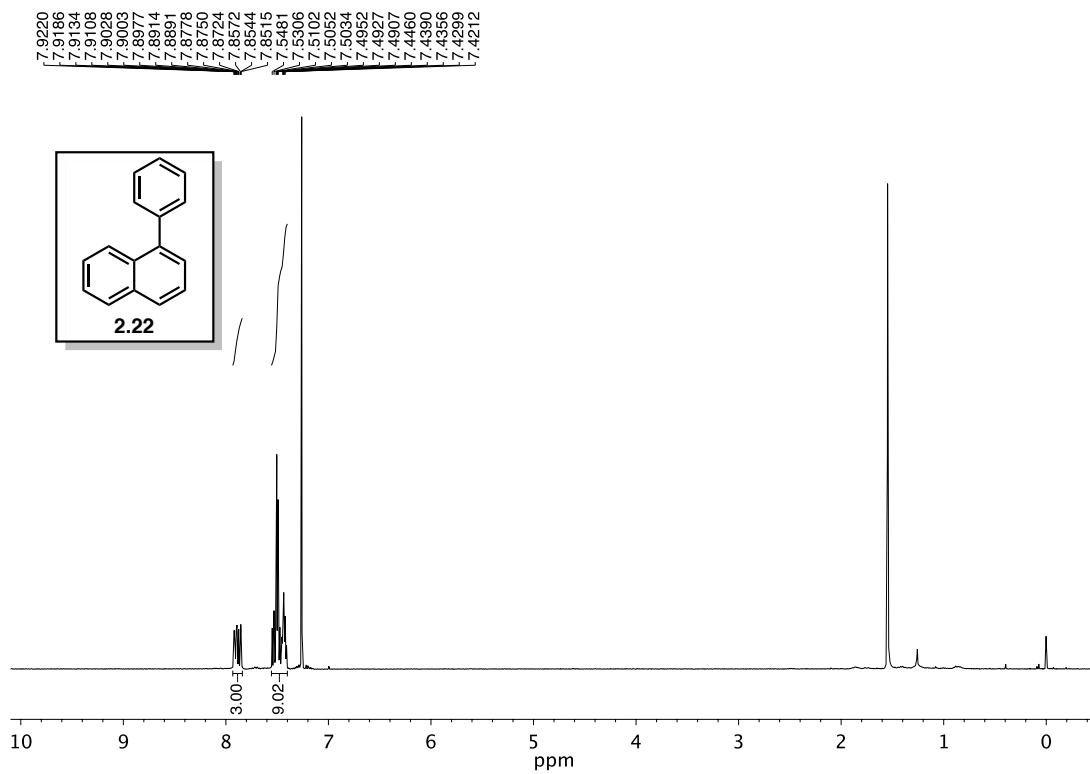
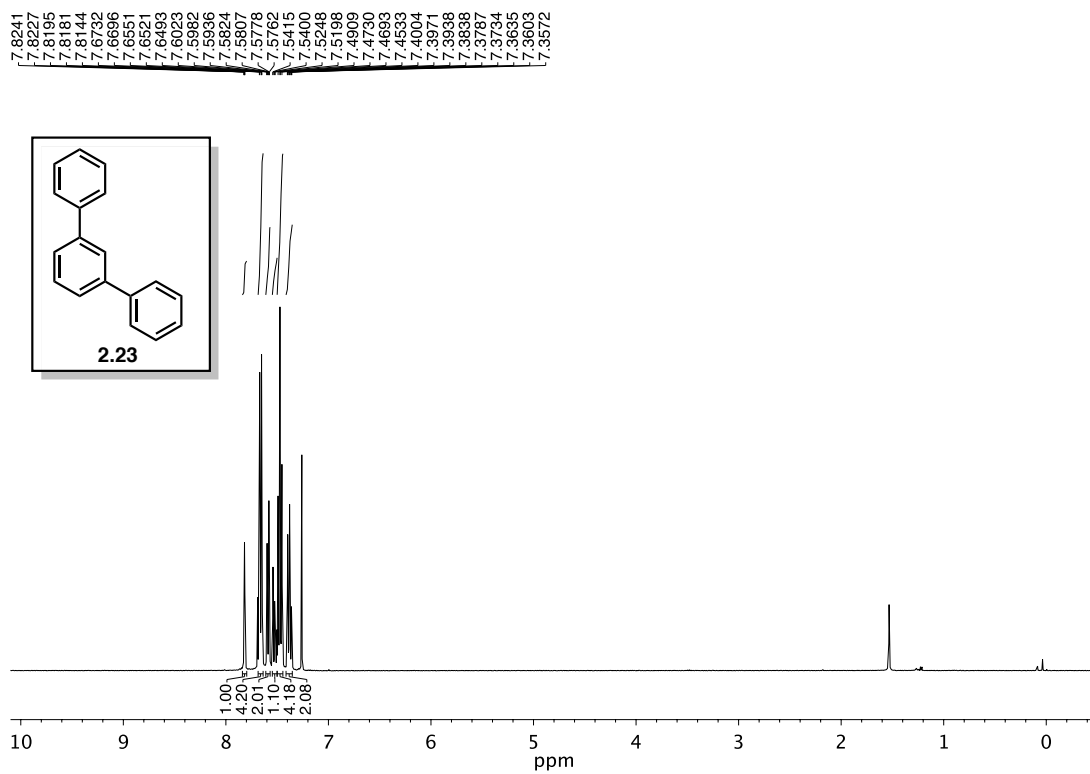


Figure 2.72  $^1\text{H}$  NMR (400 MHz,  $\text{CDCl}_3$ ) of compound 2.20, 2.21.





**Figure 2.73**  $^1\text{H}$  NMR (400 MHz,  $\text{CDCl}_3$ ) of compound **2.22**.



**Figure 2.74**  $^1\text{H}$  NMR (400 MHz,  $\text{CDCl}_3$ ) of compound **2.23**.

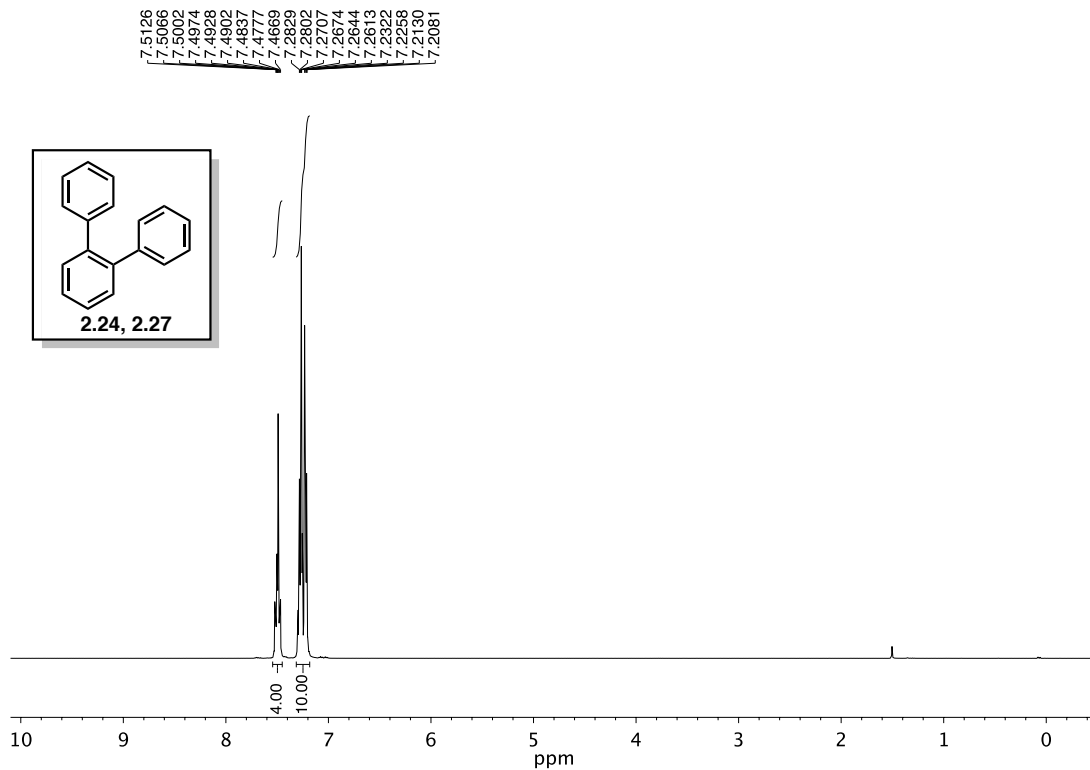


Figure 2.75  $^1\text{H}$  NMR (400 MHz,  $\text{CDCl}_3$ ) of compound 2.24, 2.27.

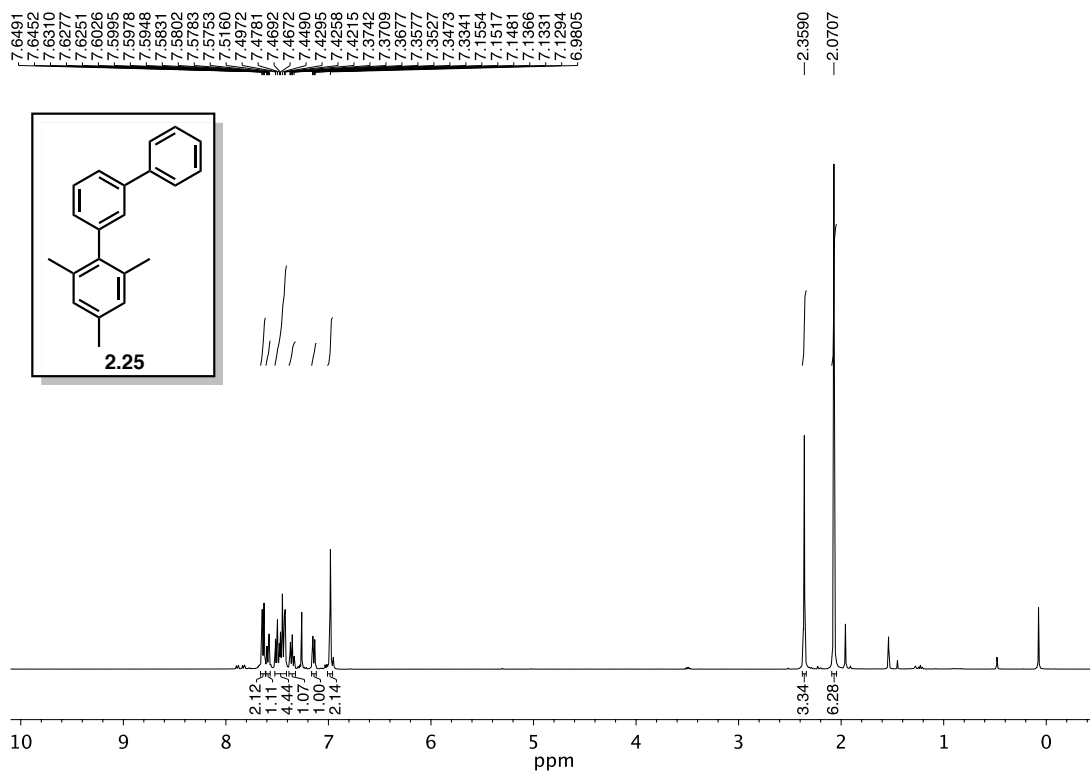


Figure 2.76  $^1\text{H}$  NMR (400 MHz,  $\text{CDCl}_3$ ) of compound 2.25.

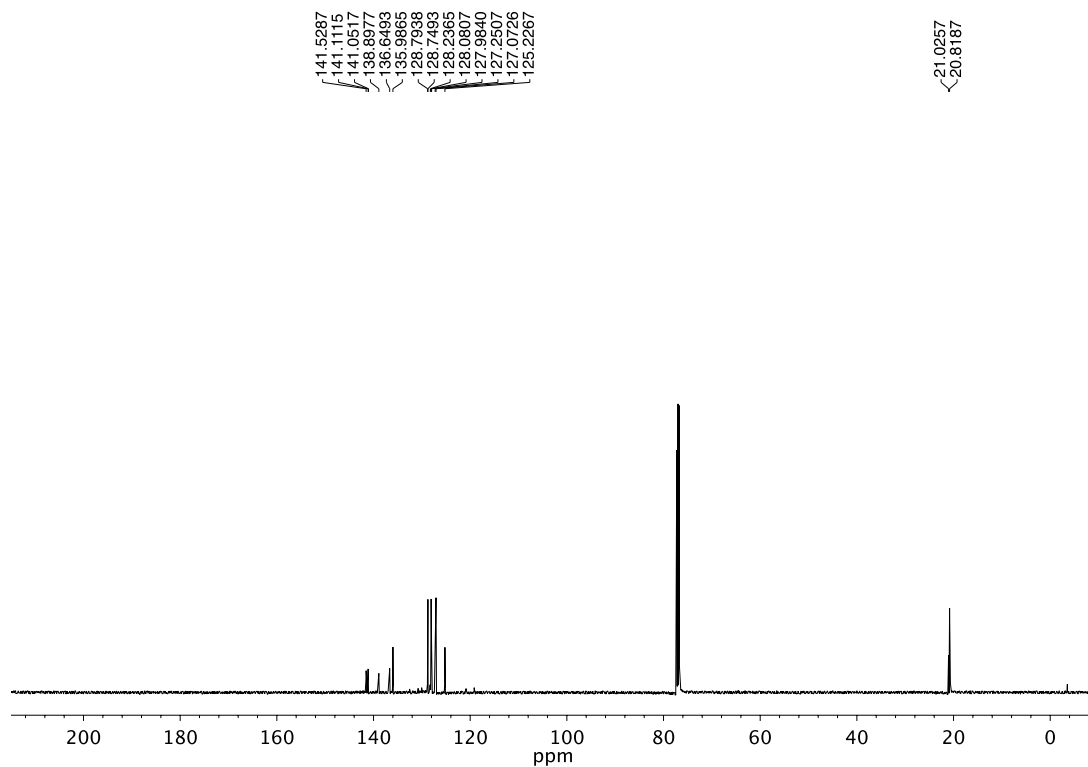


Figure 2.77  $^{13}\text{C}$  NMR (125 MHz,  $\text{CDCl}_3$ ) of compound 2.25.

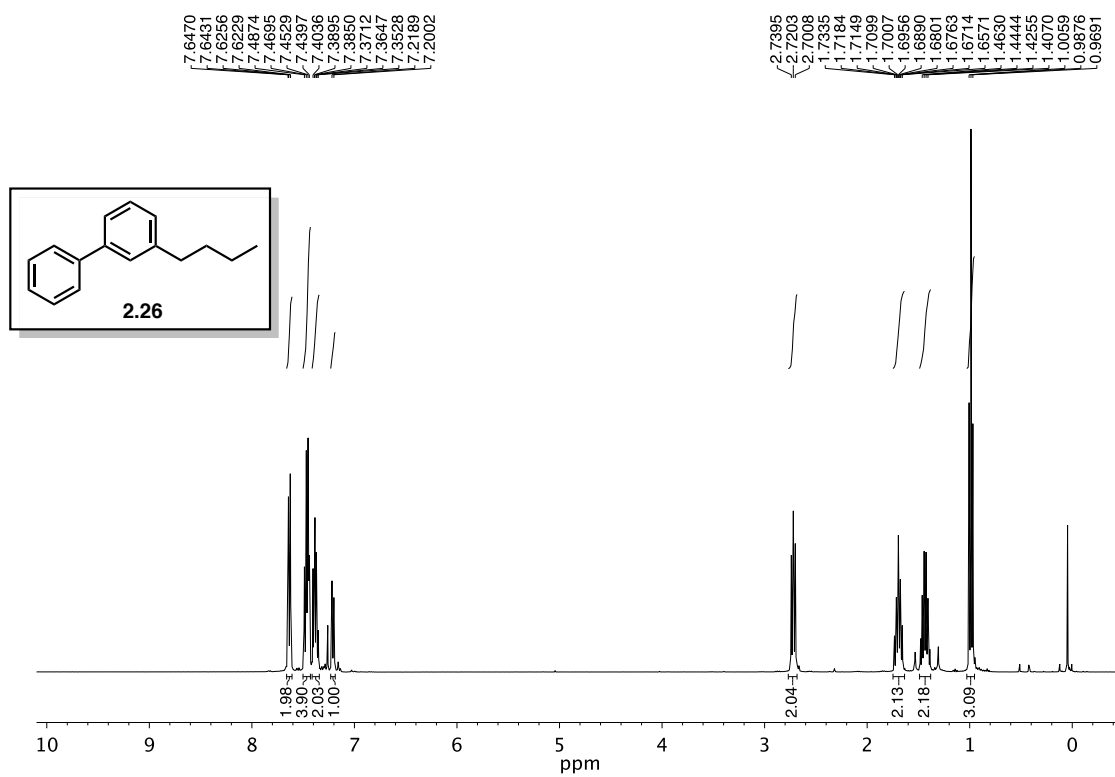


Figure 2.78  $^1\text{H}$  NMR (400 MHz,  $\text{CDCl}_3$ ) of compound 2.26.

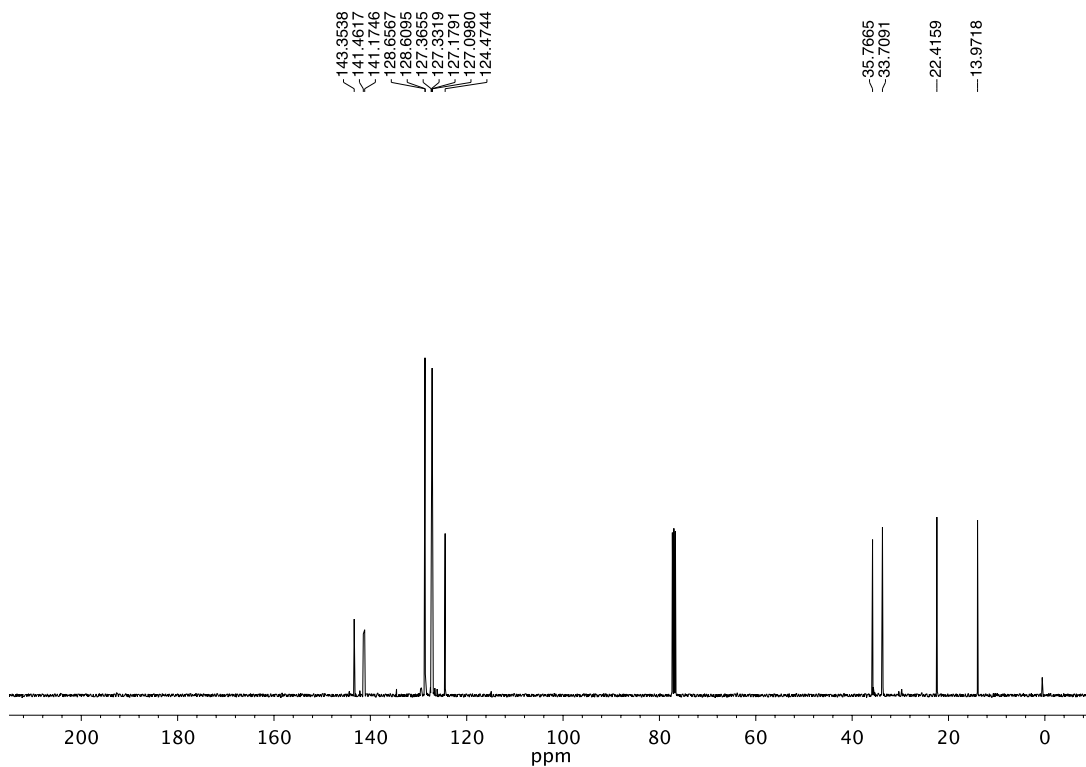


Figure 2.79  $^{13}\text{C}$  NMR (100 MHz,  $\text{CDCl}_3$ ) of compound 2.26.

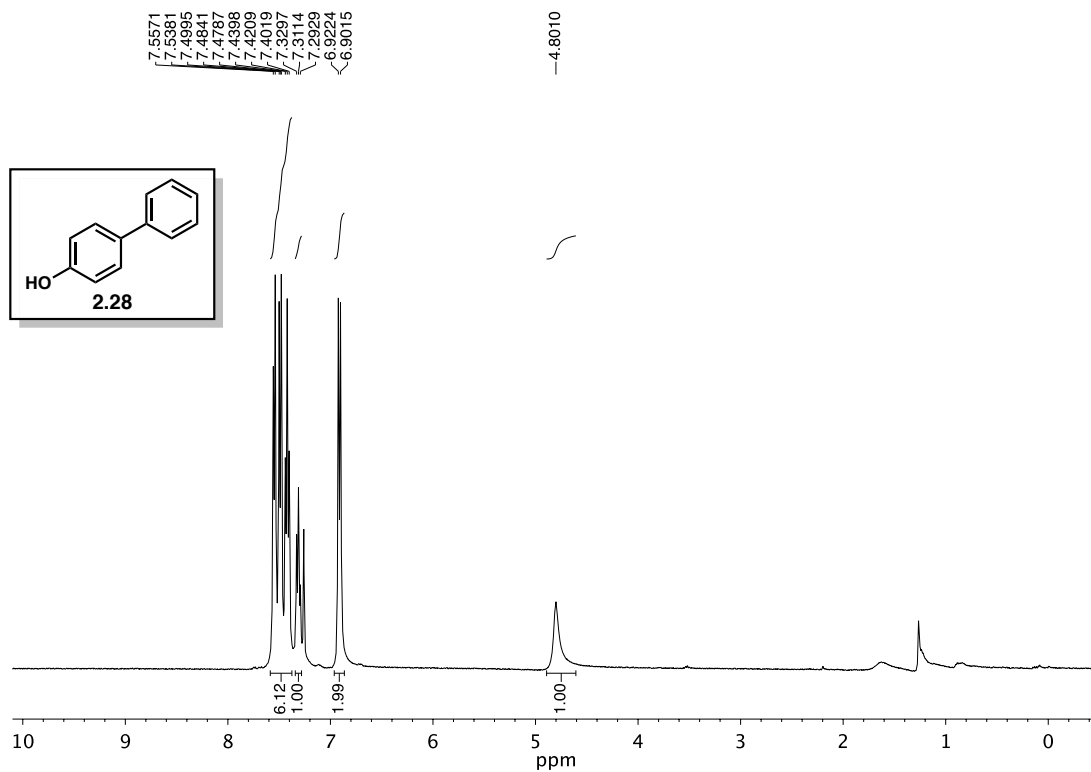


Figure 2.80  $^1\text{H}$  NMR (400 MHz,  $\text{CDCl}_3$ ) of compound 2.28.

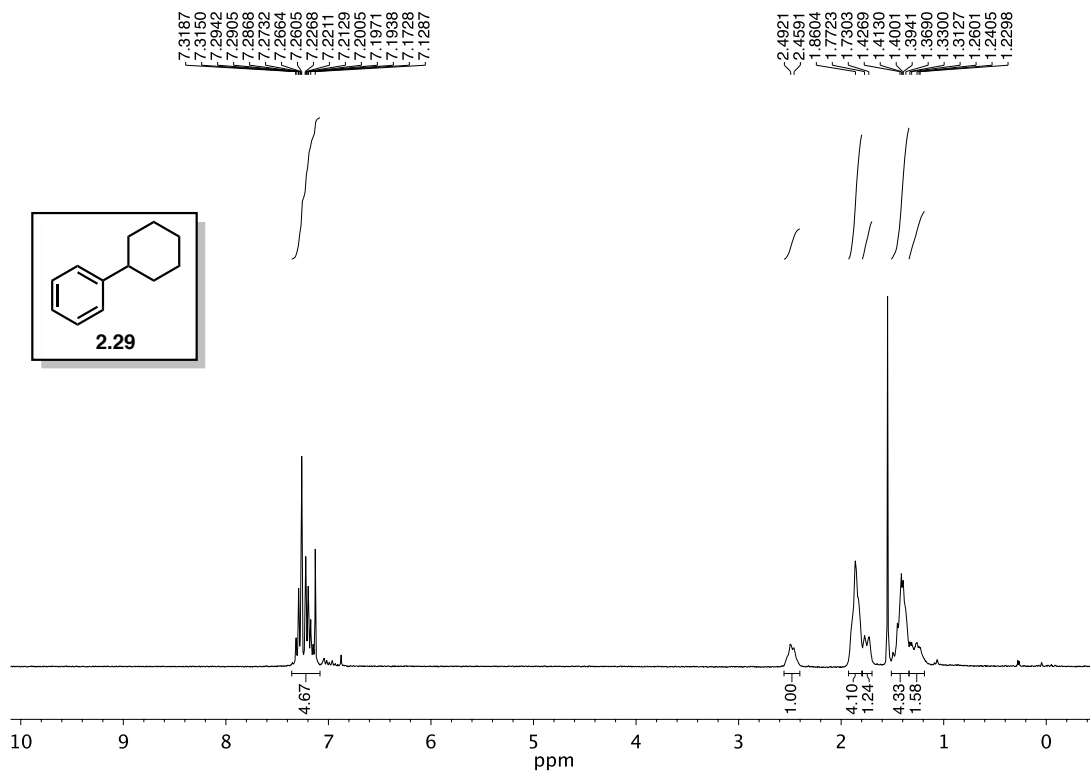


Figure 2.81 <sup>1</sup>H NMR (400 MHz, CDCl<sub>3</sub>) of compound 2.29.

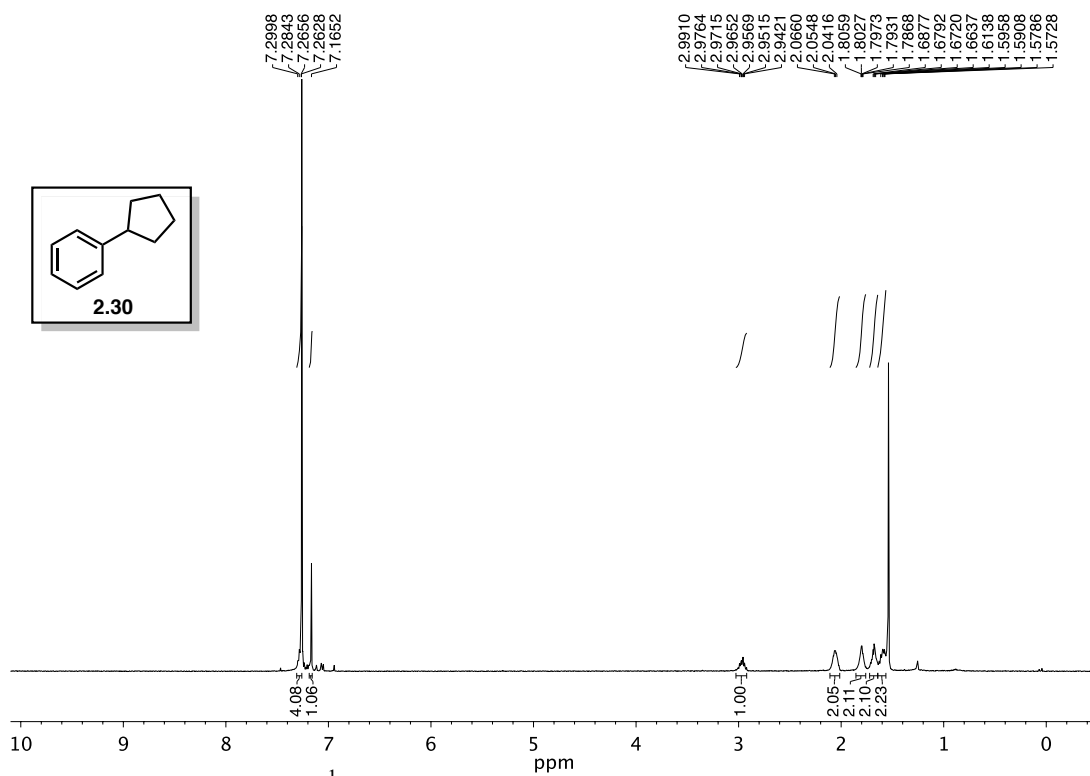
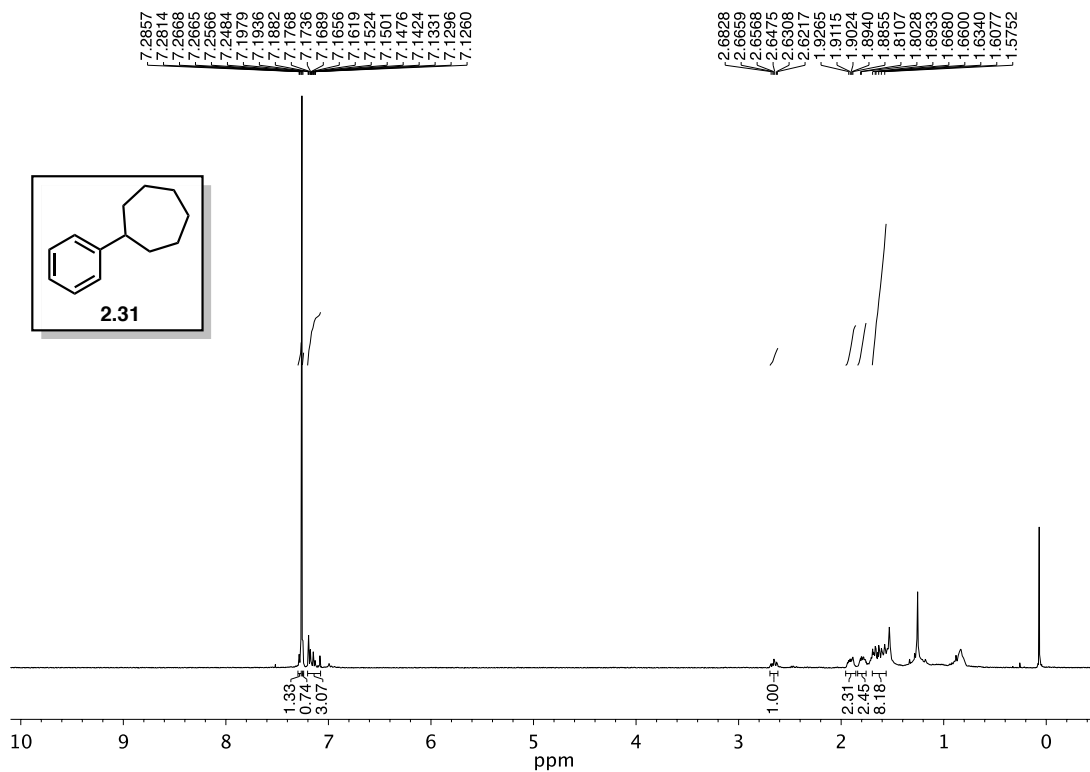
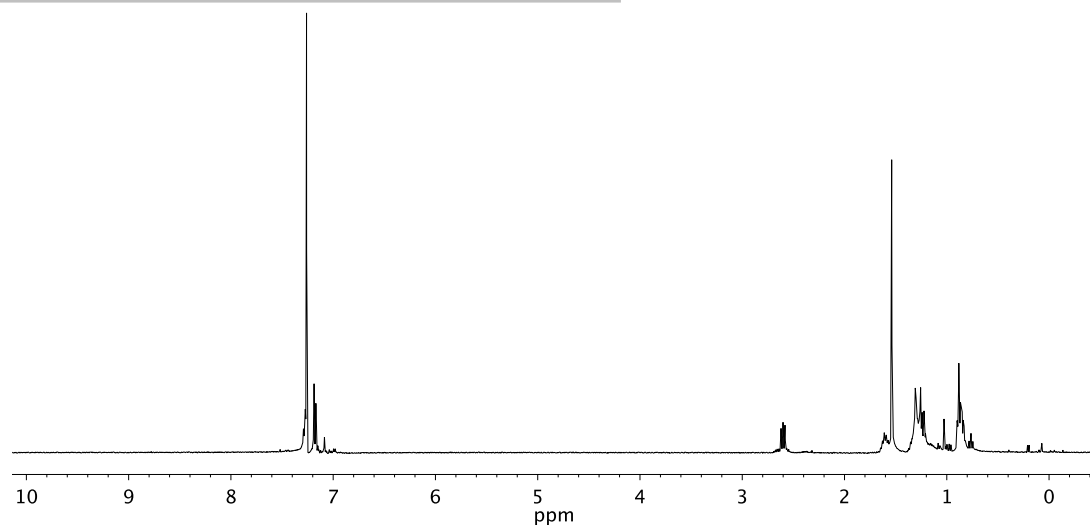
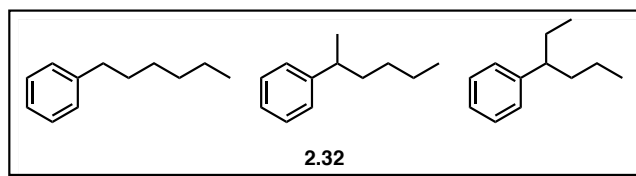


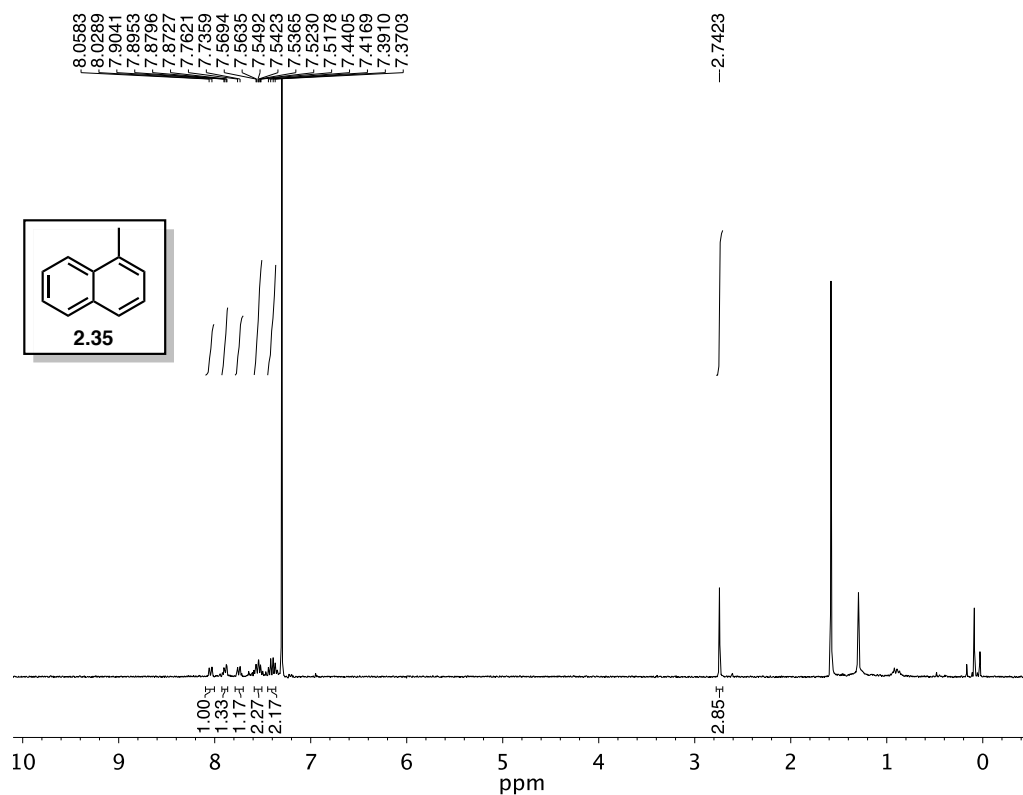
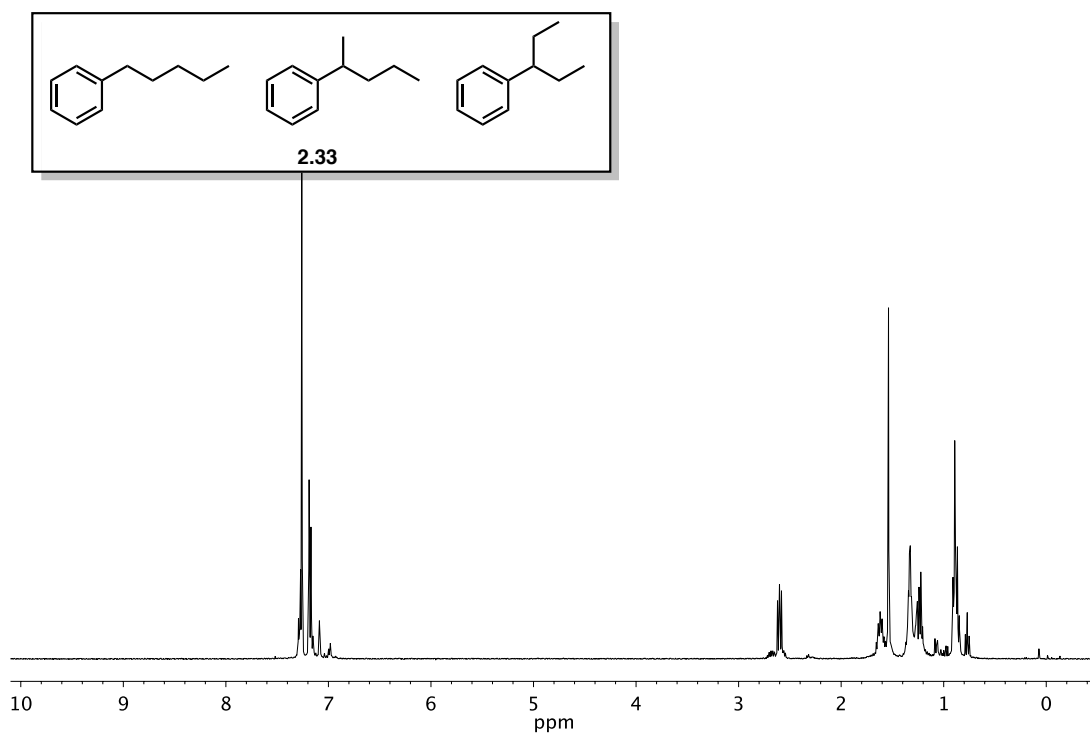
Figure 2.82 <sup>1</sup>H NMR (500 MHz, CDCl<sub>3</sub>) of compound 2.30.



**Figure 2.83**  $^1\text{H}$  NMR (400 MHz,  $\text{CDCl}_3$ ) of compound 2.31.



**Figure 2.84**  $^1\text{H}$  NMR (400 MHz,  $\text{CDCl}_3$ ) of compound 2.32.



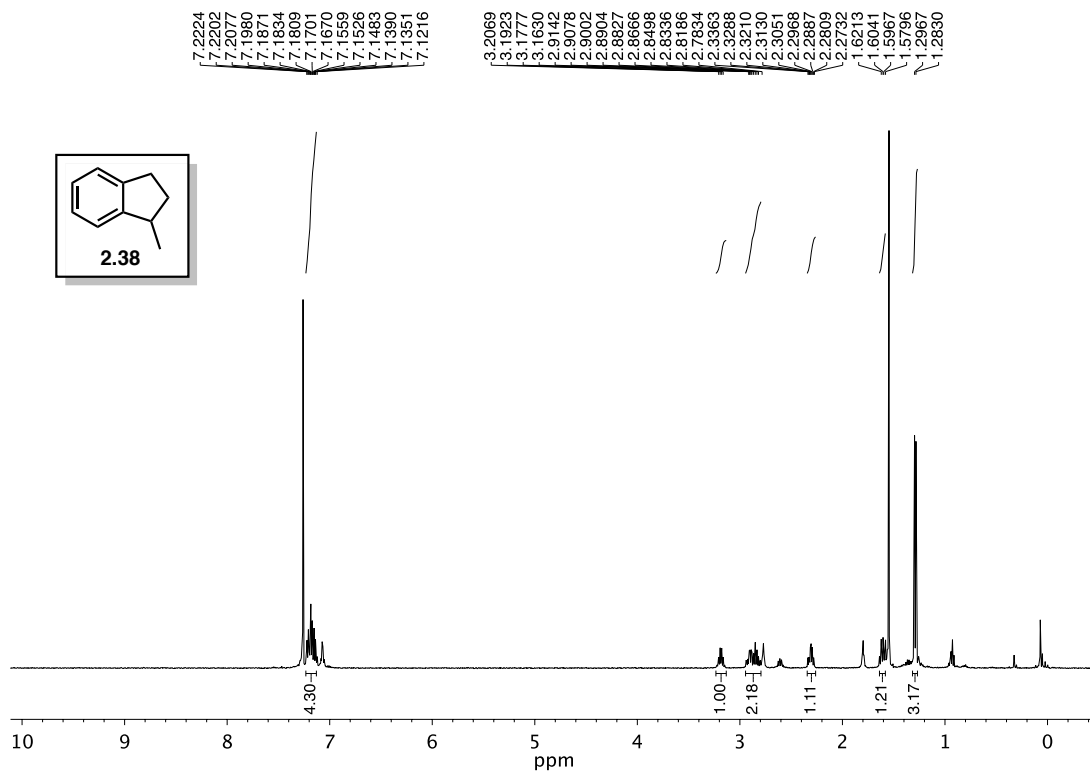


Figure 2.87  $^1\text{H}$  NMR (500 MHz,  $\text{CDCl}_3$ ) of compound 2.38.

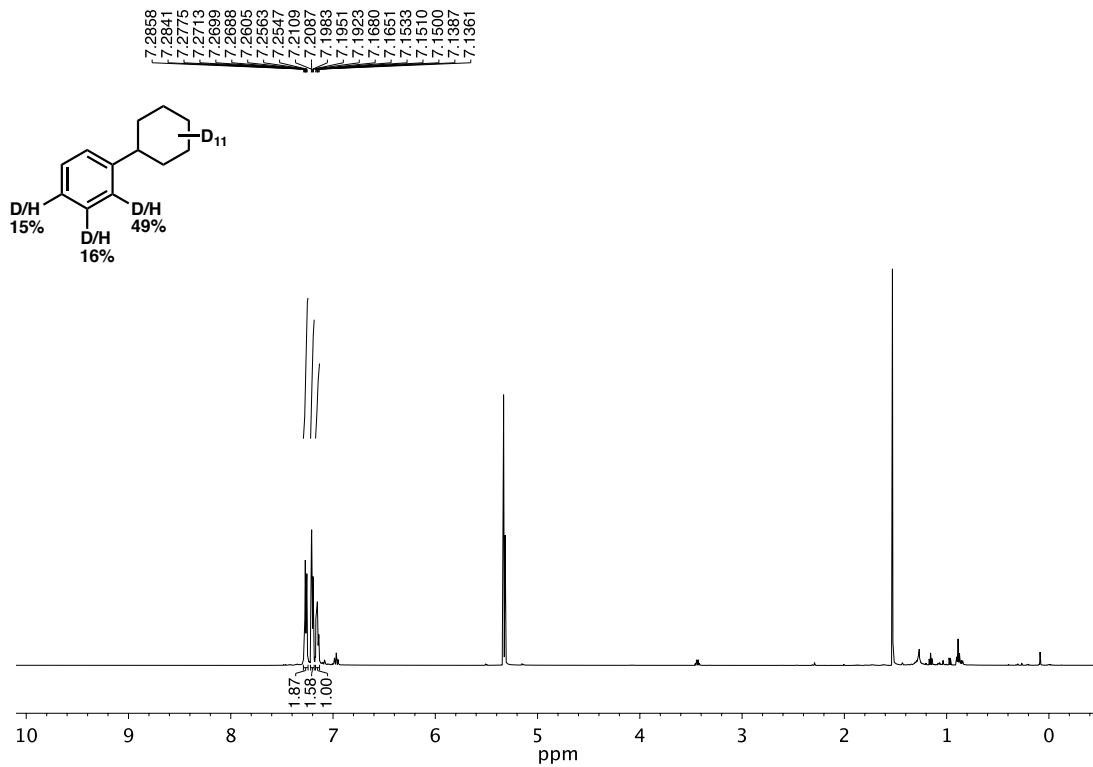


Figure 2.88  $^1\text{H}$  NMR (500 MHz,  $\text{CDCl}_3$ ) of compound 2.43.



## 2.9 Notes and References

- (1) Müller, T.; Juhasz, M.; Reed, C. A. *Angew. Chem. Int. Ed.* **2004**, *43*, 1543–1546.
- (2) Duttwyler, S., et al. *Angew. Chem.* **2010**, *122*, 7681–7684.
- (3) For reviews on the monocarborane clusters, see: (a) Körbe, S.; Schreiber, P. J.; Michl, J. *Chem. Rev.* **2006**, *106*, 5208–5249. (b) Reed, C. A. *Acc. Chem. Res.* **2009**, *43*, 121–128.
- (4) Allemann, O., et al. *Science* **2011**, *332*, 574–577.
- (5) Lambert, J. B. *Tetrahedron* **1990**, *46*, 2677–2689.
- (6) For examples of cycloaddition reactivity of arynes, see: (a) Tadross, P. M.; Stoltz, B. M. *Chem. Rev.* **2012**, *112*, 3550–3577. (b) Logullo, F. M.; Seitz, A. H.; Friedman, L. *Org. Syn.* **1968**, *48*, 12.
- (7) Refer to section 2.7.
- (8) Mascarelli, L. *Gazz. Chim. Ital.* **1936**, *66*, 843–850.
- (9) Fasani, M., et al. *Chem. Commun.* **1997**, 1329–1330.
- (10) Allemann, O. Baldrige, K. K.; Siegel, J. S. *Org. Chem. Front.* **2015**, *2*, 1018–1021.
- (11) Skell, P. S.; Garner, A. V. *J. Am. Chem. Soc.* **1956**, *78*, 5430–5433.
- (12) Douvris, C.; Ozerov, O. V. *Science* **2008**, *321*, 1188–1190.
- (13) Barlett, P. D.; Condon, F. E.; Schneider, A. *J. Am. Chem. Soc.* **1944**, *66*, 1531–1539.
- (14) Shao, B.; Bagdasarian, A. L.; Popov, S.; Nelson, H. M. *Science* **2017**, *355*, 1403–1407.
- (15) Refer to section 2.6.4.
- (16) Douvris, C., et al. *J. Am. Chem. Soc.* **2010**, *132*, 4946–4953.
- (17) (a) Littke, A. F.; Fu, G. C. *Angew. Chem. Int. Ed.* **2002**, *41*, 4176–4211. (b) Blanksby, S. J.; Ellison, G. B. *Acc. Chem. Res.* **2003**, *36*, 255–263.
- (18) Refer to section 2.6.7.

- (19) Danilina, N.; Payrer, E. L.; van Bokhoven, J. A. *Chem. Commun.* **2010**, *46*, 1509–1510.
- (20) McMillen, D. F.; Golden, D. M. *Annu. Rev. Phys. Chem.* **1982**, *33*, 493–532.
- (21) (a) Cook, A. K.; Schimler, S. D.; Matzger, A. J.; Sanford, M. S. *Science* **2016**, *351*, 1421–1424. (b) Smith, K. T., et al. *Science* **2016**, *351*, 1424–1427.
- (22) Refer to section 2.6.12.
- (23) Hashiguchi, B. G., et al. *Science* **2014**, *343*, 1232–1237.
- (24) (a) Troung, T.; Daugulis, O. *J. Am. Chem. Soc.* **2011**, *133*, 4243–4245. (b) Yun, S. Y.; Wang, K. P.; Lee, N. K.; Mamidipalli, P.; Lee, D. *J. Am. Chem. Soc.* **2013**, *135*, 4668–4671.
- (25) Wada, K., et al. *J. Am. Chem. Soc.* **2003**, *125*, 7035–7048.
- (26) Fornarini, S.; Crestoni, M. E. *Acc. Chem. Res.* **1998**, *31*, 827–834.
- (27) Simmons, E. M.; Hartwig, J. F. *Angew. Chem. Int. Ed.* **2012**, *51*, 3066–3072.
- (28) Masson, E.; Schlosser, M. *Eur. J. Org. Chem.* **2005**, 4401–4405.
- (29) Ball, L. T.; Green, M.; Lloyd-Jones, G. C.; Russell, C. A. *Org. Lett.* **2010**, *12*, 4724–4727.
- (30) Heiss, C.; Marzi, E.; Mongin, F.; Schlosser, M. *Eur. J. Org. Chem.* **2007**, 669–675.
- (31) Kawamoto, T.; Sato, A.; Ryu, I. *Org. Lett.* **2014**, *16*, 2111–2113.
- (32) Zhang, H.; Wang, C.; Li, Z.; Wang, Z. *Tetrahedron Lett.* **2015**, *56*, 5371–5376.
- (33) Zhou, C.; Liu, Q.; Li, Y.; Zhang, R.; Fu, X.; Duan, C. *J. Org. Chem.* **2012**, *77*, 10468–10472.
- (34) Kan, J.; Huang, S.; Lin, J.; Zhang, M.; Su, W. *Angew. Chem. Int. Ed.* **2015**, *54*, 2199–2203.
- (35) Xu, C.; Yin, L.; Huang, B.; Liu, H.; Cai, M. *Tetrahedron* **2016**, *72*, 2065–2071.
- (36) Nakamura, K.; Yasui, K.; Tobisu, M.; Chatani, N. *Tetrahedron* **2015**, *71*, 4484–4489.
- (37) Liu, L.; Dong, Y.; Pang, B.; Ma, J. *J. Org. Chem.* **2014**, *79*, 7193–7198.

- (38) Pan, X.; Lacôte, E.; Lalevée, J.; Curran, D. P. *J. Am. Chem. Soc.* **2012**, *134*, 5669–5674.
- (39) Cahiez, G.; Chaboche, C.; Duplais, C.; Moyeux, A. *Org. Lett.* **2009**, *11*, 277–280.
- (40) Everson, D. A.; Jones, B. A.; Weix, D. J. *J. Am. Chem. Soc.* **2012**, *134*, 6146–6159.
- (41) (a) Yang, C. T.; Zhang, Z. Q.; Liu, Y. C.; Liu, L. *Angew. Chem. Int. Ed.* **2011**, *50*, 3904–3907. (b) Zhu, J.; Pérez, M.; Caputo, C. B.; Stephan, D. W. *Angew. Chem. Int. Ed.* **2016**, *55*, 1417–1421.
- (42) (a) McCann, L. C.; Hunter, H. N.; Clyburne, J. A. C.; Organ, M. G. *Angew. Chem. Int. Ed.* **2012**, *51*, 7024–7027. (b) Bedford, R. B., et al. *Chemistry* **2014**, *20*, 7935–7938. (c) Maslak, P.; Narvaez, J. N.; Kula, J.; Malinski, D. S. *J. Org. Chem.* **1990**, *55*, 4550–4559.
- (43) Joseph, J. T., et al. *Tetrahedron Lett.* **2015**, *56*, 5106–5111.

## CHAPTER THREE

### Teaching an Old Carbocation New Tricks: Intermolecular C–H Insertion Reactions of Vinyl Carbocations

Adapted from: Stasik Popov, Brian Shao, Alex L. Bagdasarian, Tyler R. Benton, Luyi Zou, Zhongyue Yang, K. N. Houk, and Hosea M. Nelson

*Science*, **2018**, *361*, 381–387.

#### 3.1 Abstract

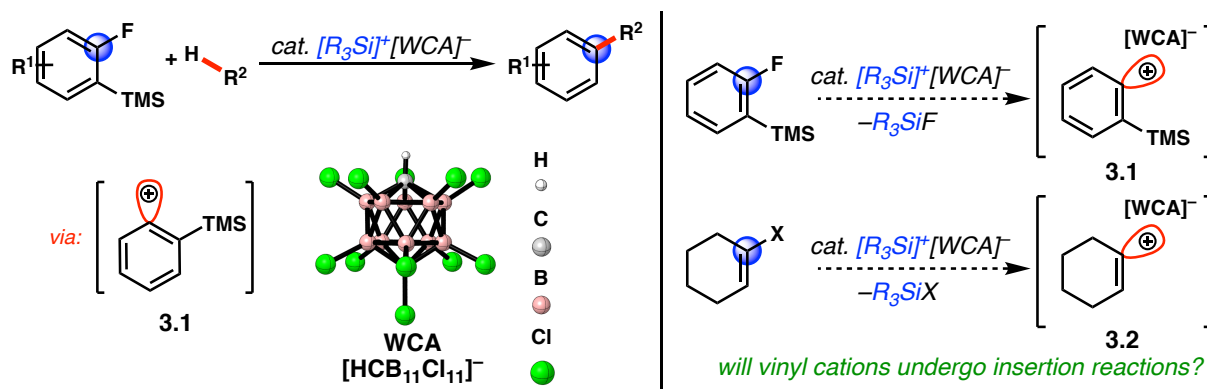
Vinyl carbocations have been the subject of extensive experimental and theoretical studies over the past five decades. Despite this long history in chemistry, the utility of vinyl cations in chemical synthesis has been limited, with most reactivity studies focusing on solvolysis reactions or intramolecular processes. Here, we report synthetic and mechanistic studies of vinyl cations generated through silylium/weakly coordinating anion (WCA) catalysis. We find that these reactive intermediates undergo mild intermolecular C–C bond forming reactions, including C–H insertion into unactivated  $sp^3$  C–H bonds and reductive Friedel–Crafts reactions with arenes. Moreover, we conducted extensive mechanistic investigations into the key C–H insertion event through experimental design. This reaction manifold provides a framework for the catalytic functionalization of hydrocarbons using simple ketone derivatives.

#### 3.2 Introduction

Our findings in the development of intermolecular  $sp^3$  C–H insertion chemistry of phenyl cations (**3.1**) led us to hypothesize about other members of the dicoordinate carbocation family.<sup>1</sup> Since they are “locally” isoelectronic to aryl cations, we naturally looked toward vinyl cations

(**3.2**) as a possible candidate for accessing similar C–H insertion reactivity (Scheme **3.1**). Challenging this hypothesis was a lack of substantial precedent for this mode of reactivity, despite the extensive experimental studies of vinyl cations over the past five decades. The vast majority of reactivity studies focused on solvolysis reactions using polar protic solvents.<sup>2</sup> This limitation has largely prevented the observation of insertion reactions due to the difficulty in generating vinyl cations and the infallible attack by polar, heteroatom-containing solvents on the cationic carbon of the vinyl cation (refer to Chapter one).

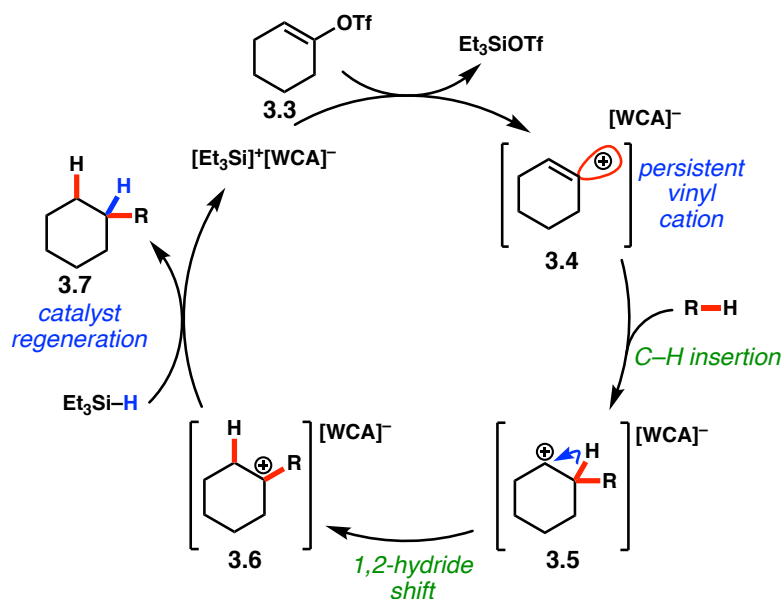
**Scheme 3.1** Inspiration for Initial Vinyl Cation Reactivity Studies



More recently, Metzger and Brewer have independently proposed the intramolecular C–H insertion of vinyl cations generated from alkynes or diazo compounds in solution.<sup>3,4</sup> While these examples relied on the use of stoichiometric Lewis acid and/or highly engineered substrates, it did grant us additional confidence in the feasibility of our proposed intermolecular vinyl cation insertion chemistry (Scheme **3.1**). We drew on our phenyl cation studies using silylium catalysis to realize our new reactivity goals.<sup>1</sup> Moreover, literature precedent informed us that vinyl triflates are superior precursors for vinyl cation generation, leading us to use cyclohexenyl triflate (**3.3**) as our base substrate.<sup>5</sup>

In this scenario, silylium-mediated ionization of vinyl triflate **3.3** would generate a kinetically persistent vinyl cation-WCA pair (**3.4**, Figure 3.1). Insertion of this reactive dicoordinate cation (**3.4**) into an alkane C–H bond would lead to formation of alkyl carbocation **3.5**. A 1,2-hydride shift would lead to the more stable tertiary cation (**3.6**) that, upon reduction by a sacrificial silane,<sup>6</sup> would generate the functionalized hydrocarbon product **3.7** and regenerate the silylium-carborane initiator.

**Figure 3.1** Proposed Catalytic Cycle for C–H Insertion of Vinyl Cations.



### 3.3 Development of Intermolecular C–H insertion Reactions of Vinyl Cations

We were pleased to find that exposure of cyclohexenyl triflate (**3.3**) to 1.5 equivalents of triethylsilane and 2 mol%  $[\text{Ph}_3\text{C}]^+[\text{HCB}_{11}\text{Cl}_{11}]^-$  in dried cyclohexane solvent at 30 °C in a nitrogen filled glovebox resulted in the formation of cyclohexylcyclohexane (**3.8**, Table 3.1) in 87% yield, after 90 minutes.<sup>7</sup> Intrigued by the remarkably mild conditions employed in this alkane alkylation reaction, we undertook a brief study of scope to further elucidate potential

synthetic applications and to gain mechanistic insight. Cycloheptane and n-pentane also reacted efficiently with the cyclohexenyl cations, albeit with poor regioselectivity in the latter case (**3.9**, **3.10**). Although cyclohexenyl triflates bearing substituents at the 2- or 6-positions led to complex mixtures of products, presumably due to non-productive unimolecular decompositions,<sup>8</sup> other positions of the cyclohexenyl ring were tolerant of substitution. For example, exposure of the enol triflate derived from 5 $\alpha$ -cholestan-3-one (**3.11**) to our reaction conditions led to formation of the alkylated steroid **3.12** in 88% yield and 15:1 diastereomeric ratio (*d.r.*). Analogous to the previously reported ring-contraction reactions of medium-sized cyclic vinyl triflates,<sup>9</sup> exposure of cyclooctenyl triflate (**3.13**) to our optimized reaction conditions led to rapid transannular C–H insertion to yield bicyclo[3.3.0]octane (**3.14**).

**Table 3.1** Reductive Alkylation Reactions of Vinyl Triflates and Alkanes.<sup>a</sup>

Entry	Substrate	Solvent	Product	Yield (%), Time (h)
1	 3.3	C <sub>6</sub> H <sub>12</sub>	 3.8	87 <sup>b</sup> , 1.5
2	 3.3	C <sub>7</sub> H <sub>14</sub>	 3.9	88 <sup>b</sup> , 2
3	 3.3	n-C <sub>5</sub> H <sub>12</sub>	 3.10	68 <sup>b</sup> , 1.5 (21:36:11)
4	 3.11	C <sub>6</sub> H <sub>12</sub>	 3.12	88 <sup>c</sup> , 3 (15:1 d.r.)
5	 3.13	C <sub>6</sub> H <sub>12</sub>	 3.14	91 <sup>b</sup> , 1

<sup>a</sup> Reactions performed at 0.1 M. <sup>b</sup> Yield determined by GC-FID with nonane as an internal standard. <sup>c</sup> Isolated Yield.

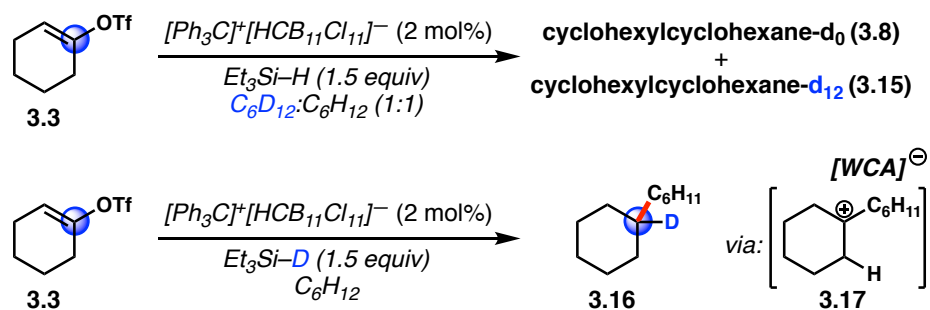
### 3.4 Deuterium Labeling Studies

Deuterium labeling studies were carried out to further probe the nature of the key C–H insertion mechanism of vinyl carbocations. First, competition experiments using a 1:1 mixture of C<sub>6</sub>H<sub>12</sub>:C<sub>6</sub>D<sub>12</sub> provided a 1:1 mixture of cyclohexylcyclohexane-d<sub>0</sub> (**3.8**) and cyclohexylcyclohexane-d<sub>12</sub>, (**3.15**) supporting a concerted reaction pathway and ruling out a rate-limiting C–H insertion event (Scheme 3.2). Use of triethylsilane-d<sub>1</sub> with cyclohexane and



cyclohexenyl triflate (**3.3**) resulted in high levels of deuterium incorporation at the tertiary carbon of alkane product **3.16**, supporting the formation of a persistent 3° carbocation (**3.17**). However, this experiment does not differentiate a 1,1- from a 1,2-insertion mechanism; the 2° carbocation (**3.5**) formed *via* 1,1-insertion will always proceed to the more stable 3° carbocation **3.6** (Figure 3.1). To tease apart these different C–H insertion mechanisms, we hypothesized that a vinyl triflate precursor capable of generating a 3-substituted cyclohexenyl vinyl cation **3.18** would allow us to distinguish between a 1,1- and a 1,2-insertion through competitive hydride and deuteride shifts (Scheme 3.3). Several mechanistic probe substrates were synthesized in hopes to test this hypothesis. While the 3-ethyl- (**3.19**) and 3-cyclohexylcyclohexenyl triflates (**3.20**) revealed promising signs of qualitative hydride/deuteride scrambling along C1 to C3, quantitative analysis of these products proved difficult. The nearly identical characteristics of each proton/deuterium and carbon in these two previous alkane examples pushed us to explore substrates with more chemically distinguishable substituents.

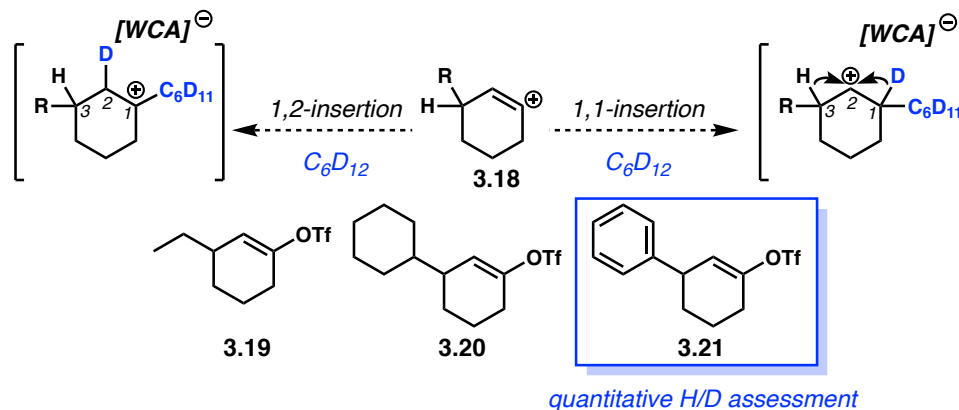
**Scheme 3.2** Initial Deuterium Labeling Studies of Triflate **3.3**



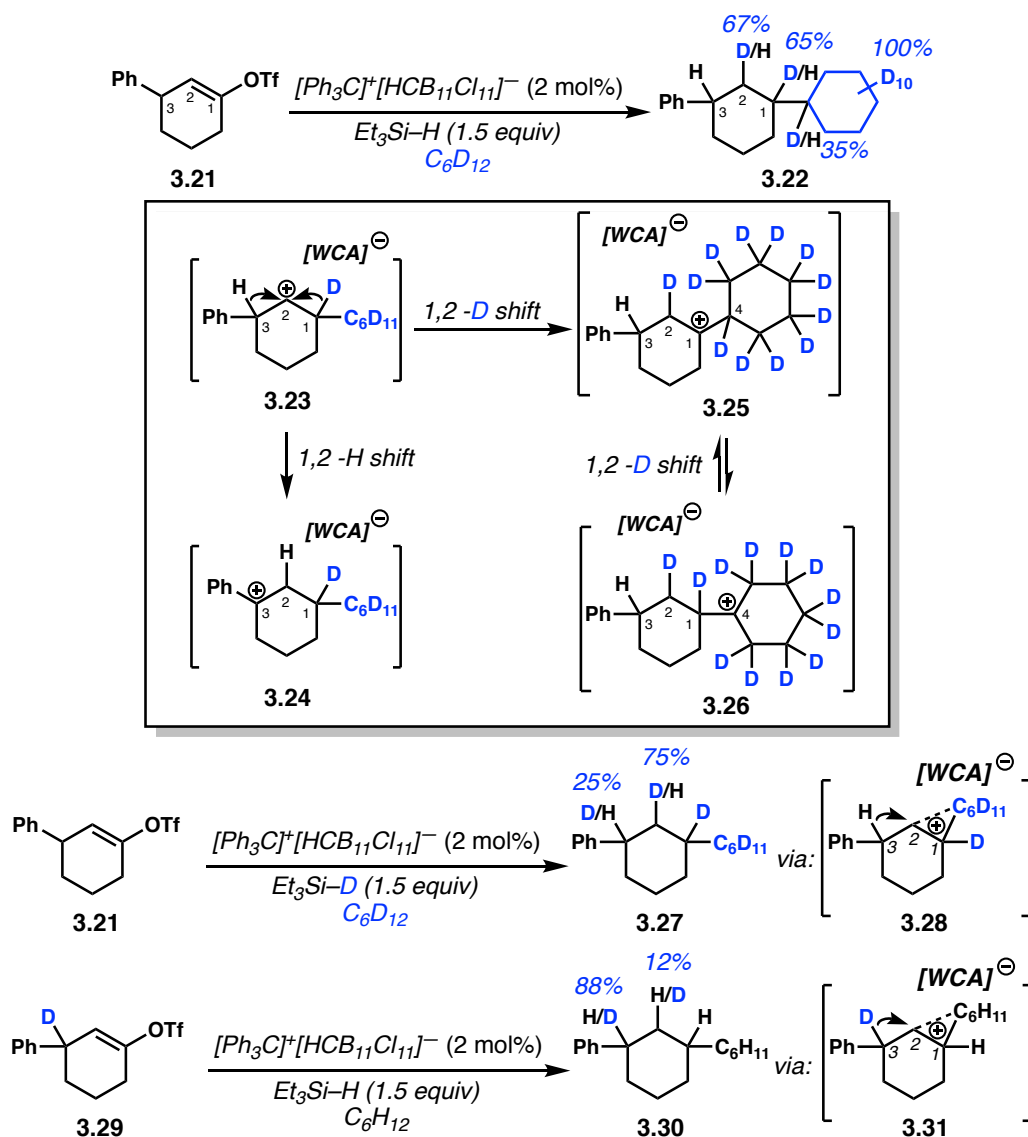
We then prepared 3-phenylcyclohexenyl triflate **3.21** in the hope that migration of the benzylic C3-hydride of carbocation intermediate **3.23** would be competitive with C1-deuteride migration, allowing for direct experimental evidence of a 1,1-insertion event (Scheme 2.4). Upon exposure of triflate **3.21** to our reaction conditions, using cyclohexane-d<sub>12</sub> solvent and triethylsilane, we observed 67% deuterium incorporation at C2, 65% at C1, and 35% at C4

(**3.22**). In total, we observed 1.6 deuterides incorporated at these three carbons (C1, C2 and C4), accounting for 80% of the two cyclohexane-d<sub>12</sub> deuterides prone to migration. Here we postulate that following 1,1-insertion, C3-hydride migration produces benzylic cation **3.24**, whereas C1-deuteride migration leads to tertiary C1 and C4 carbons **3.25** and **3.26**, respectively. All four cations (**3.24** to **3.26**) can be quenched by terminal silane. Further confirming migration of the C3-benzylic H, using C<sub>6</sub>D<sub>12</sub> and triethylsilane-d<sub>1</sub>, we observed 75% deuterium incorporation at C2 and 25% deuterium incorporation at C3 (**3.27**, Scheme **2.4**). The observation of D incorporation at the C3-carbon suggests a 1,2-hydride migration to quench a transient cation (**3.28**) that results from a 1,1-insertion event. Moreover, use of C3-deuterated substrate **3.29** with C<sub>6</sub>H<sub>12</sub> leads to D-incorporation at C2 (*ca.* 12%), further supporting the migration of the benzylic deuteride to quench the carbocation (**3.31**) generated upon insertion. The lower levels of C2 deuteride incorporation in product **3.30** can be attributed to kinetic isotope effects, as the C3-deuteride in **3.28** will migrate slower than the C3-hydride in cation **3.31**, whereas the C1 hydride of cation **3.28** will migrate faster in this system than the deuteride of transient **3.31**.<sup>10</sup> The fact that less migration of the benzylic C3 hydride is observed over the tertiary C1 hydride supports the computational findings performed by the Houk group, wherein a discrete classical secondary cation is not formed due to the nonclassical nature of our reaction. A full article with detailed discussions on computational studies done to probe the nonclassicality of our vinyl cation reactions can be viewed in our group's publication.<sup>7</sup>

**Scheme 3.3** Design of Mechanistic Probe Substrates



**Scheme 3.4** Deuterium Labeling Experiments in Support of 1,1-C–H Insertion Pathway.

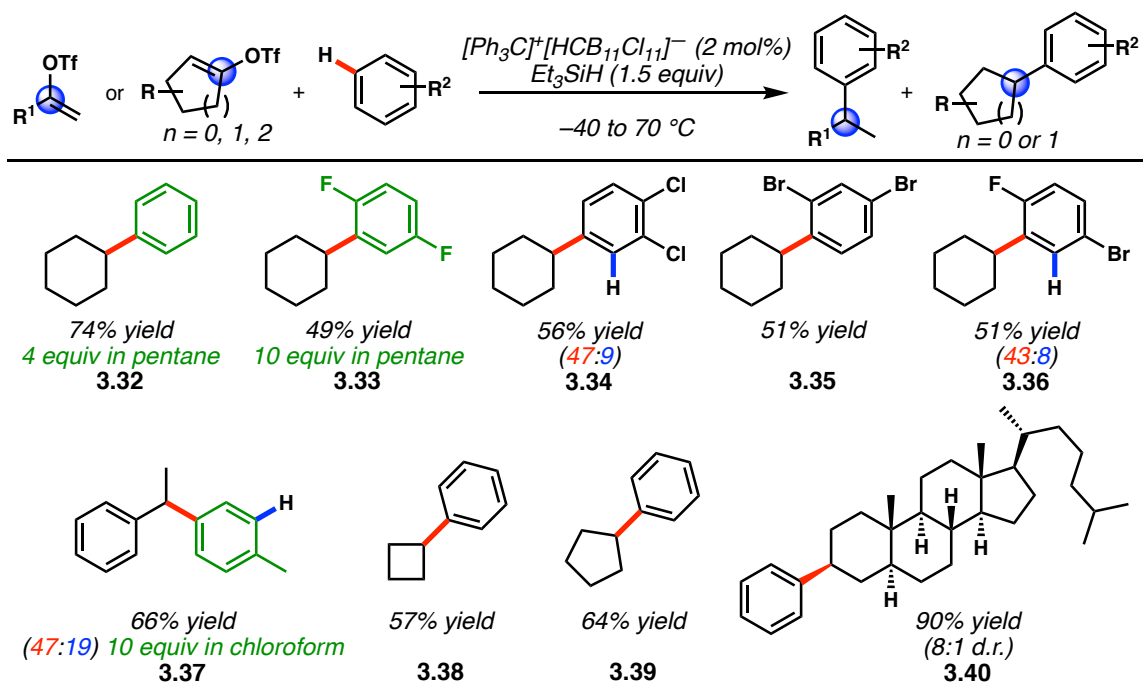


### 3.5 Reductive Friedel-Crafts Methodology of Vinyl Cations

Having established that vinyl triflates are competent vinyl cation precursors under silylium catalysis conditions, and that these reactive intermediates undergo efficient  $sp^3$  C–H functionalization reactions, we sought to investigate their reactivity with arenes. It has been reported that cyclic vinyl cations are poor electrophiles in Friedel-Crafts arylation reactions.<sup>11</sup> This finding has been attributed to the poor electrophilicity of vinyl cations<sup>12</sup> and to the slow ionization of vinyl cation precursors in arene solvents.<sup>11</sup> In early studies, cyclohexenyl triflates were completely unreactive towards arene nucleophiles, while larger ring size triflates participated in Friedel–Crafts reactions at elevated temperatures, albeit in poor yields.<sup>11</sup> We posited that use of silylium-carborane salts would allow for mild ionization of cyclic vinyl triflates in nonpolar solvents, allowing for facile Friedel–Crafts arylation reactions. We were pleased to find that with 4 equivalents of benzene in pentane solvent (1:22 ratio of benzene:pentane), cyclohexenyl triflate (**3.3**) underwent smooth reductive arylation to yield phenylcyclohexane (**3.32**) in 74% yield at room temperature (Scheme **3.5**). In this reaction, the mass balance is composed of cyclohexylpentane isomers. In addition to benzene, electron-poor haloarenes such as difluorobenzene and dichlorobenzene underwent smooth, C–C bond formation to yield cyclohexylated haloarenes (**3.33** to **3.36**) in synthetically useful yields. Likewise, electron-rich arenes were competent nucleophiles. Cyclohexenyl triflates bearing substituents at the 4- or 5-positions could also be arylated, including the enol triflate derived from  $5\alpha$ -cholestan-3-one, which yielded an arylated steroid core (**3.40**) in 90% yield and 8:1 d.r. Various ring sizes were also competent under these reaction conditions, with cyclopentenyl triflate undergoing smooth reductive alkylation with benzene reaction partners in 64% yield (**3.39**). Cyclobutenyl triflate participated in this reductive Friedel-Crafts alkylation (**3.38**), as did

aromatic alkenes (**3.37**). Simple acyclic vinyl triflates were competent electrophiles for arylation by requiring as little as 10 equivalents of arene in chloroform solvent at  $-40\text{ }^{\circ}\text{C}$ .

**Scheme 3.5** Reductive Arylation of Vinyl Triflates.



### 3.6 Conclusion

We have shown that vinyl cations, the subject of numerous computational and experimental studies, are now accessible synthetically from simple vinyl triflates using WCA salts under mild conditions. The non-nucleophilic nature of the WCA allows these unstabilized vinyl cations to engage in C–C bond forming reactions with alkanes and a variety of arenes, modes of reactivity that have been largely unreported despite extensive previous work. Through deuterium labeling studies, convincing evidence supports a 1,1-insertion pathway for the key intermolecular C–H insertion step. These findings lay the conceptual and experimental

groundwork for further discoveries in the field of alkane C–H bond functionalization using ketone derivatives and WCA catalysis.

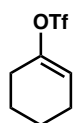
### 3.7 Experimental Section

#### 3.7.1 Materials and Methods

Unless otherwise stated, all reactions were performed in an MBraun glovebox under nitrogen atmosphere with  $\leq 0.5$  ppm O<sub>2</sub> levels. All glassware and stir-bars were dried in a 160 °C oven for at least 12 hours and dried *in vacuo* before use. All liquid substrates were either dried over CaH<sub>2</sub> or filtered through dry neutral aluminum oxide. Solid substrates were dried over P<sub>2</sub>O<sub>5</sub>. All solvents were rigorously dried before use. Benzene, *o*-dichlorobenzene, and toluene were degassed and dried in a JC Meyer solvent system and stored inside a glovebox. Cyclohexane, fluorobenzene, and *n*-hexane were distilled over potassium. Chlorobenzene and *o*-difluorobenzene were distilled over sodium. Pentane was distilled over sodium-potassium alloy. Chloroform was dried over CaH<sub>2</sub> and stored in a glovebox. All solvents were stored over 4 Å molecular sieves. Triethylsilane and triisopropylsilane were dried over sodium and stored inside a glovebox. *Closo*-Carborane catalysts were prepared according to literature procedure.<sup>13</sup> *n*-Butylcyclohexane and *n*-pentylcyclohexane were purchased from Alfa Aesar. Preparatory thin layer chromatography (TLC) was performed using Millipore silica gel 60 F<sub>254</sub> pre-coated plates (0.25 mm) and visualized by UV fluorescence quenching. SiliaFlash P60 silica gel (230-400 mesh) was used for flash chromatography. AgNO<sub>3</sub>-Impregnated silica gel was prepared by mixing with a solution of AgNO<sub>3</sub> (150% v/w of 10% w/v solution in acetonitrile), removing solvent under reduced pressure, and drying at 120 °C. NMR spectra were recorded on a Bruker AV-300 (<sup>1</sup>H, <sup>19</sup>F), Bruker AV-400 (<sup>1</sup>H, <sup>13</sup>C, <sup>19</sup>F), Bruker DRX-500 (<sup>1</sup>H), and Bruker AV-500

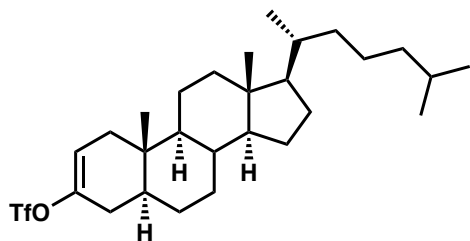
( $^1\text{H}$ ,  $^{13}\text{C}$ ).  $^1\text{H}$  NMR spectra are reported relative to  $\text{CDCl}_3$  (7.26 ppm) unless noted otherwise. Data for  $^1\text{H}$  NMR spectra are as follows: chemical shift (ppm), multiplicity, coupling constant (Hz), integration. Multiplicities are as follows: s = singlet, d = doublet, t = triplet, dd = doublet of doublet, dt = doublet of triplet, ddd = doublet of doublet of doublet, td = triplet of doublet, m = multiplet.  $^{13}\text{C}$  NMR spectra are reported relative to  $\text{CDCl}_3$  (77.16 ppm) unless noted otherwise. GC spectra were recorded on an Agilent 6850 series GC using an Agilent HP-1 (50 m, 0.32 mm ID, 0.25 mm DF) column. GCMS spectra were recorded on a Shimadzu GCMS-QP2010 using a Restek XTI-5 (50 m, 0.25 mm ID, 0.25 mm DF) column. interface at room temperature. IR Spectra were record on a Perkin Elmer 100 spectrometer and are reported in terms of frequency absorption ( $\text{cm}^{-1}$ ). High-resolution mass spectra (HR-MS) were recorded on a Waters (Micromass) GCT Premier spectrometer and are reported as follows: m/z (% relative intensity). Purification by preparative HPLC was done on an Agilent 1200 series instrument with a reverse phase Alltima  $\text{C}_{18}$  (5m, 25 cm length, 1 cm internal diameter) column.

### 3.7.2 Synthesis of Vinyl Triflate Substrates

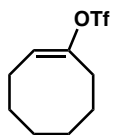


**Cyclohex-1-en-1-yl trifluoromethanesulfonate (3.3).** In a flame dried 1 L three-neck flask equipped with a dropping funnel, cyclohexanone (25.0 g, 255 mmol, 1.0 equiv) and freshly distilled anhydrous pyridine (22.2 g, 280 mmol, 1.1 equiv) were dissolved in anhydrous methylene chloride (400 mL). The solution was cooled to 0 °C. The dropping funnel was charged with a solution of triflic anhydride (79.0 g, 280 mmol, 1.1 equiv) in methylene chloride (160 mL). The solution was added dropwise to the reaction (~45 minutes). After addition ceased,

the ice bath was removed and the reaction stirred for 16 hours. The volatiles were removed under reduced pressure and the crude material was suspended in petroleum ether and filtered. The supernatant was concentrated and the resulting oil was purified by vacuum distillation at 0.2 mmHg to give cyclohexenyl triflate (**3.3**) as a colorless oil (25.8 g, 44%). NMR data match those reported in literature.<sup>14</sup>



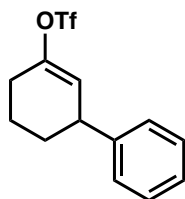
**(5S,8R,9S,10S,13R,14S,17R)-10,13-Dimethyl-17-((R)-6-methylheptan-2-yl)-4,5,6,7,8,9,10,11,12,13,14,15,16,17-tetradecahydro-1H-cyclopenta[a]phenanthren-3-yl trifluoromethanesulfonate (3.11).** Synthesized from 5 $\alpha$ -cholestan-3-one according to reported literature. NMR data match those reported in literature<sup>15</sup>



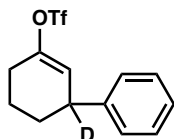
**(E)-Cyclooct-1-en-1-yl trifluoromethanesulfonate (3.13).** In a flame dried 250 mL round bottom flask, cyclooctanone (3.0 g, 23.8 mmol, 1.0 equiv) and freshly distilled 2-chloropyridine (3.0 g, 26.1 mmol, 1.1 equiv) were dissolved in anhydrous methylene chloride (90 mL). The solution was cooled to 0 °C. Triflic anhydride (8.1 g, 28.5 mmol, 1.2 equiv) was added dropwise to the solution. After addition, the ice bath was removed and the reaction stirred for 16 hours. The reaction mixture was quenched with 0.5M aqueous HCl (200 mL). The phases were separated and the aqueous layer was extracted with methylene chloride (2 x 100 mL). The combined organics were dried over magnesium sulfate, filtered and volatiles removed under



reduced pressure to give the crude material as a purple oil. The product was purified by vacuum distillation (5 mmHg, 100 °C) to give triflate (**3.13**) as a colorless oil (3.2 g, 51%). NMR data match those reported in literature.<sup>14</sup>



**1,4,5,6-Tetrahydro-[1,1'-biphenyl]-3-yl-1 trifluoromethanesulfonate (3.21).** A flame dried round bottom flask was charged with anhydrous  $\text{ZnCl}_2$  (3.7 g, 27 mmol, 2.6 equiv) and anhydrous toluene (4 mL). After cooling the mixture to  $-30\text{ }^\circ\text{C}$ , a solution of 1.0 M  $\text{PhMgBr}$  in  $\text{Et}_2\text{O}$  (54 mL, 54 mmol, 5.2 equiv) was added dropwise. The reaction was then left to warm up to room temperature over 2 hours to yield a 0.47 M solution of diphenylzinc. To a separate flame dried schlenk flask was added  $\text{Cu}(\text{OTf})_2$  (75 mg, 0.21 mmol, 0.02 equiv),  $\text{PPh}_3$  (109 mg, 0.42 mmol, 0.04 equiv) and anhydrous toluene (50 mL). After stirring for 30 minutes, cyclohex-2-en-1-one (1.00 g, 10.4 mmol, 1.0 equiv) was added and the solution cooled to  $-30\text{ }^\circ\text{C}$ . The solution of 0.47 M diphenylzinc in  $\text{Et}_2\text{O}$  (29 mL, 13.5 mmol, 1.3 equiv) was then added dropwise. After 2 hours, the reaction was brought to  $0\text{ }^\circ\text{C}$  before adding  $\text{Tf}_2\text{O}$  (3.5 mL, 20.8 mmol, 2.0 equiv) and allowed to warm to room temperature over 12 hours. The reaction was quenched with saturated aqueous sodium bicarbonate solution (80 mL). The aqueous layer was extracted with  $\text{Et}_2\text{O}$  (3 x 60 mL) and the combined organics were dried over  $\text{MgSO}_4$ . After concentrating by rotary evaporation, the crude product was purified by flash chromatography (hexanes) to yield 500 mg (16%) of colorless oil. NMR spectra match those reported in literature.<sup>16</sup>



**1,4,5,6-Tetrahydro-[1,1'-biphenyl]-3-yl-1-*d* trifluoromethanesulfonate (3.29).** Synthesized from cyclohex-2-en-1-one-3-*d* according to reported literature with modification.<sup>17</sup>

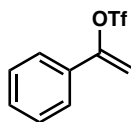
A flame dried round bottom flask was charged with anhydrous  $\text{ZnCl}_2$  (1.2 g, 9.0 mmol, 2.6 equiv) and anhydrous toluene (15 mL). After cooling the mixture to  $-30\text{ }^\circ\text{C}$ , a solution of 3.0 M  $\text{PhMgBr}$  in  $\text{Et}_2\text{O}$  (6 mL, 20 mmol, 5.2 equiv) was added dropwise. The reaction was then left to warm up to room temperature over 2 hours to yield a 0.40 M solution of diphenylzinc.

To a separate flame dried schlenk flask was added  $\text{Cu}(\text{OTf})_2$  (33 mg, 0.09 mmol, 0.02 equiv),  $\text{PPh}_3$  (48 mg, 0.18 mmol, 0.04 equiv) and anhydrous toluene (20 mL). After stirring for 30 minutes, cyclohex-2-en-1-one-3-*d* (440 mg, 4.5 mmol, 1.0 equiv) was added and the solution cooled to  $-30\text{ }^\circ\text{C}$ . The solution of 0.4 M diphenylzinc in  $\text{Et}_2\text{O}$  (14 mL, 5.9 mmol, 1.3 equiv) was then added dropwise. After 2 hours, the reaction was brought to  $0\text{ }^\circ\text{C}$  before adding  $\text{Tf}_2\text{O}$  (1.5 mL, 9.0 mmol, 2 equiv) and allowed to warm to room temperature over 12 hours. The reaction was quenched with saturated aqueous sodium bicarbonate solution (40 mL). The aqueous layer was extracted with  $\text{Et}_2\text{O}$  (3 x 30 mL) and the combined organics were dried over  $\text{MgSO}_4$ . After concentrating by rotary evaporation, the crude product was purified by flash chromatography (hexanes) to yield 260 mg (19%) of colorless oil.

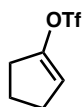
$^1\text{H}$  NMR (500 MHz,  $\text{CDCl}_3$ )  $\delta$  7.35–7.21 (m, 2H), 7.26–7.23 (m, 1H), 7.21–7.17 (m, 2H), 5.83 (br s, 1H), 2.50–2.43 (m, 1H), 2.38 (dt,  $J = 17.5, 5.2$  Hz, 1H), 2.01 (ddd,  $J = 13.2, 7.1, 2.8$  Hz, 1H), 1.95–1.87 (m, 1H), 1.82–1.73 (m, 1H), 1.56–1.51 (m, 1H);  $^{19}\text{F}$  NMR (282 MHz,  $\text{CDCl}_3$ )  $\delta$  –74.0;  $^{13}\text{C}$  NMR (125 MHz,  $\text{CDCl}_3$ )  $\delta$  150.5, 143.7, 127.5, 126.8, 121.5, 118.6 (q,  $^1J_{\text{C-F}} = 318$  Hz), 40.9 (t,  $^1J_{\text{C-D}} = 20$  Hz), 31.2, 27.6, 21.1.

FTIR (Neat film NaCl): 3062, 3027, 2945, 2864, 1683, 1603, 1414, 1246, 1202, 1139, 1049, 994, 931, 919, 907, 878, 837, 822, 700, 603, 505.

HR-MS (GCT-LIFDI): Calculated for  $[C_{13}H_{12}DF_3O_3S + Na]^+$ : 330.0498; measured: 330.0509.



**1-Phenylvinyl trifluoromethanesulfonate (3.41).** In a flame dried 500 mL roundbottom flask, phenylacetylene (5.11 g, 50.0 mmol) was dissolved in anhydrous methylene chloride (250 mL). Triflic acid (6.75 g, 45.0 mmol) was added dropwise to the solution under vigorous stirring. After 20 minutes, the reaction was quenched with saturated aqueous sodium bicarbonate (100 mL). The layers were separated and the organic layer was dried over magnesium sulfate, filtered and volatiles removed under reduced pressure to give the crude as a black oil. The crude material was vacuum distilled (0.2 mmHg, 65 °C) to give triflate **3.41** as a faint yellow oil (3.2 g, 28%). NMR data match those reported in literature.<sup>18</sup>



**Cyclopent-1-en-1-yl trifluoromethanesulfonate (3.42).** Synthesized according to literature procedures. NMR data match those reported in literature.<sup>19</sup>



**Cyclobut-1-en-1-yl trifluoromethanesulfonate (3.43).** To a 250 mL flame dried roundbottom flask equipped with a magnetic stirring bar were added cyclobutanone (2.00 g, 28.5 mmol), N-Phenylbis(trifluoromethanesulfonimide) (11.2 g, 31.4 mmol) and anhydrous tetrahydrofuran (56 mL). The resulting solution was cooled to 0 °C. In a separate flask, potassium hexamethyldisilazide (5.98 g, 29.9 mmol) was dissolved in anhydrous tetrahydrofuran (40 mL).

This solution was added dropwise to the cyclobutanone-containing solution. The reaction stirred at 0 °C for 2 hours at which point most of the tetrahydrofuran was removed under reduced pressure. The resulting mixture was diluted with diethyl ether (50 mL) and washed with water (3 x 30 mL) followed by brine (2 x 30 mL). The organics were dried over sodium sulfate, filtered and volatiles removed under pressure. The crude material was purified by vacuum distillation (0.2 mmHg, 25 °C) to give the product with a small amount of hexamethyldisilazane impurity. The triflate was further purified by silica column chromatography (hexanes) to give pure product as a colorless oil (400 mg, 7%). Note: the low yield is likely due to the volatility of the product.

$^1\text{H}$  NMR (400 MHz,  $\text{CDCl}_3$ )  $\delta$  5.42 (s, 1H), 2.92 – 2.90 (m, 2H), 2.26 – 2.24 (m, 2H);  $^{19}\text{F}$  NMR (376 MHz,  $\text{CDCl}_3$ )  $\delta$  -73.8;  $^{13}\text{C}$  NMR (125 MHz,  $\text{CDCl}_3$ )  $\delta$  138.0, 118.7 (q,  $^1J_{\text{C-F}} = 319$  Hz), 116.7, 33.9, 21.4.

FTIR (Neat film NaCl): 2960, 2950, 2858, 1629, 1423, 1272, 1244, 1204, 1135, 932, 909, 851, 769, 605, 575, 522.

HR-MS (GCT-LIFDI): Calculated for  $\text{C}_5\text{H}_5\text{F}_3\text{O}_3\text{S}$ : 201.9911; measured: 201.9918.

### 3.7.3 General Procedure for Yield Calculations by GC

Calibration curves were made by first preparing 5:1, 3:1, 1:1, 1:3, and 1:5 molar ratio solutions of nonane to product. GC analysis of the chromatogram integrations was plotted on Microsoft Excel to form a linear calibration curve line. All curves were tested to be within  $\leq 5\%$  error. For analysis of reactions, nonane (1.12 equiv) was added to the reaction mixture after completion and aliquots were prepared by diluting in hexanes, quenched with a saturated aqueous sodium bicarbonate solution, and the organic layer filtered through a kimwipe. Yields are then calculated

by comparing the integration ratios of nonane to the product against their respective calibration curve.

### 3.7.4 Optimization for Alkane Alkylation Reactions

This section outlines the optimization of the reaction shown below. All yields of bicyclohexyl (3.8) are GC yields.

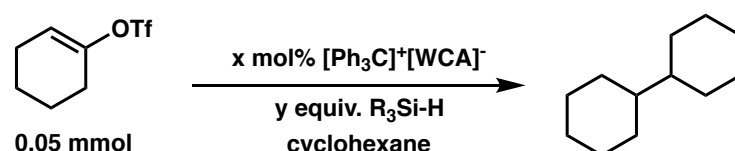
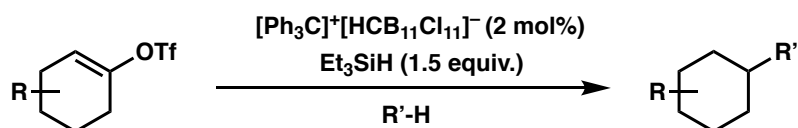


**Table 3.2** Optimization of intermolecular alkylation reaction.

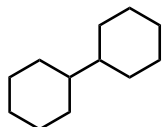
Anion	% Cat. Loading	Conc.	Temp.	Silane	Yield
[HCB <sub>11</sub> Cl <sub>11</sub> ]	2 mol%	0.1 M	30 °C	Et <sub>3</sub> SiH (150 mol%)	87%
[HCB <sub>11</sub> Cl <sub>11</sub> ]	2 mol%	0.1 M	30 °C	iPr <sub>3</sub> SiH (150 mol%)	68%
[HCB <sub>11</sub> Cl <sub>11</sub> ]	0 mol%	0.1 M	30 °C	Et <sub>3</sub> SiH (120 mol%)	0%
[HCB <sub>11</sub> Cl <sub>11</sub> ]	2 mol%	0.1 M	30 °C	none	0%
[HCB <sub>11</sub> H <sub>5</sub> Cl <sub>6</sub> ]	2 mol%	0.1 M	30 °C	Et <sub>3</sub> SiH (150 mol%)	50%
[HCB <sub>11</sub> Br <sub>11</sub> ]	2 mol%	0.1 M	30 °C	Et <sub>3</sub> SiH (150 mol%)	69%
[B(C <sub>6</sub> F <sub>5</sub> ) <sub>4</sub> ]	2 mol%	0.1 M	30 °C	Et <sub>3</sub> SiH (150 mol%)	6%

### 3.7.5 General Procedure for Intermolecular Alkane Insertion Reactions.



In a well-kept glovebox, H<sub>2</sub>O, O<sub>2</sub> ≤ 0.5 ppm, a dram vial was charged with [Ph<sub>3</sub>C]<sup>+</sup>[HCB<sub>11</sub>Cl<sub>11</sub>]<sup>-</sup> (0.02 equiv) and this was suspended in alkane (0.1 M). Triethylsilane (1.5 equiv) along with a magnetic stirring bar were added to the mixture, and the resulting suspension stirred for 10

minutes. At this point, vinyl triflate (1.0 equiv) was added to the reaction and stirred for 0.2–12 hours at 30 °C (see substrates for specific details). Upon completion, the reaction mixture was passed through a short plug of silica gel inside the glovebox and washed with hexanes. The solution was brought out and volatiles removed under reduced pressure. Some substrates needed further purification by silica column chromatography.



**Bicyclohexyl (3.8).** Synthesized according to general procedure 3.7.5. A dram vial was charged with  $[\text{Ph}_3\text{C}]^+[\text{HCB}_{11}\text{Cl}_{11}]^-$  (0.8 mg, 0.001 mmol, 0.02 equiv) and this was suspended in cyclohexane (0.5 mL, 4.63 mmol). Triethylsilane (12 mL, 0.075 mmol, 1.5 equiv) along with a magnetic stirring bar were added to the mixture and the resulting suspension stirred for 10 minutes. Cyclohexenyl triflate (**3.3**) (11.5 mg, 0.05 mmol, 1.0 equiv) was added to the reaction and stirred for 1.5 hours at 30 °C. Upon completion the reaction was plugged through silica and bicyclohexyl was obtained in 87% GC yield. The crude could be further purified by flash column chromatography (hexanes) to give bicyclohexyl as a colorless oil. NMR spectra match those reported in literature.<sup>20</sup>



**Figure 3.2** GC Trace Showing 1:1 Mixture of Nonane to Bicyclohexyl.

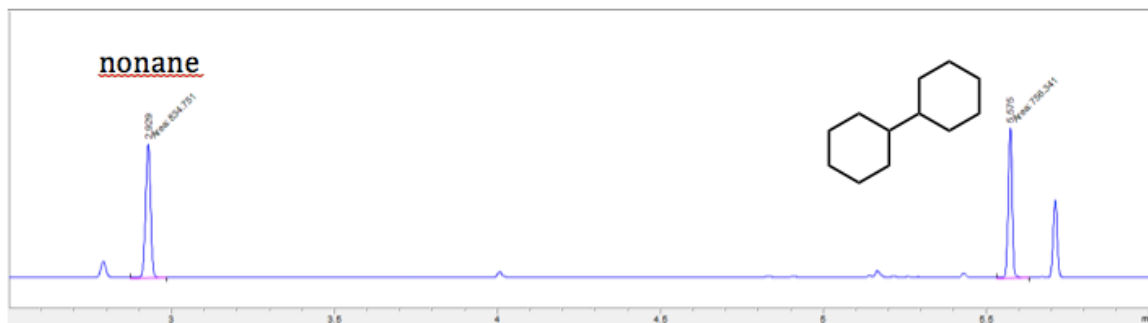
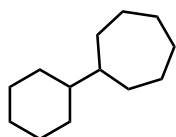


**Figure 3.3** GC Trace Showing 87% Yield of Bicyclohexyl.



**Cyclohexylcycloheptane (3.9).** Synthesized according to general procedure 3.7.5. A dram vial was charged with  $[\text{Ph}_3\text{C}]^+[\text{HCB}_{11}\text{Cl}_{11}]^-$  (0.8 mg, 0.001 mmol, 0.02 equiv) and this was suspended in cycloheptane (0.5 mL). Triethylsilane (12 mL, 0.075 mmol, 1.5 equiv) along with a magnetic stirring bar were added to the mixture and the resulting suspension stirred for 10 minutes. Cyclohexenyl triflate (**3.3**) (11.5 mg, 0.05 mmol, 1 equiv) was added to the reaction and stirred for 2 hours at 30 °C. Upon completion the reaction was plugged through silica and cyclohexylcycloheptane was obtained in 88% GC yield. The crude could be further purified by flash column chromatography (hexanes) to give cyclohexylcycloheptane as a colorless oil.

$^1\text{H}$  NMR (500 MHz,  $\text{CDCl}_3$ )  $\delta$  1.74–1.68 (m, 2H), 1.68–1.52 (m, 9H), 1.50–1.43 (m, 2H), 1.42–1.34 (m, 2H), 1.32–1.07 (m, 7H), 1.06–0.96 (m, 2H);  $^{13}\text{C}$  NMR (125 MHz,  $\text{CDCl}_3$ )  $\delta$  45.0, 44.9, 31.5, 30.0, 28.6, 27.6, 27.2, 27.1.

FTIR (Neat film NaCl): 2918, 2850, 2670, 1448, 1349, 1263, 972, 893, 844.

HR-MS (GCT-LIFDI): Calculated for  $\text{C}_{13}\text{H}_{24}$ : 180.1878; measured: 180.1881.

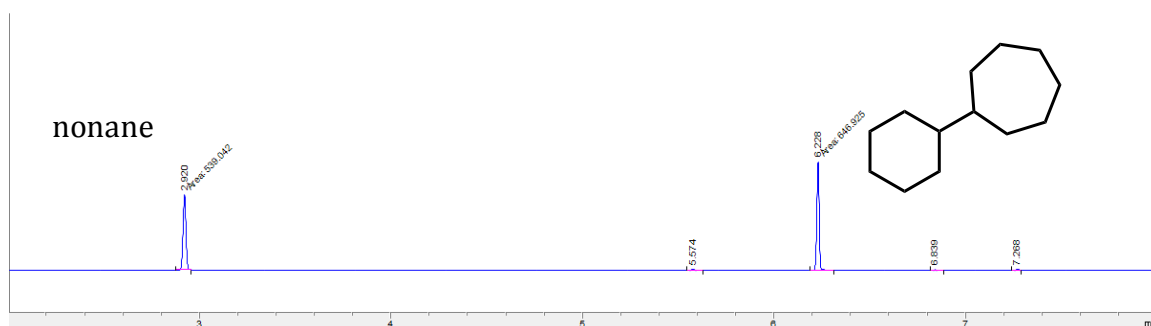


**Figure 3.4** GC Trace Showing 1:1 Mixture of Nonane to Cyclohexylcycloheptane.

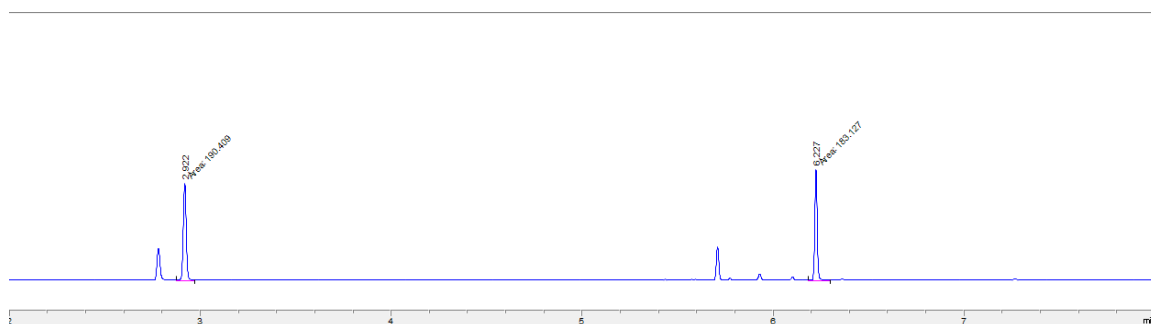
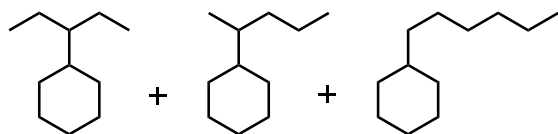


**Figure 3.5** GC Trace Showing 88% Yield of Cyclohexylcycloheptane.



**Pentylcyclohexane (mixture of isomers, 3.10).** Synthesized according to general procedure 3.7.5. A dram vial was charged with  $[\text{Ph}_3\text{C}]^+[\text{HCB}_{11}\text{Cl}_{11}]^-$  (0.8 mg, 0.001 mmol, 0.02 equiv) and this was suspended in pentane (0.5 mL). Triethylsilane (12 mL, 0.075 mmol, 1.5 equiv) along with a magnetic stirring bar were added to the mixture and the resulting suspension stirred for 10 minutes. Cyclohexenyl triflate (**3.3**) (11.5 mg, 0.05 mmol, 1.0 equiv) was added to the reaction and it stirred for 1.5 hours at 30 °C to give 11% of 3-cyclohexylpentane, 36% of 2-cyclohexylpentane and 21% of 1-cyclohexylpentane (GC). Upon completion the reaction was passed through silica and an inseparable mixture of the three isomers were obtained as a colorless oil (4.3 mg, 56%). The NMR data of this mixture matched those of the three authentic samples (experimental data of authentic samples can be found in adapted article).



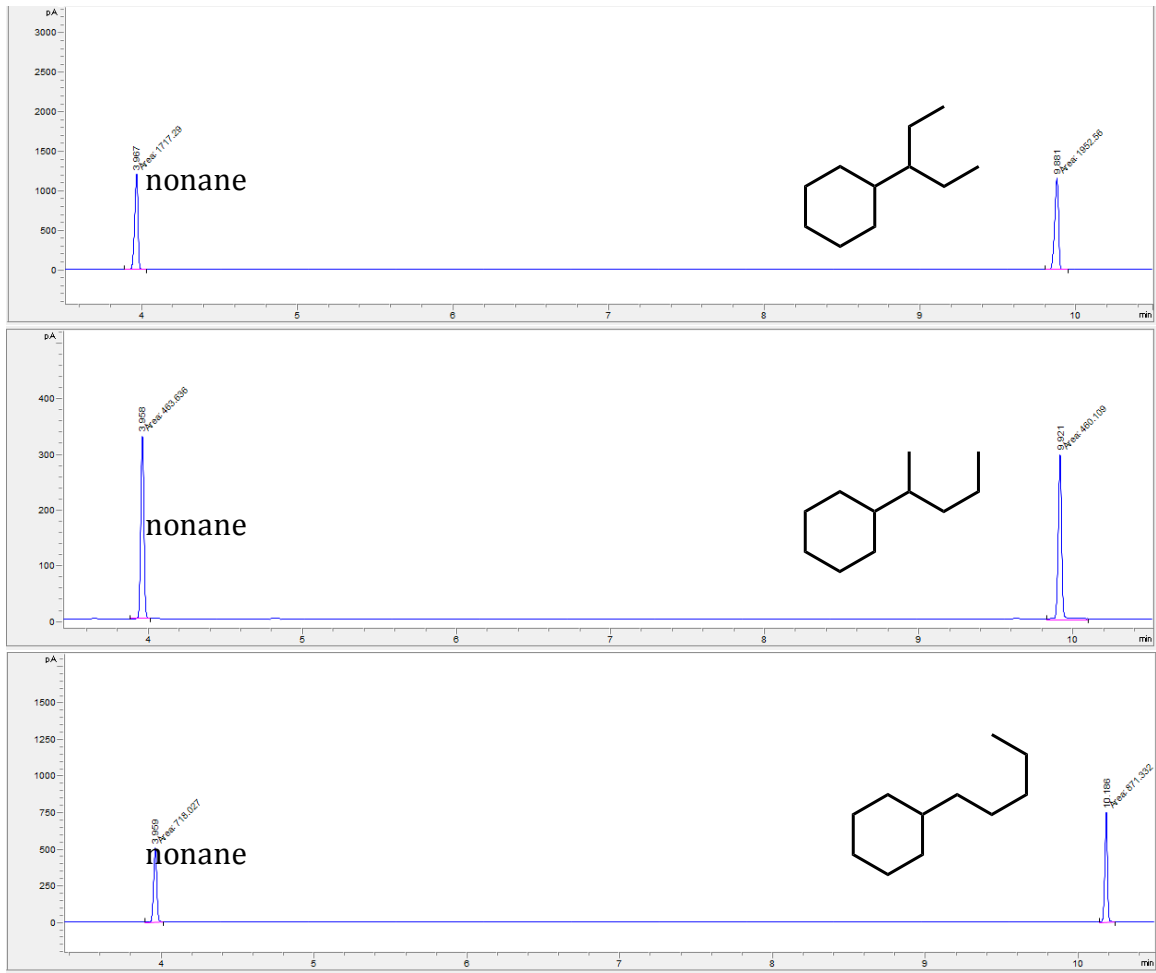


**Figure 3.6** GC Traces Showing 1:1 Mixture of Nonane to 3-cyclohexylpentane (Top), Nonane to 2-cyclohexylpentane (Middle), and Nonane to 1-cyclohexylpentane (Bottom).

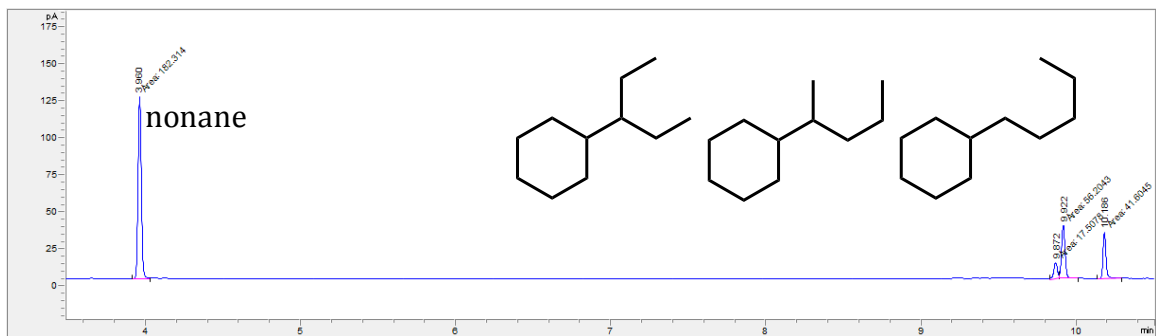
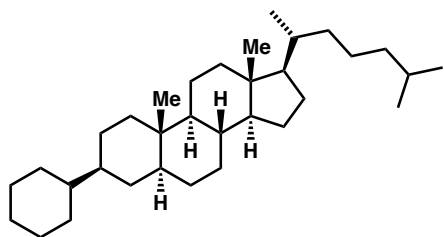


**Figure 3.7** GC Trace Showing 11% of 3-cyclohexylpentane, 36% of 2-cyclohexylpentane and 21% of 1-cyclohexylpentane.



**(3*S*,5*S*,8*R*,9*S*,10*S*,13*R*,14*S*,17*R*)-3-Cyclohexyl-10,13-dimethyl-17-((*R*)-6-methylheptan-2-yl)hexadecahydro-1*H*-cyclopenta[*a*]phenanthrene (3.12)**. Synthesized according to general procedure 3.7.5. A dram vial was charged with  $[\text{Ph}_3\text{C}]^+[\text{HCB}_{11}\text{Cl}_{11}]^-$  (0.8 mg, 0.001 mmol, 0.02 equiv) and this was suspended in cyclohexane (0.5 mL, 4.63 mmol). Triethylsilane (12 mL, 0.075 mmol, 1.5 equiv) along with a magnetic stirring bar were added to the mixture and the resulting suspension stirred for 10 minutes. Triflate **3.11** (26.0 mg, 0.05 mmol, 1.0 equiv) was added to the reaction and it stirred for 3 hours at 30 °C. Upon completion the reaction was passed through silica and volatiles removed under reduced pressure to give product **3.12** as a white solid (19.5 mg, 88%). GC-FID analysis showed ~15:1 d.r. In order to assign the stereochemistry of the newly formed C–C bond, the material was crystallized by vapor diffusion in the following manner: ~3 mg of the material was dissolved in a minimal amount of cyclohexane in a small crystallization tube. This was placed into a 20 mL vial of acetone and the vial was capped. After 3 days, a crystal suitable for single crystal X-ray diffraction was grown (crystallographic data can be viewed in the adapted article).

$^1\text{H}$  NMR (500 MHz,  $\text{CDCl}_3$ )  $\delta$  0.79–0.66 (m, 4H), 0.83 (s, 3H), 0.96 (dd,  $J = 6.7, 2.3$  Hz, 8H), 1.00 (d,  $J = 6.5$  Hz, 3H), 1.37–1.04 (m, 22H), 1.49–1.37 (m, 4H), 1.69–1.56 (m, 3H), 1.85–1.70 (m, 7H), 1.95–1.86 (m, 1H), 2.05 (dt,  $J = 12.5, 3.4$  Hz, 1H);  $^{13}\text{C}$  NMR (125 MHz,  $\text{CDCl}_3$ )  $\delta$  56.8, 56.5, 54.9, 47.0, 43.8, 43.6, 42.8, 40.3, 39.7, 39.1, 36.4, 36.2, 36.0, 35.7, 32.6, 32.4, 30.5, 30.4, 29.4, 28.4, 28.2, 27.1, 27.0, 25.8, 24.4, 24.0, 23.0, 22.7, 21.2, 18.8, 12.5, 12.3.

FTIR (Neat film NaCl): 2917, 2848, 1446, 1383, 1172, 930, 890.

HR-MS (GCT-LIFDI): Calculated for C<sub>33</sub>H<sub>58</sub>: 454.4539; measured: 454.4536.

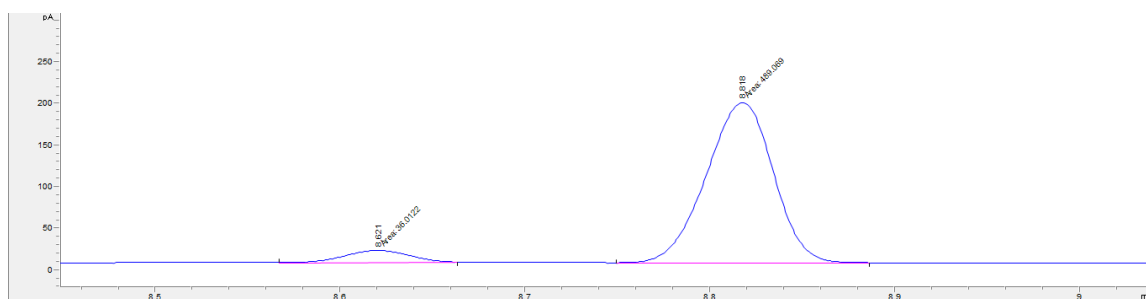
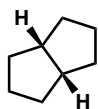


**Figure 3.8** GC Trace Showing ~15:1 d.r. **3.12**.



**(3a,6a)-Octahdropentalene (3.14)**. Synthesized according to general procedure 3.7.5. A dram vial was charged with [Ph<sub>3</sub>C]<sup>+</sup>[HCB<sub>11</sub>Cl<sub>11</sub>]<sup>-</sup> (0.8 mg, 0.001 mmol) and this was suspended in cyclohexane (0.5 mL, 4.63 mmol). Triethylsilane (12 mL, 0.075 mmol) along with a magnetic stirring bar were added to the mixture and the resulting suspension stirred for 10 minutes. Cyclooctenyl triflate (**3.13**) (18.0 mg, 0.07 mmol, 1.0 equiv) was added to the reaction and it stirred for 1 hours at 30 °C. The reaction was passed through silica in the glovebox and volatiles removed under reduced pressure to give product **3.14** as a colorless oil (91% GC yield). NMR spectra match those reported in literature.<sup>21</sup>

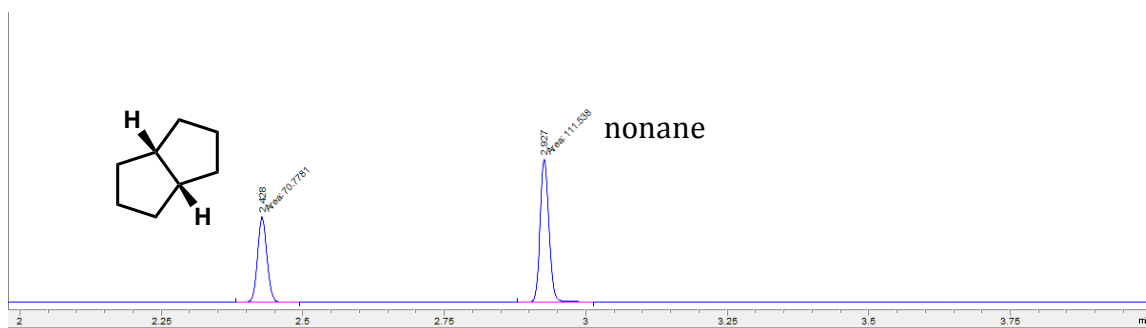
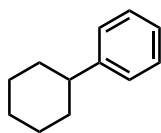


**Figure 3.9** GC Trace Showing 1:1 Mixture of Nonane to Octahdropentalene.



0.1 M solution of vinyl triflate). Arene (10-50 equiv.) and vinyl triflate (1 equiv.) were added along with a magnetic stirring bar to the solution. The solution was cooled to  $-40\text{ }^{\circ}\text{C}$ . At this point, silane (1.5 equiv.) was added to the reaction and it stirred at this temperature until completion (see substrates for specific details). Upon completion, the reaction mixture was pushed through a short plug of silica gel inside the glovebox and washed with hexanes. The solution was brought out and volatiles removed under reduced pressure. Some substrates needed further purification by silica column chromatography (see below) or preparative high-pressure liquid chromatography (HPLC).



**Phenylcyclohexane (3.32).** Synthesized according to general procedure A. A dram vial was charged with  $[\text{Ph}_3\text{C}]^+[\text{HCB}_{11}\text{Cl}_{11}]^-$  (0.8 mg, 0.002 mmol) and this was suspended in pentane (0.5 mL, 11.1 mmol). Triethylsilane (9.6 mL, 0.060 mmol), benzene (18 mL, 0.2 mmol, 4 equiv), and a magnetic stirring bar were added respectively to the mixture and stirred for 10 minutes. Cyclohexenyl triflate (**3.3**) (12.0 mg, 0.050 mmol) was added to the reaction and stirred for 2 hour at  $30\text{ }^{\circ}\text{C}$ . The reaction was plugged through silica in the glovebox and volatiles removed under reduced pressure to give product **3.32** in 74% yield (GC). NMR spectra match those reported in literature.<sup>1</sup>

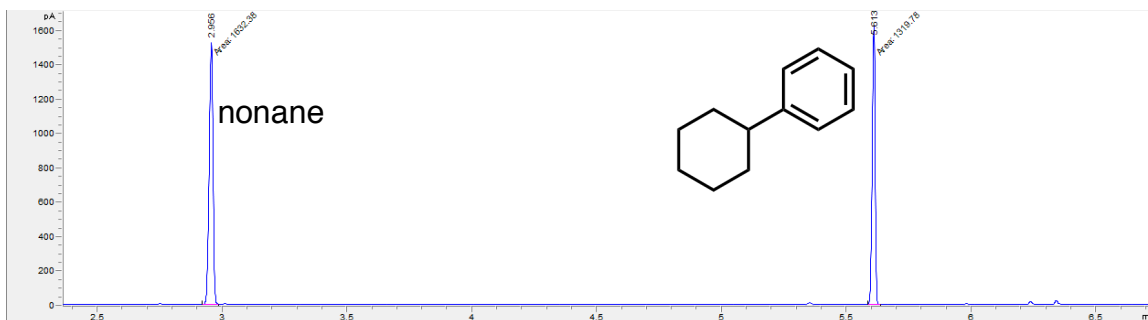


**Figure 3.11** GC Trace Showing 1:1 Mixture of Nonane to Phenylcyclohexane.

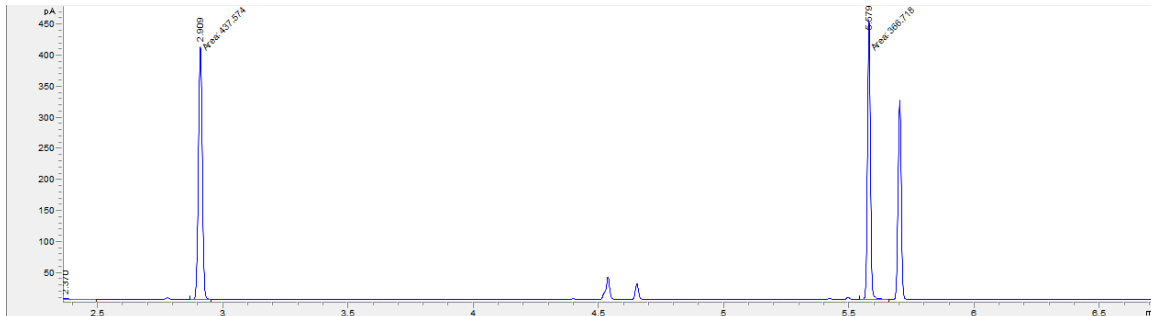
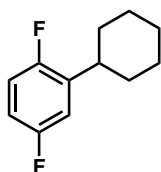


**Figure 3.12** GC Trace Showing 74% Yield of Phenylcyclohexane.



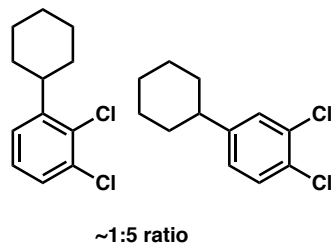
**2-cyclohexyl-1,4-difluorobenzene (3.33).** Synthesized according to general procedure A. A dram vial was charged with  $[\text{Ph}_3\text{C}]^+[\text{HCB}_{11}\text{Cl}_{11}]^-$  (3.2 mg, 0.004 mmol) and this was suspended in pentane (0.5 mL) and 1,4-difluorobenzene (51 mL, 0.50 mmol). Triethylsilane (9.6 mL, 0.06 mmol) along with a magnetic stirring bar were added to the mixture and stirred for 10 minutes. Cyclohexenyltriflate (**3.3**) (12.0 mg, 0.05 mmol) was added to the reaction and stirred for 3 hours at 30 °C. The reaction was plugged through silica in the glovebox and volatiles removed under reduced pressure to yield **3.33** in 49% yield (NMR). **3.33** was also synthesized as described above in 1,4-difluorobenzene solvent (0.5 mL). Crude material was purified by flash column chromatography (hexanes) to yield a colorless oil (22 mg, 56%).

$^1\text{H}$  NMR (500 MHz,  $\text{CDCl}_3$ )  $\delta$  6.96 – 6.88 (m, 2H), 6.83 – 6.78 (m, 1H), 2.84 (t,  $J = 10.8$  Hz, 1H), 1.85 (br d,  $J = 10.5$  Hz, 4H), 1.76 (br d,  $J = 12.9$  Hz, 1H), 1.47 – 1.32 (m, 4H), 1.29 – 1.20 (m, 1H);  $^{19}\text{F}$   $\{^1\text{H}\}$  NMR (376 MHz,  $\text{CDCl}_3$ )  $\delta$  -119.4 ( $J = 17.7$  Hz), -125.7 ( $J = 17.7$  Hz);  $^{13}\text{C}$  NMR (125 MHz,  $\text{CDCl}_3$ )  $\delta$  158.9 (dd,  $^1J_{\text{C-F}} = 240.8$  Hz,  $^4J_{\text{C-F}} = 2.3$  Hz), 156.4 (dd,  $^1J_{\text{C-F}} = 239.9$  Hz,  $^4J_{\text{C-F}} = 2.4$  Hz), 136.3 (dd,  $^2J_{\text{C-F}} = 17.4$  Hz,  $^3J_{\text{C-F}} = 7.0$  Hz), 115.9 (dd,  $^2J_{\text{C-F}} = 26.2$  Hz,  $^3J_{\text{C-F}} =$

8.7 Hz), 114.1 (dd,  $^2J_{C-F} = 24.0$  Hz,  $^3J_{C-F} = 5.5$  Hz), 113.1 (dd,  $^2J_{C-F} = 24.1$  Hz,  $^3J_{C-F} = 8.8$  Hz), 37.1, 32.9, 26.7, 26.0.

FTIR (Neat film NaCl): 2928, 2854, 1625, 1596, 1493, 1450, 1425, 1232, 1178, 866, 810, 780, 731.

HR-MS (GCT-LIFDI): Calculated for  $C_{12}H_{14}F_2$ : 196.1064; measured: 196.1067.



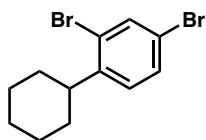
**1,2-dichloro-4-cyclohexylbenzene (3.34)**. Synthesized according to general procedure A. A dram vial was charged with  $[Ph_3C]^+[HCB_{11}Cl_{11}]^-$  (3.2 mg, 0.004 mmol) and this was suspended in 1,4-difluorobenzene (2 mL, 19.5 mmol). Triethylsilane (48 mL, 0.3 mmol) along with a magnetic stirring bar were added to the mixture and stirred until colorless. Cyclohexenyltriflate (**3.3**) (46.0 mg, 0.20 mmol) was added the reaction and it stirred for 1 hour at 30 °C. The reaction was plugged through silica in the glovebox and volatiles removed under reduced pressure to give product **3.34** as a mixture of isomers in 47% yield (NMR) and 9% yield (NMR). Crude material was further purified via flash column chromatography (hexanes) to give product **3.34** (mixture of isomers) as a colorless oil. Major isomer was assigned based on the coupling constants in the  $^1H$  NMR. These coupling constants are consistent with a 1,2,4-substituted benzene ring, but not with a 1,2,3-substituted benzene ring. HSQC and HMBC were used to determine which carbon peaks in  $^{13}C$  NMR belonged to the major isomer.

$^1H$  NMR major isomer (500 MHz,  $CDCl_3$ )  $\delta$  7.33 (d,  $J = 8.3$  Hz, 1H), 7.28 (d,  $J = 1.9$  Hz, 1H), 7.03 (dd,  $J = 8.3, 1.9$  Hz, 1H), 2.46 (dd,  $J = 10.2, 7.5$  Hz, 1H), 1.84 (br d,  $J = 12.9$  Hz, 4H), 1.75

(br d,  $J = 12.9$  Hz, 1H), 1.41 – 1.33 (m, 4H), 1.28 – 1.19 (m, 2H);  $^{13}\text{C}$  NMR major isomer (125 MHz,  $\text{CDCl}_3$ )  $\delta$  148.4, 132.2, 130.3, 129.6, 129.0, 126.5, 44.0, 34.4, 26.8, 26.1.

FTIR (Neat film NaCl): 2924, 2852, 1584, 1560, 1475, 1461, 1449, 1131, 1028, 671, 592.

HR-MS (GCT-LIFDI): Calculated for  $\text{C}_{12}\text{H}_{14}\text{Cl}_2$ : 228.0473; measured: 228.0473.



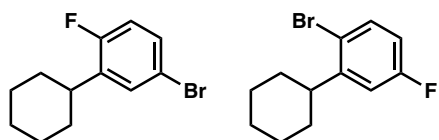
**2,4-dibromo-1-cyclohexylbenzene (3.35).** Synthesized according to general procedure A. A dram vial was charged with  $[\text{Ph}_3\text{C}]^+[\text{HCB}_{11}\text{Cl}_{11}]^-$  (0.8 mg, 0.001 mmol) and this was dissolved in 1,3-dibromobenzene (0.5 mL, 3.4 mmol). Triethylsilane (12 mL, 0.075 mmol) along with a magnetic stirring bar were added to the mixture and the resulting solution stirred for 10 minutes. Triflate **3.3** (12.0 mg, 0.05 mmol) was added to the reaction and stirred for 2 hours at 30 °C. The reaction was plugged through silica in the glovebox and volatiles removed under reduced pressure to give product **3.35** in 51% yield (NMR). The crude product was further purified by reverse phase HPLC (9:1 acetonitrile\_water) to give pure product as a colorless oil.

$^1\text{H}$  NMR (500 MHz,  $\text{CDCl}_3$ )  $\delta$  7.68 (d,  $J = 2.0$  Hz, 2H), 7.38 (dd,  $J = 8.3, 2.0$  Hz, 2H), 7.11 (d,  $J = 8.3$  Hz, 1H), 2.90 (tt,  $J = 11.6, 3.0$  Hz, 1H), 1.90 – 1.81 (m, 4H), 1.49 – 1.18 (m, 5H);  $^{13}\text{C}$  NMR (125 MHz,  $\text{CDCl}_3$ )  $\delta$  145.6, 135.1, 130.8, 128.6, 125.1, 119.7, 43.0, 33.3, 26.9, 26.2.

FTIR (Neat film NaCl): 2924, 2851, 1730, 1577, 1551, 1465, 1448, 1379, 1083, 1033, 998, 812, 779, 720, 700, 553.

HR-MS (GCT-LIFDI): Calculated for  $\text{C}_{12}\text{H}_{14}\text{Br}_2$ : 317.9442; measured: 317.9455.





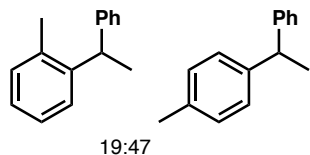
5.4:1

**4-bromo-2-cyclohexyl-1-fluorobenzene (3.36)** . Synthesized according to general procedure A. A dram vial was charged with  $[\text{Ph}_3\text{C}]^+[\text{HCB}_{11}\text{Cl}_{11}]^-$  (0.8 mg, 0.001 mmol) and this was dissolved in 1,4-bromofluorobenzene (0.5 mL, 4.6 mmol). Triethylsilane (12 mL, 0.075 mmol) along with a magnetic stirring bar were added to the mixture and the resulting solution stirred for 10 minutes. Triflate **3.3** (12.0 mg, 0.05 mmol) was added to the reaction and stirred for 2 hours at 30 °C. The reaction was plugged through silica in the glovebox and volatiles removed under reduced pressure to give product **3.36** as a mixture of isomers in 43% and 8% yield (NMR), respectively. The reaction mixture was purified by reverse phase HPLC (85:15 acetonitrile:water) to give the product **3.36** and a regioisomer as a mixture (~5:1 ratio) as a colorless oil. Major isomer was assigned by looking at the  $^{13}\text{C}$  NMR and the HSQC. By  $^{13}\text{C}$  NMR, the carbon on the fluorine and the carbons *ortho* to the fluorine could be assigned by their large  $^1J_{\text{C-F}}$  and  $^2J_{\text{C-F}}$  values respectively. Of the two carbons *ortho* to the fluorine, only one of them was attached to a hydrogen, meaning that the other position was cyclohexylated.

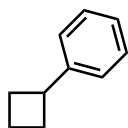
$^1\text{H}$  NMR major isomer (500 MHz,  $\text{CDCl}_3$ )  $\delta$  7.33 (dd,  $J = 6.5, 2.5$  Hz, 1H), 7.25 – 7.22 (m, 1H), 6.87 (dd,  $J = 9.9, 8.7$  Hz, 1H), 2.85 – 2.77 (m, 1H), 1.87 – 1.80 (m, 4H), 1.79 – 1.72 (m, 1H), 1.44 – 1.36 (m, 4H), 1.30 – 1.21 (m, 1H);  $^{19}\text{F}$   $\{^1\text{H}\}$  NMR (376 MHz,  $\text{CDCl}_3$ )  $\delta$  -119.4;  $^{13}\text{C}$  NMR major isomer (125 MHz,  $\text{CDCl}_3$ )  $\delta$  159.8 (d,  $^1J_{\text{C-F}} = 244.9$  Hz), 137.0 (d,  $^2J_{\text{C-F}} = 16.3$  Hz), 130.9 (d,  $^3J_{\text{C-F}} = 5.4$  Hz), 130.0 (d,  $^3J_{\text{C-F}} = 5.7$  Hz), 117.1 (d,  $^2J_{\text{C-F}} = 24.8$  Hz), 116.7 (d,  $^4J_{\text{C-F}} = 3.3$  Hz), 37.2 (d,  $^3J_{\text{C-F}} = 1.7$  Hz, 33.0, 26.8, 26.2).

FTIR (Neat film NaCl): 2929, 2853, 1605, 1579, 1480, 1449, 1232, 1181, 1168, 1099, 1005, 869, 810, 612.

HR-MS (GCT-LIFDI): Calculated for  $C_{12}H_{14}BrF$ : 256.0263; measured: 256.0260.

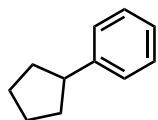


**1-methyl-4-(1-phenylethyl)benzene (3.37).** Synthesized according to general procedure B. A dram vial was charged with  $[Ph_3C]^+[HCB_{11}Cl_{11}]^-$  (1.6 mg, 0.002 mmol) and this was dissolved in chloroform (1 mL). Toluene (92 mg, 1 mmol) and 1-phenylvinyl trifluoromethanesulfonate (**3.41**) (25.2 mg, 0.1 mmol) were added along with a magnetic stirring bar to the solution. The solution was cooled to  $-40\text{ }^\circ\text{C}$ . At this point, triethylsilane (17.4 mg, 0.15 mmol) was added to the reaction and stirred at  $-40\text{ }^\circ\text{C}$  for 1 hour. The reaction mixture was warmed to room temperature and was plugged through silica in the glovebox and volatiles removed under reduced pressure. The crude material was purified by flash column chromatography (hexanes) to give an inseparable mixture of products **3.37** in 47% and 19% yield, para and ortho isomers, respectively, as a colorless oil. NMR spectra match those reported in literature.<sup>22,23</sup>

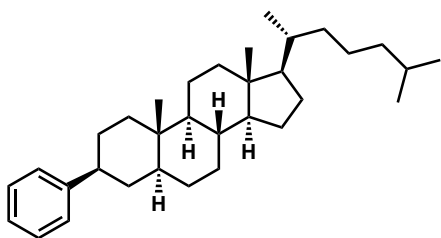


**Phenylcyclobutane (3.38).** Synthesized according to a modified general procedure A. A dram vial was charged with  $[Ph_3C]^+[HCB_{11}Cl_{11}]^-$  (0.8 mg, 0.001 mmol) and this was dissolved in benzene (10 mL, 112 mmol). Triisopropylsilane (15 mL, 0.075 mmol) along with a magnetic stirring bar were added to the mixture and stirred until colorless. Cyclobutenyl triflate (**3.43**) (10.0 mg, 0.05 mmol) was added to the reaction and stirred for 0.5 hours at  $30\text{ }^\circ\text{C}$ . The reaction was plugged through silica in the glovebox and volatiles removed under reduced pressure to give

product **3.38** in 57% yield (NMR). The crude product was purified *via* silica column chromatography (hexanes) to give phenylcyclobutane as a colorless oil. NMR data match those reported in literature.<sup>24</sup>



**Phenylcyclopentane (3.39).** Synthesized according to general procedure A. A dram vial was charged with  $[\text{Ph}_3\text{C}]^+[\text{HCB}_{11}\text{Cl}_{11}]^-$  (1.6 mg, 0.002 mmol) and this was suspended in benzene (1 mL, 11.2 mmol). Triethylsilane (24 mL, 0.15 mmol) along with a magnetic stirring bar were added to the mixture and stirred until colorless. Cyclopentenyl triflate (**3.3**) (22.0 mg, 0.10 mmol) was added to the reaction and stirred for 6 days at 70 °C. The reaction was plugged through silica in the glovebox and volatiles removed under reduced pressure to give phenylcyclopentane (**3.39**) in 64% yield (NMR). The crude product was further purified by flash column chromatography (hexanes) to give phenylcyclopentane as a colorless oil (7.6 mg, 52%). NMR spectra match those reported in literature.<sup>24</sup>



**(3S,5S,8R,9S,10S,13R,14S,17R)-10,13-dimethyl-17-((R)-6-methylheptan-2-yl)-3-phenylhexadecahydro-1H-cyclopenta[a]phenanthrene (3.40).** Synthesized according to general procedure A. A dram vial was charged with  $[\text{Ph}_3\text{C}]^+[\text{HCB}_{11}\text{Cl}_{11}]^-$  (0.8 mg, 0.001 mmol) and this was suspended in benzene (0.5 mL, 5.6 mmol). Triethylsilane (12 mL, 0.075 mmol) along with a magnetic stirring bar were added to the mixture and the resulting suspension stirred for 10 minutes. Triflate **3.3** (26.0 mg, 0.05 mmol) was added to the reaction and stirred for 2

hours at 30 °C. The reaction was plugged through silica in the glovebox and volatiles removed under reduced pressure to give product **3.40** as a diastereomeric mixture in 79% and 11% yield (NMR) of the major and minor diastereomers, respectively. The crude mixture was purified via silica column chromatography (hexanes) to give an inseparable mixture of diastereomers as a white solid (18.5 mg, 85% of mixture). Assignment of major isomer was based on key cross-peaks in <sup>1</sup>H COSY and <sup>1</sup>H NOESY spectroscopy experiments. From the major benzylic proton, adjacent protons were identified at 1.47 ppm and 1.72 ppm through COSY. The same peaks were observed in NOESY in addition to two peaks at 1.08 ppm and 1.26 ppm corresponding to 1,3-diaxial interactions of the benzylic proton. Through 2D HSQC and HMBC experiments, the cross-peak at 1.26 ppm was determined to be the *trans*-decalin proton.

Major Isomer: <sup>1</sup>H NMR (500 MHz, CDCl<sub>3</sub>) δ 7.33 – 7.29 (m, 2H), 7.27 – 7.24 (m, 2H), 7.22 – 7.18 (m, 1H), 2.58 (tt, *J* = 11.5, 5.0 Hz, 1H), 2.02 (dt, *J* = 12.5, 3.4 Hz, 1H), 1.90 – 1.80 (m, 2H), 1.77 – 1.66 (m, 3H), 1.65 – 1.58 (m, 2H), 1.56 – 1.46 (m, 3H), 1.43 – 1.25 (m, 9H), 1.23 – 1.00 (m, 11H), 0.94 (d, *J* = 6.6 Hz, 3H), 0.91 (d, *J* = 2.3 Hz, 3H), 0.90 (s, 3H), 0.89 (d, *J* = 2.3 Hz, 3H), 0.77 – 0.71 (m, 1H), 0.70 (s, 3H); <sup>13</sup>C NMR (125 MHz, CDCl<sub>3</sub>) δ 147.9, 128.4, 127.0, 125.9, 56.8, 56.5, 54.8, 47.2, 45.0, 42.8, 39.7, 39.1, 36.8, 36.4, 36.0, 35.9, 35.7, 30.0, 28.2, 24.0, 23.0, 22.7, 18.9, 12.7, 12.3.

FTIR (Neat film NaCl): 3070, 3023, 2926, 2846, 1466, 1381, 757, 696, 513.

HR-MS (GCT-LIFDI): Calculated for C<sub>33</sub>H<sub>52</sub>: 448.4069; measured: 448.4058.

### 3.7.7 Procedure for Deuterium Competition Experiments

In order to probe the kinetics of our reaction, we subjected **3.3** to a competition experiment with 1:1 C<sub>6</sub>H<sub>12</sub>:C<sub>6</sub>D<sub>12</sub>. Lack of deuterium crossover (Figure **3.13**) and a kinetic isotope effect (KIE) of

0.96 suggest that the C–H insertion step is not rate-determining. Outlined below is the procedure for conducting our alkane competition experiment.

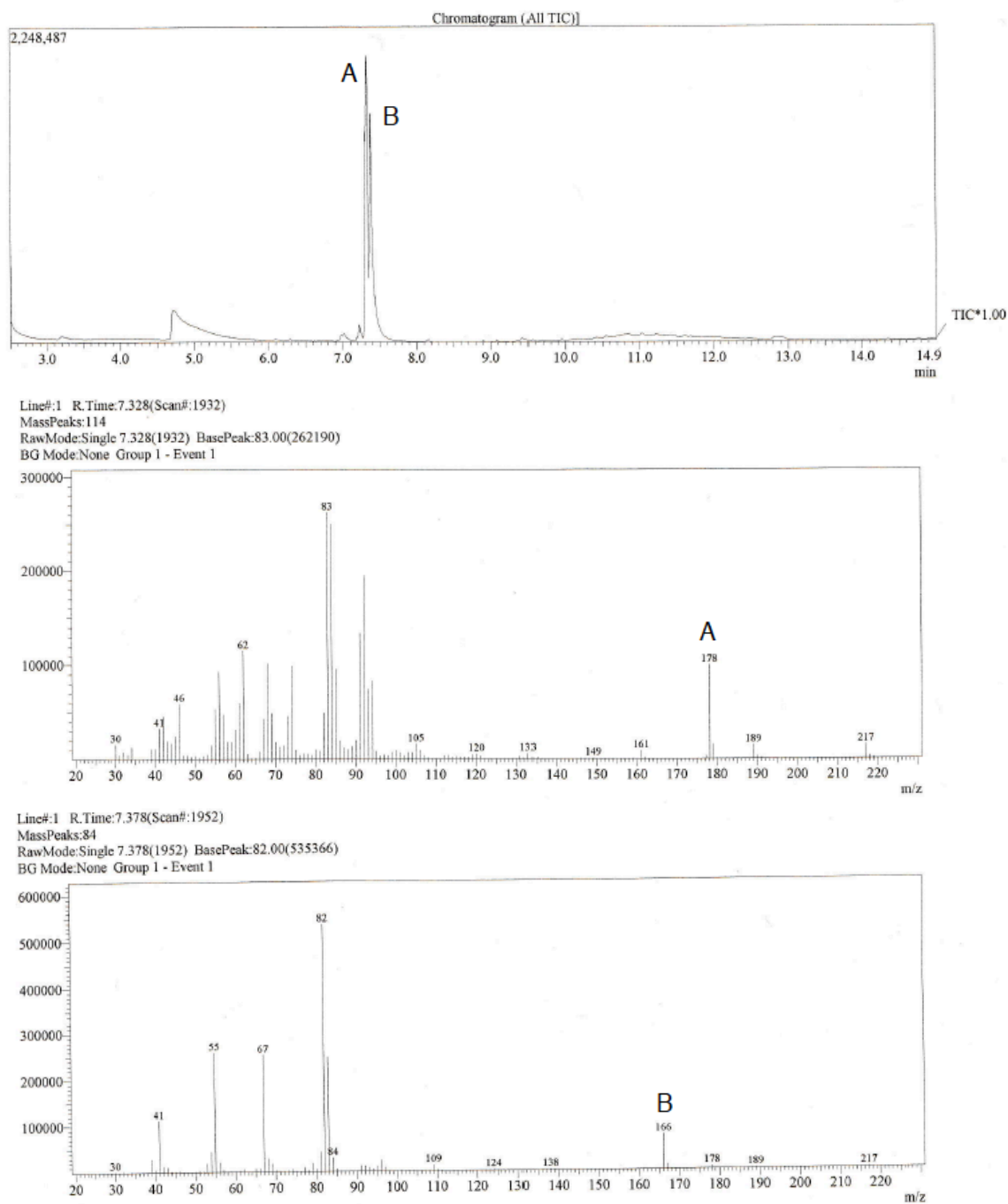


**Figure 3.13** GCMS Spectrum of  $C_6H_{12}/C_6D_{12}$  Crossover Experiment. A = Cyclohexylcyclohexane- $d_{12}$  ( $m/z = 178$ ); B = Cyclohexylcyclohexane ( $m/z = 166$ ).

Similarly, we also subjected **3.3** to a competition experiment with 1:1 Et<sub>3</sub>SiH:Et<sub>3</sub>SiD. An equal distribution of D<sub>1</sub>:D<sub>0</sub> products by qualitative GCMS analysis (Figure 3.14) suggests that the silane quench is also not rate-determining. Outlined below is the procedure for conducting our alkane competition experiment.

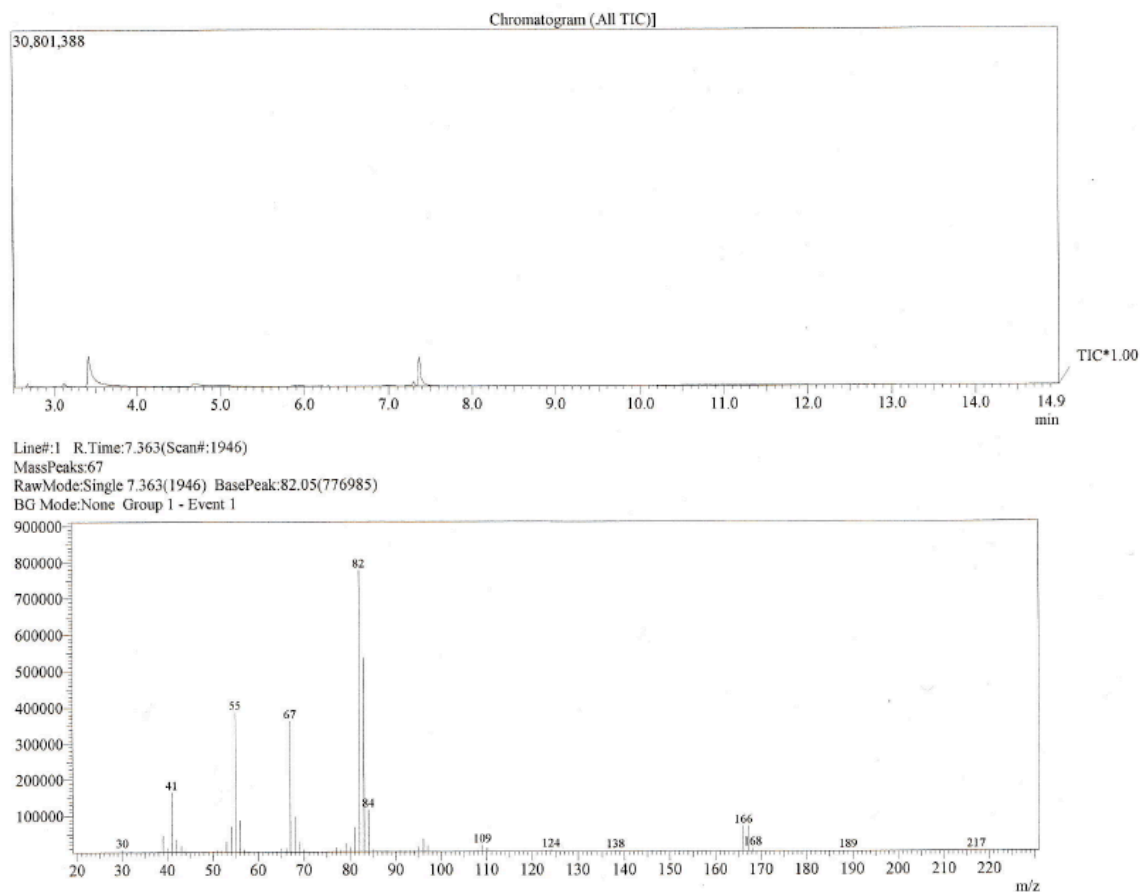
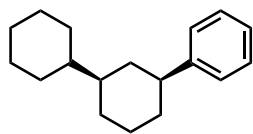


**Figure 3.14** GCMS Spectrum of Et<sub>3</sub>SiH/Et<sub>3</sub>SiD Competition Experiment.

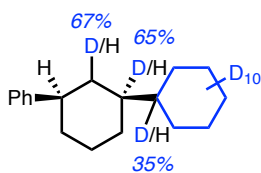
### 3.7.8 Procedure for D-labeling Experiments

In order to distinguish between a *1,1*- and *1,2*-insertion event, we used a modified procedure from general procedure 3.7.5 using C<sub>6</sub>D<sub>12</sub> in place of cyclohexane. NMR data reveals both *1,2*-hydride and deuterium shifts in our substrate, suggestive of an incipient secondary carbocation

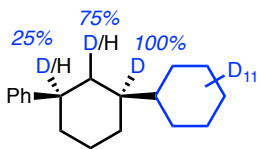
intermediate resulting from a *I,I*-insertion.



**(*cis*)-3-Phenyl-1,1'-bi(cyclohexane) (3.44).** Compound was purchased from Sigma Aldrich as a mixture of isomers. Major *cis* isomer was isolated by reverse phase preparatory HPLC (95:5 acetonitrile:water).

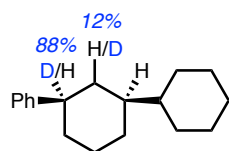


**D<sub>12</sub>-(*cis*)-3-Phenyl-1,1'-bi(cyclohexane) (3.22).** [Ph<sub>3</sub>C]<sup>+</sup>[HCB<sub>11</sub>Cl<sub>11</sub>]<sup>-</sup> (2.4 mg, 3.0 μmol, 0.02 equiv) was suspended in cyclohexane-d<sub>12</sub> (1.5 mL) before addition of triethylsilane (29 μL, 0.18 mmol, 1.2 equiv). After stirring for 10 minutes, vinyl triflate **3.21** (46 mg, 0.15 mmol, 1.0 equiv) was added and the reaction was stirred at room temperature for 17 hours. The reaction was passed through a small layer of silica gel to remove excess silylium reagent inside a well-kept glovebox, ≤ 0.5 ppm O<sub>2</sub>. Crude material was purified by flash chromatography (hexanes) to yield a mixture of diastereomers. Major *cis* product was isolated by reverse phase preparatory HPLC (95:5 acetonitrile:water) to yield 7.3 mg (19%) of colorless oil.

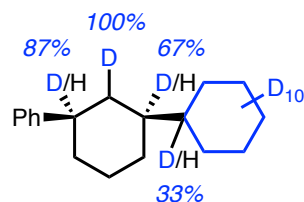


**D<sub>13</sub>-(*cis*)-3-Phenyl-1,1'-bi(cyclohexane) (3.27).** [Ph<sub>3</sub>C]<sup>+</sup>[HCB<sub>11</sub>Cl<sub>11</sub>]<sup>-</sup> (2.4 mg, 3.0 μmol, 0.02 equiv) was suspended in cyclohexane-d<sub>12</sub> (1.5 mL) before addition of triethylsilane-d<sub>1</sub> (29 μL, 0.18 mmol, 1.2 equiv). After stirring for 10 minutes, vinyl triflate **3.21** (46 mg, 0.15 mmol, 1.0 equiv) was added and the reaction was stirred at room temperature for 17 hours. The reaction

was passed through a small layer of silica gel to remove excess silylium reagent inside a well-kept glovebox,  $\leq 0.5$  ppm O<sub>2</sub>. Crude material was purified by flash chromatography (hexanes) to yield a mixture of diastereomers. Major *cis* product was isolated by reverse phase preparatory HPLC (95:5 acetonitrile:water) to yield 6.0 mg (16%) of colorless oil.



**D<sub>1</sub>-(*cis*)-3-Phenyl-1,1'-bi(cyclohexane) (3.30).** [Ph<sub>3</sub>C]<sup>+</sup>[HCB<sub>11</sub>Cl<sub>11</sub>]<sup>-</sup> (2.4 mg, 3.0 μmol, 0.02 equiv) was suspended in cyclohexane (1.5 mL) before addition of triethylsilane (36 μL, 0.18 mmol, 1.5 equiv). After stirring for 10 minutes, vinyl triflate **3.29** (46 mg, 0.15 mmol, 1.0 equiv) was added and the reaction was stirred at room temperature for 1 hour. The reaction was passed through a small layer of silica gel to remove excess silylium reagent inside a well-kept glovebox,  $\leq 0.5$  ppm O<sub>2</sub>. Crude material was purified by flash chromatography (hexanes) to yield a mixture of diastereomers. Major *cis* product was isolated by reverse phase preparatory HPLC (95:5 acetonitrile:water) to yield 6.2 mg (17%) of colorless oil.



**D<sub>13</sub>-(*cis*)-3-Phenyl-1,1'-bi(cyclohexane) (3.45).** [Ph<sub>3</sub>C]<sup>+</sup>[HCB<sub>11</sub>Cl<sub>11</sub>]<sup>-</sup> (2.4 mg, 3.0 μmol, 0.02 equiv) was suspended in D<sub>12</sub>-cyclohexane (1.5 mL) before addition of triethylsilane (36 μL, 0.18 mmol, 1.5 equiv). After stirring for 10 minutes, vinyl triflate **3.29** (46 mg, 0.15 mmol, 1.0 equiv) was added and the reaction was stirred at room temperature for 17 hours. The reaction was passed through a small layer of silica gel to remove excess silylium reagent inside a well-kept glovebox,  $\leq 0.5$  ppm O<sub>2</sub>. Crude material was purified by flash chromatography (hexanes) to yield



a mixture of diastereomers. Major *cis* product was isolated by reverse phase preparatory HPLC (95:5 acetonitrile:water) to yield 8.8 mg (23%) of colorless oil.

### 3.8 Spectra Relevant to Chapter Three:

#### **Teaching An Old Carbocation New Tricks: Intermolecular C–H Insertion Reactions of Vinyl Carbocations**

Adapted from: Stasik Popov, Brian Shao, Alex L. Bagdasarian, Tyler R. Benton, Luyi Zou,

Zhongyue Yang, K. N. Nouk, and Hosea M. Nelson

*Science*, **2018**, *361*, 381–387.

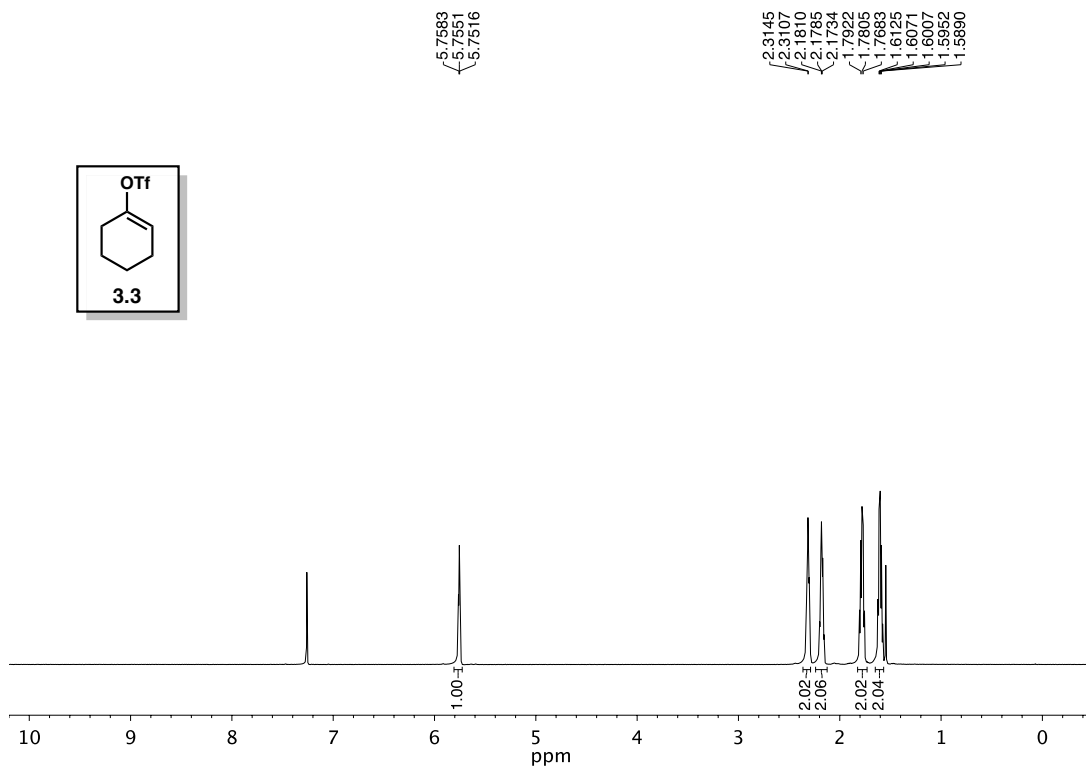


Figure 3.15 <sup>1</sup>H NMR (400 MHz, CDCl<sub>3</sub>) of compound 3.3.

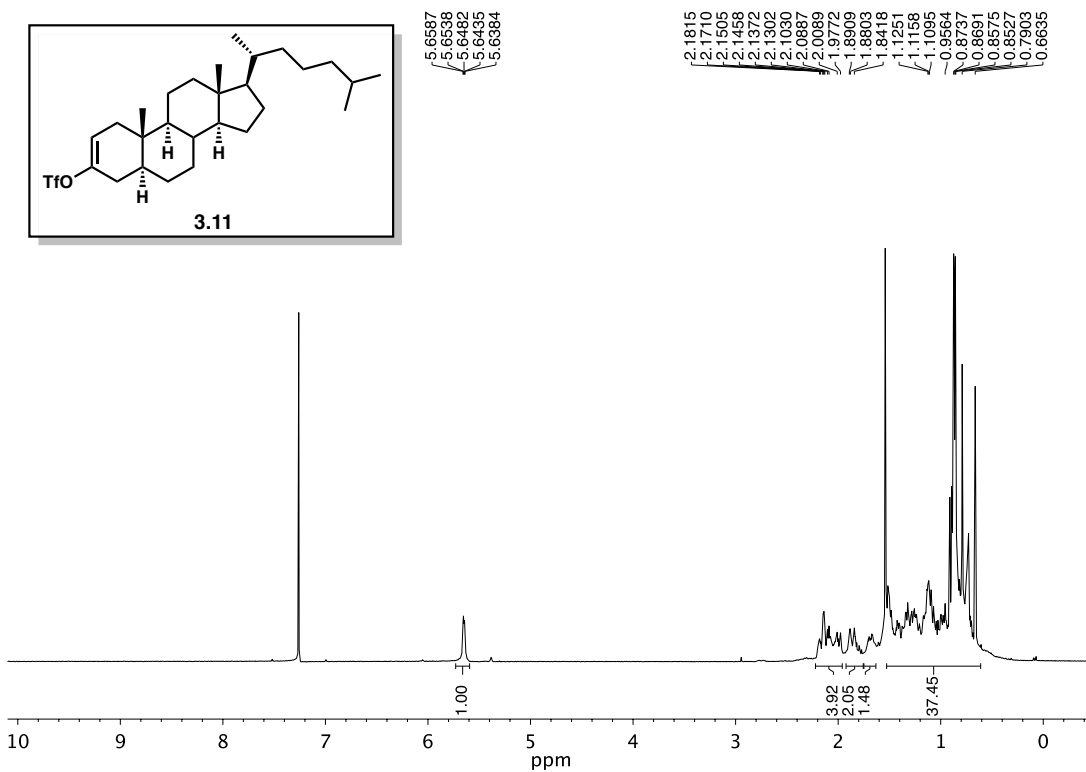
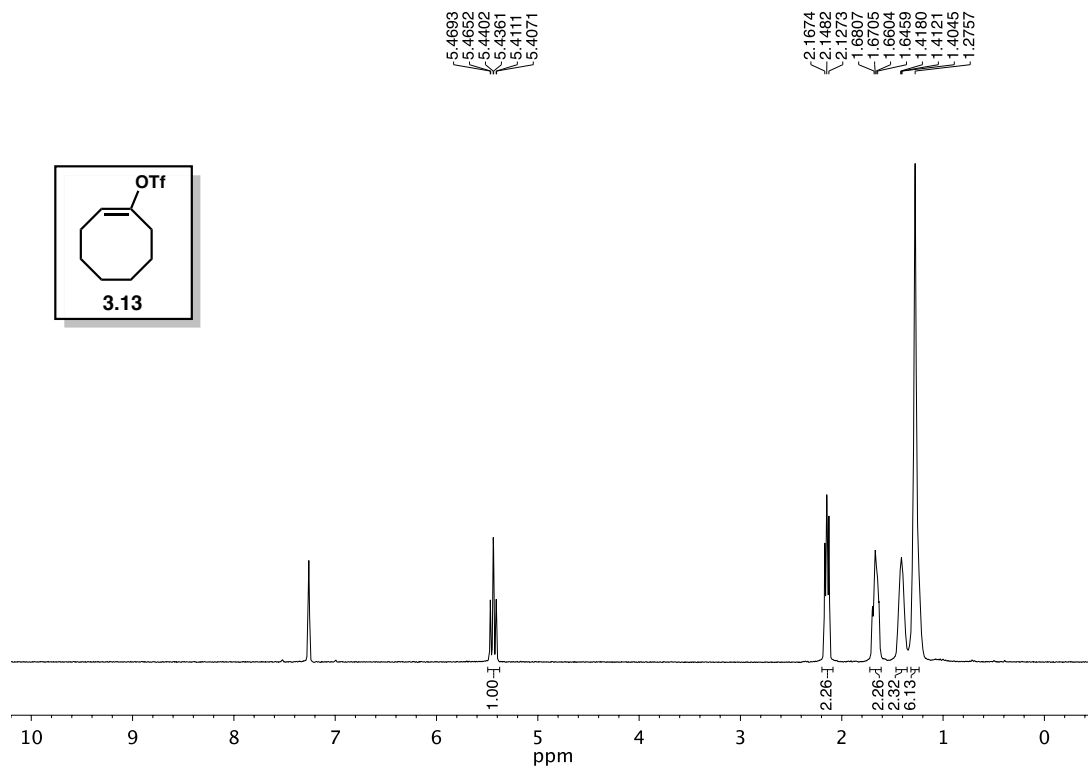
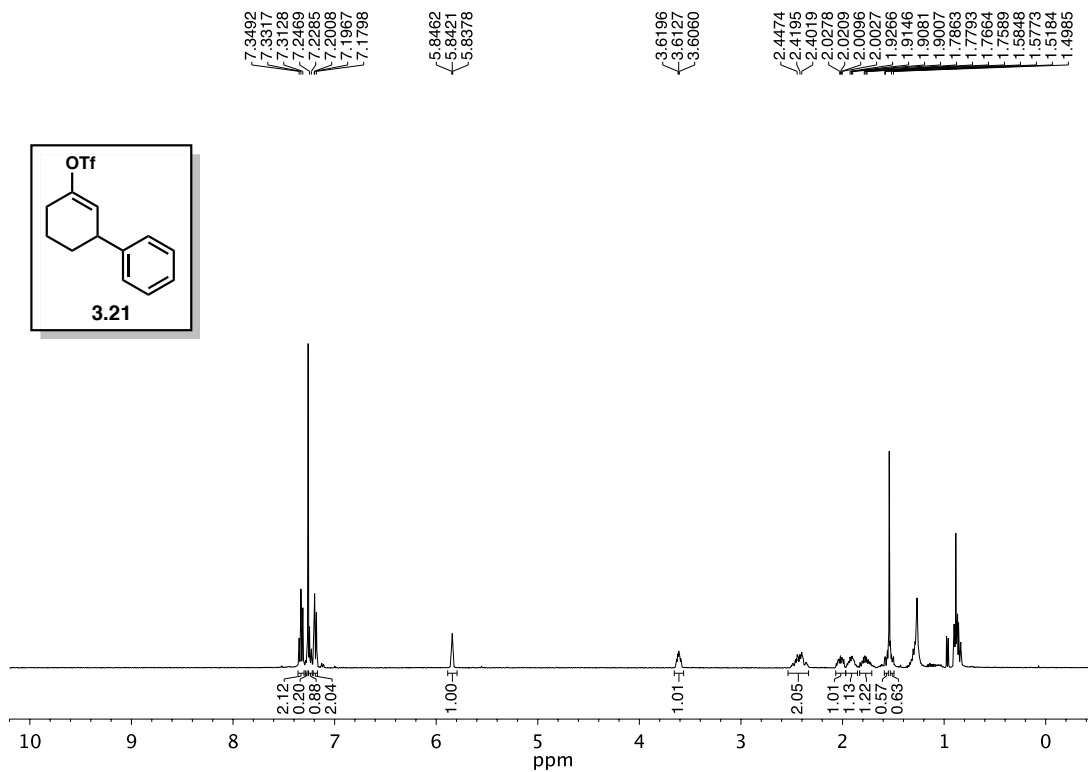


Figure 3.16 <sup>1</sup>H NMR (500 MHz, CDCl<sub>3</sub>) of compound 3.11.



**Figure 3.17**  $^1\text{H NMR}$  (400 MHz,  $\text{CDCl}_3$ ) of compound **3.13**.



**Figure 3.18**  $^1\text{H NMR}$  (400 MHz,  $\text{CDCl}_3$ ) of compound **3.21**.

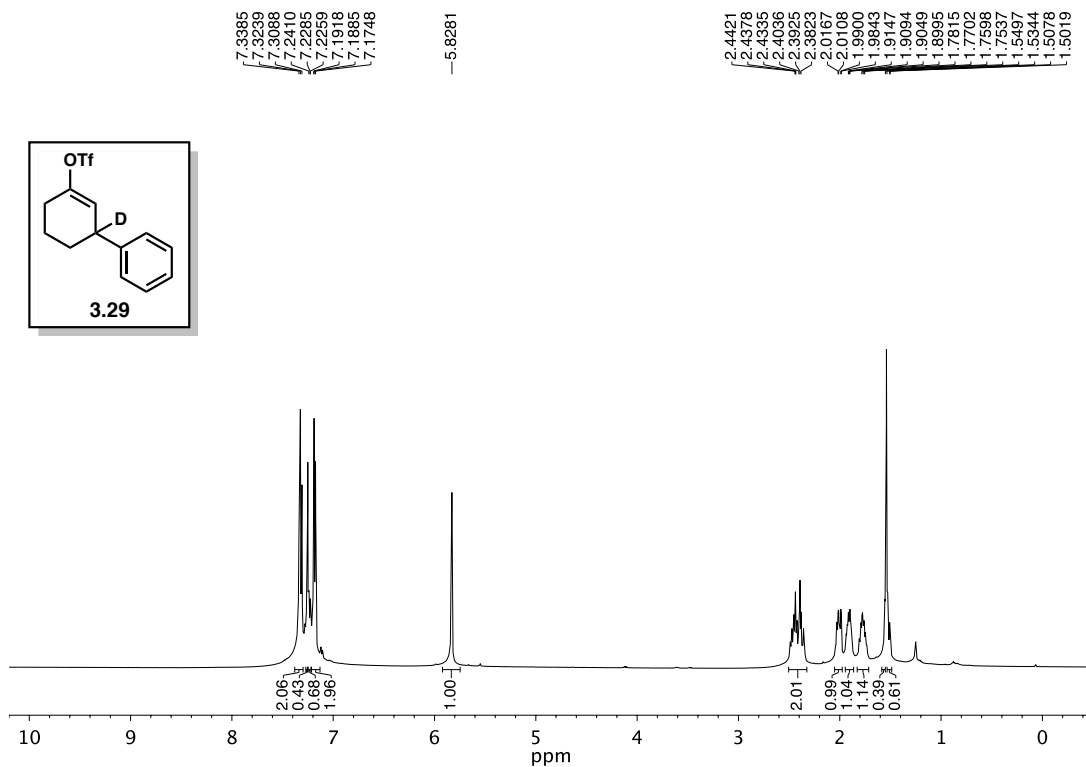


Figure 3.19 <sup>1</sup>H NMR (400 MHz, CDCl<sub>3</sub>) of compound 3.29.

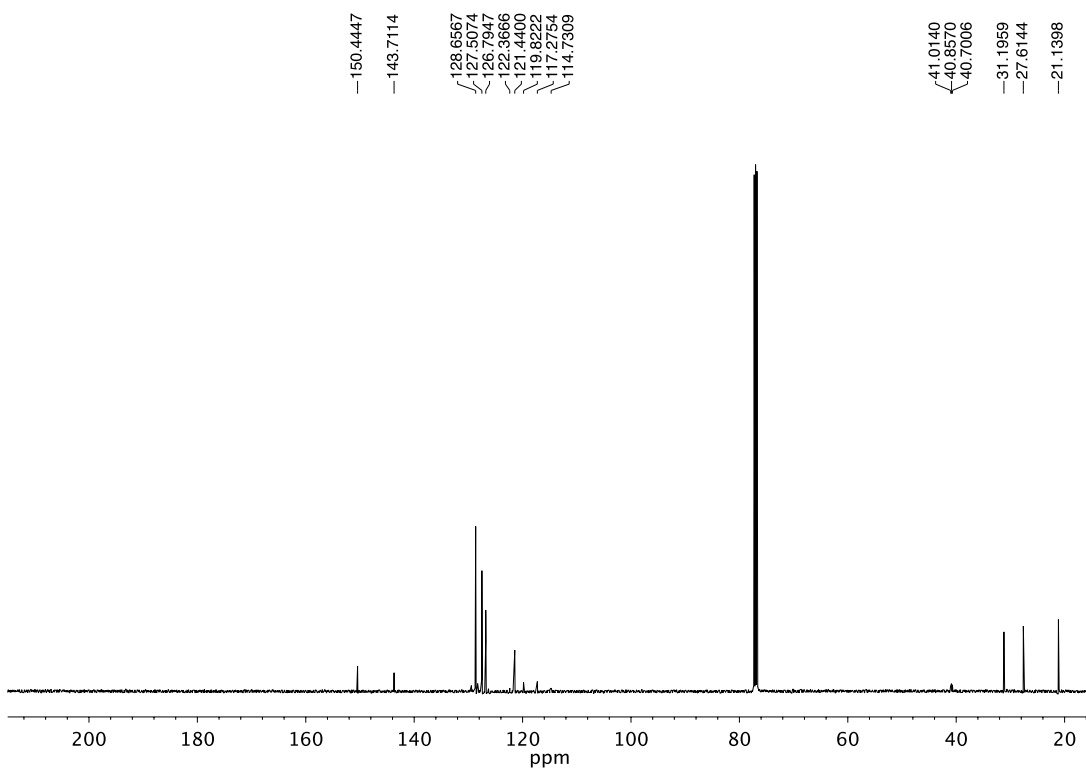


Figure 3.20 <sup>13</sup>C NMR (125 MHz, CDCl<sub>3</sub>) of compound 3.29.

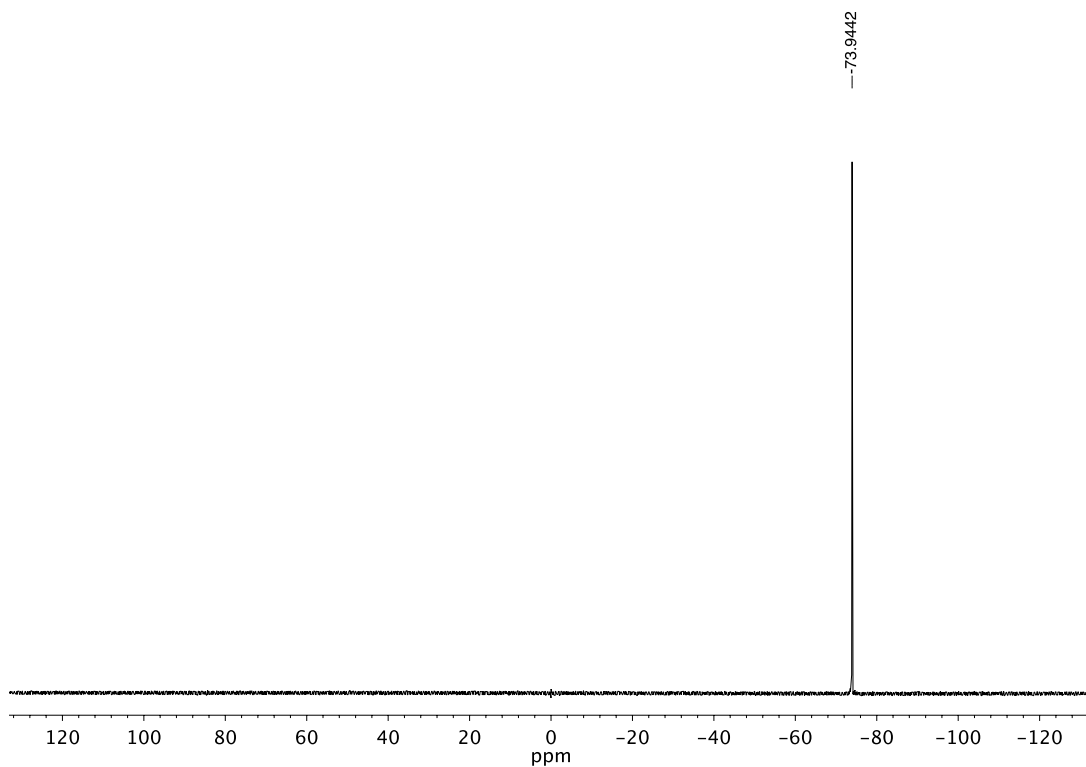


Figure 3.21  $^{19}\text{F}$  NMR (376 MHz,  $\text{CDCl}_3$ ) of compound 3.29.

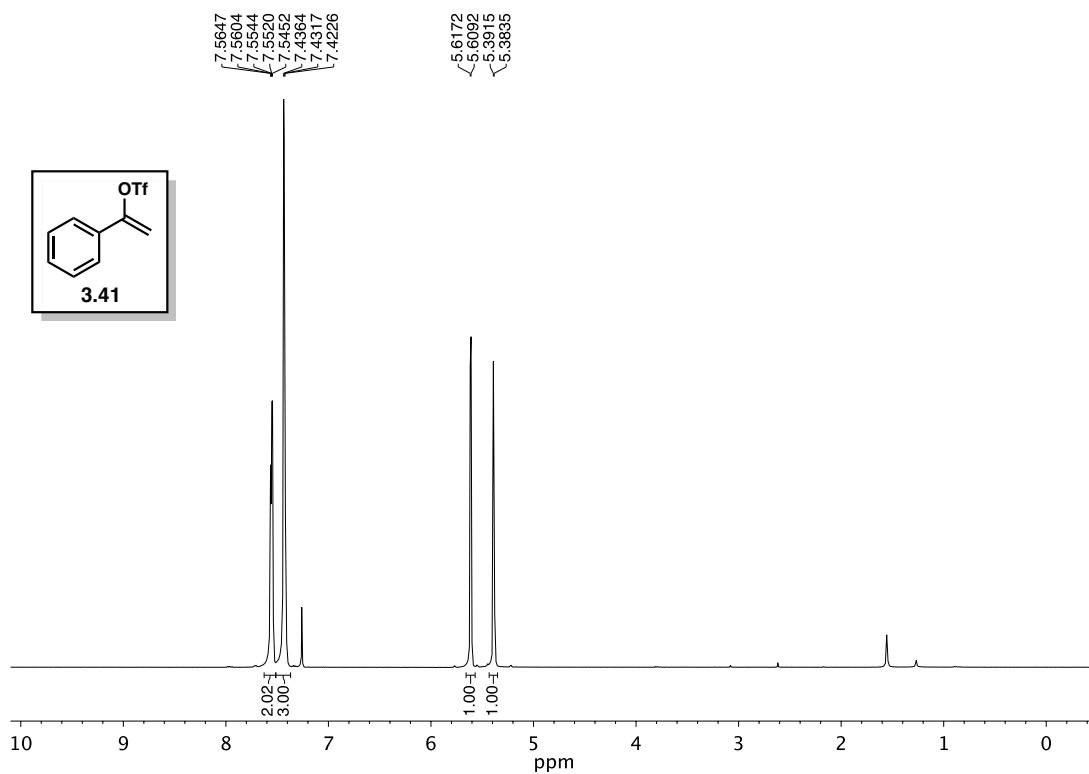


Figure 3.22  $^1\text{H}$  NMR (400 MHz,  $\text{CDCl}_3$ ) of compound 3.41.

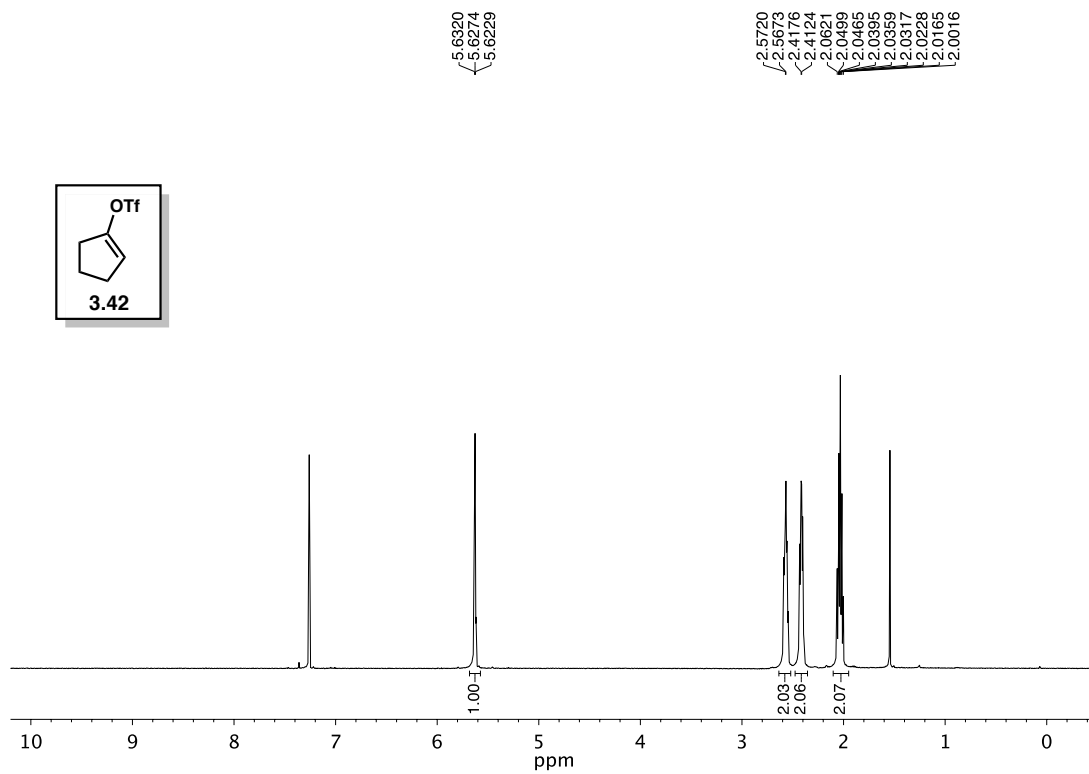


Figure 3.23  $^1\text{H}$  NMR (400 MHz,  $\text{CDCl}_3$ ) of compound 3.42.

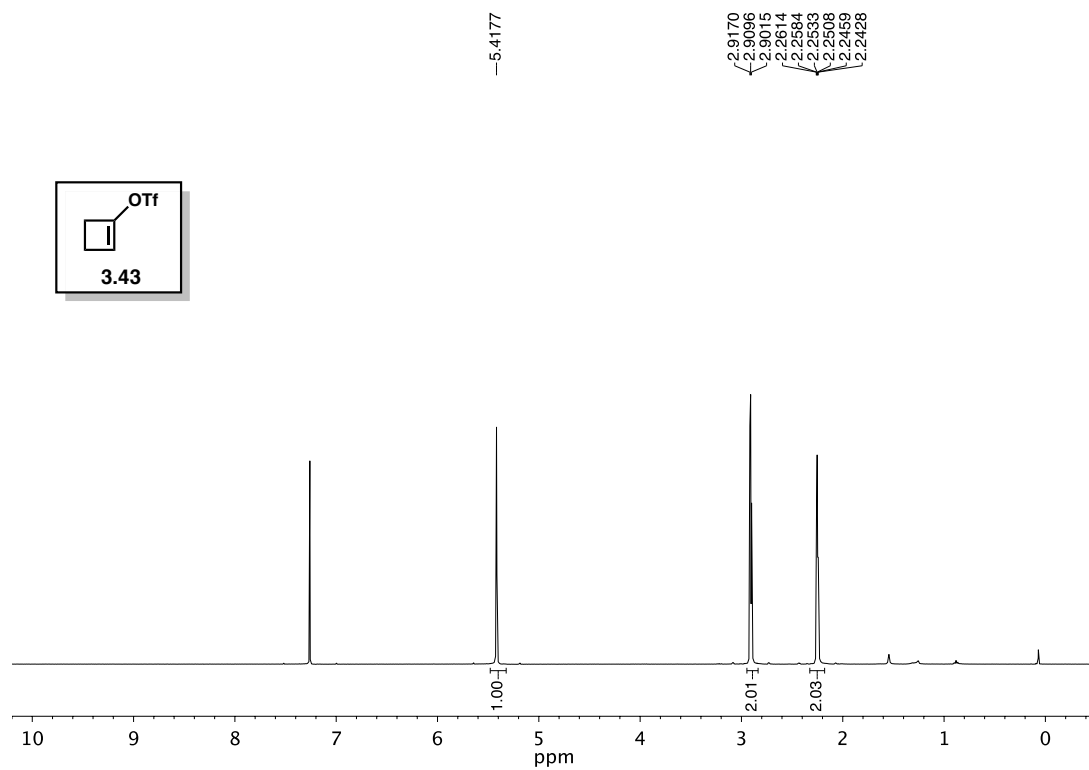
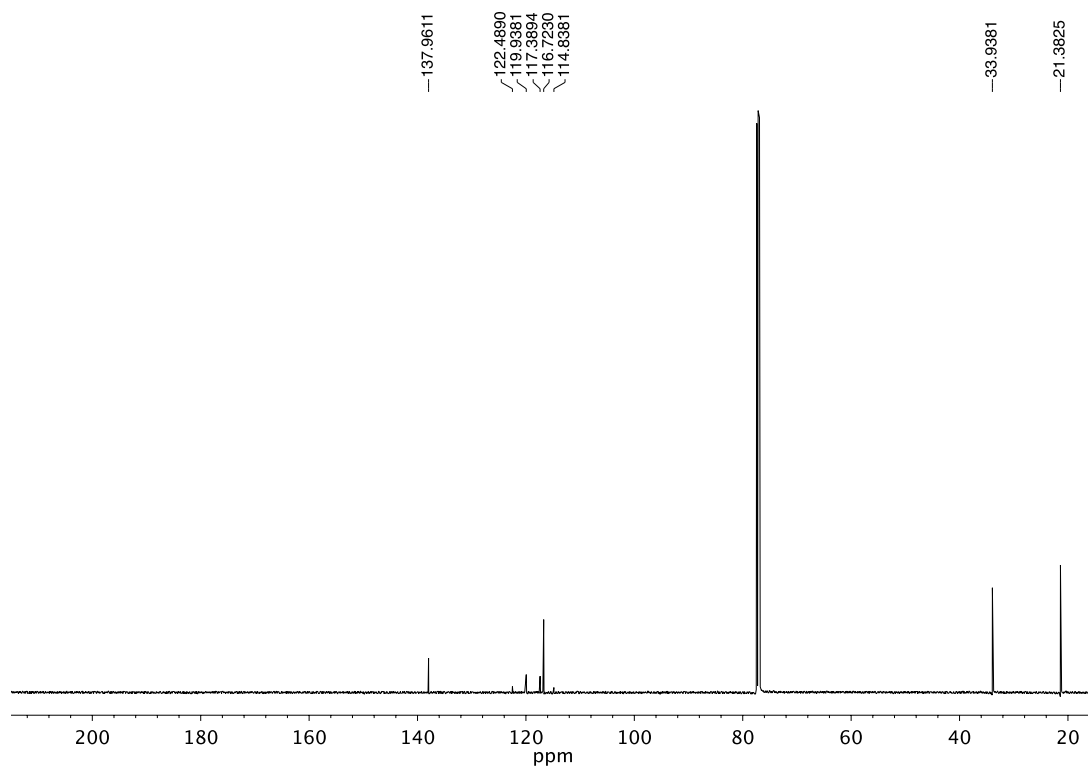
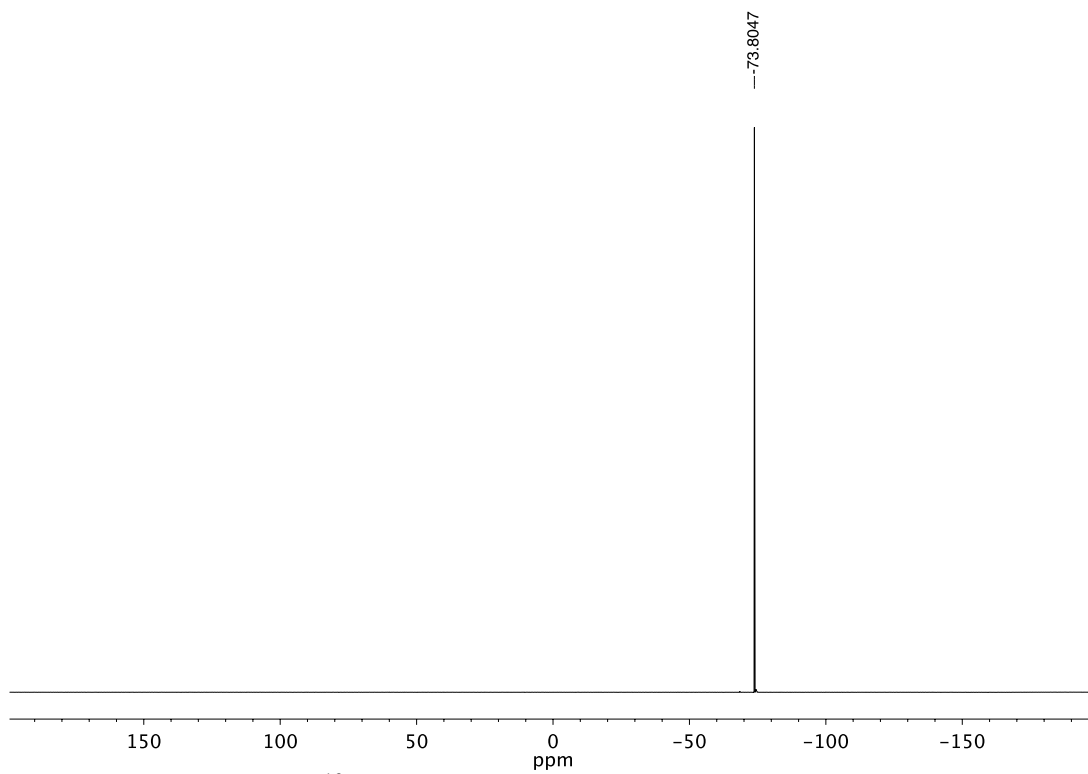


Figure 3.24  $^1\text{H}$  NMR (400 MHz,  $\text{CDCl}_3$ ) of compound 3.43.



**Figure 3.25**  $^{13}\text{C}$  NMR (125 MHz,  $\text{CDCl}_3$ ) of compound **3.43**.



**Figure 3.26**  $^{19}\text{F}$  NMR (376 MHz,  $\text{CDCl}_3$ ) of compound **3.43**.



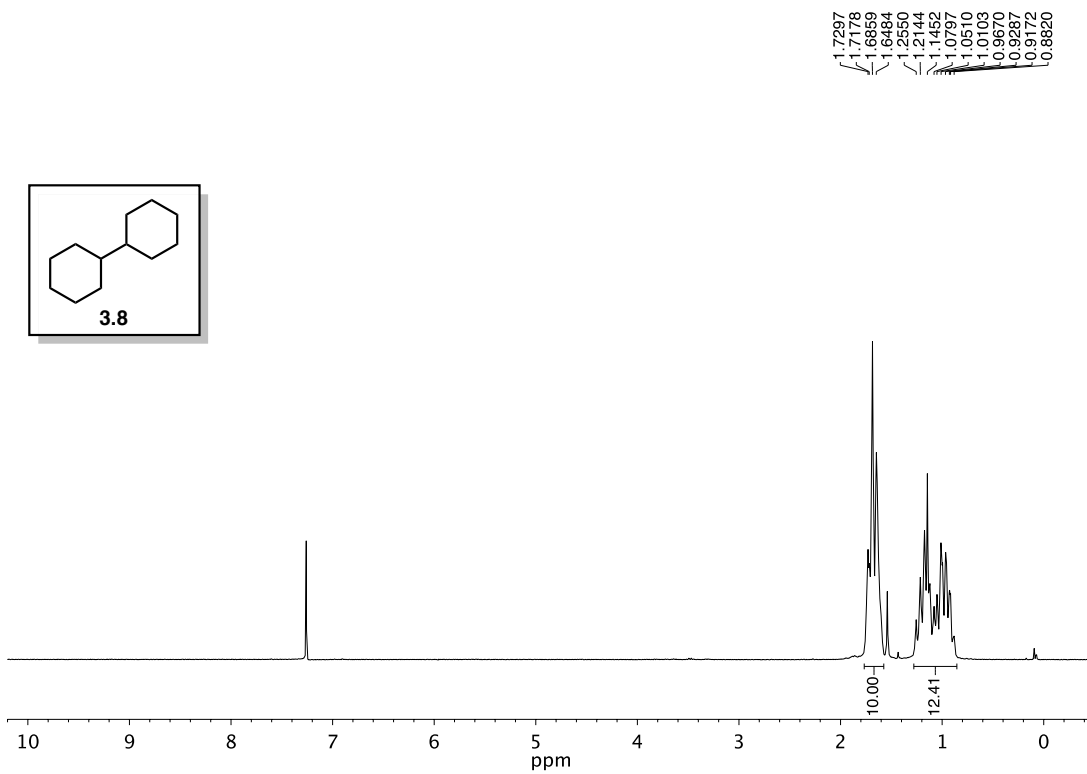


Figure 3.27  $^1\text{H}$  NMR (400 MHz,  $\text{CDCl}_3$ ) of compound 3.8.

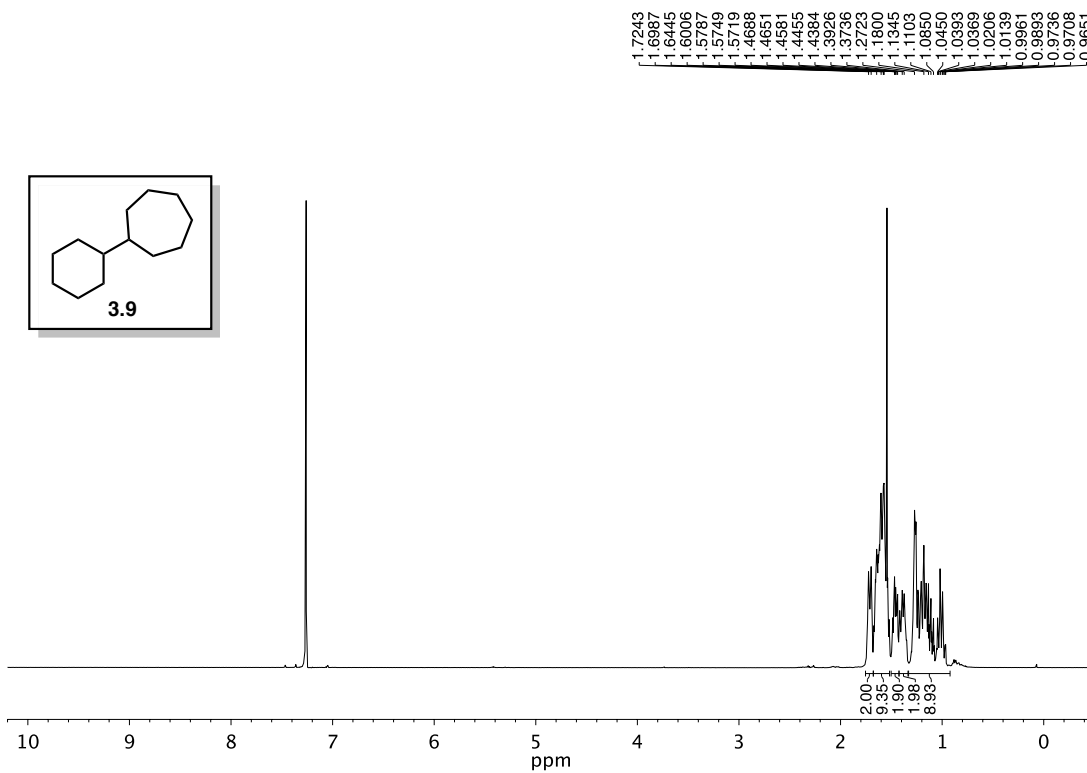
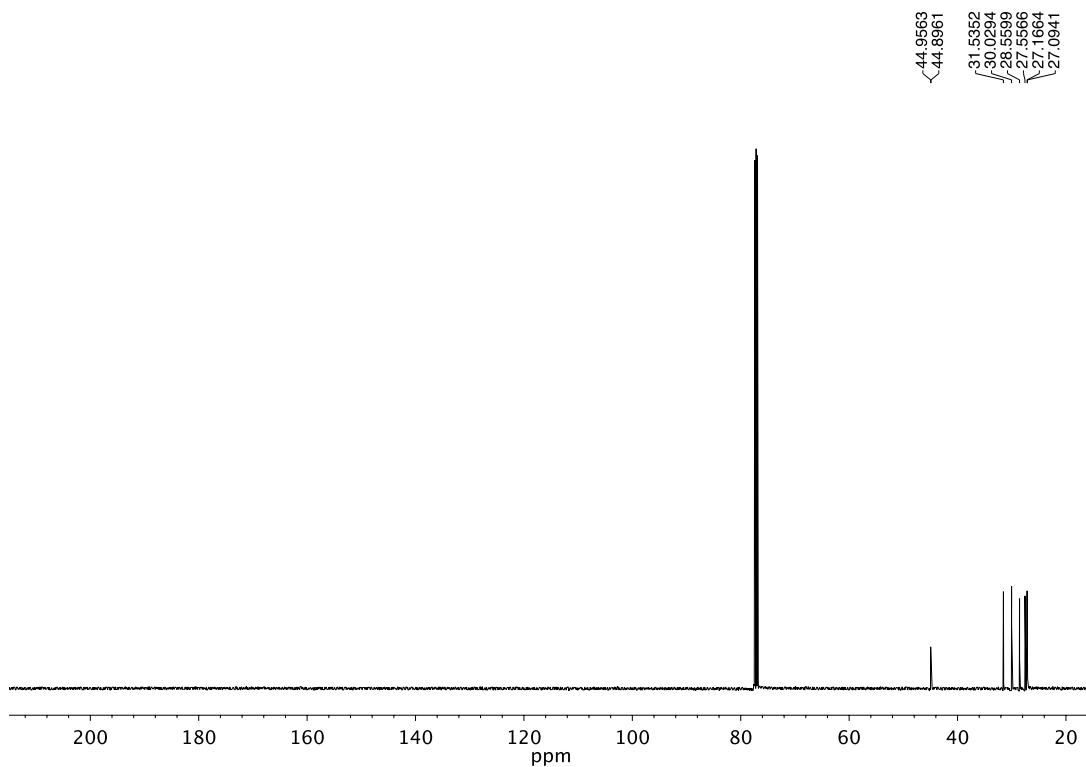
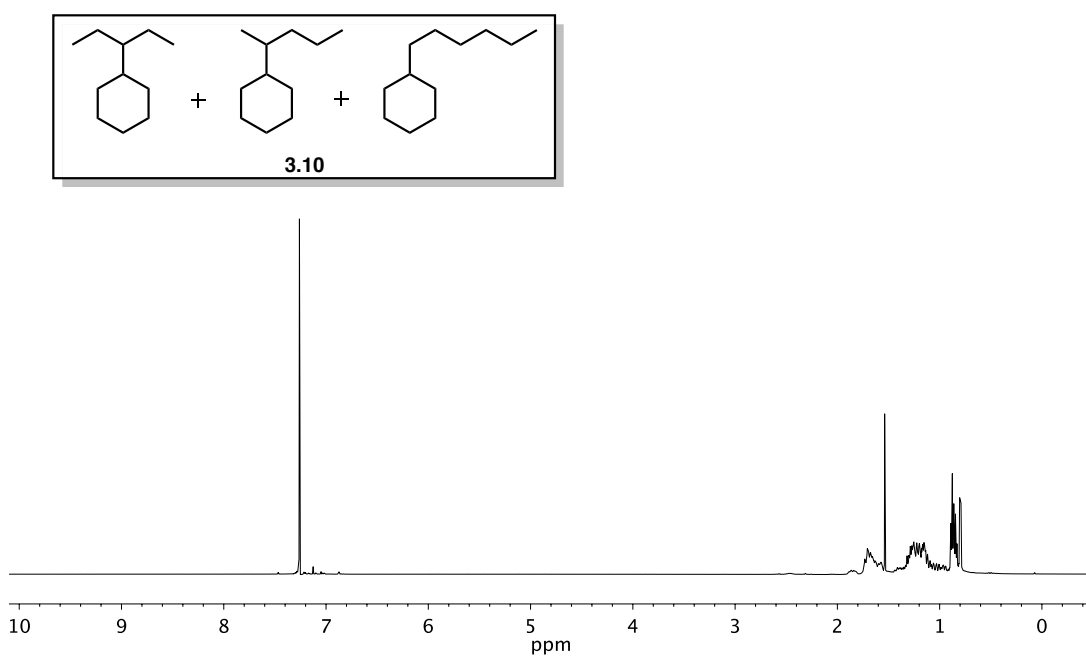


Figure 3.28  $^1\text{H}$  NMR (400 MHz,  $\text{CDCl}_3$ ) of compound 3.9.



**Figure 3.29**  $^{13}\text{C}$  NMR (125 MHz,  $\text{CDCl}_3$ ) of compound **3.9**.



**Figure 3.30**  $^1\text{H}$  NMR (400 MHz,  $\text{CDCl}_3$ ) of compound **3.10**.

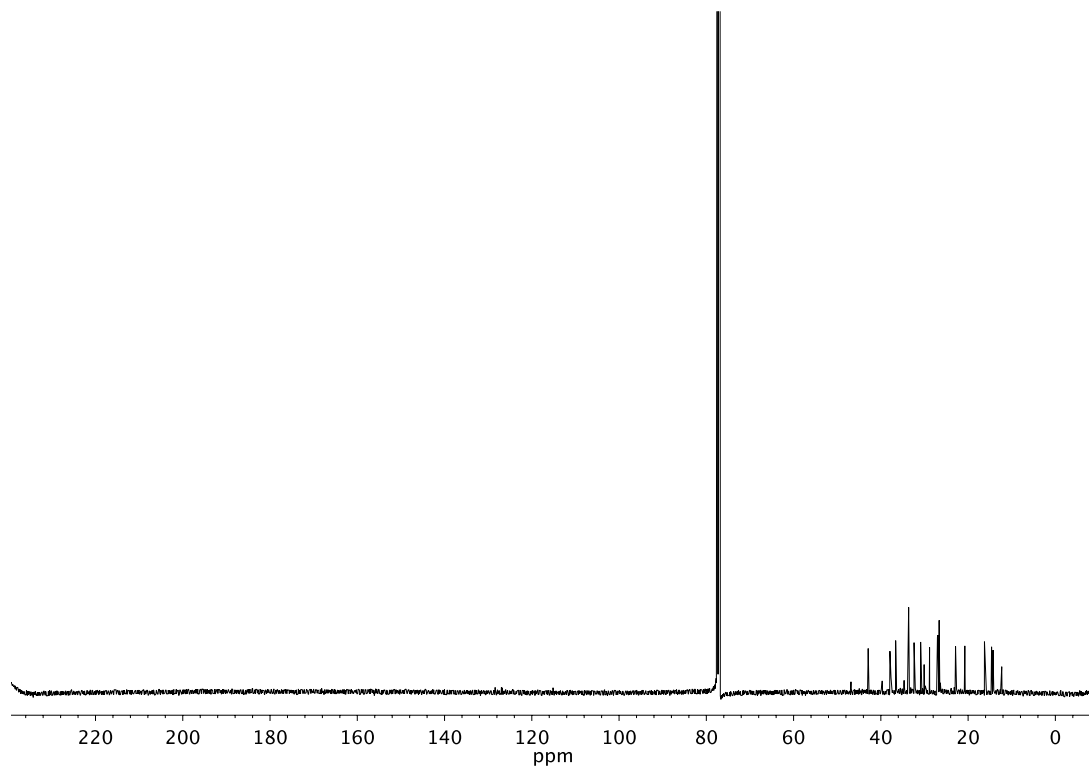


Figure 3.31  $^{13}\text{C}$  NMR (125 MHz,  $\text{CDCl}_3$ ) of compound **3.10**.

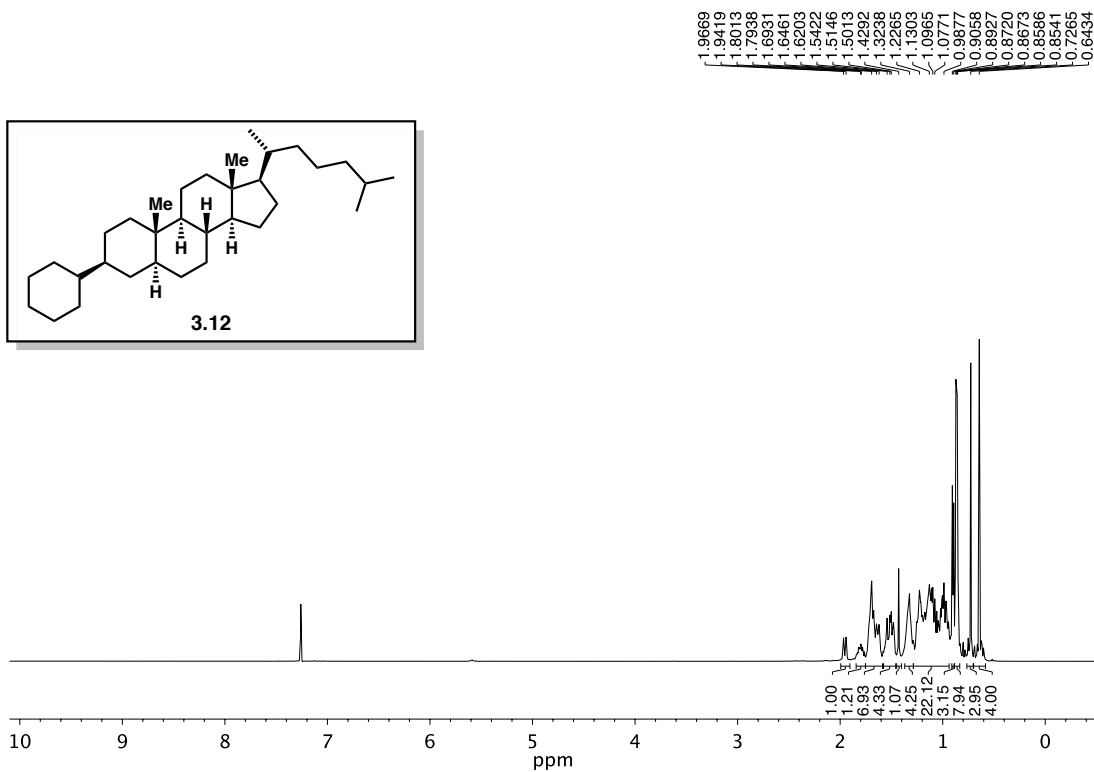


Figure 3.32  $^1\text{H}$  NMR (500 MHz,  $\text{CDCl}_3$ ) of compound **3.12**.

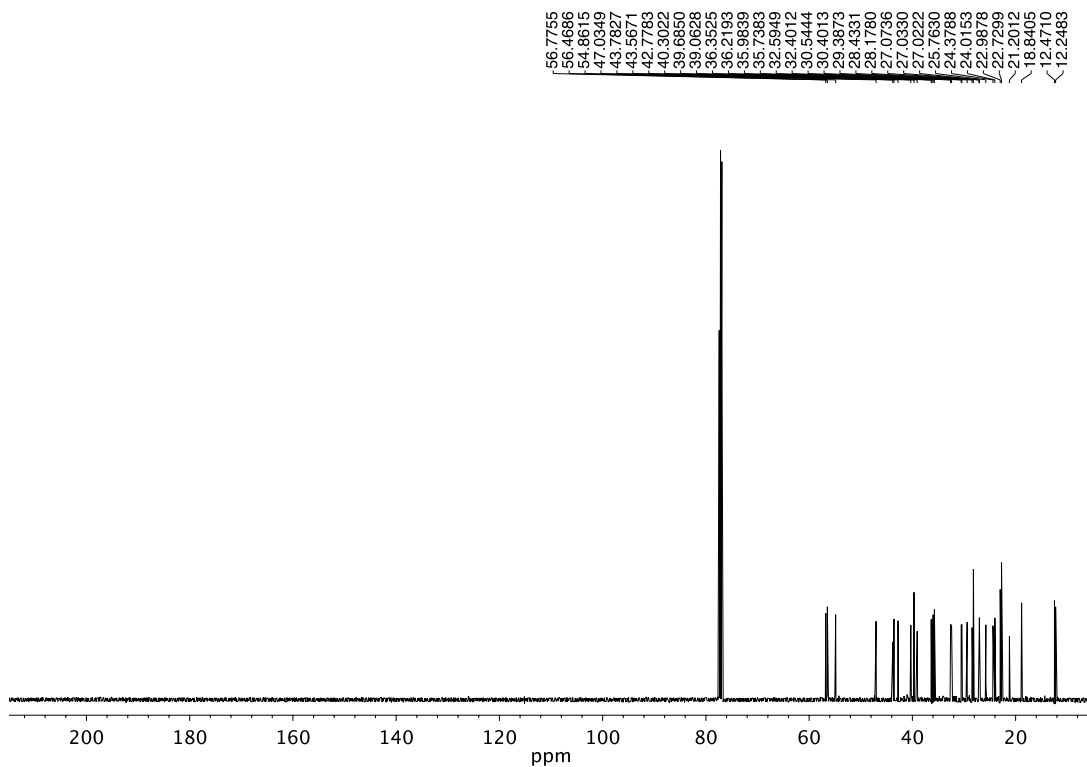


Figure 3.33  $^{13}\text{C}$  NMR (125 MHz,  $\text{CDCl}_3$ ) of compound **3.12**.

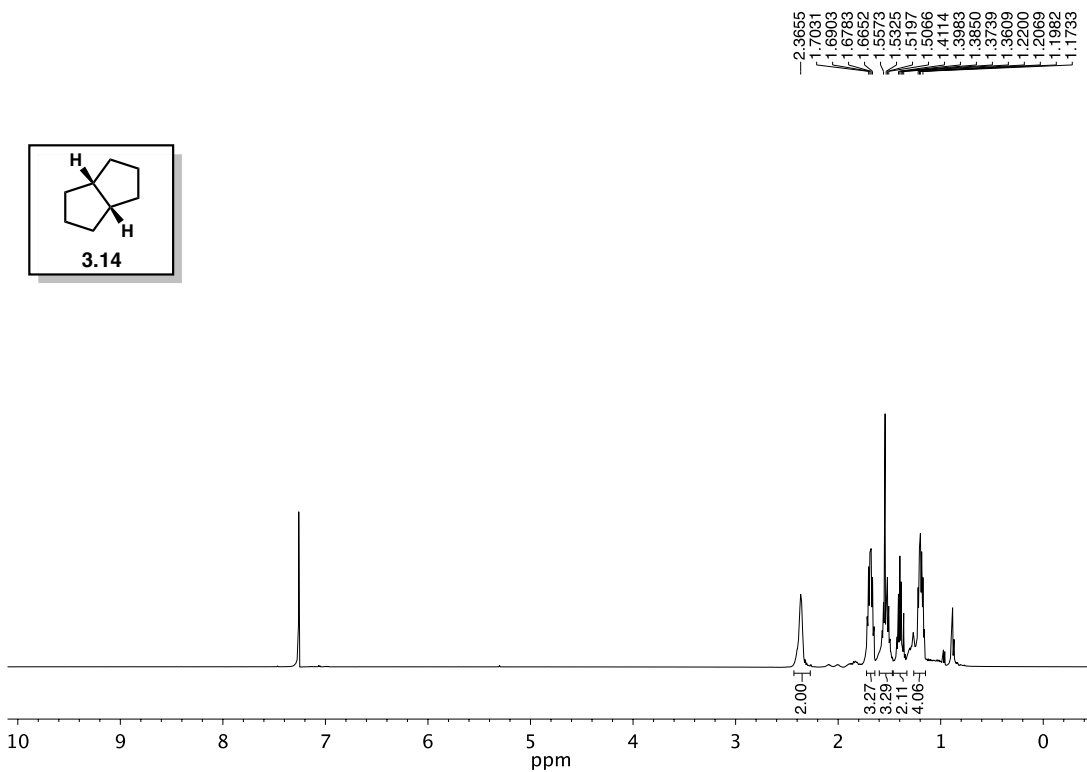


Figure 3.34  $^1\text{H}$  NMR (400 MHz,  $\text{CDCl}_3$ ) of compound **3.14**.

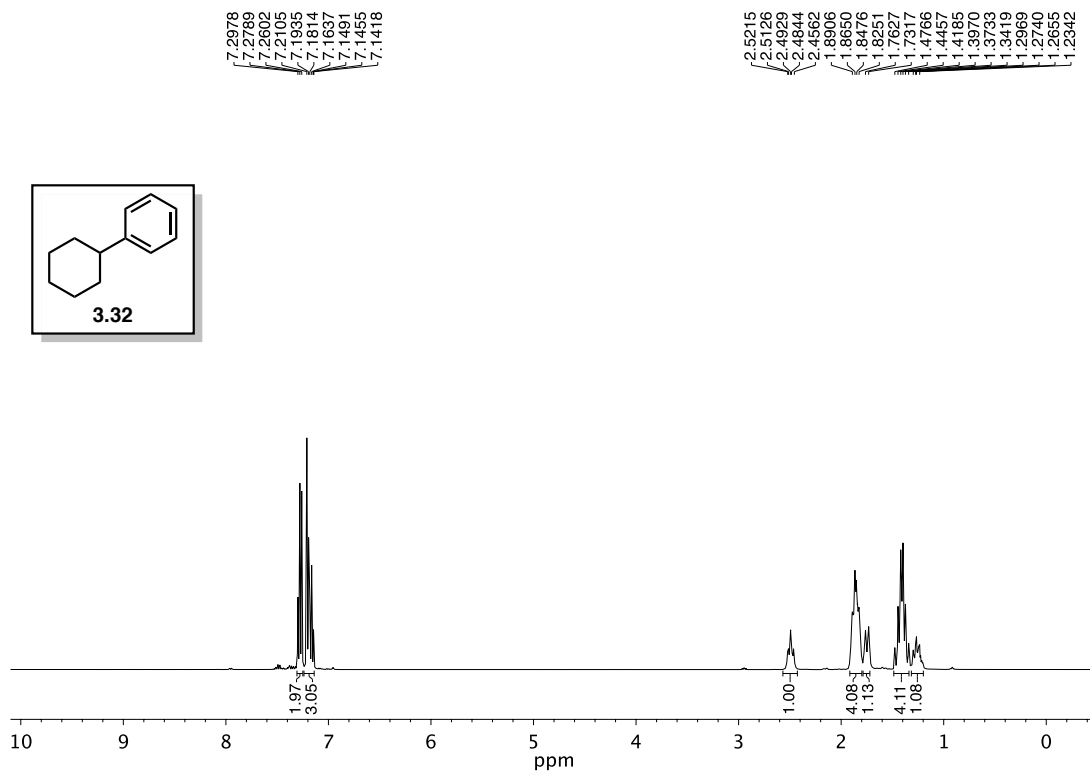


Figure 3.35 <sup>1</sup>H NMR (400 MHz, CDCl<sub>3</sub>) of compound 3.32.

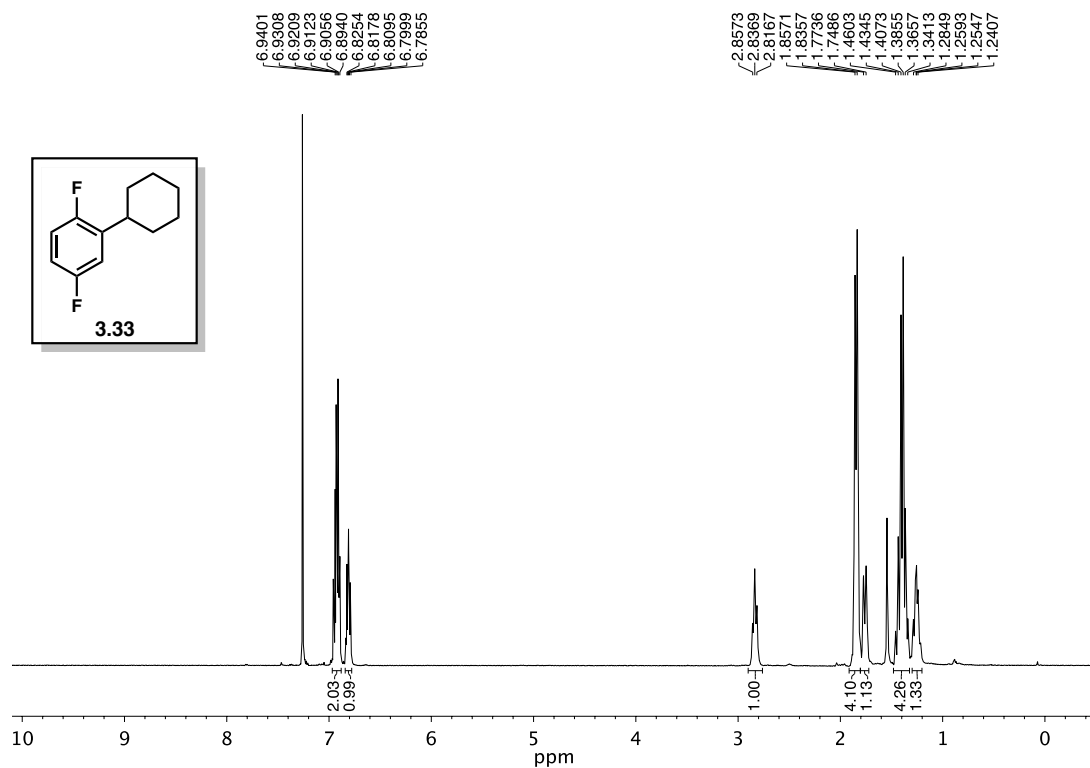


Figure 3.36 <sup>1</sup>H NMR (500 MHz, CDCl<sub>3</sub>) of compound 3.33.

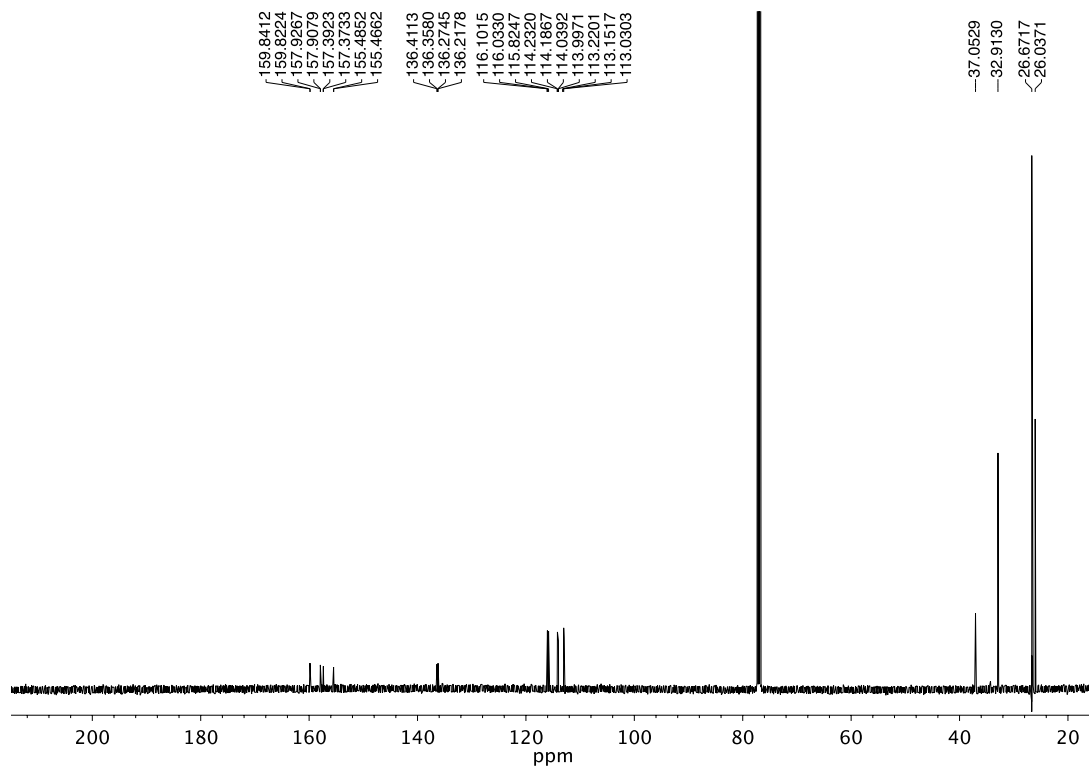


Figure 3.37  $^{13}\text{C}$  NMR (125 MHz,  $\text{CDCl}_3$ ) of compound 3.33.

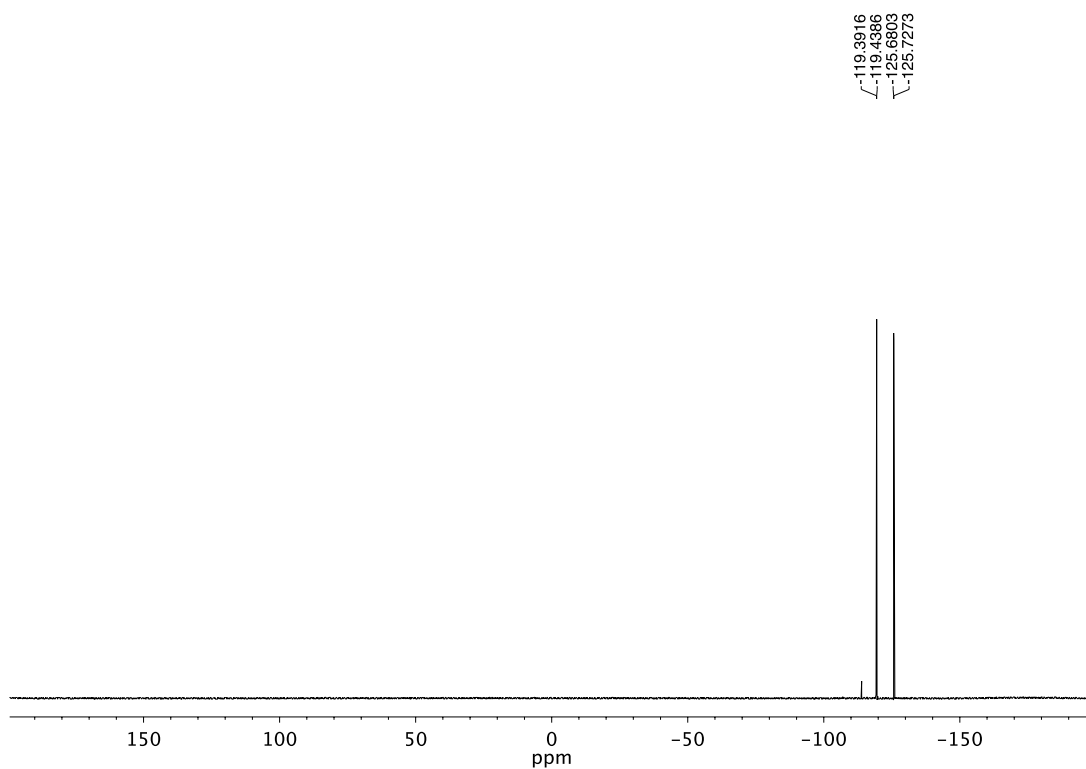
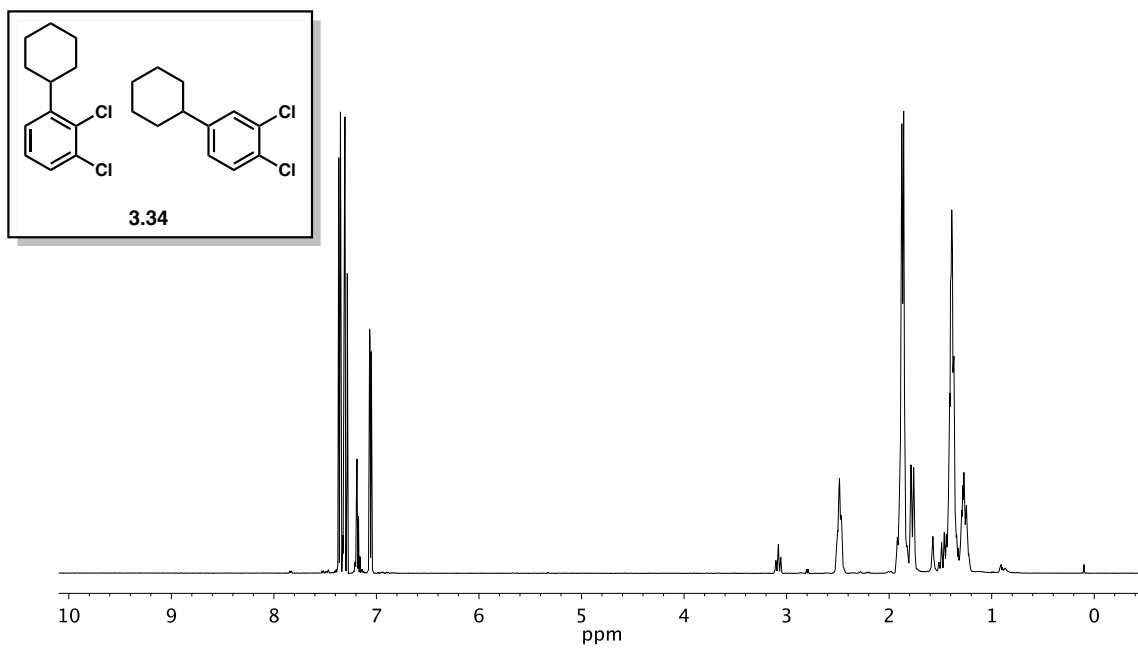
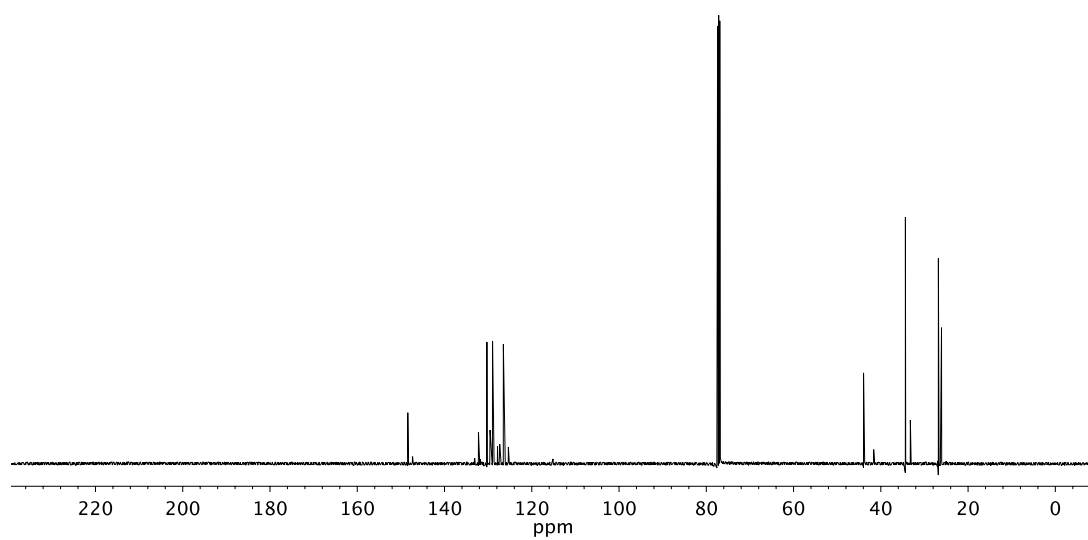


Figure 3.38  $^{19}\text{F}$  NMR (376 MHz,  $\text{CDCl}_3$ ) of compound 3.33.



**Figure 3.39** <sup>1</sup>H NMR (500 MHz, CDCl<sub>3</sub>) of compound **3.34**.



**Figure 3.40** <sup>13</sup>C NMR (125 MHz, CDCl<sub>3</sub>) of compound **3.34**.

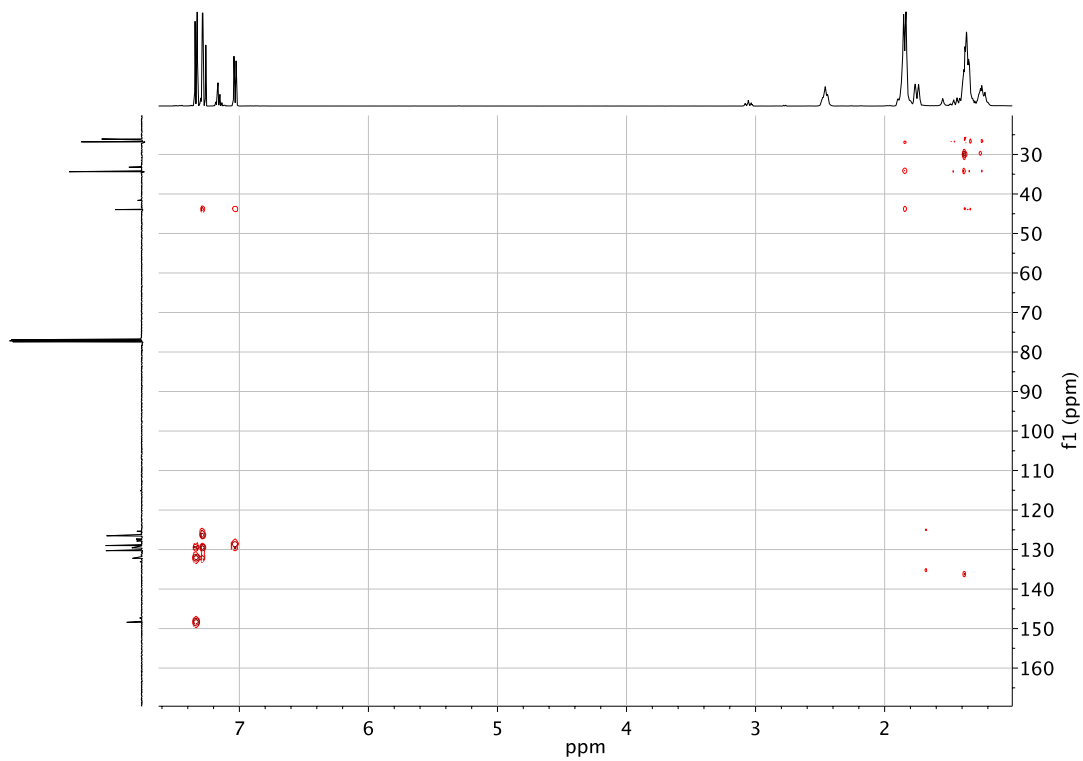


**Figure 3.41** 2D HMBC NMR (500 MHz, CDCl<sub>3</sub>) of compound **3.34**.

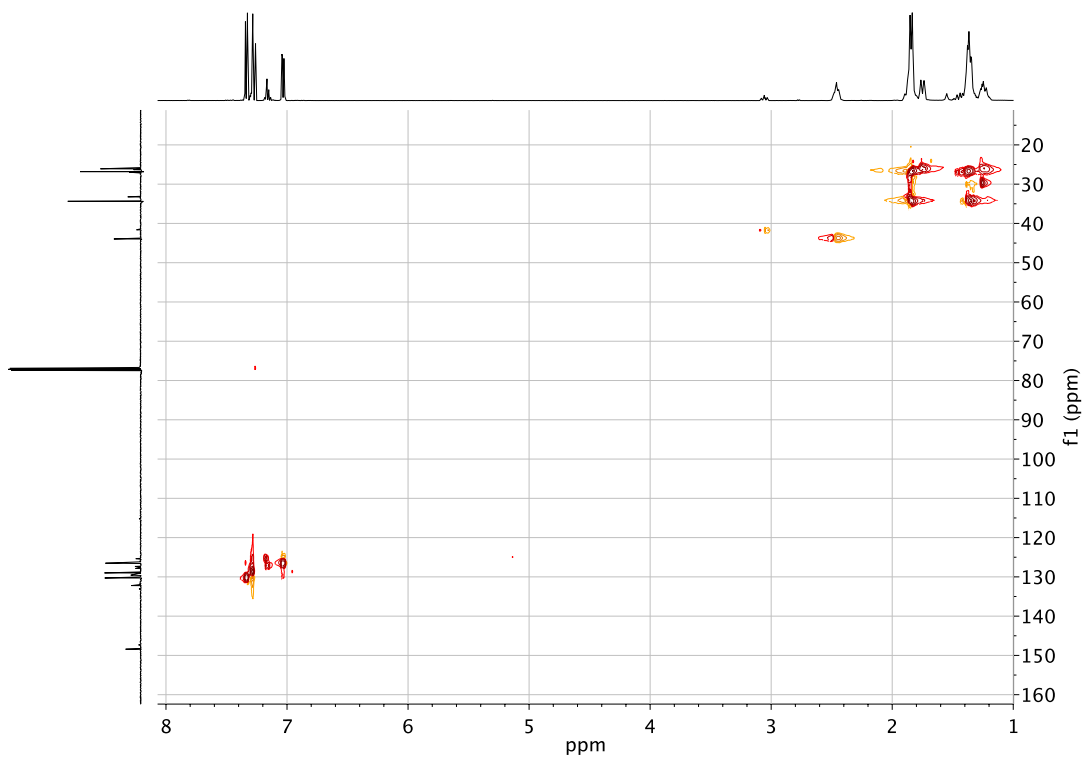


**Figure 3.42** 2D HSQC NMR (500 MHz, CDCl<sub>3</sub>) of compound **3.34**.



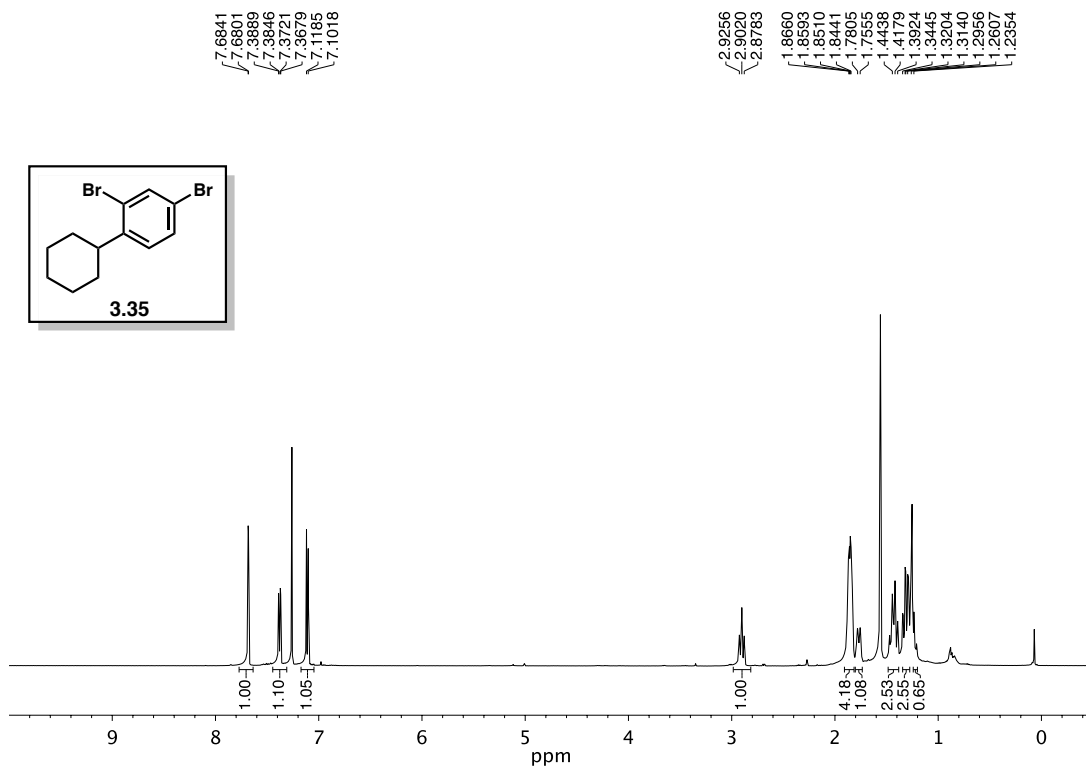


**Figure 3.43**  $^1\text{H NMR}$  (500 MHz,  $\text{CDCl}_3$ ) of compound 3.35.

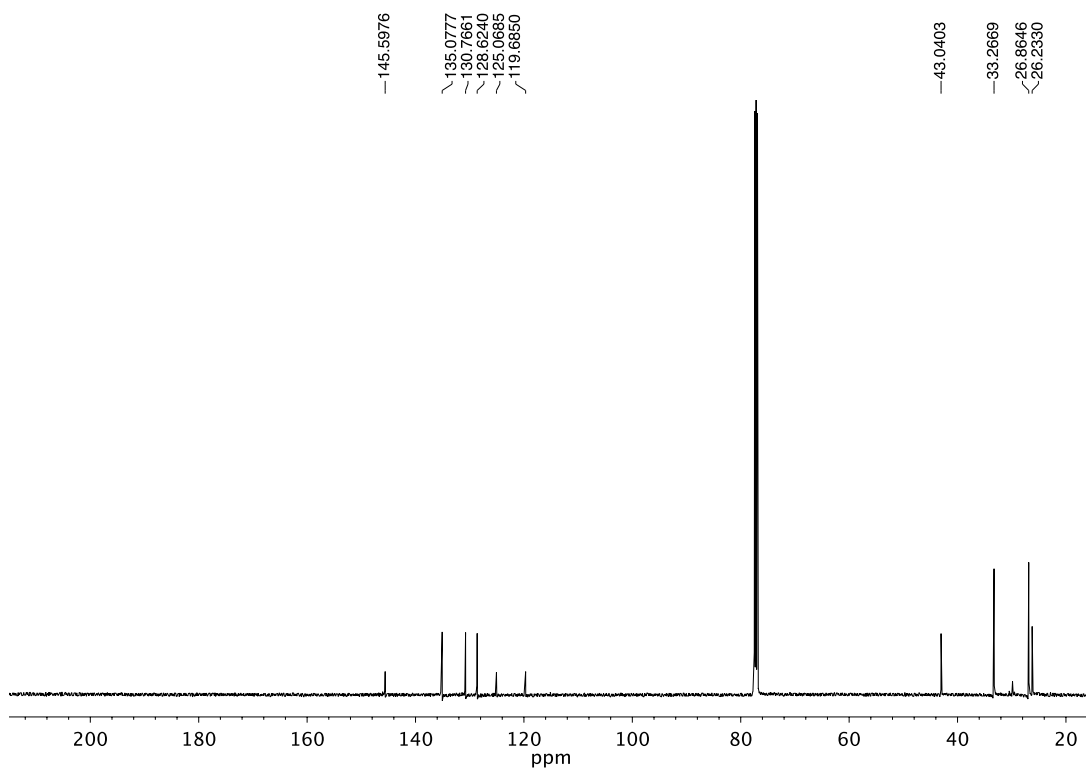


**Figure 3.44**  $^{13}\text{C NMR}$  (125 MHz,  $\text{CDCl}_3$ ) of compound 3.35.

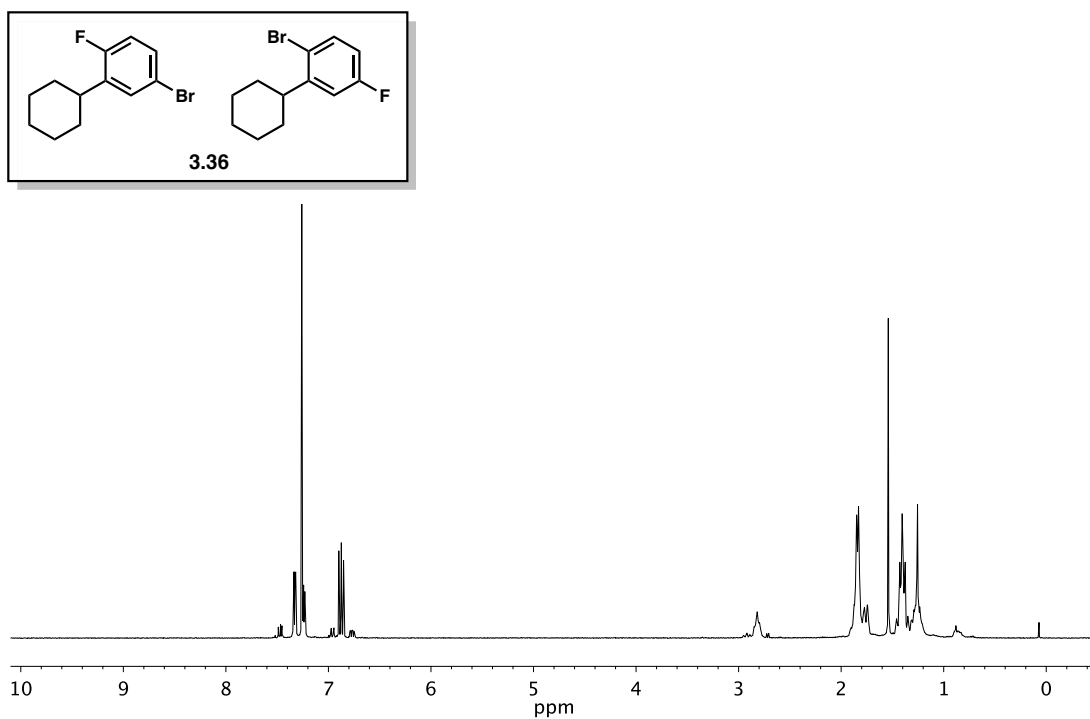


**Figure 3.45** <sup>1</sup>H NMR (500 MHz, CDCl<sub>3</sub>) of compound **3.36**.

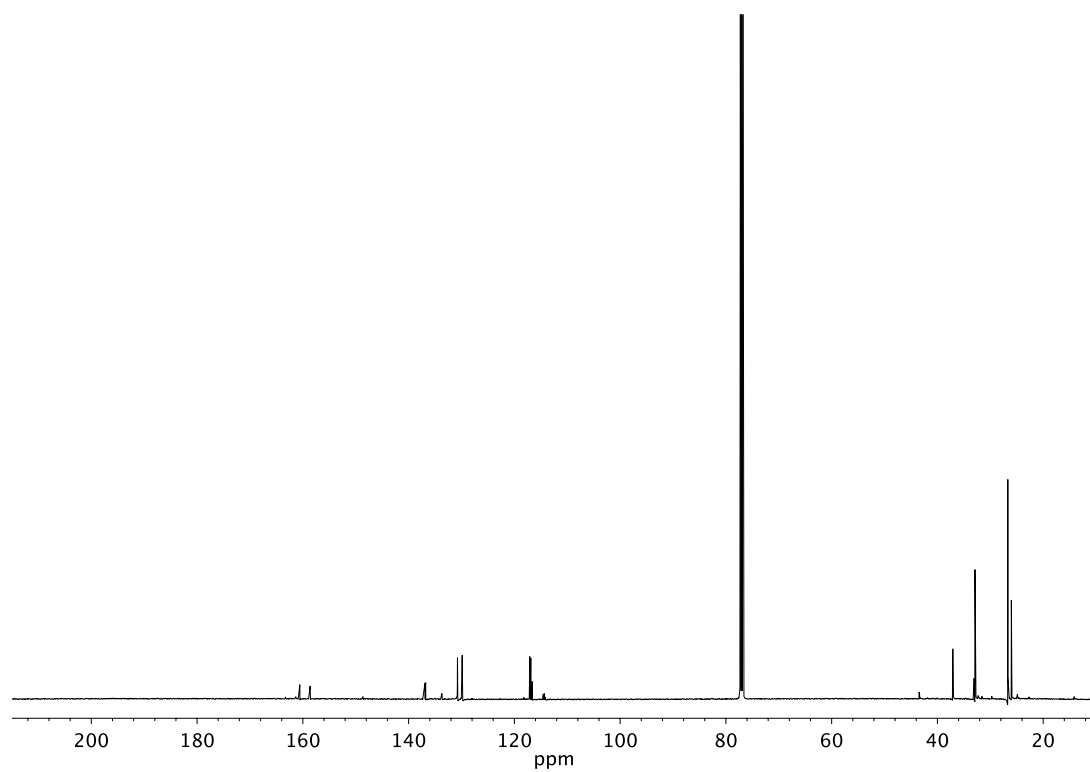


**Figure 3.46** <sup>13</sup>C NMR (125 MHz, CDCl<sub>3</sub>) of compound **3.36**.

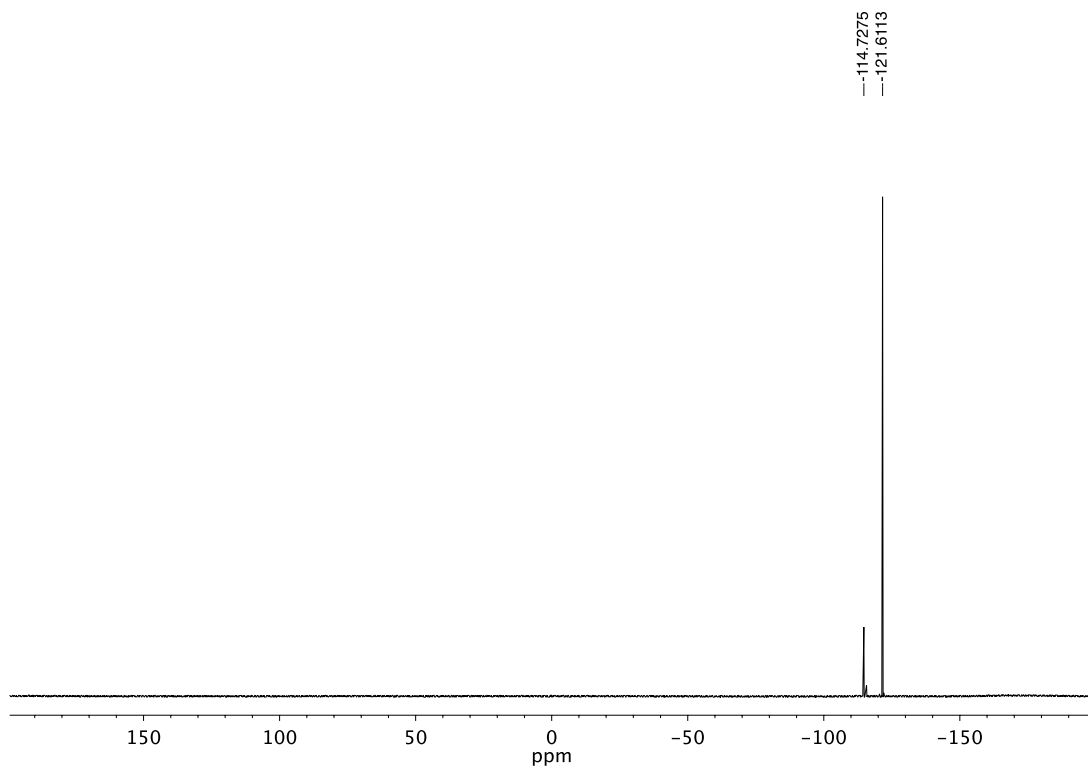


**Figure 3.47**  $^{19}\text{F}$  NMR (376 MHz,  $\text{CDCl}_3$ ) of compound **3.36**.

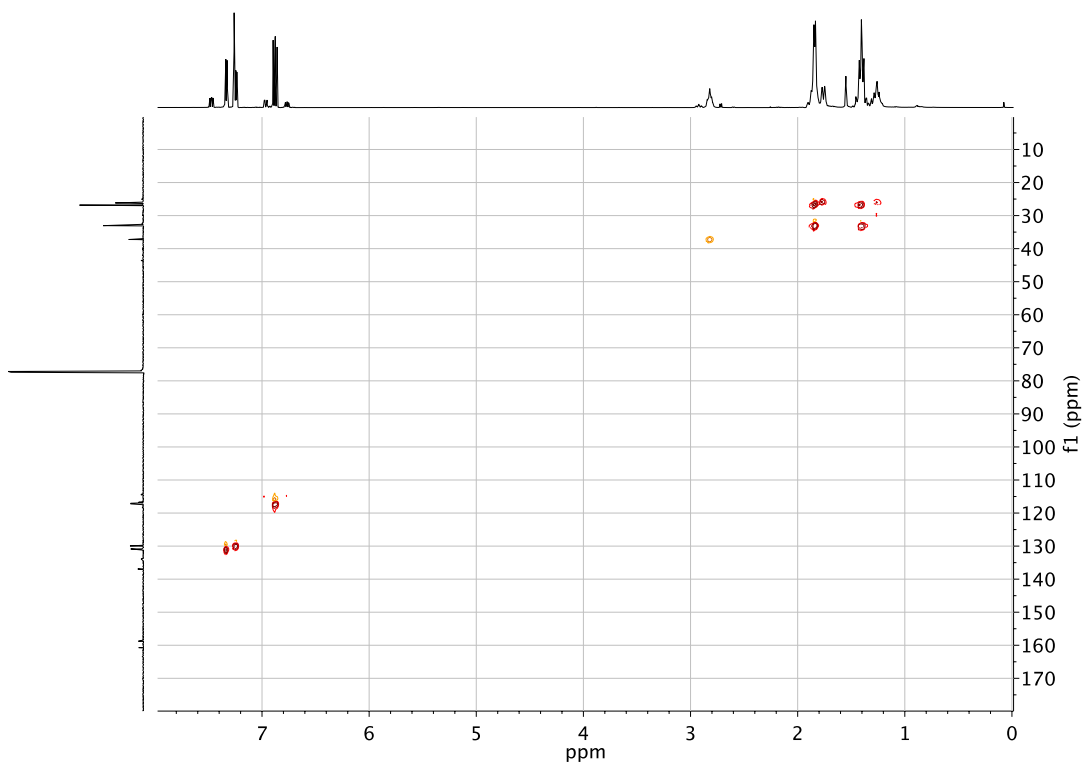


**Figure 3.48** 2D HSQC NMR (500 MHz,  $\text{CDCl}_3$ ) of compound **3.36**.

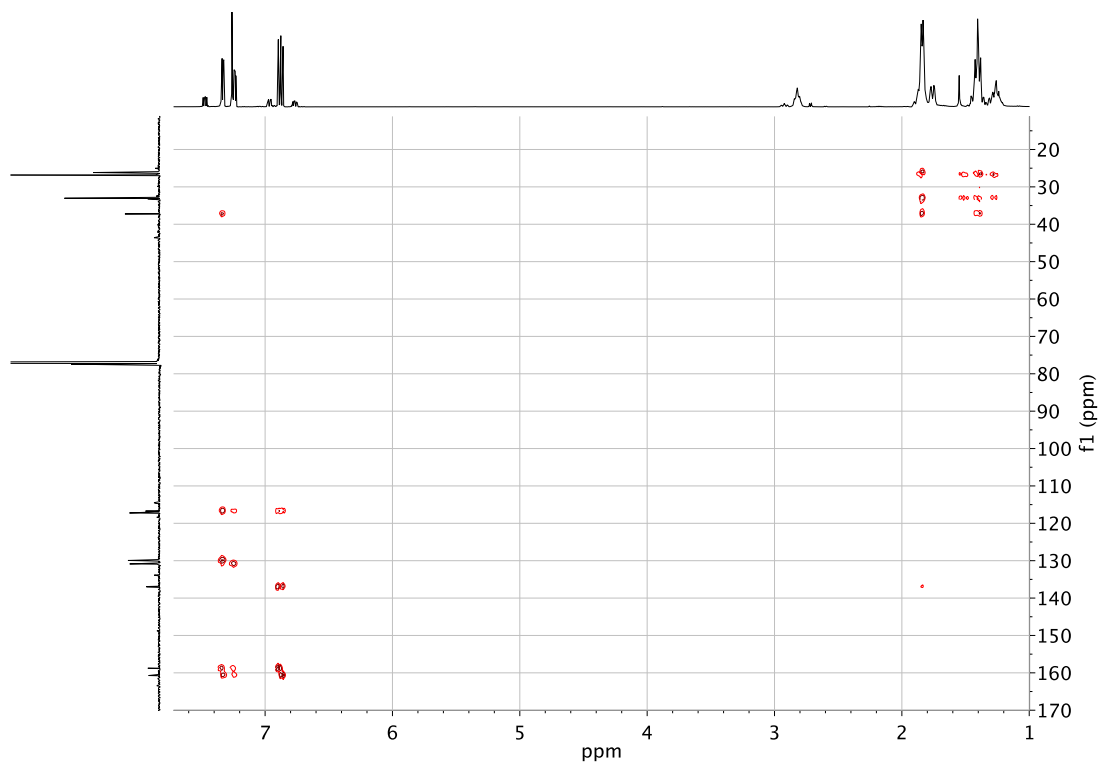


**Figure 3.49** 2D HMBC NMR (500 MHz,  $\text{CDCl}_3$ ) of compound **3.36**.

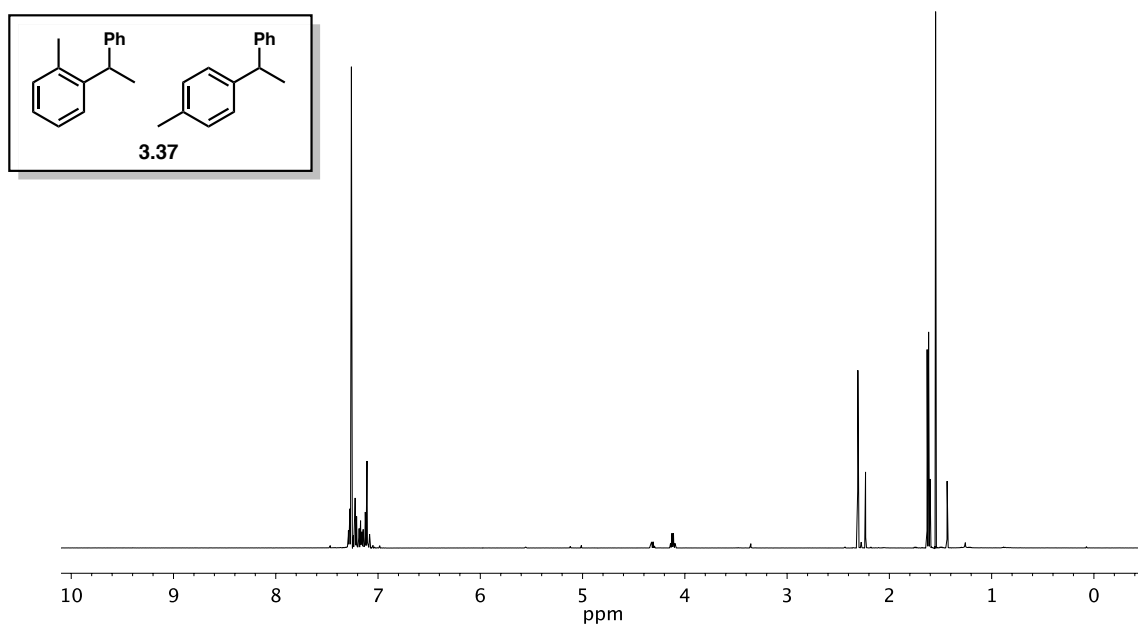


**Figure 3.50**  $^1\text{H}$  NMR (400 MHz,  $\text{CDCl}_3$ ) of compound **3.37**.

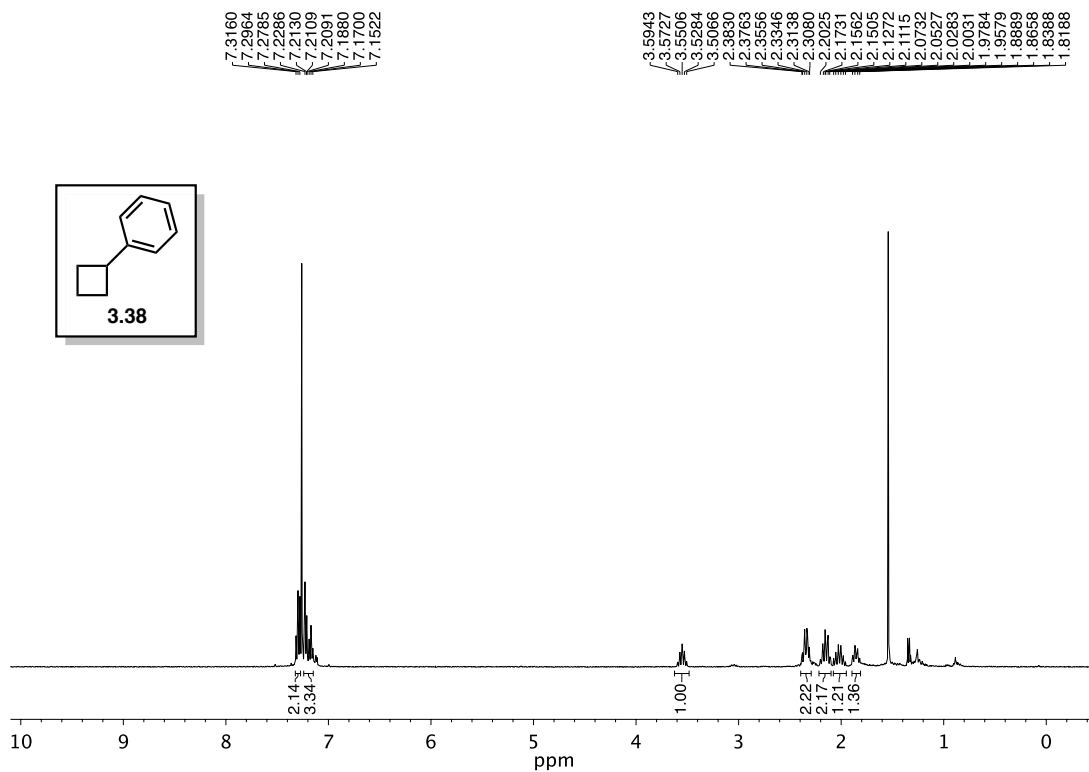


Figure 3.51 <sup>1</sup>H NMR (400 MHz, CDCl<sub>3</sub>) of compound 3.38.

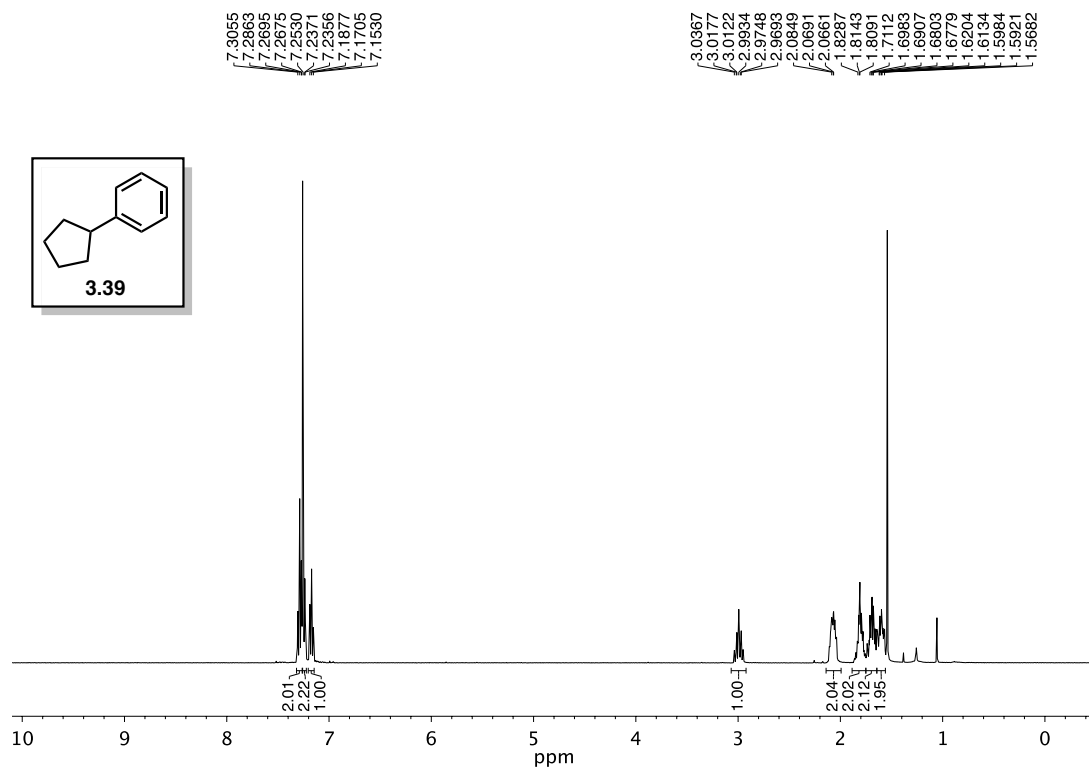
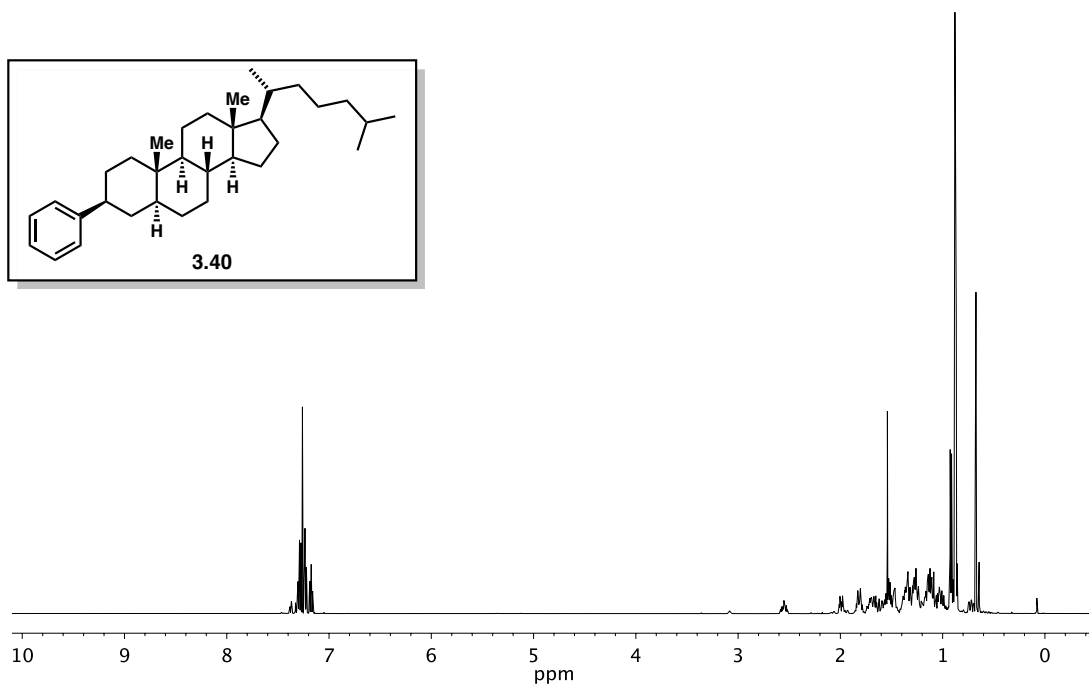
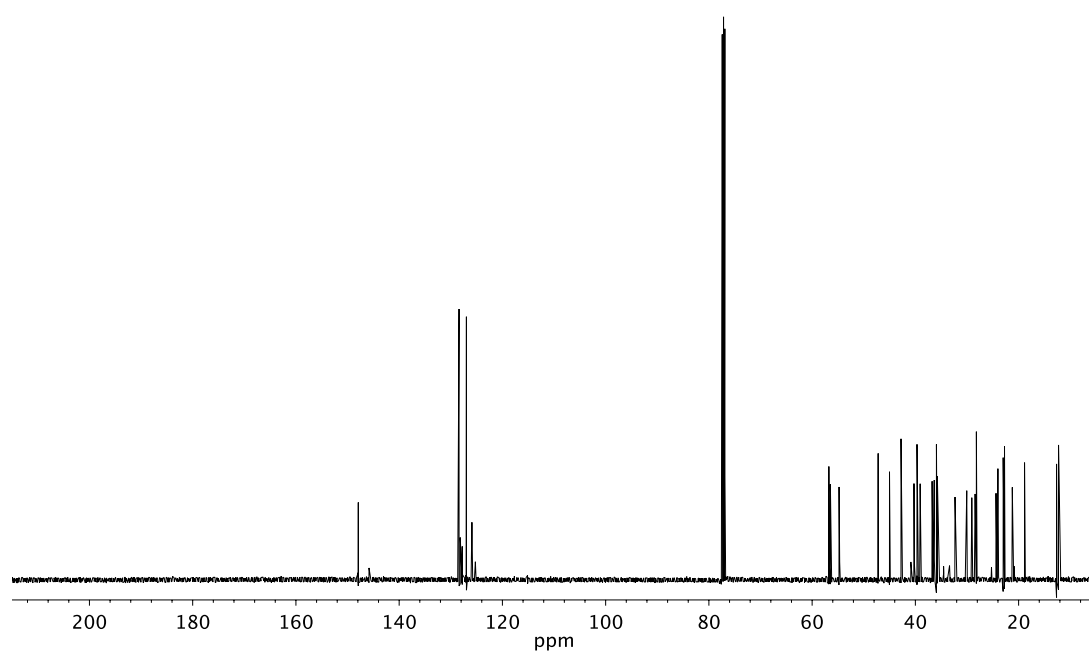


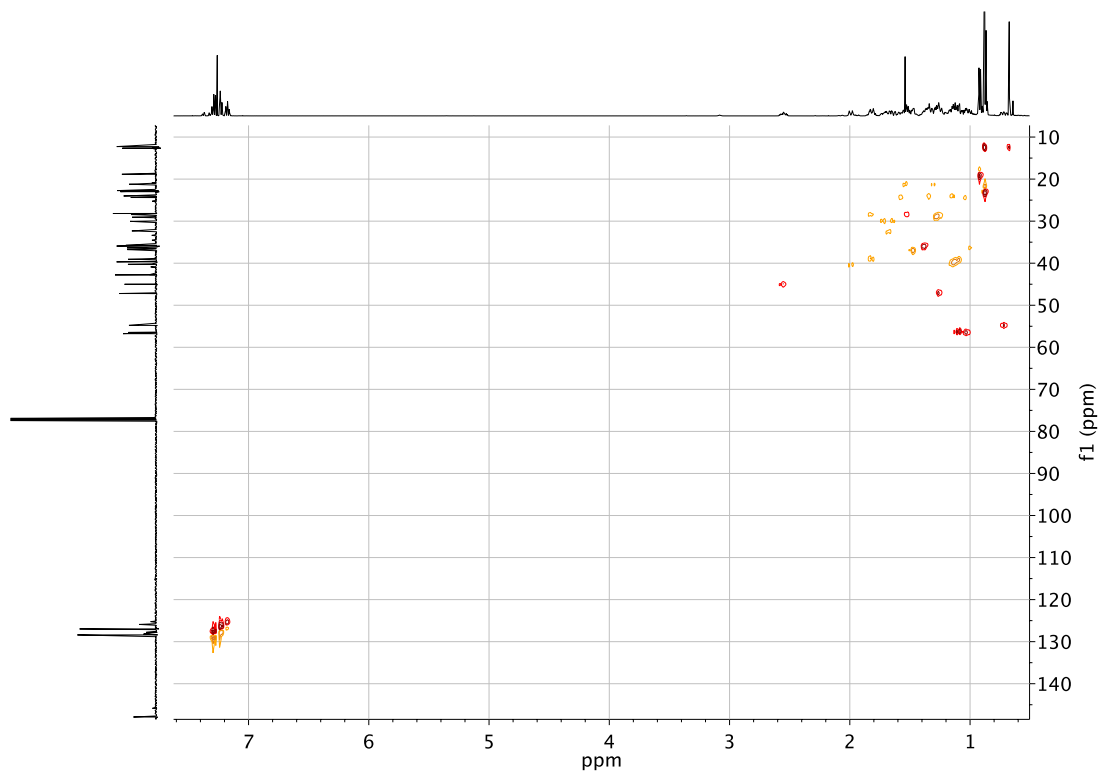
Figure 3.52 <sup>1</sup>H NMR (400 MHz, CDCl<sub>3</sub>) of compound 3.39.



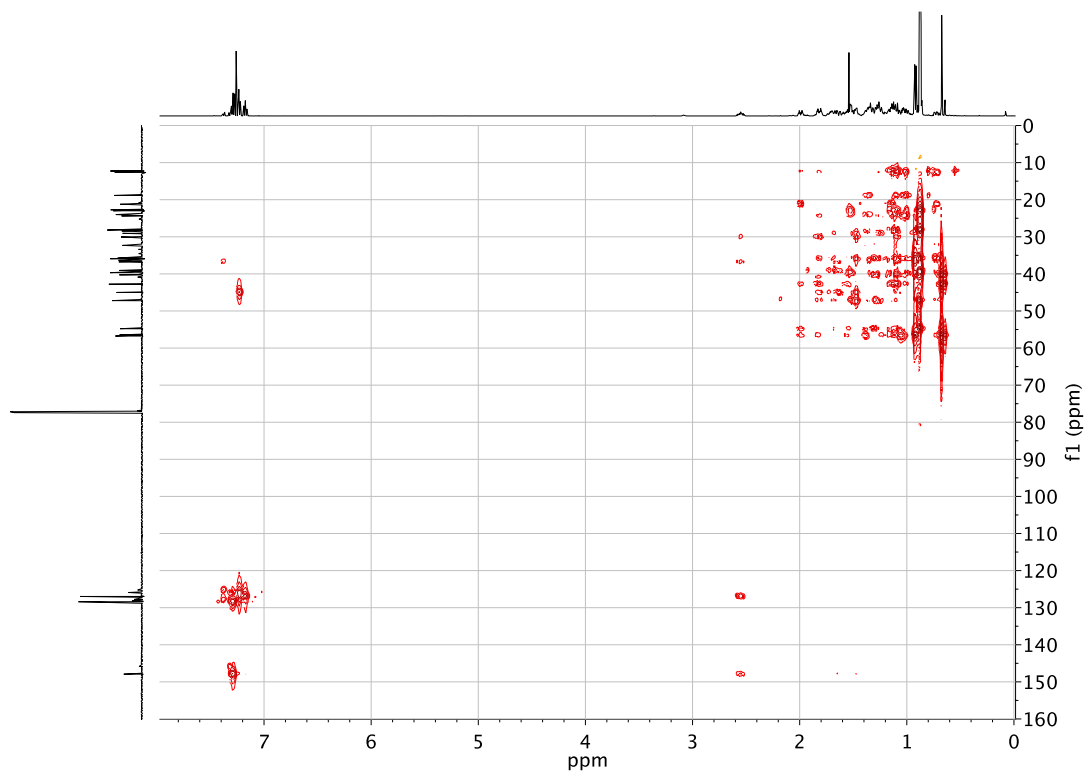
**Figure 3.53** <sup>1</sup>H NMR (500 MHz, CDCl<sub>3</sub>) of compound **3.40**.



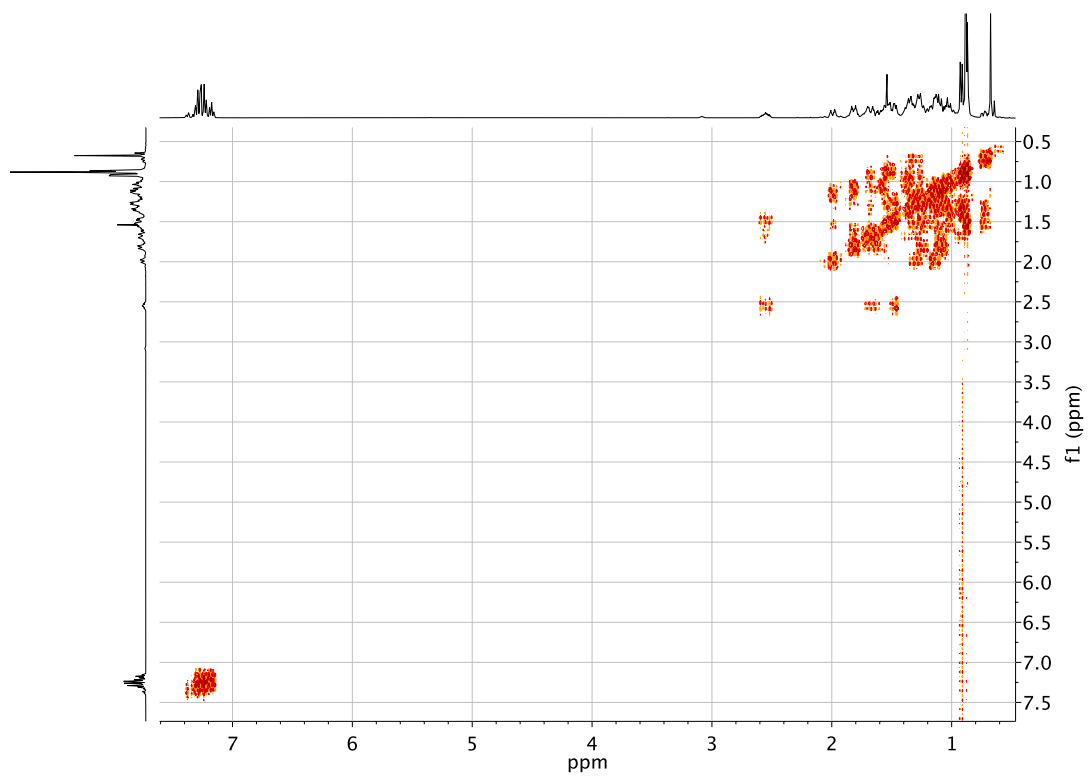
**Figure 3.54** <sup>13</sup>C NMR (125 MHz, CDCl<sub>3</sub>) of compound **3.40**.



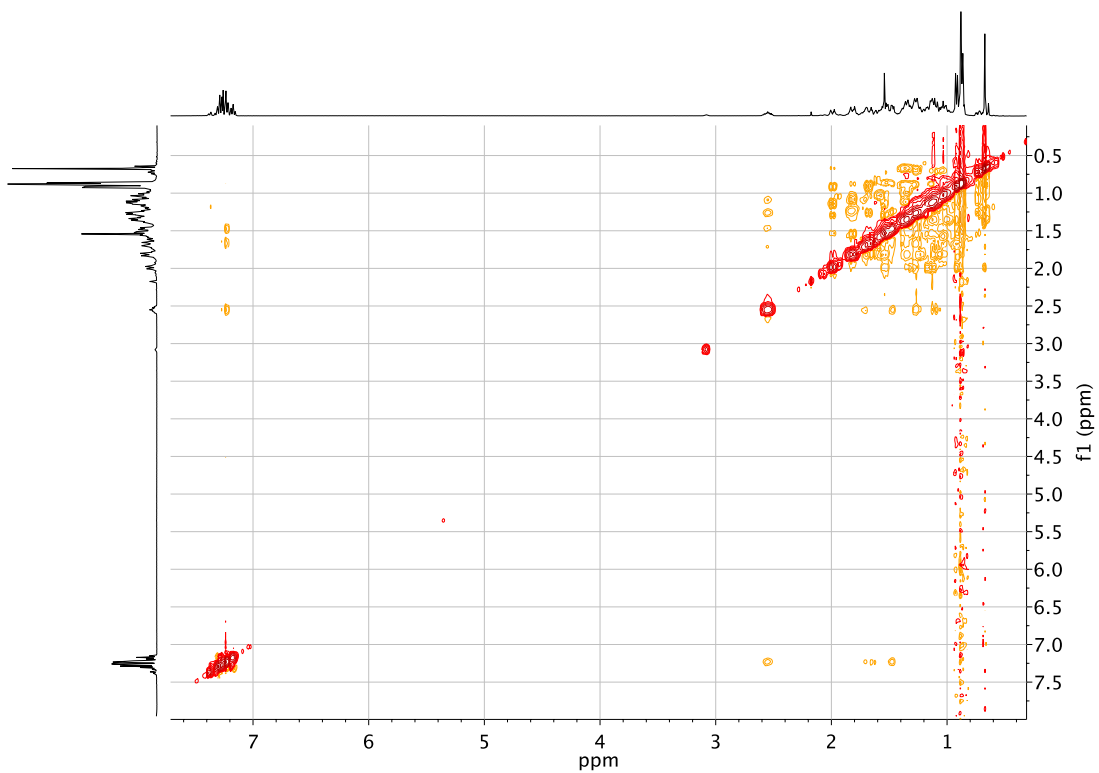
*Figure 3.55* 2D HSQC NMR (500 MHz, CDCl<sub>3</sub>) of compound **3.40**.



*Figure 3.56* 2D HMBC NMR (500 MHz, CDCl<sub>3</sub>) of compound **3.40**.

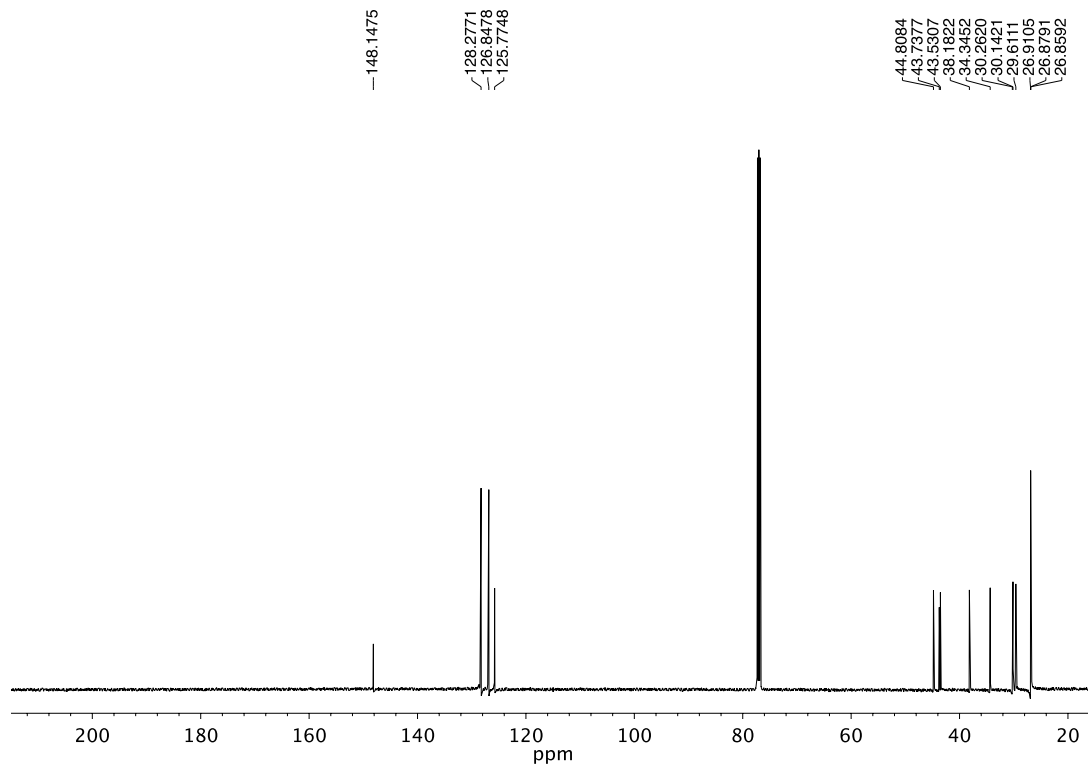
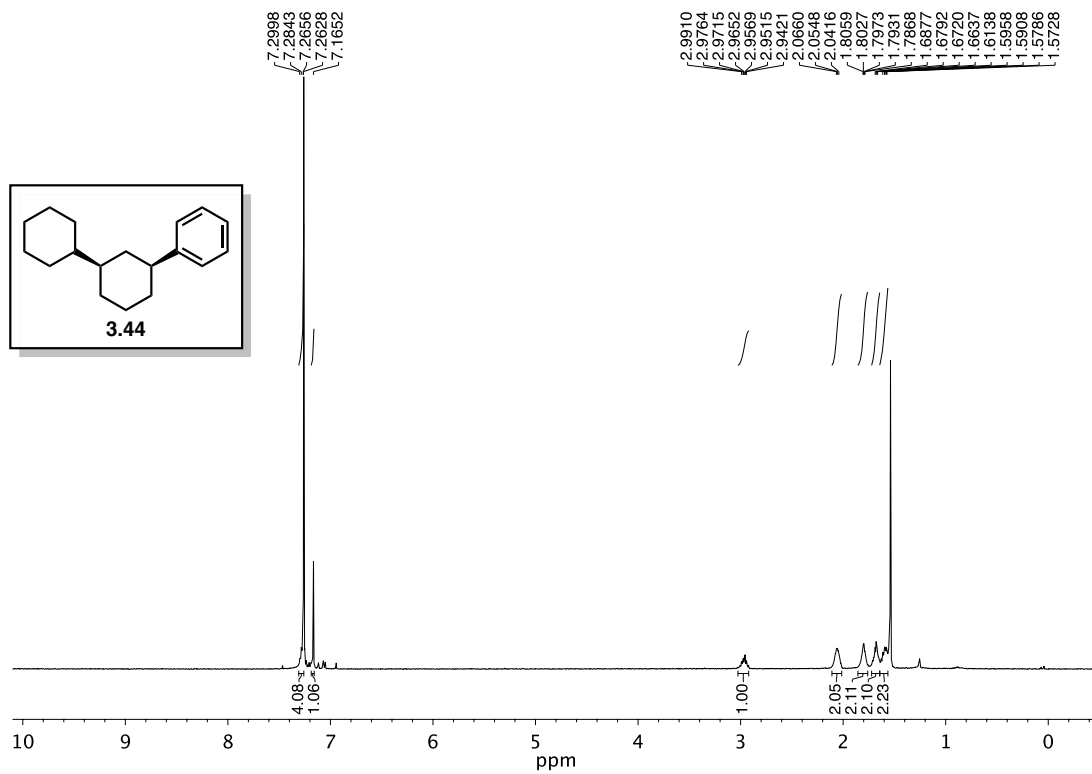


**Figure 3.57** <sup>1</sup>H COSY NMR (500 MHz, CDCl<sub>3</sub>) of compound **3.40**.



**Figure 3.58** <sup>1</sup>H NOESY NMR (500 MHz, CDCl<sub>3</sub>) of compound **3.40**.





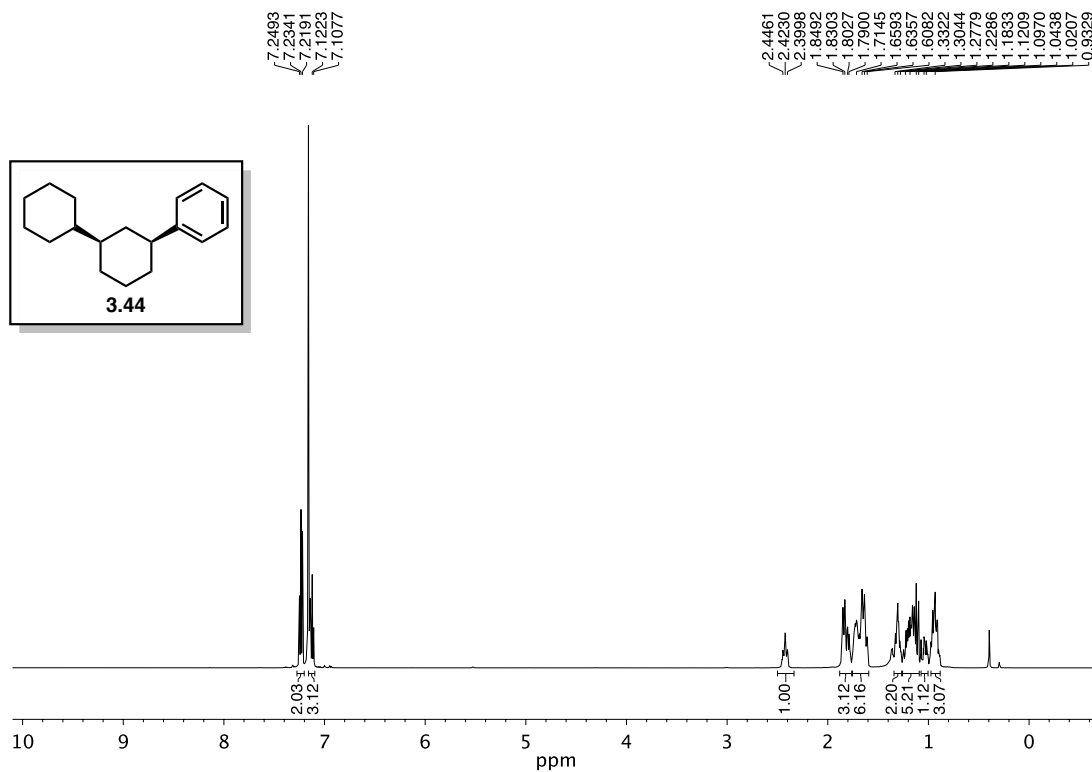


Figure 3.61  $^1\text{H}$  NMR (500 MHz,  $\text{C}_6\text{D}_6$ ) of compound 3.44.

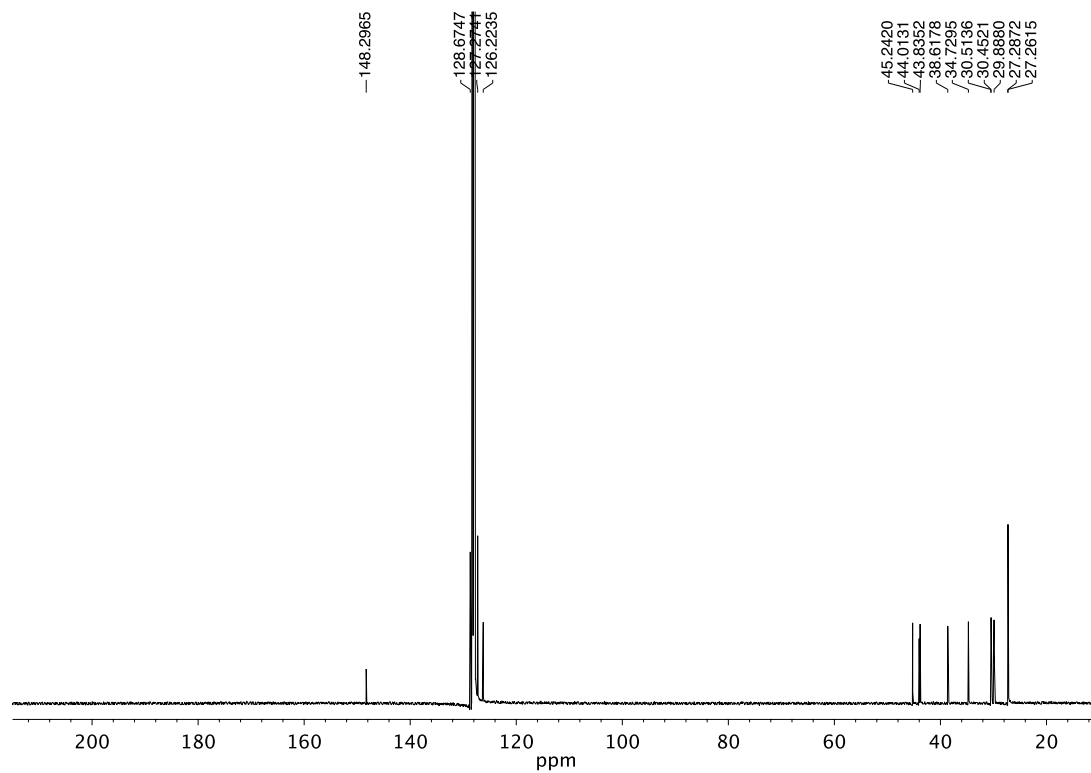


Figure 3.62  $^{13}\text{C}$  NMR (125 MHz,  $\text{C}_6\text{D}_6$ ) of compound 3.44.

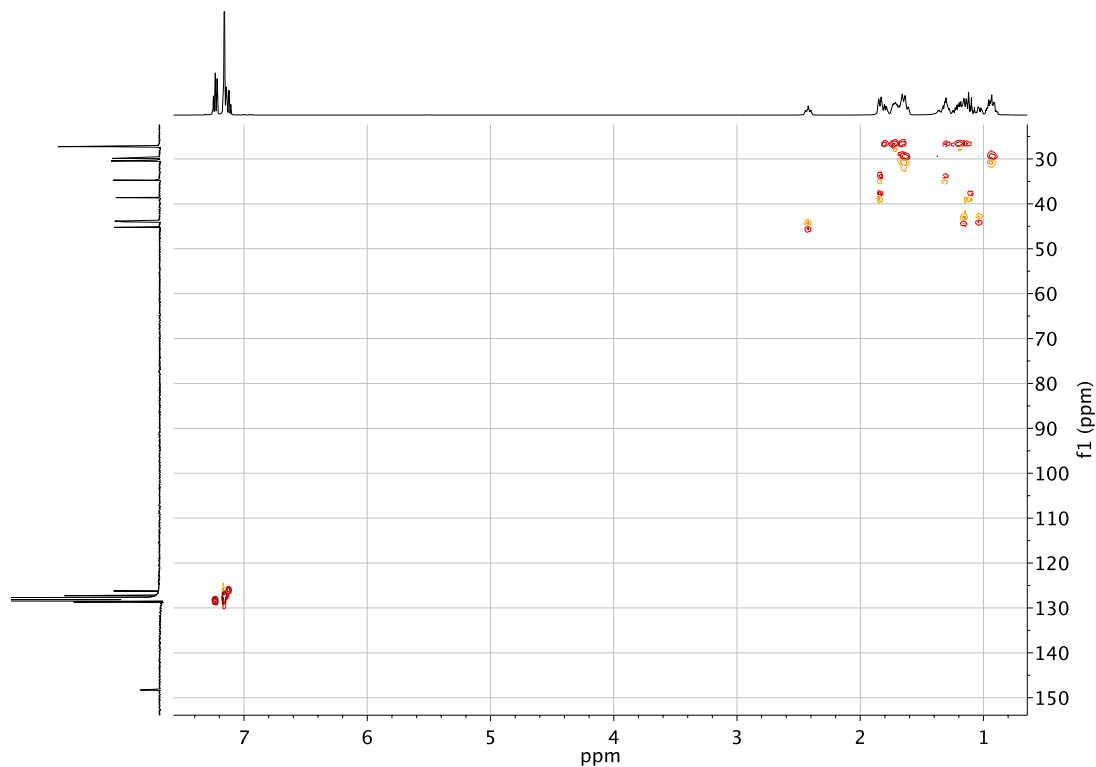


Figure 3.63 2D HSQC NMR (500 MHz, C<sub>6</sub>D<sub>6</sub>) of compound **3.44**.

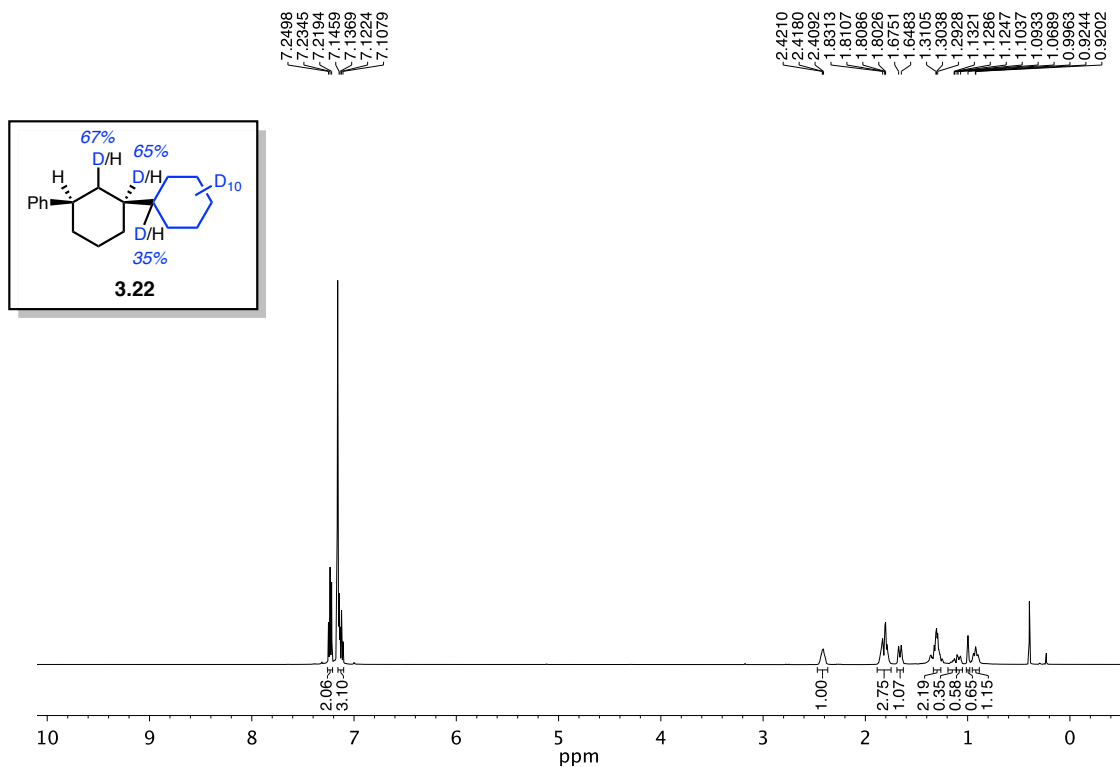


Figure 3.64 <sup>1</sup>H NMR (500 MHz, C<sub>6</sub>D<sub>6</sub>) of compound **3.22**.

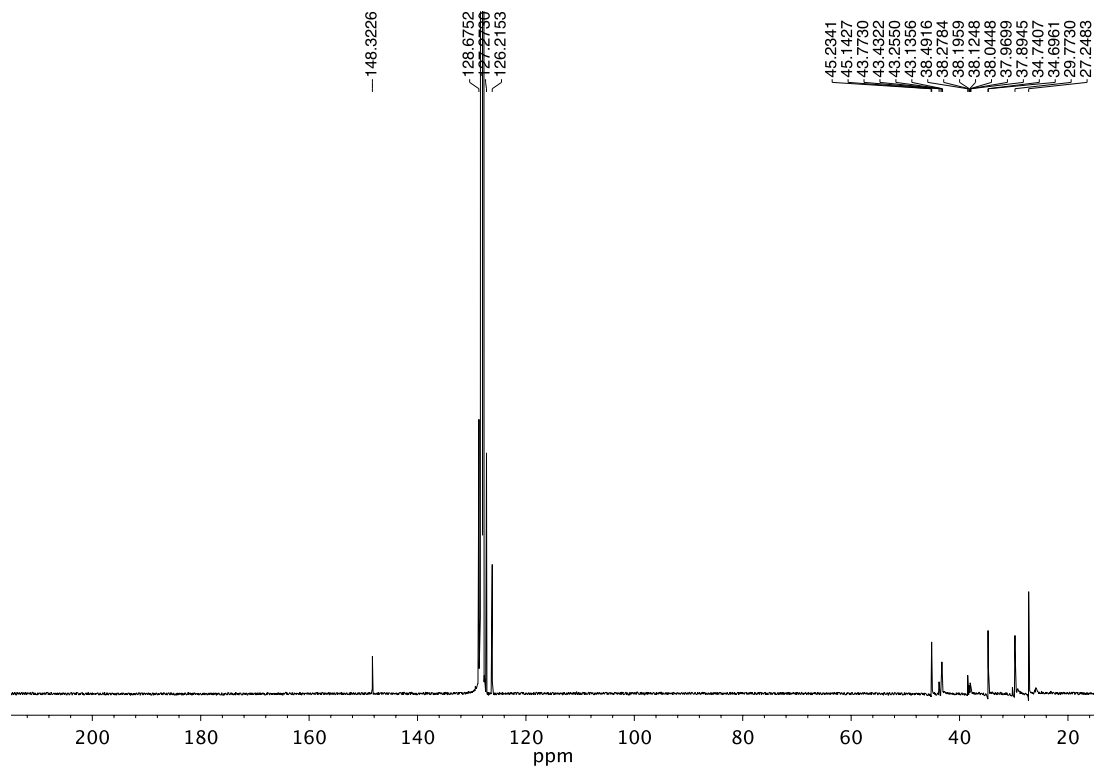


Figure 3.65  $^{13}\text{C}$  NMR (125 MHz,  $\text{C}_6\text{D}_6$ ) of compound 3.22.

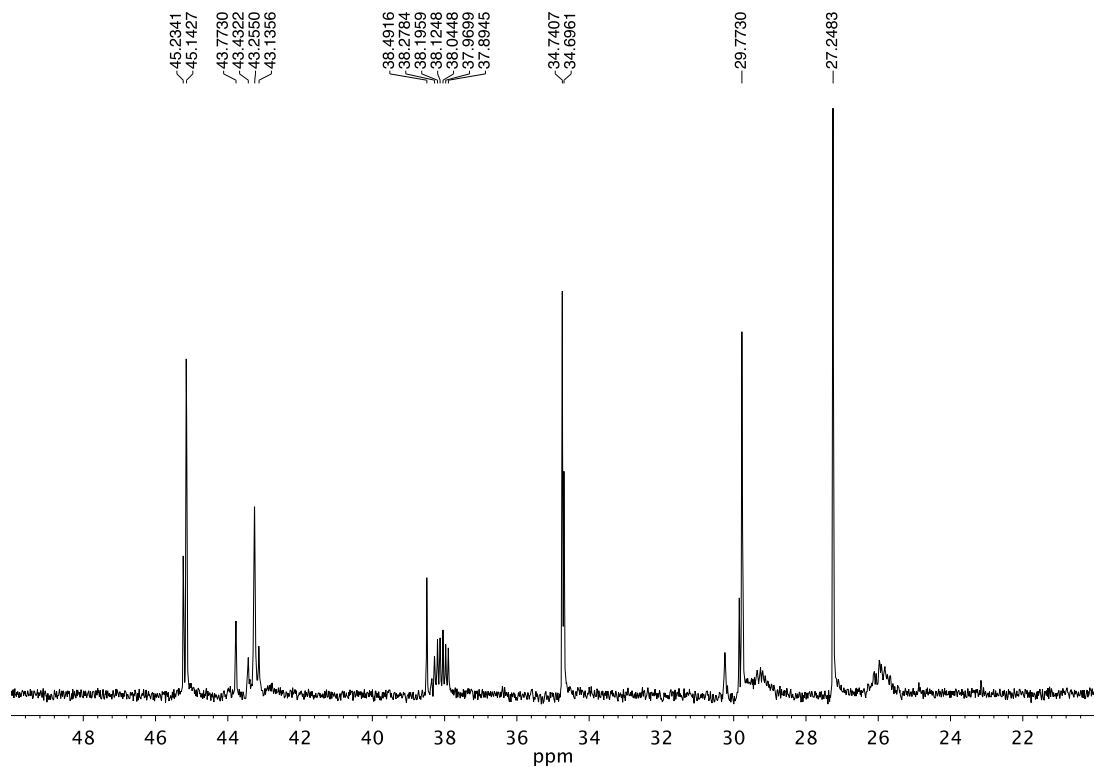
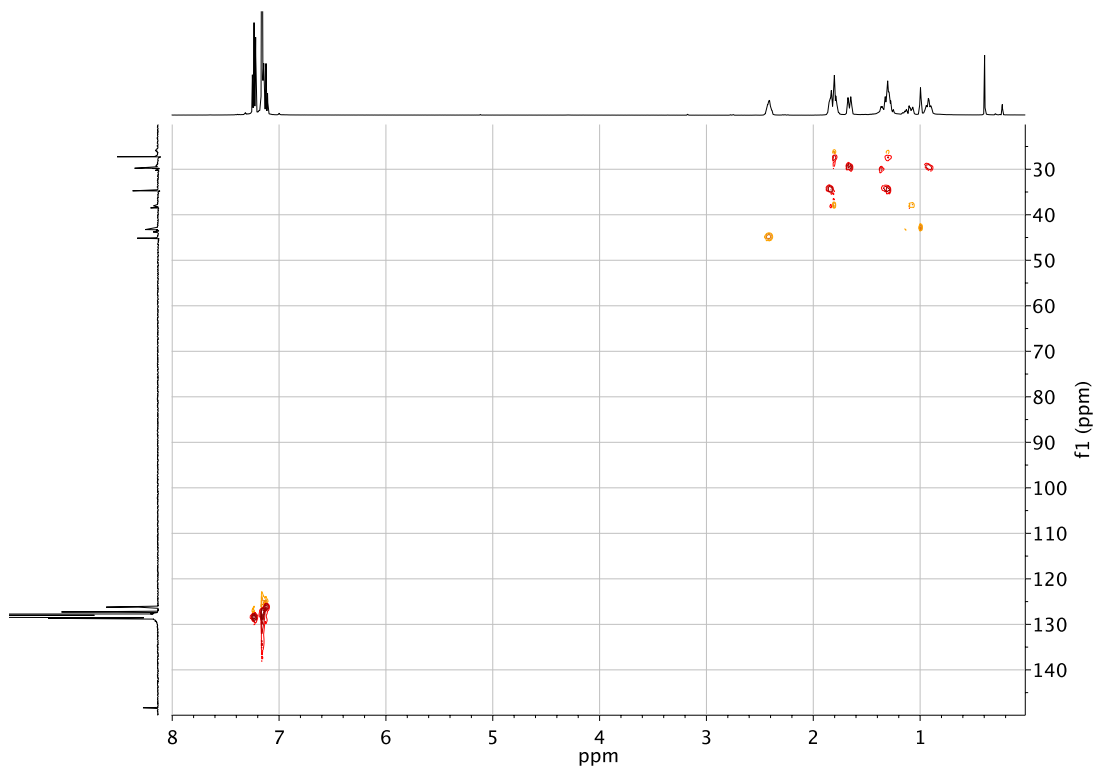
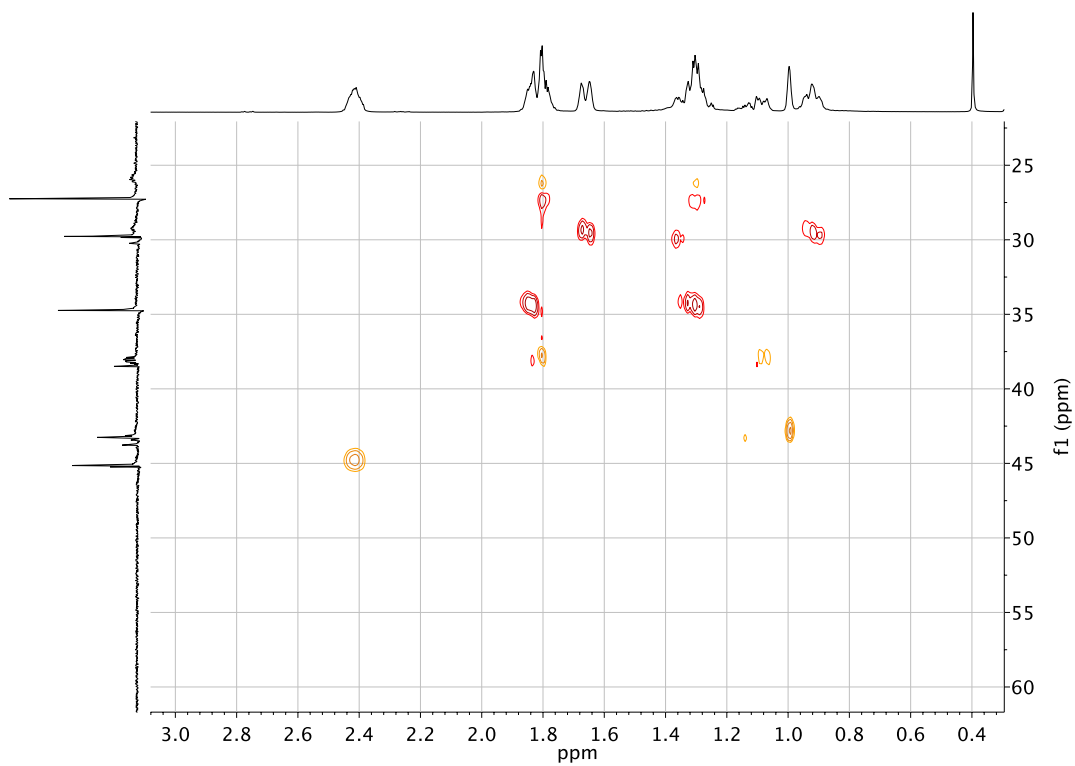


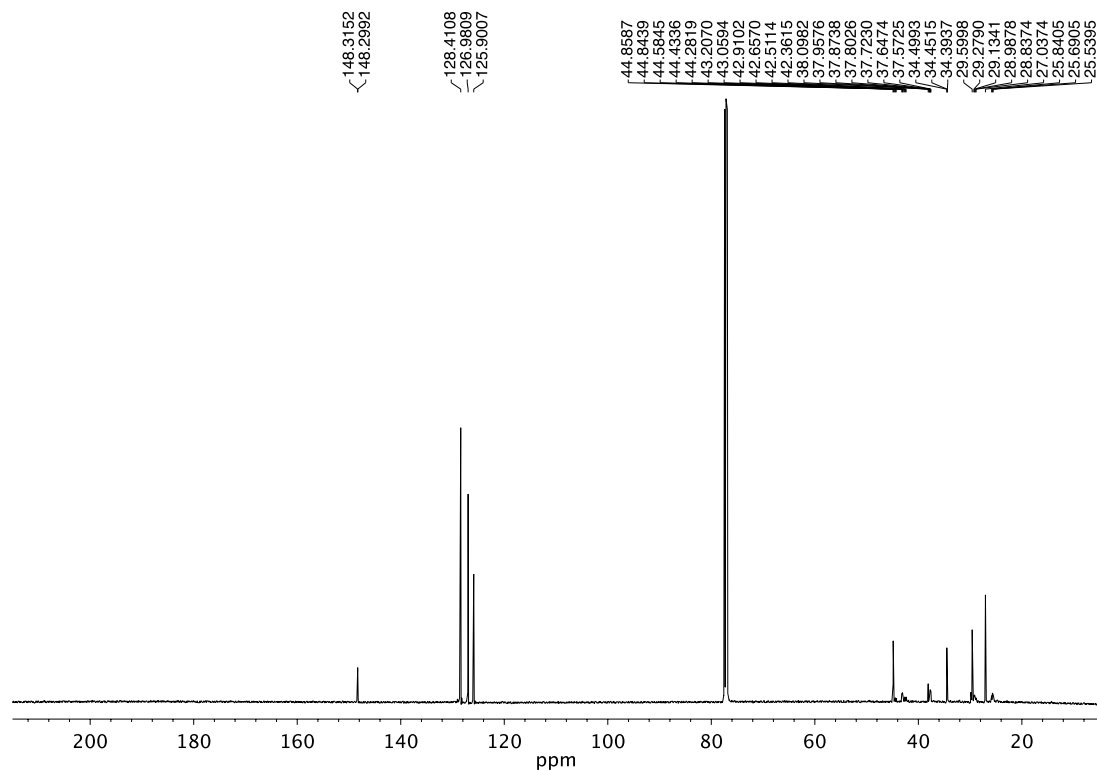
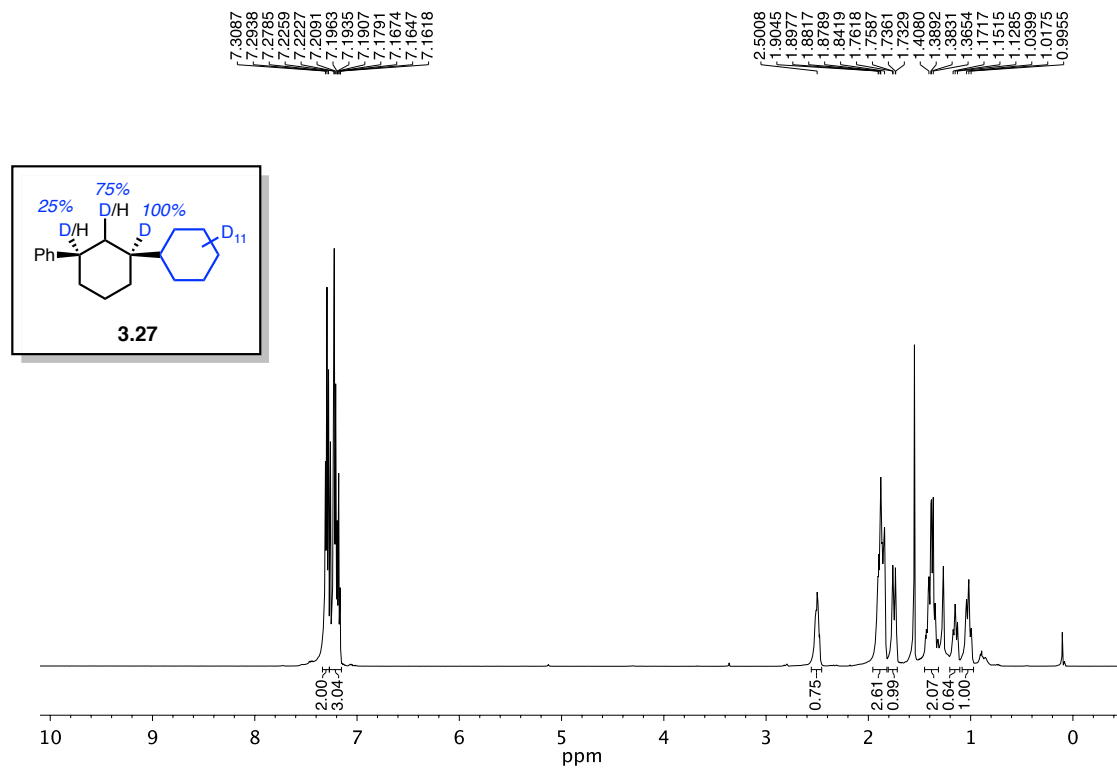
Figure 3.66  $^{13}\text{C}$  NMR (125 MHz,  $\text{C}_6\text{D}_6$ ) of compound 3.22.

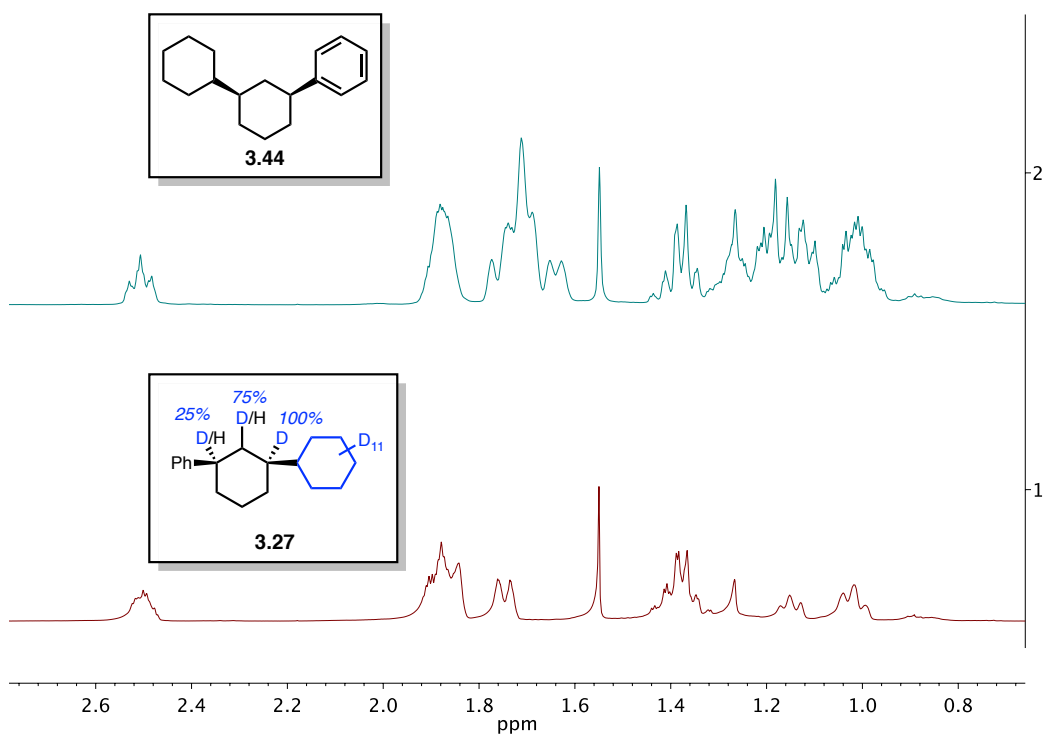


**Figure 3.67** 2D HSQC NMR (500 MHz, C<sub>6</sub>D<sub>6</sub>) of compound **3.22**.

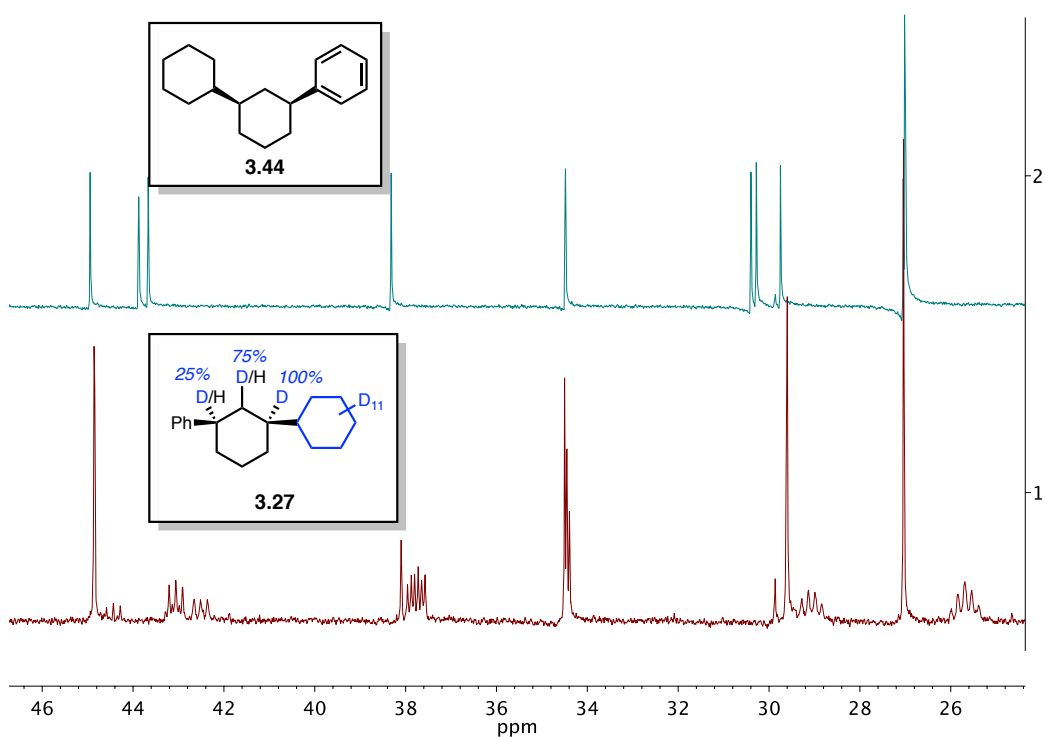


**Figure 3.68** 2D HSQC NMR (500 MHz, C<sub>6</sub>D<sub>6</sub>) of compound **3.22**.

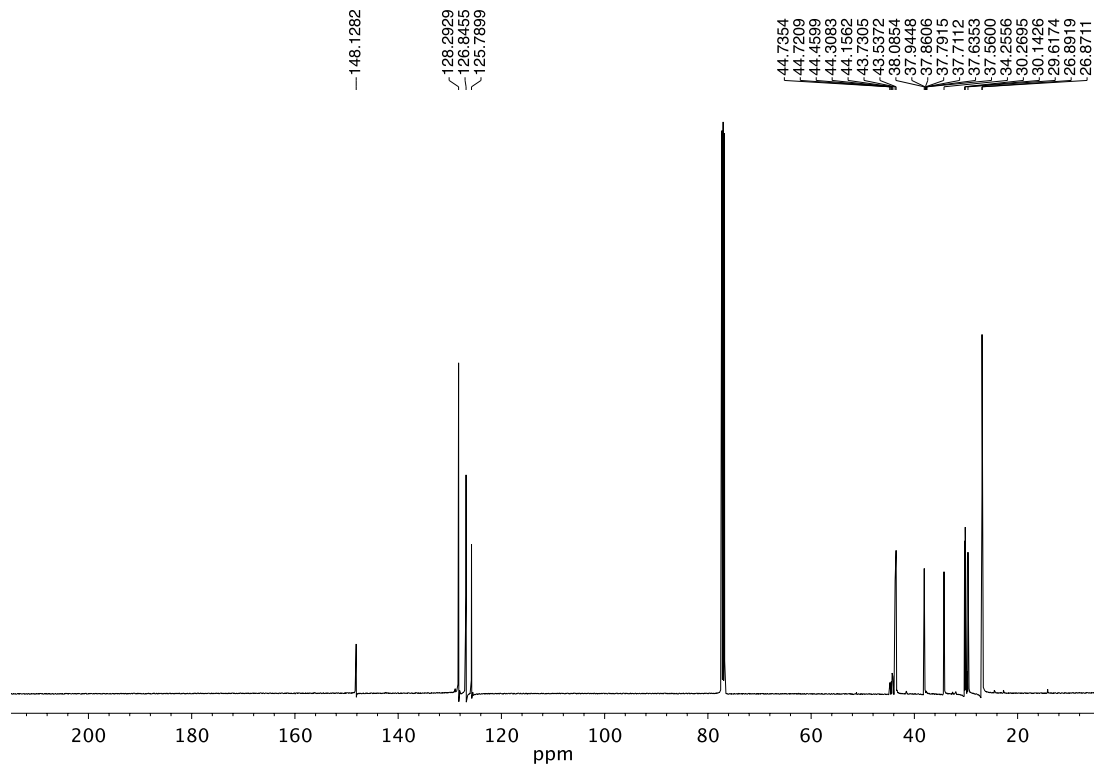
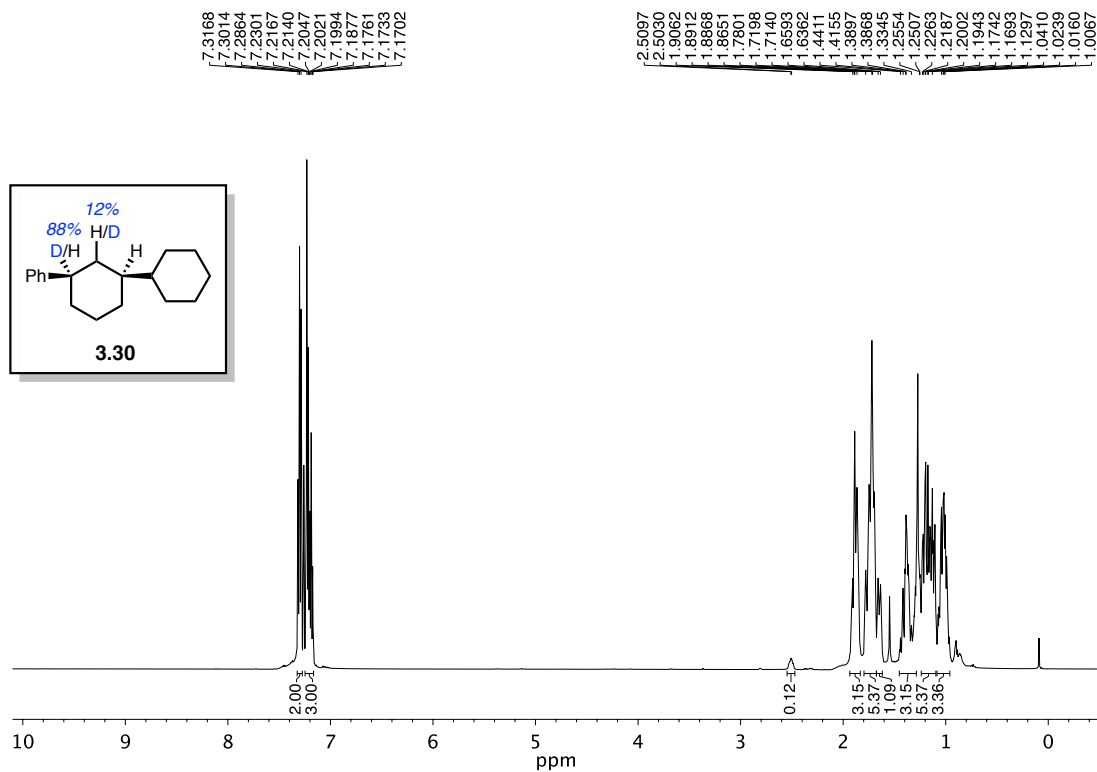




**Figure 3.71**  $^1\text{H}$  NMR (500 MHz,  $\text{CDCl}_3$ ) comparison of compound **3.27** with **3.44**.



**Figure 3.72**  $^{13}\text{C}$  NMR (125 MHz,  $\text{CDCl}_3$ ) comparison of compound **3.27** with **3.44**.





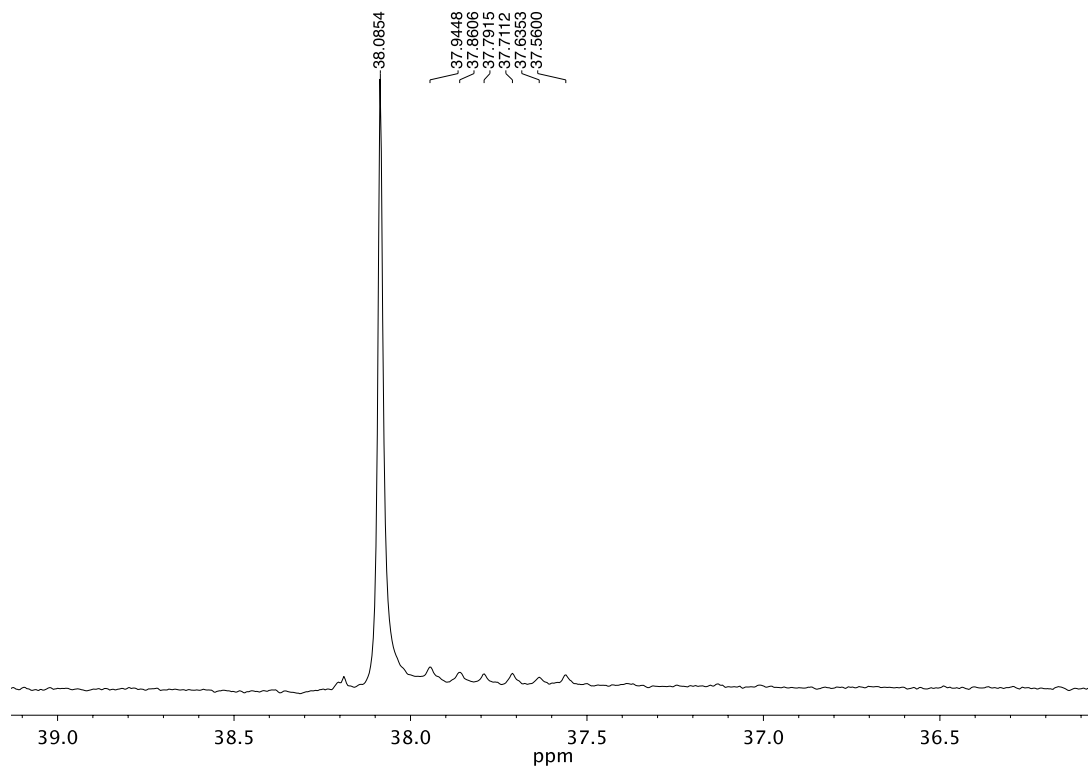


Figure 3.75  $^{13}\text{C}$  NMR (125 MHz,  $\text{CDCl}_3$ ) of compound **3.30**.

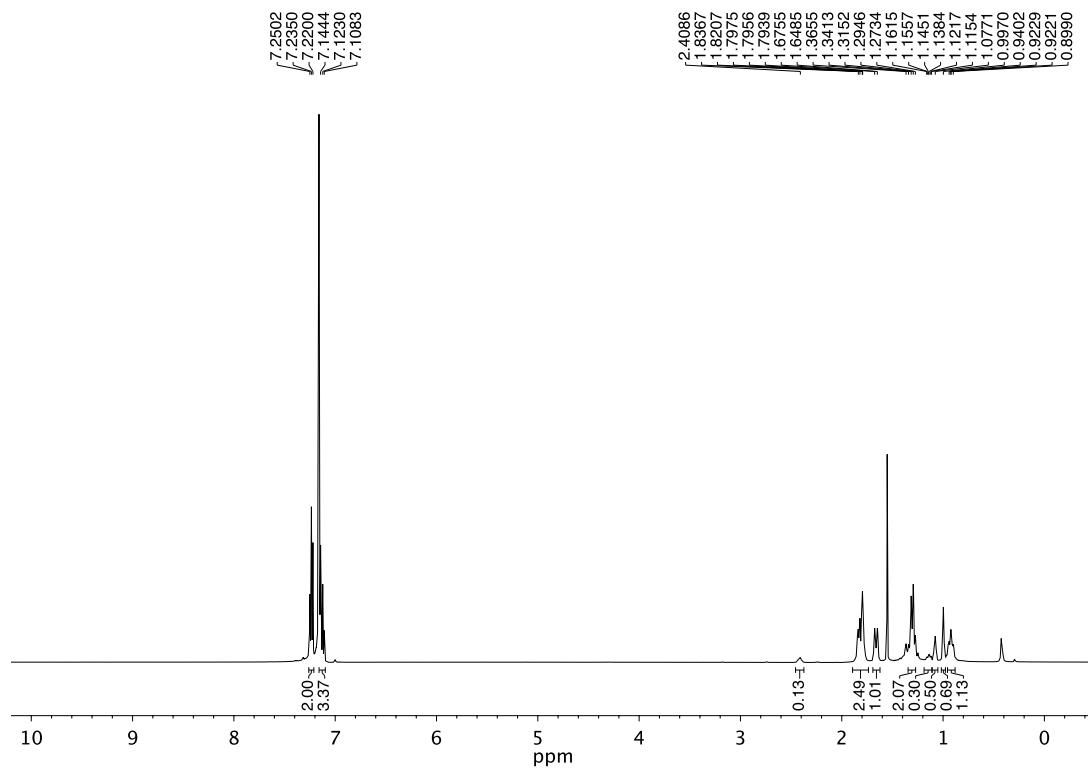
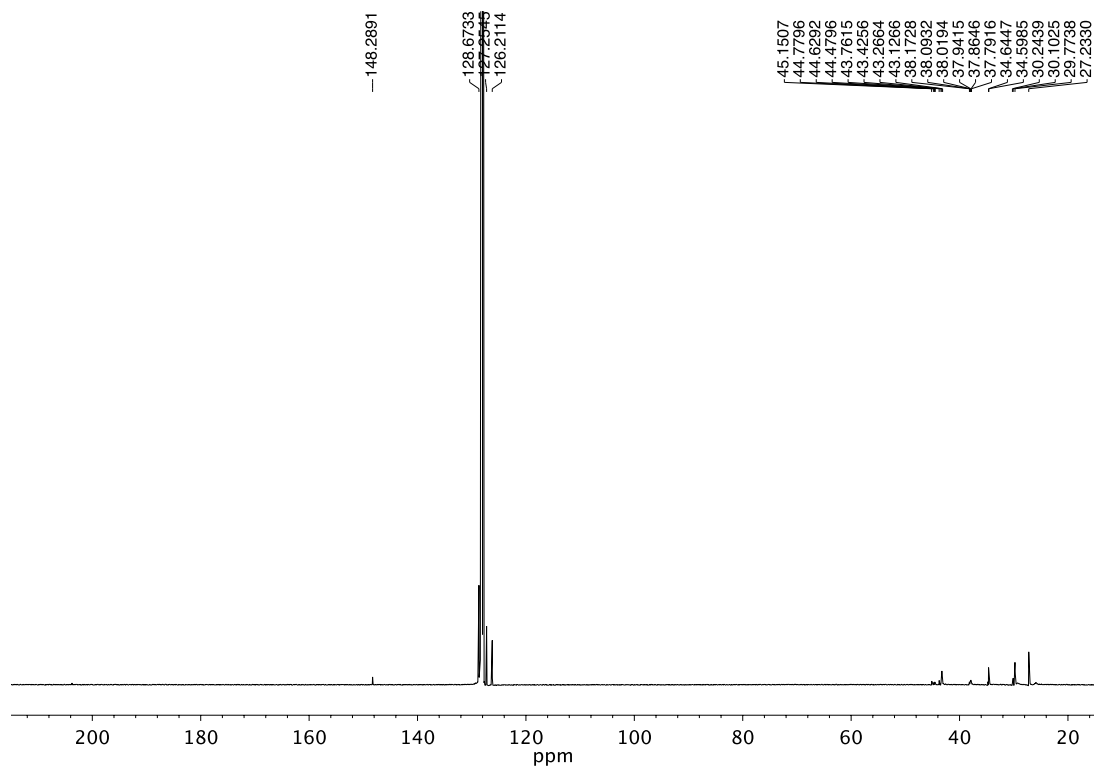
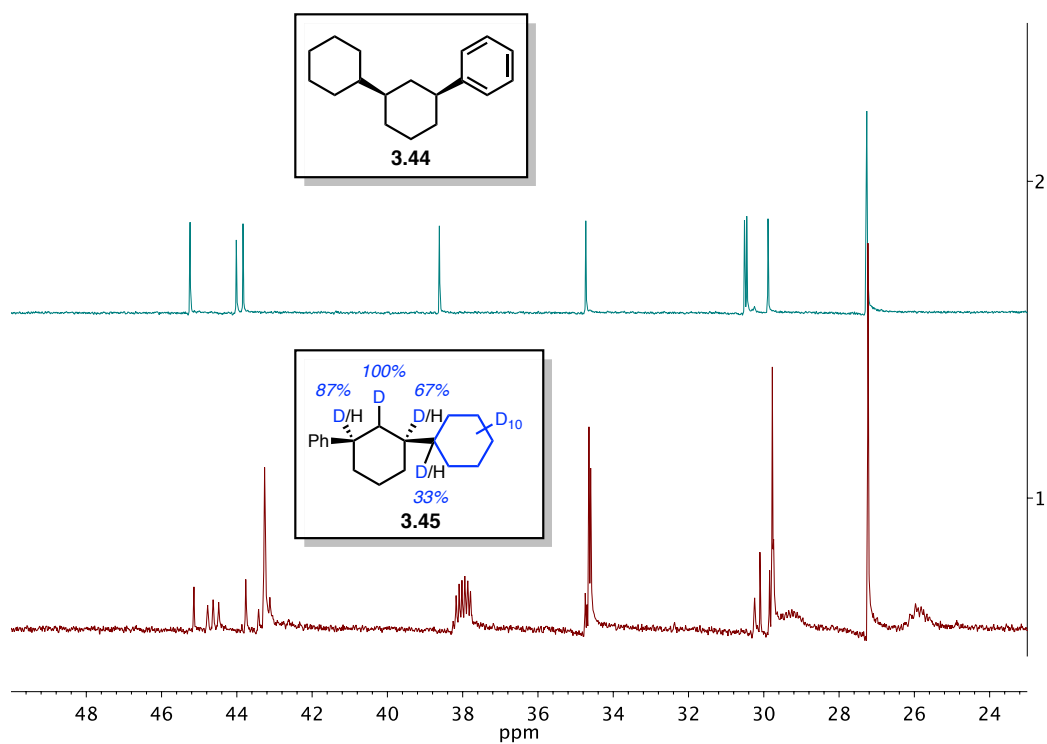


Figure 3.76  $^1\text{H}$  NMR (500 MHz,  $\text{C}_6\text{D}_6$ ) of compound **3.45**.



**Figure 3.77**  $^{13}\text{C}$  NMR (125 MHz,  $\text{C}_6\text{D}_6$ ) of compound **3.45**.



**Figure 3.78**  $^{13}\text{C}$  NMR (125 MHz,  $\text{C}_6\text{D}_6$ ) comparison of compound **3.45** with **3.44**.

### 3.9 Notes and References

- (1) Shao, B.; Bagdasarian, A. L.; Popov, S.; Nelson, H. M. *Science*, **2017**, *355*, 1403–1407.
- (2) (a) Stang, P. J.; Rappoport, Z.; Hanack, M.; Subramanian, L. R. *Vinyl Cations*; Academic Press: New York, NY, 1979. (b) Rappoport, Z.; Stang P. J., Eds. *Dicoordinated Carbocations*; John Wiley & Sons: New York, NY, 1997. (c) Hanack, M. *Angew. Chem. Int. Ed.* **1978**, *17*, 333–341. (d) Byrne, P. A., et al. *J. Am. Chem. Soc.* **2017**, *139*, 1499–1511.
- (3) Biermann, U.; Koch, R.; Metzger, J. O. *Angew. Chem. Int. Ed.* **2006**, *45*, 3076–3079.
- (4) Cleary, S. E.; Hensinger, M. J.; Brewer, M. *Chem. Sci.* **2017**, *8*, 6810–6814.
- (5) (a) Stang, P. J.; Summerville, R. H. *J. Am. Chem. Soc.* **1969**, *91*, 4600–4601. (b) Stang, P. *J. Acc. Chem. Res.* **1978**, *11*, 107–114.
- (6) Carey, F. A.; Tremper, H. S. *J. Org. Chem.* **1971**, *36*, 758–761.
- (7) Popov, S., et al. *Science* **2018**, *361*, 381–387.
- (8) Pfeifer, W. D.; Bahn, C. A.; Schleyer, P. v. R. *J. Am. Chem. Soc.* **1971**, *93*, 1513–1516.
- (9) Lamparter, E.; Hanack, M. *Eur. J. Inorg. Chem.* **1972**, *105*, 3789–3793.
- (10) Coxon, J. M.; Thorpe, J. *J. Org. Chem.* **2000**, *65*, 8421–8429.
- (11) Stang, P. J.; Anderson, A. *J. Am. Chem. Soc.* **1978**, *100*, 1520–1525.
- (12) Byrne, P. A., et al. *J. Am. Chem. Soc.* **2017**, *139*, 1499–1511.
- (13) Reed, C. A. *Acc. Chem. Res.* **2010**, *43*, 121–128.
- (14) Su, X.; Huang, H.; Yuan, Y.; Li, Y. *Angew. Chem. Int. Ed.* **2017**, *56*, 1338–1341.
- (15) Hioki, Y.; Okano, K.; Mori, A. *Chem. Commun. (Camb.)* **2017**, *53*, 2614–2617.
- (16) Alonso, P., et al. *Angew. Chem. Int. Ed.* **2015**, *54*, 15506–15510.
- (17) Lim, B. Y.; Jung, B. E.; Cho, C. G. *Org. Lett.* **2014**, *16*, 4492–4495.

- (18) Kawamoto, T.; Sasaki, R.; Kamimura, A. *Angew. Chem. Int. Ed.* **2017**, *56*, 1342–1345.
- (19) Nogi, K.; Fujihara, T.; Terao, J.; Tsuji, Y. *J. Org. Chem.* **2015**, *80*, 11618–11623.
- (20) Xu, X.; Cheng, D.; Pei, W. *J. Org. Chem.* **2006**, *71*, 6637–6639.
- (21) Günbas, D. D., et al. *Tetrahedron*, **2005**, *61*, 11177–11183.
- (22) Podder, S.; Choudhury, J.; Roy, S. *J. Org. Chem.* **2007**, *72*, 3129–3132.
- (23) vom Stein, T., et al. *Angew. Chem. Int. Ed.* **2015**, *54*, 10178–10182.
- (24) Maercker, A.; Oeffner, K. S.; Girreser, U. *Tetrahedron* **2004**, *60*, 8245–8256.

## CHAPTER FOUR

### Vinyl Carbocations Generated Under Basic Conditions and Their Intramolecular C–H Insertion Reactions

Adapted from: Benjamin Wigman, Stasik Popov, Alex L. Bagdasarian, Brian Shao, Tyler R. Benton, Chloé G. Williams, Steven P. Fisher, Vincent Lavallo, K. N. Houk, and Hosea M.

Nelson

*J. Am. Chem. Soc.* **2019**, *141*, 9140–9144.

#### 4.1 Abstract

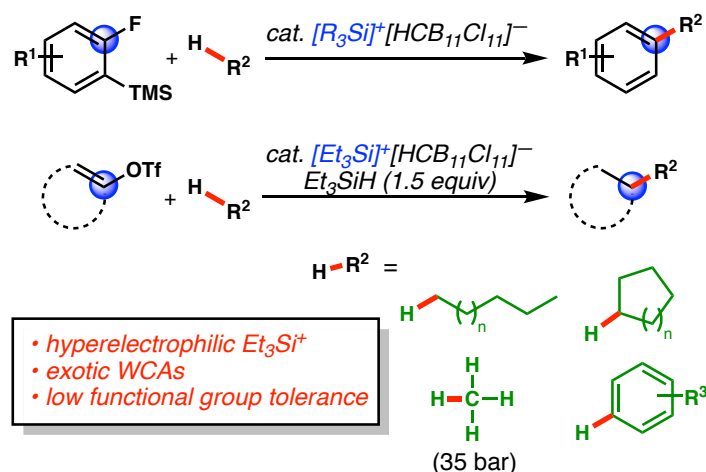
Here we report the surprising discovery that high-energy vinyl carbocations can be generated under strongly basic conditions, and that they engage in intramolecular  $sp^3$  C–H insertion reactions through the catalysis of weakly coordinating anion salts. This approach relies on the unconventional combination of lithium hexamethyldisilazide base and the commercially available catalyst, triphenylmethylium tetrakis(pentafluorophenyl)borate. These reagents form a catalytically active lithium species that enables the application of vinyl cation C–H insertion reactions to heteroatom-containing substrates.

#### 4.2 Introduction

Our discovery of the unique intermolecular C–H insertion chemistry in both phenyl and vinyl cations marks an important fundamental advancement in the field of carbocation research.<sup>1</sup> However, the conditions in which we are able to generate our desired carbenium species utilized less than ideal conditions for use in more broadly applicable chemical spaces (Scheme 4.1). While potent electrophiles like silylium ions are useful in generating such reactive carbocations

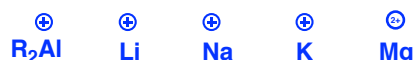
for the conversion of hydrocarbons, they hinder the application of these strategies in the syntheses of heteroatom-rich complex molecules, such as those utilized for materials and pharmaceuticals.<sup>2-4</sup>

**Scheme 4.1** Pitfalls of Silylium-mediated Reactions



For example, vinyl cations were shown to engage in high yielding reductive alkane alkylation reactions using silylium-carborane catalysis (Scheme 4.1).<sup>1</sup> This approach can often lead to limited substrate scope due to the electrophilicity of the reagents. While our group is heavily focused on fundamental reactivity, we are also equally interested in being able to employ our new discoveries (e.g the C–H insertion of carbocations) to a wide range of synthetic applications. We posited that using a milder Lewis acid initiator (Figure 4.1) would greatly expand the scope of vinyl carbocation C–H insertion reactions.

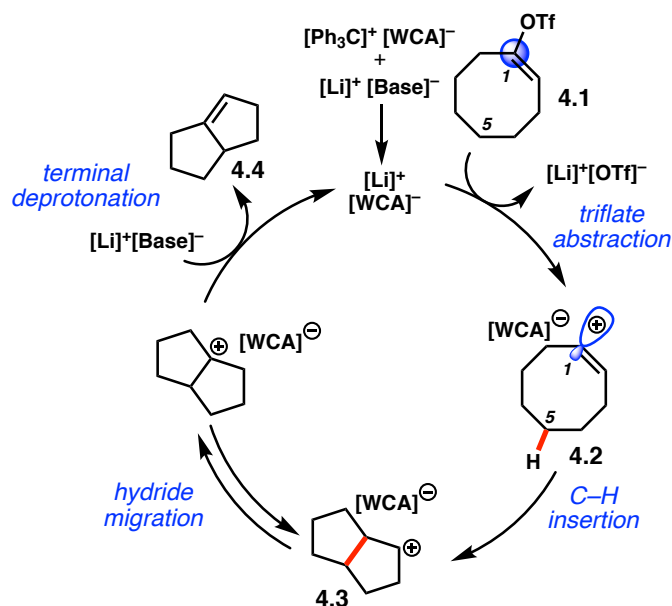
**Figure 4.1** Milder Initiators



Inspired by work from Michl and others, we hypothesized that Li cations, paired with WCAs, could serve as Lewis acids capable of converting vinyl triflates into reactive vinyl

cations.<sup>5-7</sup> To evaluate this hypothesis, we considered cyclooctenyl triflates (e.g. **4.1**, Figure **4.2**) that undergo facile ionization by silylium cations to form vinyl carbocations. These cations subsequently engage in transannular C–H insertion reactions to generate bicyclooctane products in excellent yield. We postulated that nucleophilic attack of a lithium base on  $[\text{Ph}_3\text{C}]^+[\text{WCA}]^-$  would yield the active  $[\text{Li}]^+[\text{WCA}]^-$  catalyst.  $[\text{Li}]^+[\text{WCA}]^-$ -mediated triflate abstraction would then afford a persistent vinyl cation **4.2** which would undergo transannular C–H insertion to form bicyclic secondary cation **4.3**. Importantly, we envisioned that deprotonation of this cation by a lithium base would generate the desired alkene products **4.4** and concomitantly regenerate the active  $[\text{Li}]^+[\text{WCA}]^-$  catalyst.

**Figure 4.2** Proposed Catalytic Cycle of Li-mediated C–H Insertion

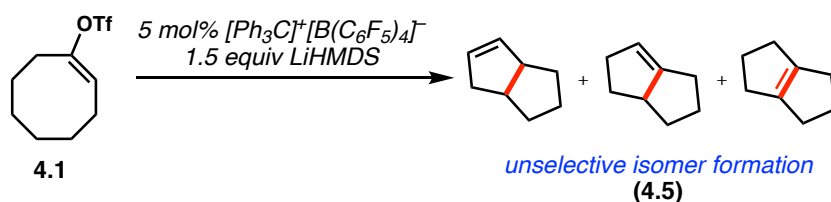


### 4.3 Development of Lithium-Mediated Insertion Reactions of Vinyl Cations

Beginning with cyclooctenyl triflate **4.1**, a screen of several Li-bases, trityl salt catalysts, and general reaction conditions was undertaken (Table **4.2**). We were gratified to find that using

a catalytic amount (5 mol%) of  $[\text{Ph}_3\text{C}]^+[\text{HCB}_{11}\text{Cl}_{11}]^-$  and 1.5 equivalents of LiHMDS base in *o*-difluorobenzene (*o*-DFB) solvent produced a mixture of bicyclooctene products (**4.5**) in four hours, in a combined yield of 84%. Remarkably, deleterious nucleophilic quenching or elimination products were not observed despite the utilization of the highly basic hexamethyldisilazide anion in the presence of a high-energy, reactive vinyl cation intermediate. Pleasingly, commercially available  $[\text{Ph}_3\text{C}]^+[\text{B}(\text{C}_6\text{F}_5)_4]^-$  was superior in this reaction, providing the bicyclooctene products (**4.5**) in 98% yield in 30 minutes at room temperature, obviating the need for the rarer  $[\text{HCB}_{11}\text{Cl}_{11}]^-$  anion. Moreover, unlike silylium-mediated reductive coupling conditions, here we generate olefinic products that can be further functionalized.<sup>8,9</sup>

**Scheme 4.2** Unselective Products of Model Substrate



#### 4.4 Incorporating Heteroatom Compatibility and Olefin Selectivity

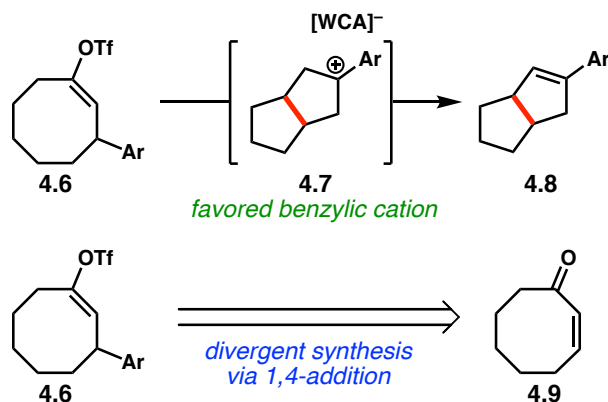
While our initial studies of  $\text{Li}^+$  ion-generated vinyl cations demonstrated exquisite reactivity and conversion, the unselective isomer formation posed an issue for synthetic relevance (Scheme 4.2). Additionally, we had yet to validate our hypothesis that the use of  $\text{Li}^+$  ions would improve the substrate compatibility of vinyl cation reactions.

We hypothesized that having aryl substitution at the 3- position of our starting cyclooctenyl triflate substrate would address the concern of unselective isomer formation. In the reaction, triflate **4.6** should give rise to a favored benzylic carbocation (**4.7**) to allow for selective deprotonation to yield styrene products (**4.8**). Furthermore, the aryl substituents could also serve



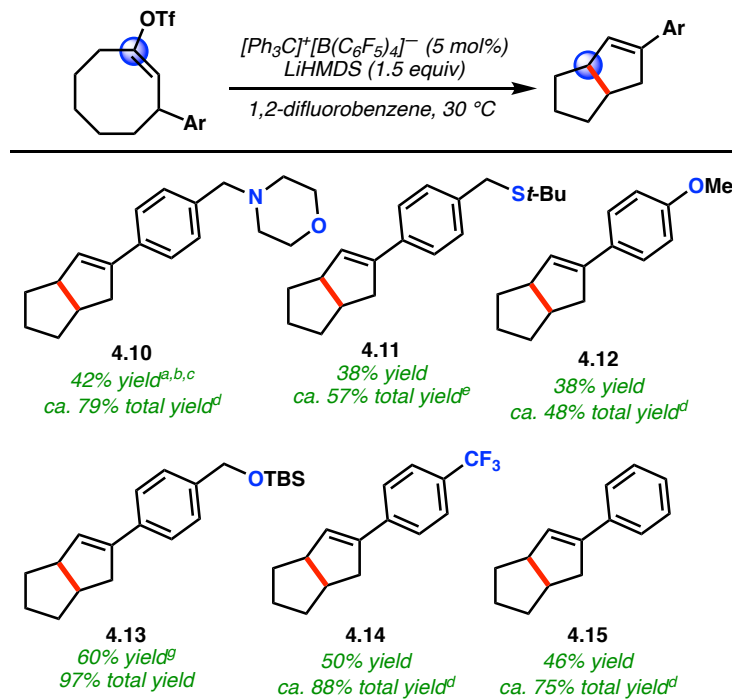
as a platform to append functional groups to test heteroatom compatibility. Starting from cyclooct-2-en-1-one (**4.9**), a wide variety of 3-arylcyclooctenyl triflates were prepared.

**Scheme 4.3** Hypothesis for New Substrate Class



We were pleased to find that benzyl morpholine derivative underwent conversion to bicyclic styrene **4.10**, in 42% yield after one hour. Similarly, heteroatom-containing thioethers and ethers were also competent under the reaction conditions (**4.11** to **4.13**, 38%, 38% and 60% yield of the depicted olefin isomer, respectively). An electron-deficient arene was tolerated, producing styrenyl trifluoromethyl derivative **4.14** in 50% yield. We also found that 3-phenylcyclooctenyl triflate provided bicyclic styrene **4.15** in 46% yield. The overall efficiency of the transannular C–H insertion reactions was high, with the total yields of the styrenyl, tri- and tetra- substituted olefin isomer products ranging from 48% to 97% (Table **4.1**). These examples highlight the functional group tolerance of these newly discovered conditions, standing in stark contrast to the previously reported Lewis acid-mediated insertion reactions of vinyl cations. In fact, when heteroatom-containing substrates (**4.10** and **4.12**) were subjected to the previously optimized silylium conditions, no reactivity was observed.<sup>1,2,10</sup>

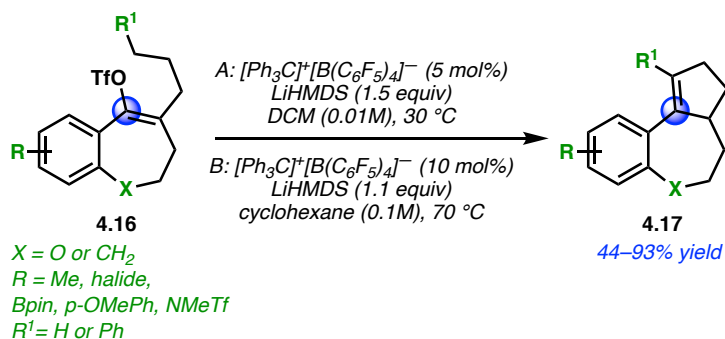
**Table 4.1** Scope of Cyclooctenyl Triflates



<sup>a</sup>3 equiv LiHMDS. <sup>b</sup>Cyclohexane as solvent. C70 °C. <sup>d</sup>Yield determined by GC-FID. <sup>e</sup>Yield determined by LCMS. <sup>f</sup>Methylene chloride as solvent.

Having demonstrated that cyclic vinyl triflates undergo transannular C–H insertion reactions under Li-WCA catalysis, we sought to further expand the scope of our method to annulation reactions. Benzosuberone-derived triflates **4.16** with tethered alkyl chains were also shown to be competent under our reaction conditions (Scheme 4.4). Gratifyingly, improved heteroatom compatibility including pinacol boronic ester, anisole, protected aniline and halogen substitution were all tolerated, yielding tricyclic products **4.17** in moderate to excellent yields (44–93%). A full report of our benzosuberone-derived triflates, as well as the mechanistic investigations not presently discussed can be viewed in our publication in *J. Am. Chem. Soc.*<sup>11</sup>

#### Scheme 4.4 Benzosuberone-derived Triflates



## 4.5 Conclusion

In the pursuit of bringing our fundamental advances in dicoordinate carbocation chemistry to broader applications, we find that it is possible to generate such species in highly basic media. Importantly, this catalytic regime represents a new strategy where lithium bases can be utilized to fuel  $[\text{Li}]^+[\text{WCA}]^-$ -catalyzed, intramolecular C–H insertion reactions of vinyl cations. With beginnings rooted in the historical and conceptual importance of long-studied carbocation intermediates, we have now entered the realm of incorporating heteroatom compatibility for application in the fine chemicals field. Considering the commercial availability of the catalyst and the simple reaction protocols, this strategy becomes an attractive approach to synthesis in both academic and industrial settings.

## 4.6 Experimental Section

### 4.6.1 Materials and Methods

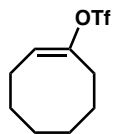
Unless otherwise stated, all reactions were performed in an MBraun glovebox under nitrogen atmosphere with  $\leq 0.5$  ppm  $\text{O}_2$  levels. All glassware and stir-bars were dried in a 160 °C oven for at least 12 hours and dried *in vacuo* before use. All liquid substrates were either dried

over  $\text{CaH}_2$  or filtered through dry neutral aluminum oxide. Solid substrates were dried over  $\text{P}_2\text{O}_5$ . All solvents were rigorously dried before use. Benzene, *o*-dichlorobenzene, and toluene were degassed and dried in a JC Meyer solvent system and stored inside a glovebox. Cyclohexane, fluorobenzene, and *n*-hexane were distilled over potassium. Chlorobenzene was distilled over sodium. *o*-Difluorobenzene was distilled over  $\text{CaH}_2$ . Pentane was distilled over sodium-potassium alloy. Chloroform was dried over  $\text{CaH}_2$  and stored in a glovebox. Triethylsilane and triisopropylsilane were dried over sodium and stored inside a glovebox. *Closo*-Carborane catalysts were prepared according to literature procedure.<sup>1</sup>  $[\text{Li}]^+[\text{B}(\text{C}_6\text{F}_5)_4]^-$  and  $[\text{K}]^+[\text{B}(\text{C}_6\text{F}_5)_4]^-$  salts were synthesized according to literature procedure.<sup>2</sup> Preparatory thin layer chromatography (TLC) was performed using Millipore silica gel 60 F<sub>254</sub> pre-coated plates (0.25 mm) and visualized by UV fluorescence quenching. SiliaFlash P60 silica gel (230-400 mesh) was used for flash chromatography.  $\text{AgNO}_3$ -Impregnated silica gel was prepared by mixing with a solution of  $\text{AgNO}_3$  (150% v/w of 10% w/v solution in acetonitrile), removing solvent under reduced pressure, and drying at 120 °C. NMR spectra were recorded on a Bruker AV-300 ( $^1\text{H}$ ,  $^{19}\text{F}$ ), Bruker AV-400 ( $^1\text{H}$ ,  $^{13}\text{C}$ ,  $^{19}\text{F}$ ), Bruker DRX-500 ( $^1\text{H}$ ), and Bruker AV-500 ( $^1\text{H}$ ,  $^{13}\text{C}$ ).  $^1\text{H}$  NMR spectra are reported relative to  $\text{CDCl}_3$  (7.26 ppm) unless noted otherwise. Data for  $^1\text{H}$  NMR spectra are as follows: chemical shift (ppm), multiplicity, coupling constant (Hz), integration. Multiplicities are as follows: s = singlet, d = doublet, t = triplet, dd = doublet of doublet, dt = doublet of triplet, ddd = doublet of doublet of doublet, td = triplet of doublet, m = multiplet.  $^{13}\text{C}$  NMR spectra are reported relative to  $\text{CDCl}_3$  (77.0 ppm) unless noted otherwise. GC spectra were recorded on an Agilent 6850 series GC using an Agilent HP-1 (50 m, 0.32 mm ID, 0.25 mm DF) column. GCMS spectra were recorded on a Shimadzu GCMS-QP2010 using a Restek XTI-5 (50 m, 0.25 mm ID, 0.25 mm DF) column interface at room temperature. IR Spectra were recorded on

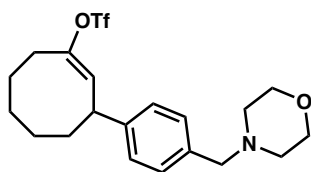
a Perkin Elmer 100 spectrometer and are reported in terms of frequency absorption ( $\text{cm}^{-1}$ ). High resolution mass spectra (HR-MS) were recorded on a Waters (Micromass) GCT Premier spectrometer, a Waters (Micromass) LCT Premier, or an Agilent GC EI-MS, and are reported as follows:  $m/z$  (% relative intensity). Purification by preparative HPLC was done on an Agilent 1200 series instrument with a reverse phase Alltima  $\text{C}_{18}$  (5m, 25 cm length, 1 cm internal diameter) column.

*Note: Experimental information for compounds 4.5, 4.9, 4.16 and 4.17 can be found in adapted article.*

#### 4.6.2 Synthesis of Cyclooctenyl Substrate Class 4.6



**(E)-Cyclooct-1-en-1-yl trifluoromethanesulfonate (4.1).** Synthesized according to literature procedure. NMR data match those reported in literature.<sup>1</sup>



**(E)-3-(4-(morpholinomethyl)phenyl)cyclooct-1-en-1-yl trifluoromethanesulfonate (4.18).** To a degassed solution of 4-(4-bromobenzyl)morpholine (1.2 g, 4.8 mmol, 2.0 equiv) at  $-78\text{ }^{\circ}\text{C}$  in THF (10 mL) was added a solution of 2.0 M *n*-BuLi in hexanes (2.5 mL, 2.0 equiv). After 30 minutes of stirring, this solution was cannula transferred to a degassed  $-78\text{ }^{\circ}\text{C}$  solution of copper iodide in  $\text{Et}_2\text{O}$  (2.5 mL). The reaction was allowed to stir at  $-78\text{ }^{\circ}\text{C}$  for 5 minutes before

removing the cooling bath to stir at room temperature. Once the solution turned dark purple in color, the reaction was placed in a 0 °C bath. Cyclooct-2-en-1-one (300 mg, 2.4 mmol, 1.0 equiv) in Et<sub>2</sub>O (5 mL) was added while maintaining this temperature. After 30 minutes of stirring, Comin's reagent (1.0 g, 2.5 mmol, 1.1 equiv) in THF (5 mL) was added and the reaction was allowed to warm to room temperature over 12 hours. The reaction was quenched by addition of saturated aqueous solution of ammonium chloride (20 mL) and extracted with Et<sub>2</sub>O (3 x 20 mL). The combined organics were washed with brine, dried over MgSO<sub>4</sub>, filtered and concentrated. The crude product was purified by flash column chromatography (30% diethyl ether in hexanes) to yield 320 mg (31%) of light yellow solid.

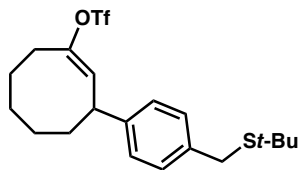
<sup>1</sup>H NMR (500 MHz, CDCl<sub>3</sub>) δ 7.31 – 7.25 (m, 2H), 7.20 – 7.15 (m, 2H), 5.72 (d, *J* = 9.4 Hz, 1H), 3.70 (t, *J* = 4.7 Hz, 4H), 3.57 (ddd, *J* = 12.5, 9.5, 4.4 Hz, 1H), 3.47 (s, 2H), 2.75 (ddd, *J* = 15.7, 12.4, 3.3 Hz, 1H), 2.46 – 2.39 (m, 4H), 1.98 – 1.90 (m, 1H), 1.87 – 1.67 (m, 6H), 1.63 (s, 1H), 1.58 – 1.50 (m, 1H).

<sup>13</sup>C NMR (125 MHz, CDCl<sub>3</sub>) δ 149.6, 142.7, 136.2, 129.5, 126.9, 124.7, 122.3, 119.7, 117.2, 114.6, 67.0, 63.0, 53.6, 41.9, 37.8, 30.5, 27.5, 26.2, 25.4.

<sup>19</sup>F NMR (282 MHz, CDCl<sub>3</sub>) δ –74.2.

FTIR (Neat Film NaCl): 2829, 2855, 2806, 1678, 1513, 1455, 1414, 1206, 1143, 1117, 1037, 1008, 931, 867, 614 3093, 3027, 2934, 2856, 2805, 1512, 1453, 1332, 1264, 1118, 1008, 876, 827, 787, 614 cm<sup>-1</sup>.

HRMS (GCT-LIFDI): Calculated for [C<sub>20</sub>H<sub>26</sub>F<sub>3</sub>NO<sub>4</sub>S + H]: 434.1535; Measured: 434.1539.



**(E)-3-(4-((*tert*-butylthio)methyl)phenyl)cyclooct-1-en-1-yl trifluoromethanesulfonate (4.19).**

To a degassed solution of 4-(4-bromobenzyl)(*tert*-butyl)sulfane (1.3g, 4.8 mmol, 2.0 equiv) at  $-78$  °C in Et<sub>2</sub>O (5 mL) was added a solution of 1.57 M *t*-BuLi in pentane (6.2 mL, 4.0 equiv). After 30 minutes of stirring, this solution was cannula transferred to a degassed  $-78$ °C solution of copper iodide (460 mg, 2.4 mmol, 1.0 equiv) in Et<sub>2</sub>O (2.5 mL). The reaction was allowed to stir at  $-78$  °C for 50 minutes before warming to 0 °C. After stirring at 0 °C for 5 minutes, cyclooct-2-en-1-one (300 mg, 2.4 mmol, 1.0 equiv) in Et<sub>2</sub>O (5 mL) was added while maintaining this temperature. After 30 minutes of stirring, Comin's reagent (1.0 g, 2.5 mmol, 1.1 equiv) in THF (5 mL) was added and the reaction was allowed to warm to room temperature over 36 hrs. The reaction was quenched by addition of saturated aqueous solution of ammonium chloride (20 mL) and extracted with Et<sub>2</sub>O (3 x 20 mL). The combined organics were washed with brine and dried over MgSO<sub>4</sub>. The crude product was purified by flash column chromatography (25% benzene in hexanes) to yield 265 mg (25%) of white solid.

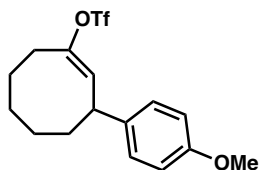
<sup>1</sup>H NMR (500 MHz, CDCl<sub>3</sub>)  $\delta$  7.30 (d,  $J$  = 8.2 Hz, 2H), 7.15 (d,  $J$  = 8.1 Hz, 2H), 5.71 (d,  $J$  = 9.4 Hz, 1H), 3.74 (s, 2H), 3.56 (ddd,  $J$  = 13.3, 9.4, 4.3 Hz, 1H), 2.75 (ddd,  $J$  = 15.5, 12.2, 3.4 Hz, 1H), 2.40 (dt,  $J$  = 15.8, 4.3 Hz, 1H), 1.93 (tt,  $J$  = 9.5, 3.8 Hz, 1H), 1.88 – 1.66 (m, 5H), 1.36 (s, 9H).

<sup>13</sup>C NMR (126 MHz, CDCl<sub>3</sub>)  $\delta$  149.8, 142.5, 137.1, 129.5, 127.3, 124.9, 118.6 (q,  $J$  = 320.0 Hz), 43.1, 42.1, 37.9, 33.1, 31.0, 30.7, 27.7, 26.3, 25.5.

<sup>19</sup>F NMR (376 MHz, CDCl<sub>3</sub>)  $\delta$   $-74.1$ .

FTIR (Neat film NaCl): 2928, 2860, 1678, 1513, 1457, 1415, 1365, 126, 1208, 1144, 1038, 1011, 982, 931, 871, 837, 732, 648, 608, 507.

HR-MS (GCT-LIFDI): Calculated for C<sub>20</sub>H<sub>27</sub>F<sub>3</sub>O<sub>3</sub>S<sub>2</sub>: 436.1354; measured: 436.1335.



**(E)-3-(4-methoxyphenyl)cyclooct-1-en-1-yl trifluoromethanesulfonate (4.20).** Synthesized using (*Z*)-cyclooct-2-en-1-one according to reported literature.<sup>12</sup>

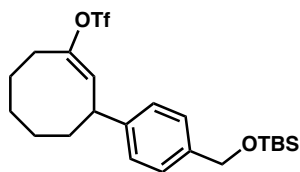
<sup>1</sup>H NMR (500 MHz, CDCl<sub>3</sub>) δ 7.18 – 7.12 (m, 2H), 6.90 – 6.83 (m, 2H), 5.69 (d, *J* = 9.5 Hz, 1H), 3.80 (s, 3H), 3.54 (ddd, *J* = 12.4, 9.4, 4.4 Hz, 1H), 2.81 – 2.70 (m, 1H), 2.41 (dt, *J* = 15.5, 4.3 Hz, 1H), 1.98 – 1.89 (m, 1H), 1.87 – 1.66 (m, 6H), 1.59 – 1.51 (m, 1H).

<sup>13</sup>C NMR (125 MHz, CDCl<sub>3</sub>) δ 158.3, 149.5, 135.9, 127.9, 125.0, 122.3, 119.8, 117.2, 115.0, 114.1, 55.3, 41.4, 37.8, 30.5, 27.6, 26.2, 25.4.

<sup>19</sup>F NMR (282 MHz, CDCl<sub>3</sub>) δ -74.2.

FTIR (Neat Film NaCl): 3045, 3005, 2933, 2857, 1678, 1613, 1514, 1414, 1248, 1209, 1144, 1039, 932, 871, 826, 607 cm<sup>-1</sup>.

HRMS (GCT-LIFDI): Calculated for C<sub>16</sub>H<sub>19</sub>F<sub>3</sub>O<sub>4</sub>S: 364.0956; Measured: 364.0954.



**(E)-3-(4-(((*tert*-butyldimethylsilyloxy)methyl)phenyl)cyclooct-1-en-1-yl**

**trifluoromethanesulfonate (4.21).** To a degassed solution of ((4-bromobenzyl)oxy)(*tert*-butyl)dimethylsilane (1.5 g, 4.8 mmol, 2.0 equiv) at -78 °C in Et<sub>2</sub>O (5 mL) was added a solution of 1.57 M *t*-BuLi in pentane (6.2 mL, 4.0 equiv). After 30 minutes of stirring, this solution was



cannula transferred to a degassed  $-78\text{ }^{\circ}\text{C}$  solution of copper iodide (460 mg, 2.4 mmol, 1.0 equiv) in  $\text{Et}_2\text{O}$  (2.5 mL). The reaction was allowed to stir at  $-78\text{ }^{\circ}\text{C}$  for 50 minutes before warming to  $0\text{ }^{\circ}\text{C}$ . After stirring at  $0\text{ }^{\circ}\text{C}$  for 15 minutes, cyclooct-2-en-1-one (300 mg, 2.4 mmol, 1.0 equiv) in  $\text{Et}_2\text{O}$  (5 mL) was added while maintaining this temperature. After 45 minutes of stirring, Comin's reagent (1.0 g, 2.5 mmol, 1.1 equiv) in THF (5 mL) was added and the reaction was allowed to warm to room temperature overnight. The reaction was quenched by addition of saturated aqueous solution of ammonium chloride (20 mL) and extracted with  $\text{Et}_2\text{O}$  (3 x 20 mL). The combined organics were washed with brine and dried with  $\text{MgSO}_4$ . The crude product was purified by flash column chromatography (25% chloroform in pentane) to yield 325 mg (28%) of yellow oil.

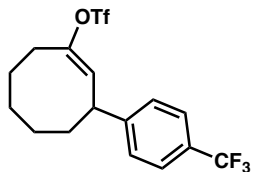
$^1\text{H}$  NMR (500 MHz,  $\text{CDCl}_3$ )  $\delta$  7.28 (d,  $J = 7.8$  Hz, 1H), 7.19 (d,  $J = 8.1$  Hz, 2H), 5.73 (d,  $J = 9.5$  Hz, 1H), 4.72 (s, 2H), 3.57 (ddd,  $J = 13.2, 9.4, 4.3$  Hz, 1H), 2.83 – 2.67 (m, 1H), 2.41 (dt,  $J = 15.6, 4.3$  Hz, 1H), 2.02 – 1.89 (m, 1H), 1.87 – 1.65 (m, 4H), 0.94 (s, 10H), 0.10 (s, 6H).

$^{13}\text{C}$  NMR (126 MHz,  $\text{CDCl}_3$ )  $\delta$  149.6, 142.4, 139.9, 126.8, 126.4, 124.8, 118.4 (q,  $J = 320.1$  Hz), 64.6, 41.9, 37.8, 30.4, 27.5, 26.1, 25.9, 25.40, 18.4,  $-5.2$ .

$^{19}\text{F}$  NMR (376 MHz,  $\text{CDCl}_3$ )  $\delta$   $-74.1$ .

FTIR (Neat film NaCl): 2930, 2858, 1416, 1248, 1210, 1145, 1092, 1039, 1009, 982, 932, 838, 777, 610, 507.

HR-MS (LCT-ESI): Calculated for  $[\text{C}_{22}\text{H}_{33}\text{F}_3\text{O}_4\text{SSi} + \text{Na}]$ : 501.1719; Measured: 501.1700.



**(E)-3-(4-(trifluoromethyl)phenyl)cyclooct-1-en-1-yl trifluoromethanesulfonate (4.22).** A flame dried round bottom flask was charged with anhydrous  $\text{ZnCl}_2$  (4.4 g, 32 mmol, 1.0 equiv) and anhydrous toluene (32 mL). After cooling the mixture to  $-30\text{ }^\circ\text{C}$ , a 0.42 M aryl lithium solution (116 mL, 21 mmol, 1.3 equiv), made from reacting 1-bromo-4-(trifluoromethyl)benzene (8.9 mL, 64 mmol) in  $\text{Et}_2\text{O}$  (124 mL) with a solution of 2.63 M *n*-BuLi in hexanes (25 mL, 65 mmol) at  $-78\text{ }^\circ\text{C}$ , was added dropwise. The reaction was then left to warm up to room temperature over 2 hours to yield a 0.18 M solution of diarylzinc by iodine titration.<sup>4</sup> To a separate flame dried schlenk flask was added  $\text{Cu}(\text{OTf})_2$  (116 mg, 0.32 mmol, 0.02 equiv),  $\text{PPh}_3$  (169 mg, 0.64 mmol, 0.04 equiv) and anhydrous toluene (80 mL). Reaction was degassed and stirred for 30 minutes. Cyclooct-2-en-1-one (2.0 g, 16 mmol, 1.0 equiv) was added and the solution cooled to  $-30\text{ }^\circ\text{C}$ . The solution of 0.18 M diarylzinc in  $\text{Et}_2\text{O}$  (116 mL, 21 mmol, 1.3 equiv) was then added dropwise. After 2 hours, the reaction was brought to  $0\text{ }^\circ\text{C}$  before adding  $\text{Tf}_2\text{O}$  (5.4 mL, 32 mmol, 2.0 equiv) and allowed to warm to room temperature over 12 hours. The reaction was quenched with saturated aqueous sodium bicarbonate solution (150 mL), extracted with  $\text{Et}_2\text{O}$  (3 x 100 mL), and the combined organics were dried over  $\text{MgSO}_4$  filtered and concentrated. Crude product was purified by flash chromatography (hexanes) to yield 540 mg (8%) of colorless oil.

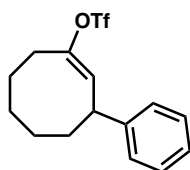
$^1\text{H}$  NMR (500 MHz,  $\text{CDCl}_3$ )  $\delta$  7.59 (d,  $J = 8.1\text{ Hz}$ , 2H), 7.35 (d,  $J = 8.0\text{ Hz}$ , 2H), 5.70 (d,  $J = 9.4\text{ Hz}$ , 1H), 3.65 (ddd,  $J = 13.1, 9.4, 4.3\text{ Hz}$ , 1H), 2.76 (ddd,  $J = 15.7, 12.3, 3.4\text{ Hz}$ , 1H), 2.43 (dt,  $J = 15.6, 4.2\text{ Hz}$ , 1H), 2.02 – 1.91 (m, 1H), 1.90 – 1.69 (m, 6H), 1.62 – 1.52 (m, 1H).

$^{13}\text{C}$  NMR (125 MHz,  $\text{CDCl}_3$ )  $\delta$  150.1, 147.7, 129.2, 129.0, 127.4, 125.7 (q,  $J_{\text{C-F}} = 3.8$  Hz), 125.6, 123.7, 123.0, 119.7, 117.2, 114.6, 42.2, 37.6, 30.5, 27.5, 26.1, 25.3.

$^{19}\text{F}$  NMR (282 MHz,  $\text{CDCl}_3$ )  $\delta$  -74.1, -64.5.

FTIR (Neat Film NaCl): 3060, 2933, 2859, 1679, 1619, 1415, 1326, 1210, 1124, 1070, 933, 606  $\text{cm}^{-1}$ .

HRMS (EI-MS): Calculated for  $\text{C}_{16}\text{H}_{16}\text{F}_6\text{O}_3\text{S}$ : 402.0724; Measured: 402.0745.



**(E)-3-phenylcyclooct-1-en-1-yl trifluoromethanesulfonate (4.23).** A flame dried round bottom flask was charged with anhydrous  $\text{ZnCl}_2$  (4.2 g, 31 mmol, 1.0 equiv) and anhydrous toluene (31 mL). After cooling the mixture to  $-30$   $^\circ\text{C}$ , a 1.0 M solution of  $\text{PhMgBr}$  in  $\text{Et}_2\text{O}$  (62 mL, 62 mmol, 2.0 equiv) was added dropwise. The reaction was then left to warm up to room temperature over 2 hours to yield a 0.47 M solution of diphenylzinc. To a separate flame dried schlenk flask was added  $\text{Cu}(\text{OTf})_2$  (64 mg, 0.18 mmol, 0.02 equiv),  $\text{PPh}_3$  (93 mg, 0.35 mmol, 0.04 equiv) and anhydrous toluene (45 mL). After stirring for 30 minutes, cyclooct-2-en-1-one (1.1 g, 8.8 mmol, 1.0 equiv) was added and the solution cooled to  $-30$   $^\circ\text{C}$ . The solution of 0.47 M diphenylzinc in  $\text{Et}_2\text{O}$  (30 mL, 11.5 mmol, 1.3 equiv) was then added dropwise. After 2 hours, the reaction was brought to  $0$   $^\circ\text{C}$  before adding  $\text{Tf}_2\text{O}$  (5 mL, 17.7 mmol, 2.0 equiv) and allowed to warm to room temperature over 12 hours. The reaction was quenched with saturated aqueous sodium bicarbonate solution (80 mL), extracted with  $\text{Et}_2\text{O}$  (3 x 60 mL) and the combined organics were dried over  $\text{MgSO}_4$ . After filtering and concentrating by rotary evaporation, the crude product was purified by flash chromatography (hexanes) to yield 145 mg (5%) of colorless oil.

$^1\text{H}$  NMR (500 MHz,  $\text{CDCl}_3$ )  $\delta$  7.37 – 7.30 (m, 2H), 7.29 – 7.20 (m, 3H), 5.74 (d,  $J = 9.5$  Hz, 1H), 3.59 (ddd,  $J = 12.1, 9.4, 4.4$  Hz, 1H), 2.77 (ddd,  $J = 15.5, 12.2, 3.4$  Hz, 1H), 2.45 – 2.37 (m, 1H), 2.01 – 1.91 (m, 1H), 1.89 – 1.68 (m, 6H), 1.61 – 1.55 (m, 1H).

$^{13}\text{C}$  NMR (125 MHz,  $\text{CDCl}_3$ )  $\delta$  149.7, 143.8, 128.8, 127.0, 126.7, 124.7, 122.3, 119.8, 117.2, 114.7, 42.3, 37.8, 30.5, 27.6, 26.2, 25.4.

$^{19}\text{F}$  NMR (282 MHz,  $\text{CDCl}_3$ )  $\delta$  -74.2.

FTIR (Neat Film NaCl): 3090, 3064, 2930, 2857, 1678, 1599, 1415, 1210, 1143, 932, 699, 605  $\text{cm}^{-1}$ .

HRMS (EI-MS): Calculated for  $\text{C}_{15}\text{H}_{17}\text{F}_3\text{O}_3\text{S}$ : 334.0850; Measured: 334.0848.

#### 4.6.3 Optimization Table for Cyclooctenyl triflate

**Table 4.2** Optimization of intramolecular C–H insertion reaction of cyclooctenyl triflate (**4.1**).

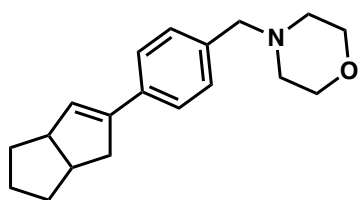
$[\text{M}]^+[\text{WCA}]^-$	% Cat. Loading	Temp.	Base	Solvent	Yield
$[\text{Ph}_3\text{C}]^+[\text{HCB}_{11}\text{Cl}_{11}]^-$	5 mol%	30 °C	LiHMDS	<i>o</i> -DFB	90%
$[\text{Ph}_3\text{C}]^+[\text{HCB}_{11}\text{Cl}_{11}]^-$	5 mol%	30 °C	LiHMDS	DCM	59%
$[\text{Ph}_3\text{C}]^+[\text{B}(\text{C}_6\text{F}_5)_4]^-$	5 mol%	30 °C	LiHMDS	<i>o</i> -DFB	98%
$[\text{Ph}_3\text{C}]^+[\text{B}(\text{C}_6\text{F}_5)_4]^-$	0 mol%	30 °C	LiHMDS	<i>o</i> -DFB	0%
$[\text{Ph}_3\text{C}]^+[\text{B}(\text{C}_6\text{F}_5)_4]^-$	5 mol%	30 °C	NaHMDS	<i>o</i> -DFB	0%
$[\text{Ph}_3\text{C}]^+[\text{B}(\text{C}_6\text{F}_5)_4]^-$	5 mol%	30 °C	KHMDS	<i>o</i> -DFB	0%
$[\text{Li}]^+[\text{B}(\text{C}_6\text{F}_5)_4]^-$	5 mol%	30 °C	LiHMDS	<i>o</i> -DFB	84%

#### 4.6.4 General Procedure for Transannular C–H Insertion Reactions.

In a well kept glovebox,  $\text{H}_2\text{O}$ ,  $\text{O}_2 \leq 0.5$  ppm, a dram vial was charged with  $[\text{Ph}_3\text{C}]^+[\text{B}(\text{C}_6\text{F}_5)_4]^-$  (0.05 equiv) and LiHMDS (1.5–3.0 equiv). Solids were stirred in solvent (0.1–0.017 M) for one minute before addition of cyclooctenyl triflate substrate. Reactions were

stirred at 30–70 °C for 0.5–3.5 hours (see substrates for exact conditions). Reactions were monitored by GC-FID spectra unless noted otherwise. Upon completion, reactions were brought out of the glovebox, diluted with hexanes, and passed through a short plug of silica. Isolation of styrene products was achieved by flash column, preparatory thin layer chromatography using silver impregnated silica or HPLC.

#### 4.6.5 Insertion Reactions of Cyclooctenyl Triflate Derivatives



**4-(4-(1,3a,4,5,6,6a-hexahydropentalen-2-yl)benzyl)morpholine (4.10).** Synthesized according to general procedure. A dram vial charged with  $[\text{Ph}_3\text{C}]^+[\text{B}(\text{C}_6\text{F}_5)_4]^-$  (1.2 mg, 1.25 mmol, 0.05 equiv) and LiHMDS (12.6 mg, 0.075 mmol, 3.0 equiv) was suspended in cyclohexane (0.25 mL, 0.017 M). After pre-stirring for one minute, corresponding triflate (10.8 mg, 0.025 mmol, 1.0 equiv) was added and stirred at 70 °C for 1 hour. Upon completion, reaction was diluted with hexanes (1 mL) and passed through a short plug of silica (1:1 hexanes: $\text{Et}_2\text{O}$ ) to yield **4.10** in 42% NMR yield. Crude product can be further purified by preparatory thin layer chromatography (10% methanol in ethyl acetate) using silver impregnated silica to give **4.10** as a colorless oil. Major byproducts observed are intractable mixtures of high molecular weight products likely due to oligomerization of the desired electron-rich styrene **4.10**.

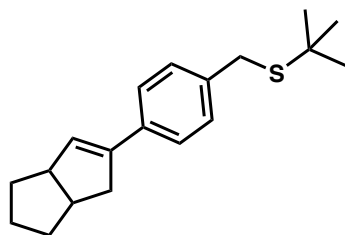
$^1\text{H}$  NMR (500 MHz,  $\text{CDCl}_3$ )  $\delta$  7.37 (d,  $J = 7.9$  Hz, 2H), 7.28 – 7.23 (m, 2H), 5.98 (q,  $J = 2.2$  Hz, 1H), 3.70 (t,  $J = 4.6$  Hz, 4H), 3.48 (s, 2H), 3.33 (tt,  $J = 8.5, 2.5$  Hz, 1H), 2.99 (ddt,  $J = 16.2, 9.3,$

2.0 Hz, 1H), 2.82 (ddq,  $J = 12.4, 8.3, 3.7$  Hz, 1H), 2.53 – 2.36 (m, 4H), 1.83 – 1.67 (m, 3H), 1.51 (dt,  $J = 7.2, 4.6$  Hz, 3H), 1.43 – 1.37 (m, 1H).

$^{13}\text{C}$  NMR (125 MHz,  $\text{CDCl}_3$ )  $\delta$  140.5, 135.6, 129.8, 129.1, 126.1, 125.5, 67.0, 63.1, 53.5, 51.1, 41.4, 40.3, 35.8, 32.5, 25.3.

FTIR (Neat Film NaCl): 3093, 3027, 2934, 2856, 2805, 1512, 1453, 1332, 1264, 1118, 1008, 876, 827, 787  $\text{cm}^{-1}$ .

HRMS (EI-MS): Calculated for  $\text{C}_{19}\text{H}_{25}\text{NO}$ : 283.1936; Measured: 283.1934.



***tert*-butyl(4-(1,3a,4,5,6,6a-hexahydropentalen-2-yl)benzyl)sulfane (4.11).** Synthesized according to general procedure. A dram vial charged with  $[\text{Ph}_3\text{C}]^+[\text{B}(\text{C}_6\text{F}_5)_4]^-$  (2.3 mg, 2.50 mmol, 0.05 equiv) and LiHMDS (12.5 mg, 0.075 mmol, 1.5 equiv) was dissolved in *o*-difluorobenzene (0.5 mL). After pre-stirring for one minute, corresponding triflate (21.8 mg, 0.05 mmol 1.0 equiv) was added and stirred at 30°C for 0.5 hours. Upon completion, reaction was diluted with ether (1 mL) and passed through a short plug of silica ( $\text{Et}_2\text{O}$ ) to yield **4.11** in 38% NMR yield. Crude product can be further purified by HPLC (10% water in acetonitrile) to give **4.11** as a white solid. The low yield observed is attributed to the instability of the products to silica chromatography.

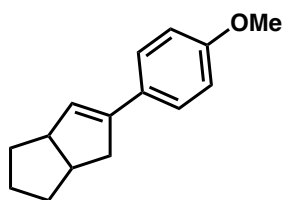
$^1\text{H}$  NMR (500 MHz,  $\text{CDCl}_3$ )  $\delta$  7.34 (d,  $J = 8.3$  Hz, 1H), 7.27 (d,  $J = 8.6$  Hz, 1H), 5.95 (q,  $J = 2.2$  Hz, 1H), 3.74 (s, 1H), 3.31 (tq,  $J = 5.5, 2.7, 2.2$  Hz, 1H), 2.97 (ddt,  $J = 16.1, 9.3, 1.9$  Hz, 1H),

2.81 (dtdd,  $J = 9.4, 8.3, 4.2, 3.1$  Hz, 1H), 2.39 (dtd,  $J = 16.2, 3.0, 1.8$  Hz, 1H), 1.82 – 1.64 (m, 1H), 1.53 – 1.45 (m, 2H), 1.34 (s, 5H).

$^{13}\text{C}$  NMR (126 MHz,  $\text{CDCl}_3$ )  $\delta$  140.5, 137.0, 135.2, 129.7, 128.8, 125.7, 51.1, 42.8, 41.3, 40.3, 35.7, 33.20, 32.5, 30.9, 25.3.

FT-IR (neat film NaCl): 2929, 2859, 1511, 1458, 1415, 1363, 1161, 1052, 830, 756, 540  $\text{cm}^{-1}$ .

HRMS (GCT-Cl): Calculated for  $\text{C}_{19}\text{H}_{26}\text{S}$ : 286.1755; Measured: 286.1768.



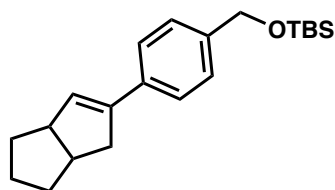
**5-(4-methoxyphenyl)-1,2,3,3a,4,6a-hexahydropentalene (4.12).** Synthesized according to general procedure. A dram vial charged with  $[\text{Ph}_3\text{C}]^+[\text{B}(\text{C}_6\text{F}_5)_4]^-$  (1.2 mg, 1.25 mmol, 0.05 equiv) and LiHMDS (6.3 mg, 0.038 mmol, 1.5 equiv) was dissolved in *o*-difluorobenzene (1.5 mL, 0.017 M). After pre-stirring for one minute, corresponding triflate (9.1 mg, 0.025 mmol, 1.0 equiv) was added and stirred at 30 °C for 1 hour. Upon completion, reaction was diluted with hexanes (1 mL) and passed through a short plug of silica to yield **4.12** in 38% NMR yield. Crude product can be further purified by flash column chromatography (50% benzene in hexanes) using silver impregnated silica to give **4.12** as a colorless oil in 29% yield (1.6 mg). Major byproducts observed are intractable mixtures of high molecular weight products likely due to oligomerization of the desired electron-rich styrene **4.12**.

$^1\text{H}$  NMR (400 MHz,  $\text{CDCl}_3$ )  $\delta$  7.38 – 7.32 (m, 2H), 6.88 – 6.80 (m, 2H), 5.85 (q,  $J = 2.2$  Hz, 1H), 3.80 (s, 3H), 3.32 (td,  $J = 8.4, 7.5, 4.4$  Hz, 1H), 2.97 (ddt,  $J = 16.1, 9.4, 2.0$  Hz, 1H), 2.87 – 2.75 (m, 1H), 2.39 (dtd,  $J = 16.1, 3.0, 1.7$  Hz, 1H), 1.82 – 1.64 (m, 2H), 1.55 – 1.46 (m, 3H), 1.45 – 1.37 (m, 1H).

$^{13}\text{C}$  NMR (125 MHz,  $\text{CDCl}_3$ )  $\delta$  158.5, 140.2, 129.5, 127.8, 126.7, 113.6, 55.2, 51.12, 4.5, 40.3, 35.8, 32.6, 25.3.

FTIR (Neat Film NaCl): 3038, 2935, 2859, 1739, 1608, 1512, 1455, 1254, 1178, 1040, 825  $\text{cm}^{-1}$ .

HRMS (EI-MS): Calculated for  $\text{C}_{15}\text{H}_{18}\text{O}$ : 214.1358; Measured: 214.1353.



***tert*-butyl((4-(1,3a,4,5,6,6a-hexahdropentalen-2-yl)benzyl)oxy)dimethylsilane (4.13).**

Synthesized according to general procedure. A dram vial charged with  $[\text{Ph}_3\text{C}]^+[\text{B}(\text{C}_6\text{F}_5)_4]^-$  (2.3 mg, 2.50 mmol, 0.05 equiv) and LiHMDS (12.5 mg, 0.075 mmol, 1.5 equiv) was dissolved in methylene chloride (0.5 mL). After pre-stirring for one minute, corresponding triflate (23.9 mg, 0.05 mmol 1.0 equiv) was added and stirred at 30°C for 0.5 hours. Upon completion, reaction was diluted with ether (1 mL) and passed through a short plug of silica ( $\text{Et}_2\text{O}$ ) to yield **4.13** in 60% NMR yield. Crude product can be further purified by flash column chromatography using silver impregnated silica (10% benzene in pentane) to give 6.6mg (46%) of **4.13** as a colorless oil.

The tetrasubstituted isomer could be isolated by preparatory thin layer chromatography (3:2 hexane:benzene) using silver impregnated silica to give **4.13** as a colorless oil.

### Characterization of styrene isomer

$^1\text{H}$  NMR (500 MHz,  $\text{CDCl}_3$ )  $\delta$  7.38 (d,  $J = 8.2$  Hz, 1H), 7.24 (d,  $J = 0.7$  Hz, 0H), 5.96 (q,  $J = 2.2$  Hz, 1H), 4.72 (s, 1H), 3.32 (tt,  $J = 8.1, 2.5$  Hz, 1H), 2.99 (ddt,  $J = 16.2, 9.4, 2.0$  Hz, 1H), 2.91 –



2.70 (m, 1H), 2.41 (dtd,  $J = 16.2, 3.0, 1.8$  Hz, 1H), 1.81 – 1.63 (m, 1H), 1.54 – 1.46 (m, 2H), 0.93 (s, 5H), 0.09 (s, 4H).

$^{13}\text{C}$  NMR (126 MHz,  $\text{CDCl}_3$ )  $\delta$  140.6, 139.9, 135.3, 129.5, 125.9, 125.5, 64.8, 51.1, 41.4, 40.3, 35.8, 32.5, 25.9, 25.3, 18.4, –5.2.

FTIR(neat film NaCl): 2931, 2858, 1513, 1463, 1376, 1256, 1212, 1091, 1006, 838, 776, 667  $\text{cm}^{-1}$ .

HRMS (GCT-CI): Calculated for  $\text{C}_{21}\text{H}_{32}\text{OSi}$ : 328.2222; Measured: 328.2227.

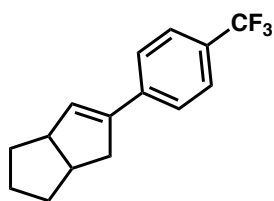
### Characterization of tetra-substituted olefin

$^1\text{H}$  NMR (500 MHz,  $\text{CDCl}_3$ )  $\delta$  7.23 (d,  $J = 8.3$  Hz, 1H), 4.71 (s, 1H), 3.84 (tt,  $J = 8.9, 6.5$  Hz, 1H), 2.74 – 2.54 (m, 1H), 2.39 – 2.10 (m, 2H), 0.94 (s, 2H), 0.10 (s, 2H).

$^{13}\text{C}$  NMR (126 MHz,  $\text{CDCl}_3$ )  $\delta$  146.6, 144.7, 138.7, 126.7, 126.1, 64.8, 48.8, 38.5, 29.4, 28.1, 25.9, 18.4, –5.2.

FTIR (neat film NaCl): 2952, 2926, 2894, 2851, 1513, 1471, 1462, 1449, 1420, 1361, 1252, 1111, 1088, 835, 775  $\text{cm}^{-1}$ .

HRMS (EI-MS): Calculated for  $[\text{C}_{21}\text{H}_{32}\text{OSi} - \text{C}_4\text{H}_9]$ : 271.1518; Measured: 271.1515.



**5-(4-(trifluoromethyl)phenyl)-1,2,3,3a,4,6a-hexahydropentalene (4.14).** Synthesized according to general procedure. A dram vial charged with  $[\text{Ph}_3\text{C}]^+[\text{B}(\text{C}_6\text{F}_5)_4]^-$  (1.2 mg, 1.25 mmol, 0.05 equiv) and LiHMDS (6.3 mg, 0.038 mmol, 1.5 equiv) was dissolved in *o*-difluorobenzene (0.25 mL, 0.1 M). After pre-stirring for one minute, corresponding triflate (10.1 mg, 0.025 mmol, 1.0 equiv) was added and stirred at 30 °C for 1 hour. Upon completion,

reaction was diluted with hexanes (1 mL) and passed through a short plug of silica to yield **4.14** in 50% NMR yield. Crude product can be further purified by flash column chromatography (hexanes) using silver impregnated silica to give **4.14** as a colorless oil.

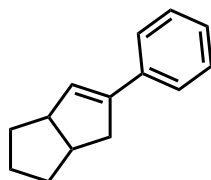
$^1\text{H}$  NMR (500 MHz,  $\text{CDCl}_3$ )  $\delta$  7.57 – 7.53 (m, 2H), 7.53 – 7.47 (m, 2H), 6.11 (q,  $J = 2.2$  Hz, 1H), 3.36 (tt,  $J = 8.6, 2.5$  Hz, 1H), 3.01 (ddt,  $J = 16.1, 9.3, 2.0$  Hz, 1H), 2.86 (dtdd,  $J = 9.3, 8.2, 4.3, 3.1$  Hz, 1H), 2.42 (dtd,  $J = 16.2, 3.0, 1.7$  Hz, 1H), 1.85 – 1.67 (m, 2H), 1.57 – 1.49 (m, 3H), 1.47 – 1.39 (m, 1H).

$^{13}\text{C}$  NMR (125 MHz,  $\text{CDCl}_3$ )  $\delta$  140.0, 139.8, 132.6, 128.9, 128.6, 128.4, 128.1, 127.5, 125.7, 125.3, 125.1 (q,  $J_{\text{C-F}} = 3.9$  Hz), 123.2, 121.0, 51.2, 41.2, 40.3, 35.7, 32.4, 25.3.

$^{19}\text{F}$  NMR (376 MHz,  $\text{CDCl}_3$ )  $\delta$  -62.4.

FTIR (Neat Film NaCl): 3049, 2943, 2864, 1615, 1449, 1412, 1324, 1163, 1122, 1110, 1070, 1016, 832, 678, 599  $\text{cm}^{-1}$ .

HRMS (EI-MS): Calculated for  $\text{C}_{15}\text{H}_{15}\text{F}_3$ : 252.1126; Measured: 252.1129.



**5-phenyl-1,2,3,3a,4,6a-hexahydropentalene (4.15).** Synthesized according to general procedure. A dram vial charged with  $[\text{Ph}_3\text{C}]^+[\text{B}(\text{C}_6\text{F}_5)_4]^-$  (1.2 mg, 1.25 mmol, 0.05 equiv) and LiHMDS (6.3 mg, 0.038 mmol, 1.5 equiv) was dissolved in *o*-difluorobenzene (1.5 mL, 0.017 M). After pre-stirring for one minute, corresponding triflate (8.4 mg, 0.025 mmol, 1.0 equiv) was added and stirred at 30 °C for 3.5 hours. Upon completion, reaction was diluted with hexanes (1 mL) and passed through a short plug of silica to yield **4.15** in 46% NMR yield. Crude product

can be further purified by flash column chromatography (hexanes) using silver impregnated silica to give **4.15** as a colorless oil.

$^1\text{H}$  NMR (400 MHz,  $\text{CDCl}_3$ )  $\delta$  7.45 – 7.39 (m, 2H), 7.30 (t,  $J = 7.6$  Hz, 2H), 7.24 – 7.17 (m, 1H), 5.99 (q,  $J = 2.2$  Hz, 1H), 3.33 (tt,  $J = 8.5, 3.4$  Hz, 1H), 3.01 (ddt,  $J = 16.2, 9.4, 2.0$  Hz, 1H), 2.88 – 2.78 (m, 1H), 2.42 (dtd,  $J = 16.1, 3.0, 1.7$  Hz, 1H), 1.83 – 1.66 (m, 2H), 1.54 – 1.48 (m, 3H), 1.47 – 1.38 (m, 1H).

$^{13}\text{C}$  NMR (125 MHz,  $\text{CDCl}_3$ )  $\delta$  140.8, 136.6, 129.9, 128.2, 126.8, 125.6, 51.1, 41.3, 40.3, 35.8, 32.5, 25.3.

FTIR (Neat Film NaCl): 3066, 3031, 2929, 2859, 1734, 1679, 1494, 1448, 1211, 752, 692  $\text{cm}^{-1}$ .

HR-MS (EI-MS): Calculated for  $\text{C}_{14}\text{H}_{16}$ : 184.1252; Measured: 184.1248.

## 4.7 Spectra Relevant to Chapter Four:

### **Vinyl Carbocations Generated Under Basic Conditions and Their Intramolecular C–H Insertion Reactions**

Adapted from: Benjamin Wigman, Stasik Popov, Alex L. Bagdasarian, Brian Shao, Tyler R. Benton, Chloé G. Williams, Steven P. Fisher, Vincent Lavallo, K. N. Houk, and Hosea M.

Nelson

*J. Am. Chem. Soc.* **2019**, *141*, 9140–9144.

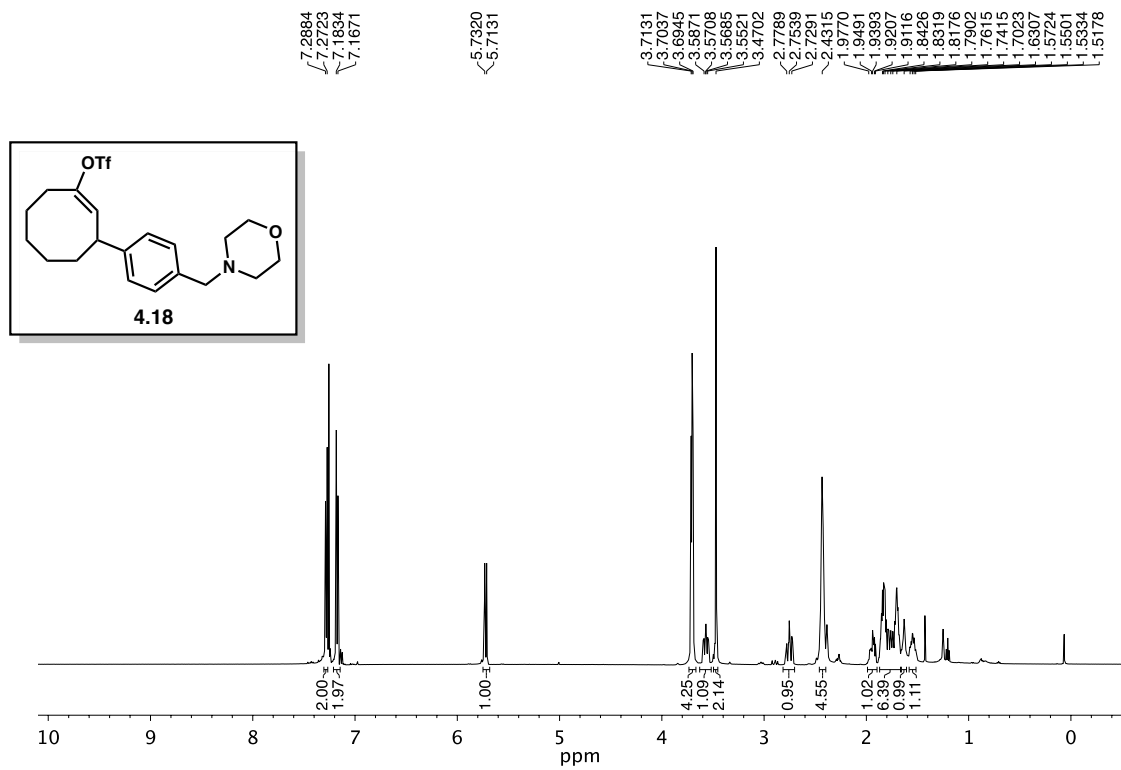


**Figure 4.3**  $^1\text{H}$  NMR (500 MHz,  $\text{CDCl}_3$ ) of compound 4.18.

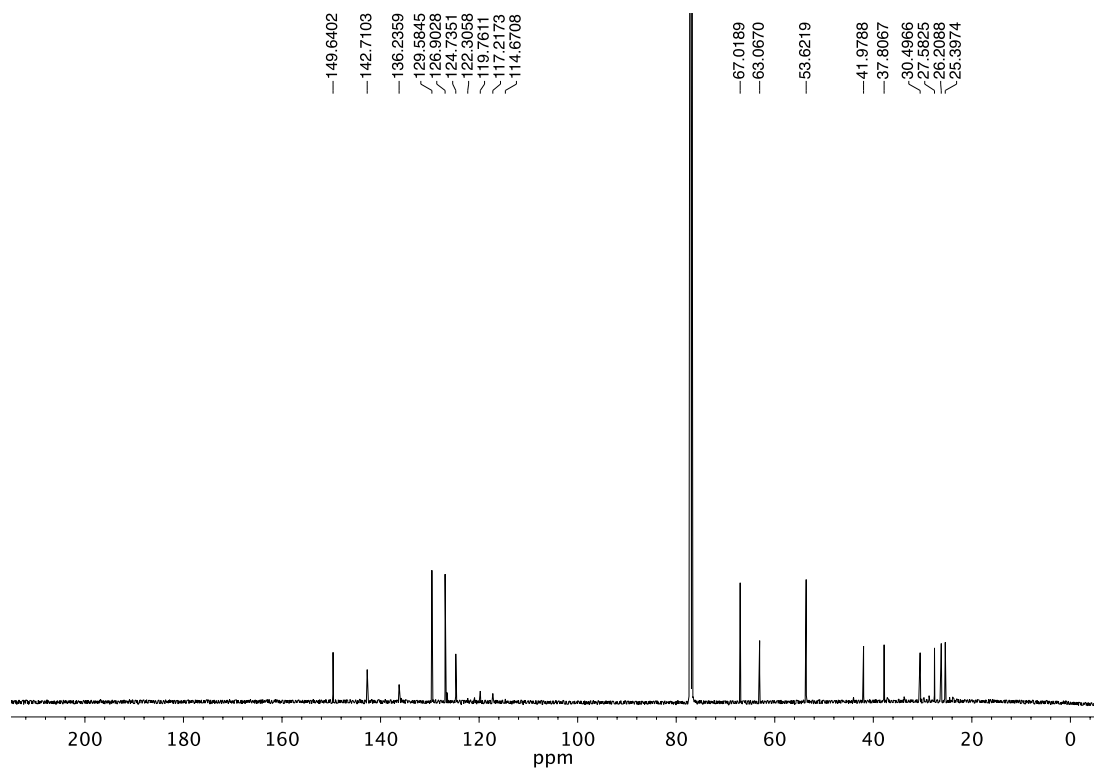


**Figure 4.4**  $^{13}\text{C}$  NMR (125 MHz,  $\text{CDCl}_3$ ) of compound 4.18.

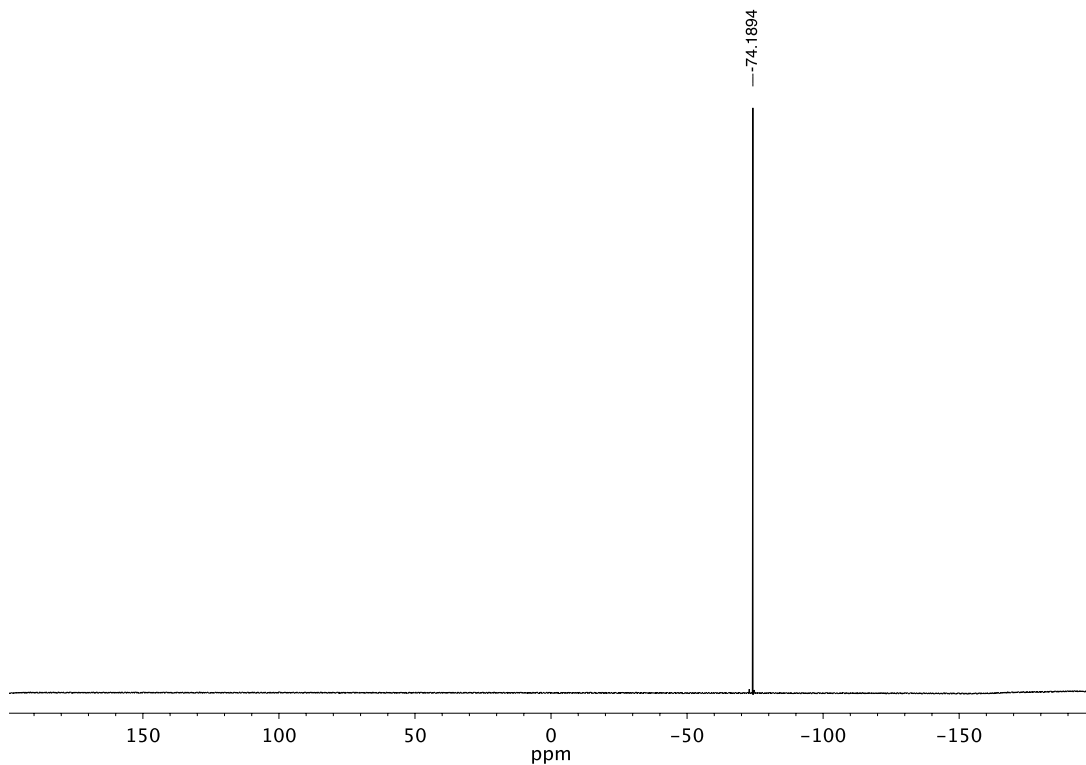


Figure 4.5  $^{19}\text{F}$  NMR (376 MHz,  $\text{CDCl}_3$ ) of compound 4.18.

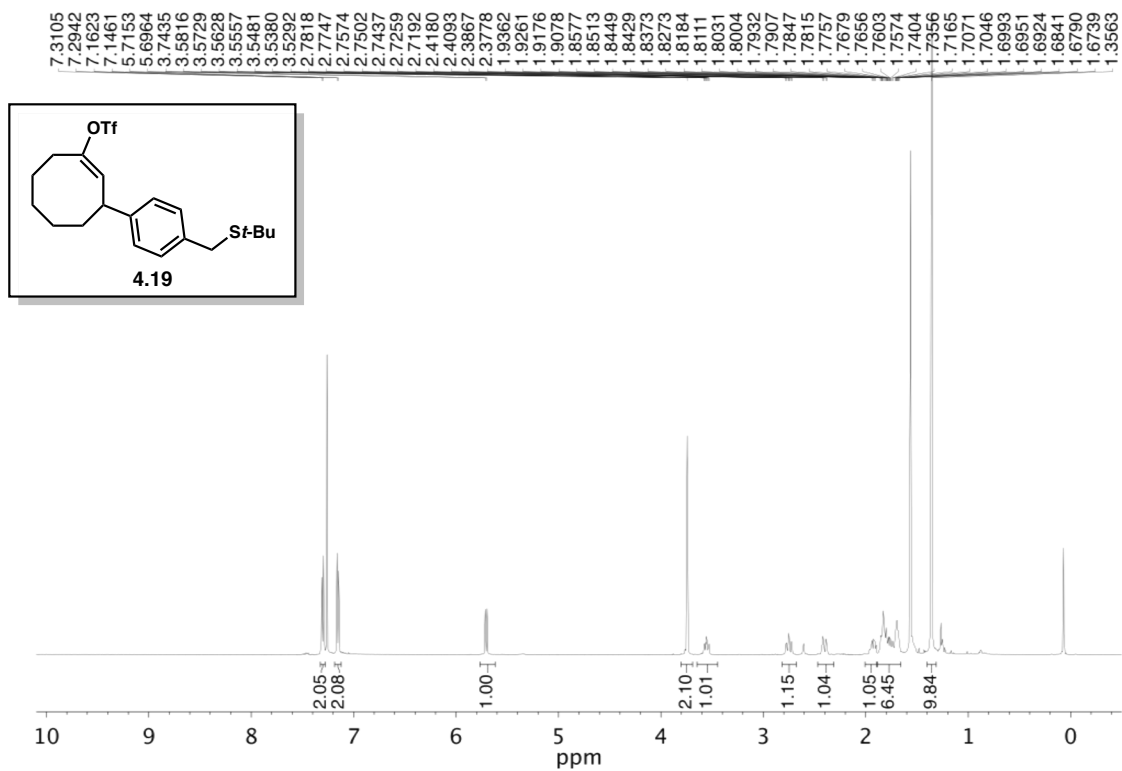
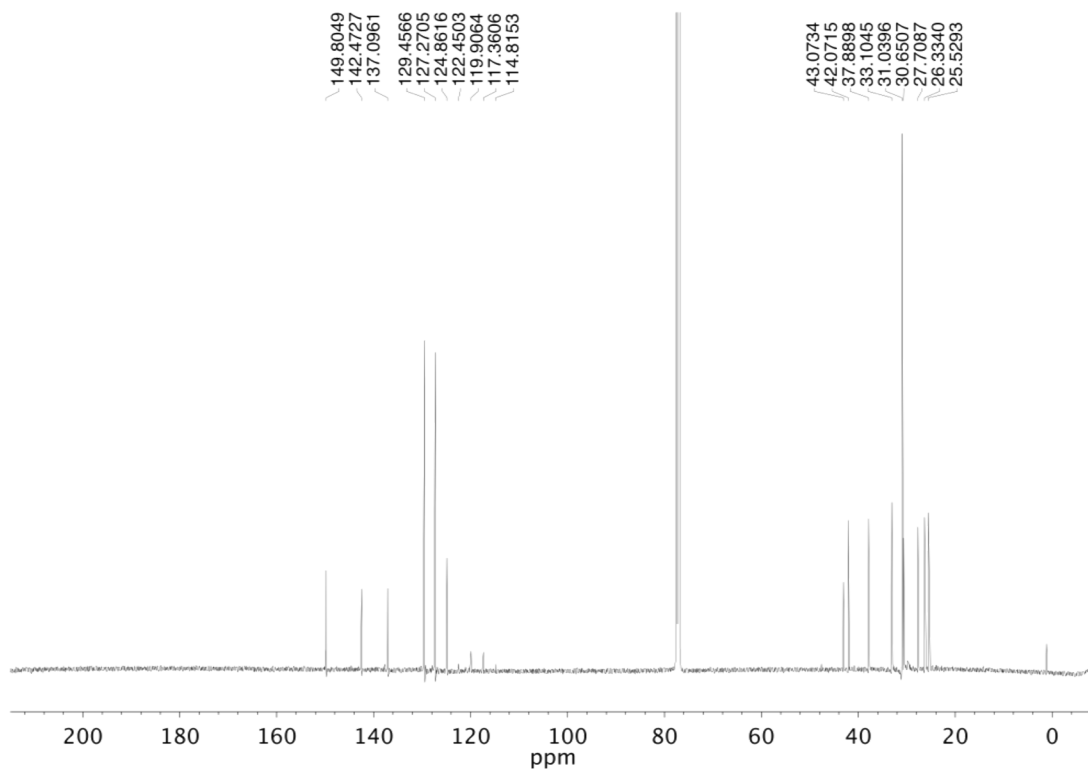
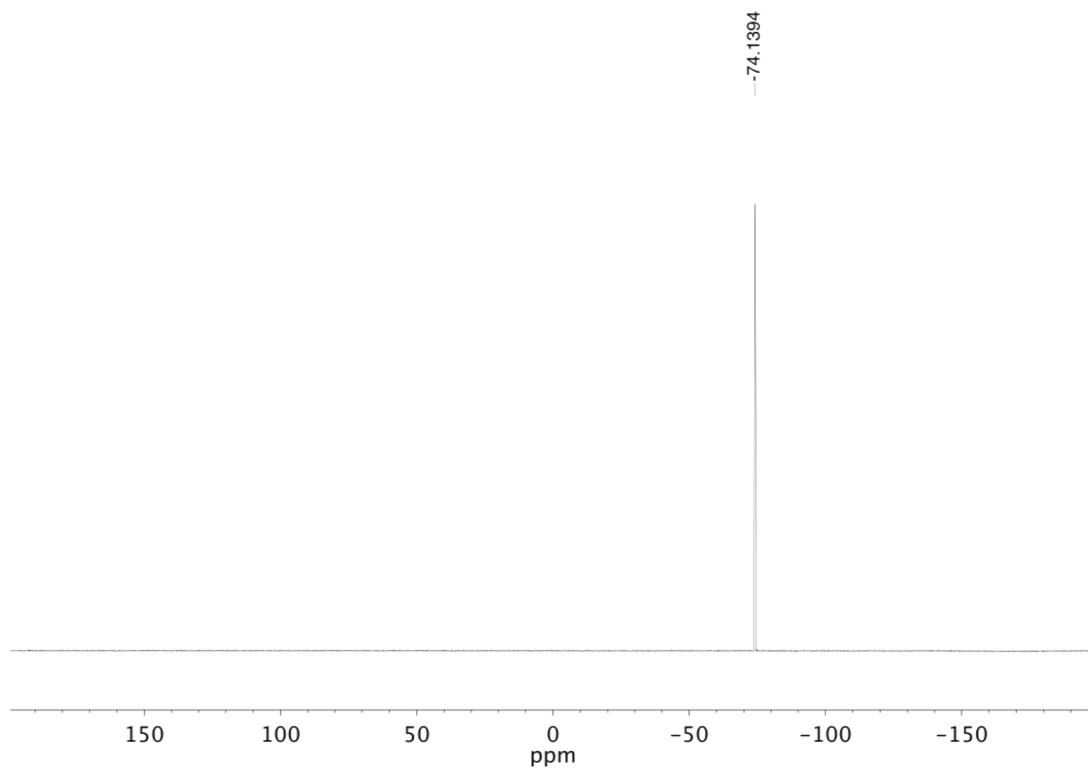


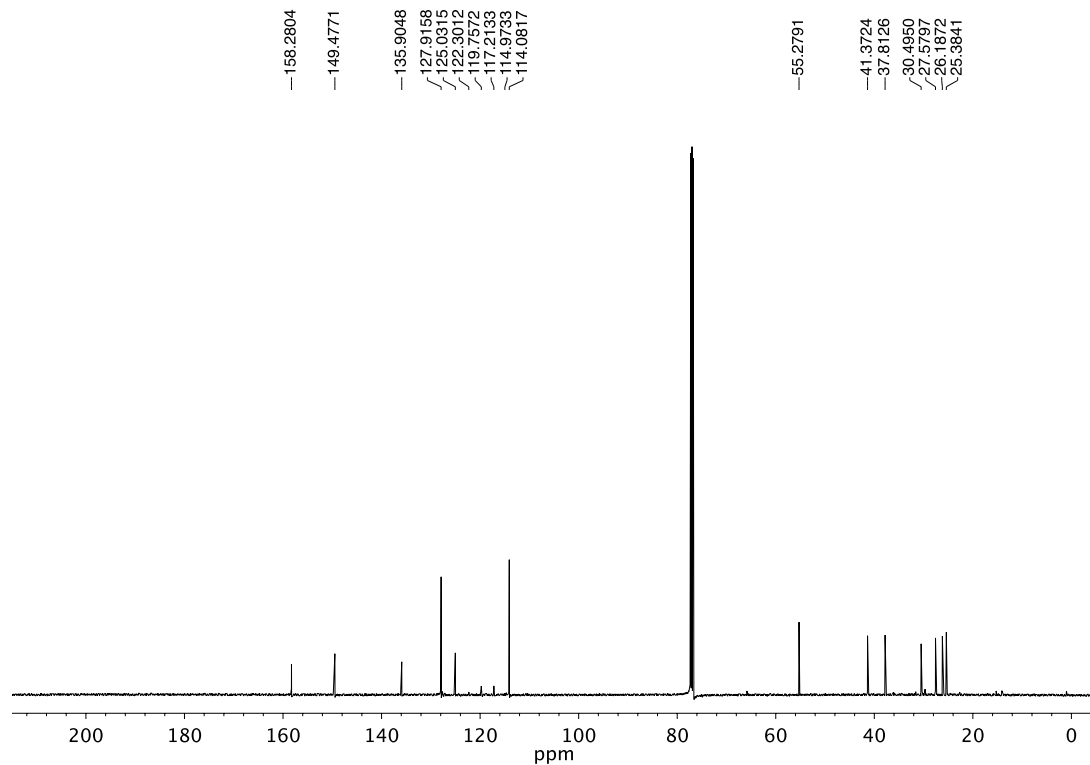
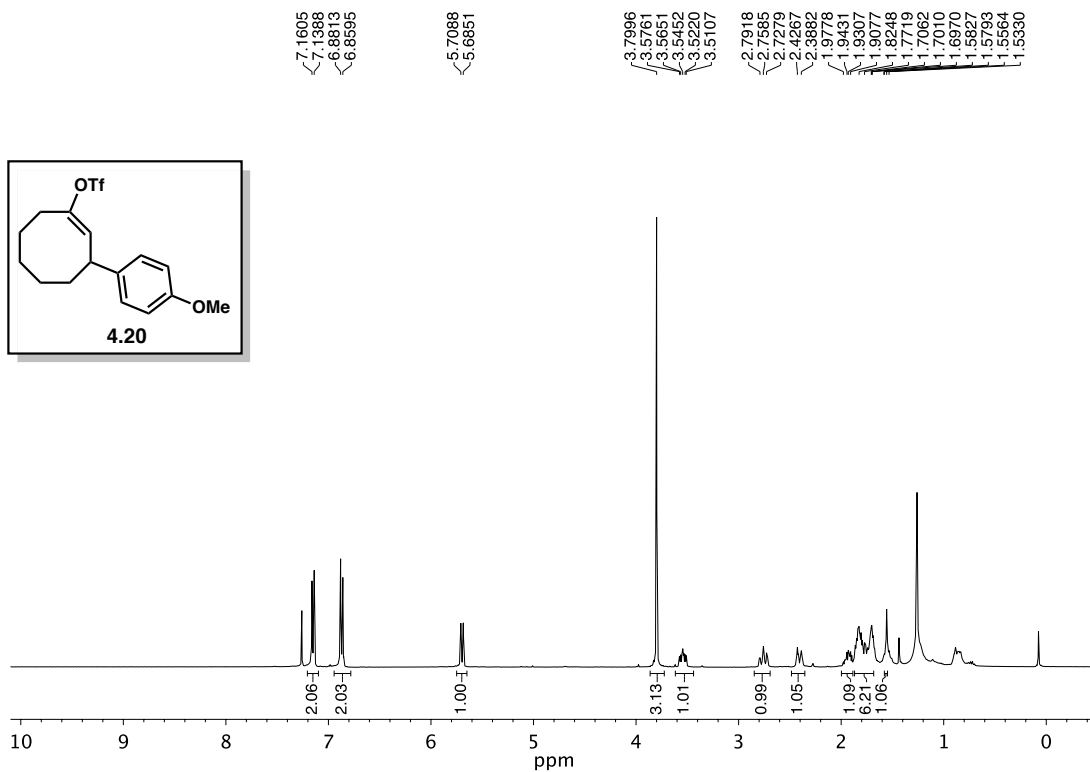
Figure 4.6  $^1\text{H}$  NMR (500 MHz,  $\text{CDCl}_3$ ) of compound 4.19.



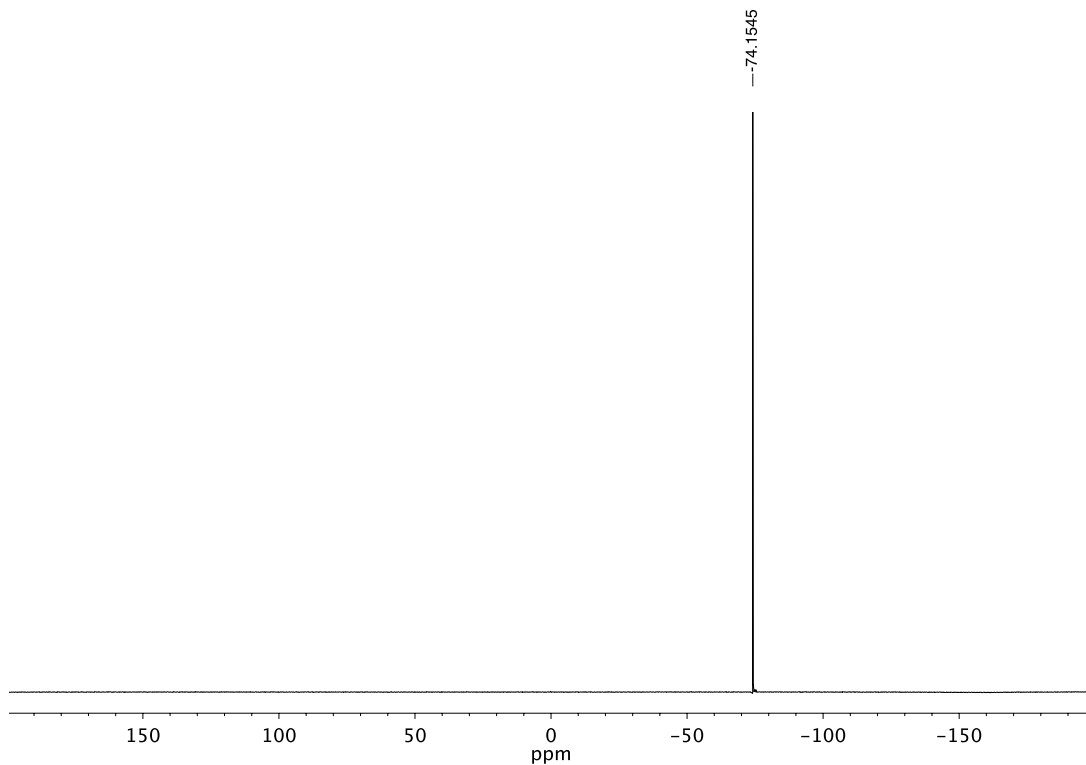
**Figure 4.7**  $^{13}\text{C}$  NMR (125 MHz,  $\text{CDCl}_3$ ) of compound **4.19**.



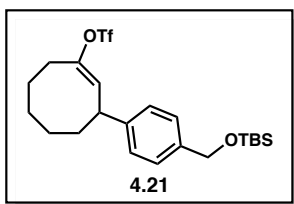
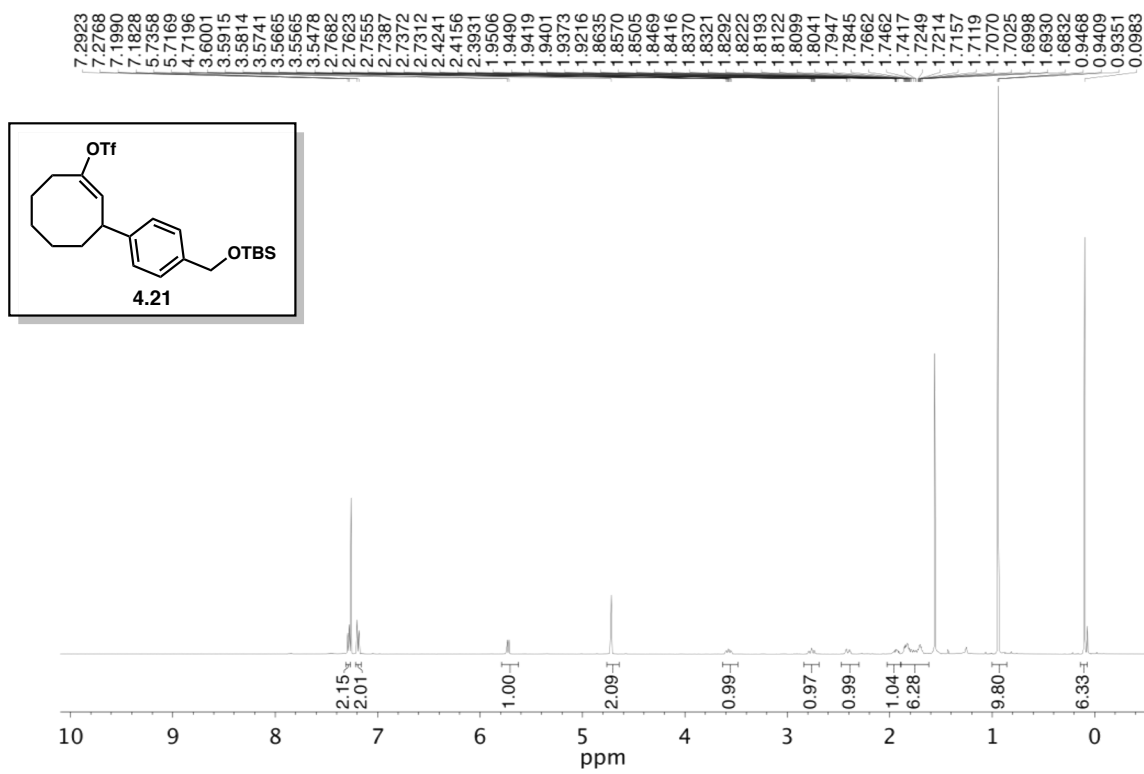
**Figure 4.8**  $^{19}\text{F}$  NMR (376 MHz,  $\text{CDCl}_3$ ) of compound **4.19**.



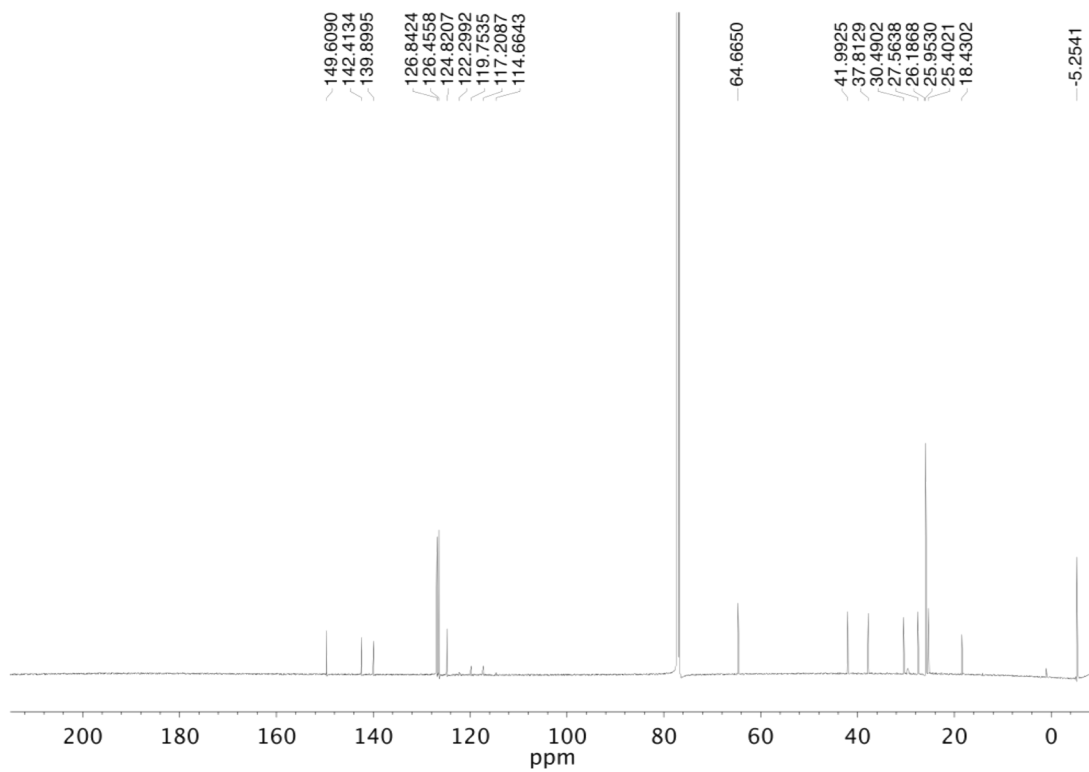




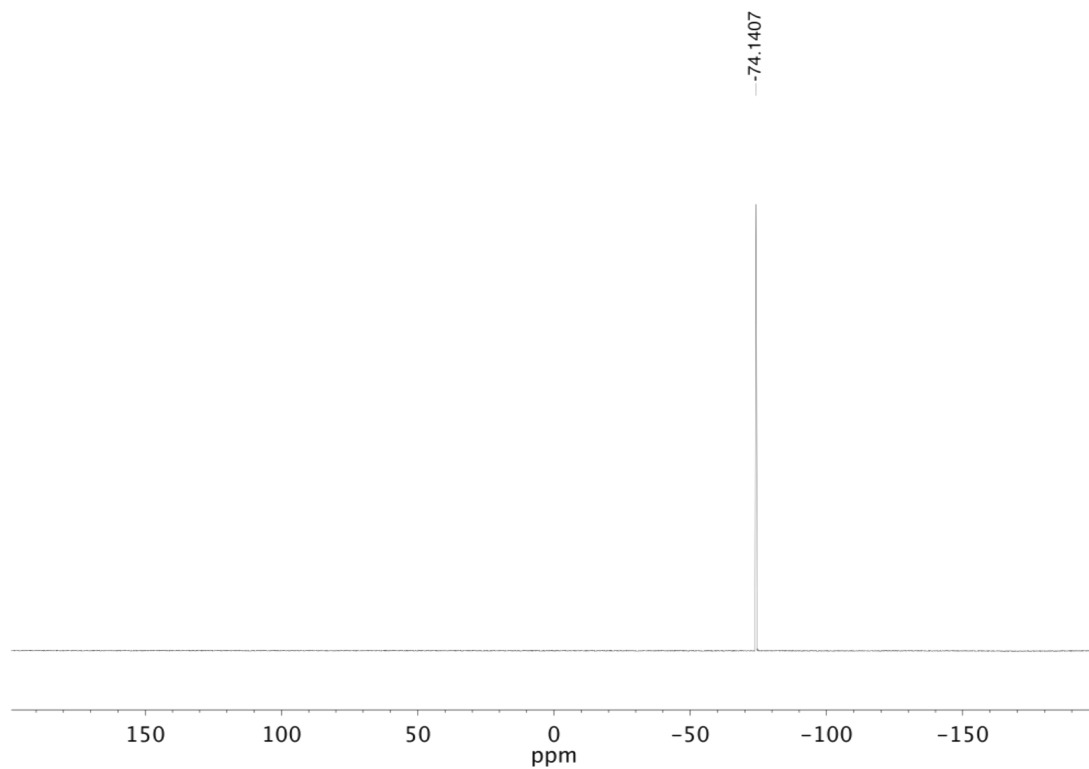
**Figure 4.11**  $^{19}\text{F}$  NMR (376 MHz,  $\text{CDCl}_3$ ) of compound **4.20**.



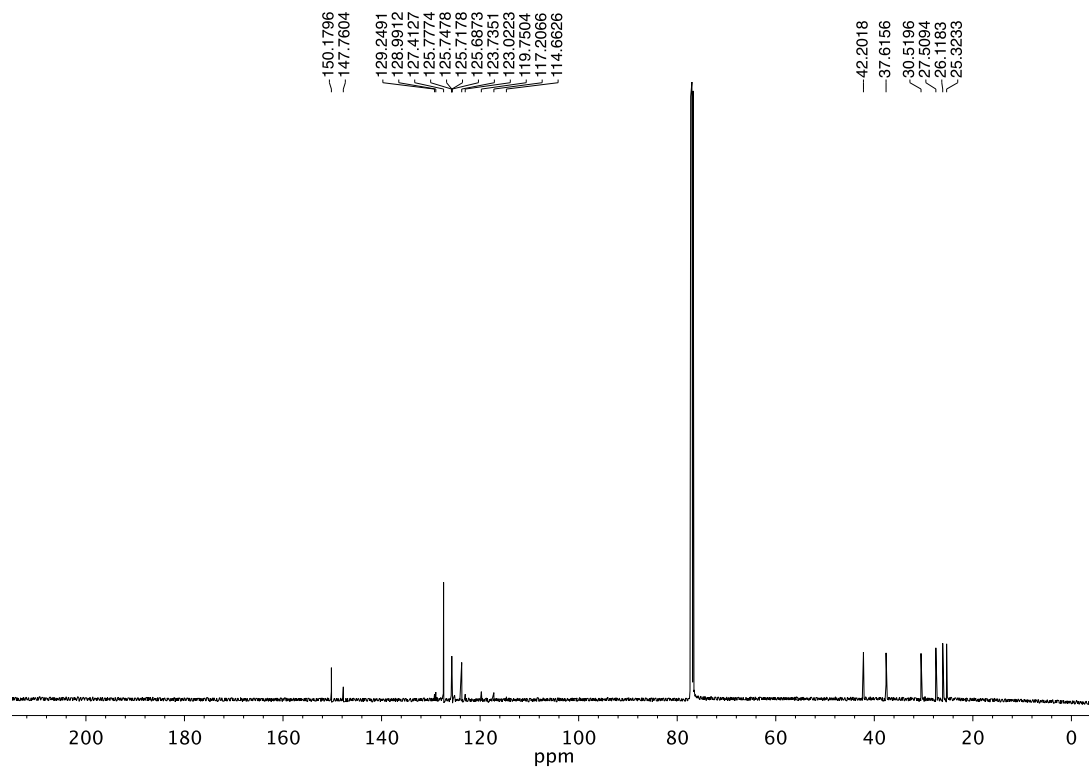
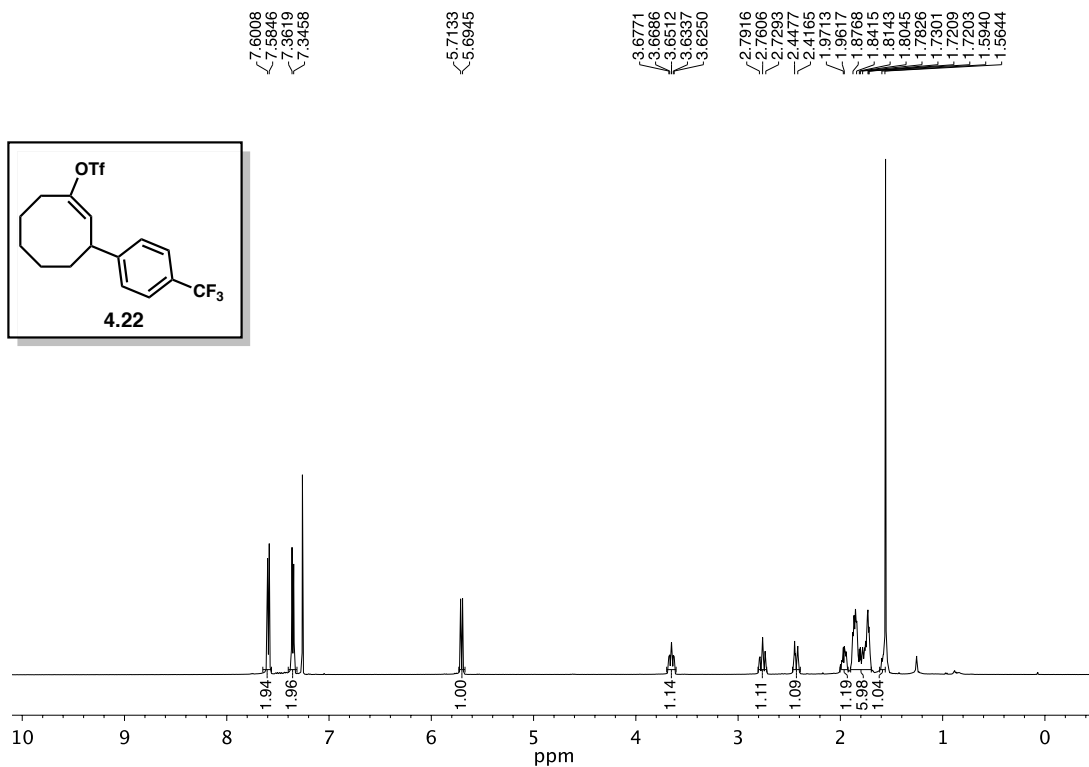
**Figure 4.12**  $^1\text{H}$  NMR (500 MHz,  $\text{CDCl}_3$ ) of compound **4.21**.



**Figure 4.13**  $^{13}\text{C}$  NMR (125 MHz,  $\text{CDCl}_3$ ) of compound **4.21**.



**Figure 4.14**  $^{19}\text{F}$  NMR (376 MHz,  $\text{CDCl}_3$ ) of compound **4.21**.



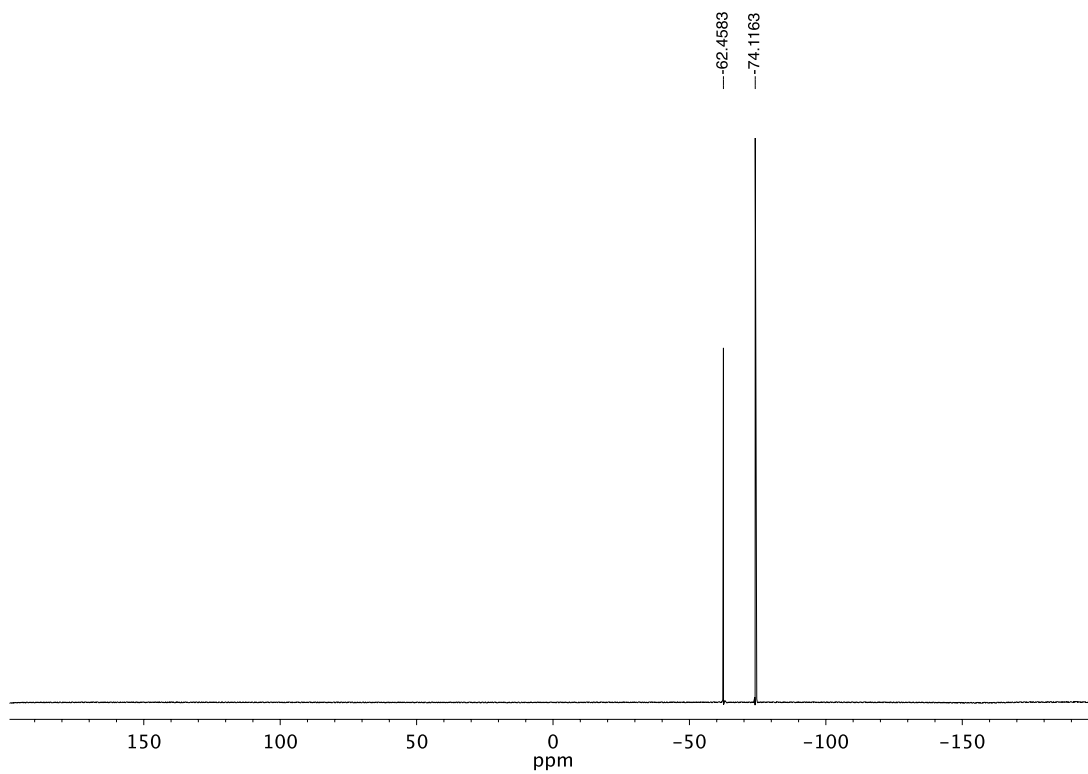


**Figure 4.17**  $^{19}\text{F}$  NMR (376 MHz,  $\text{CDCl}_3$ ) of compound **4.22**.

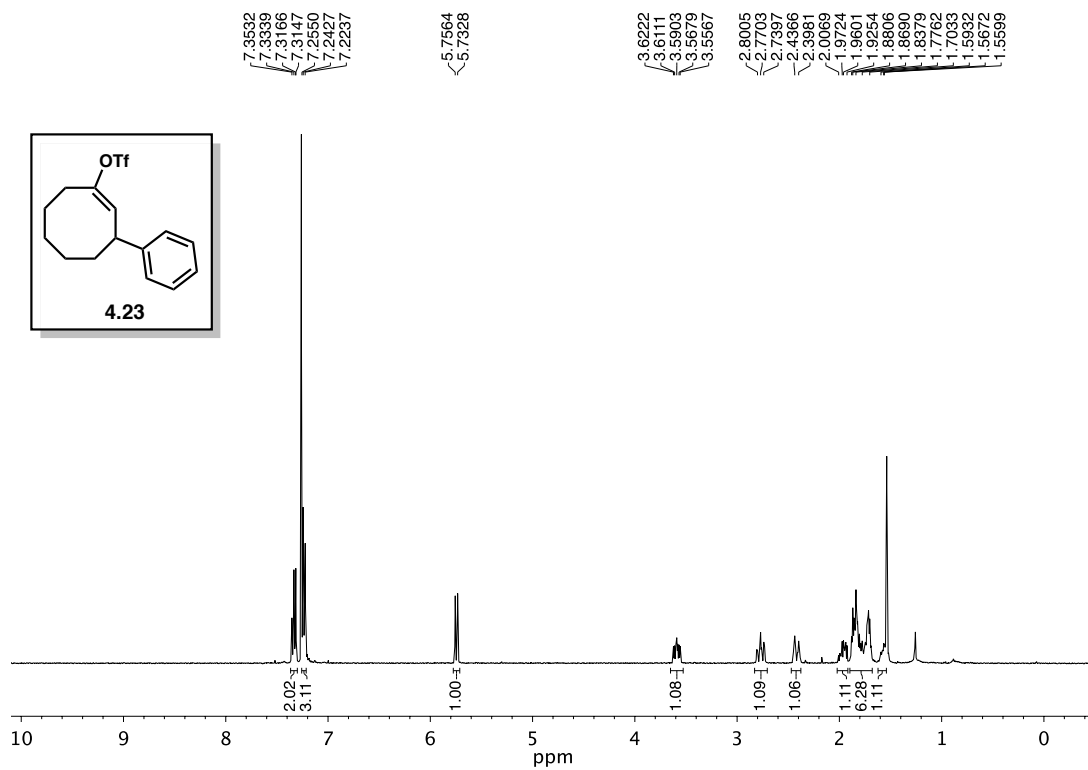


**Figure 4.18**  $^1\text{H}$  NMR (500 MHz,  $\text{CDCl}_3$ ) of compound **4.23**.

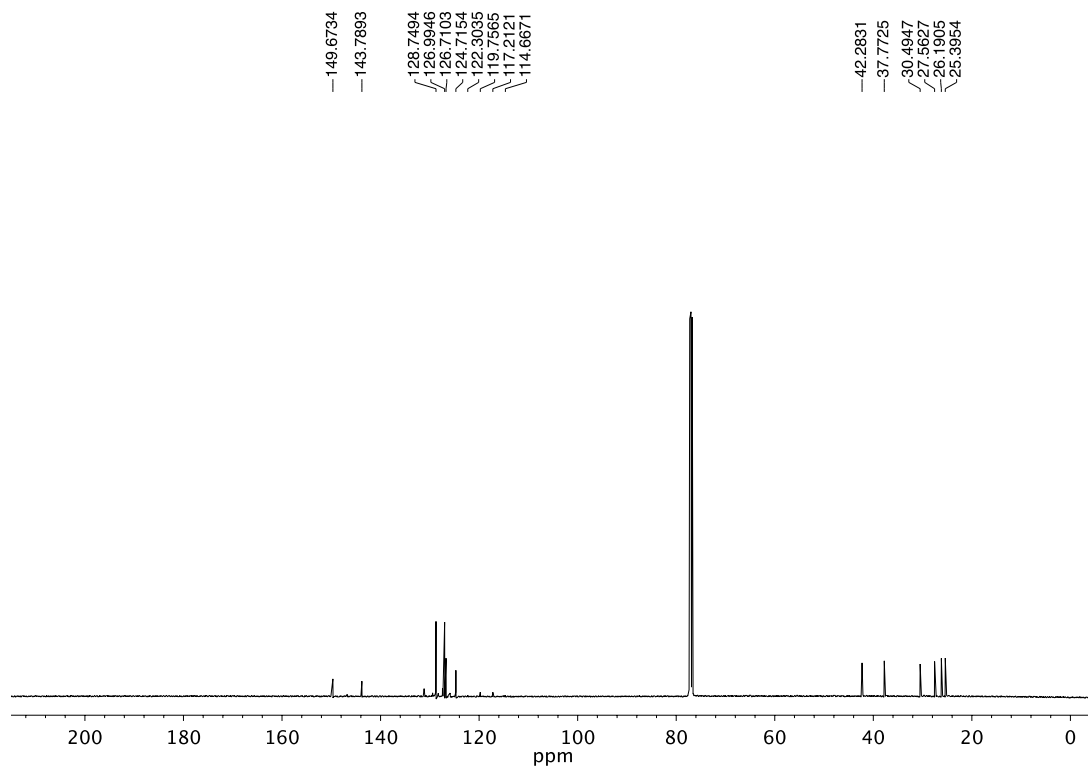


**Figure 4.19**  $^{13}\text{C}$  NMR (125 MHz,  $\text{CDCl}_3$ ) of compound **4.23**.

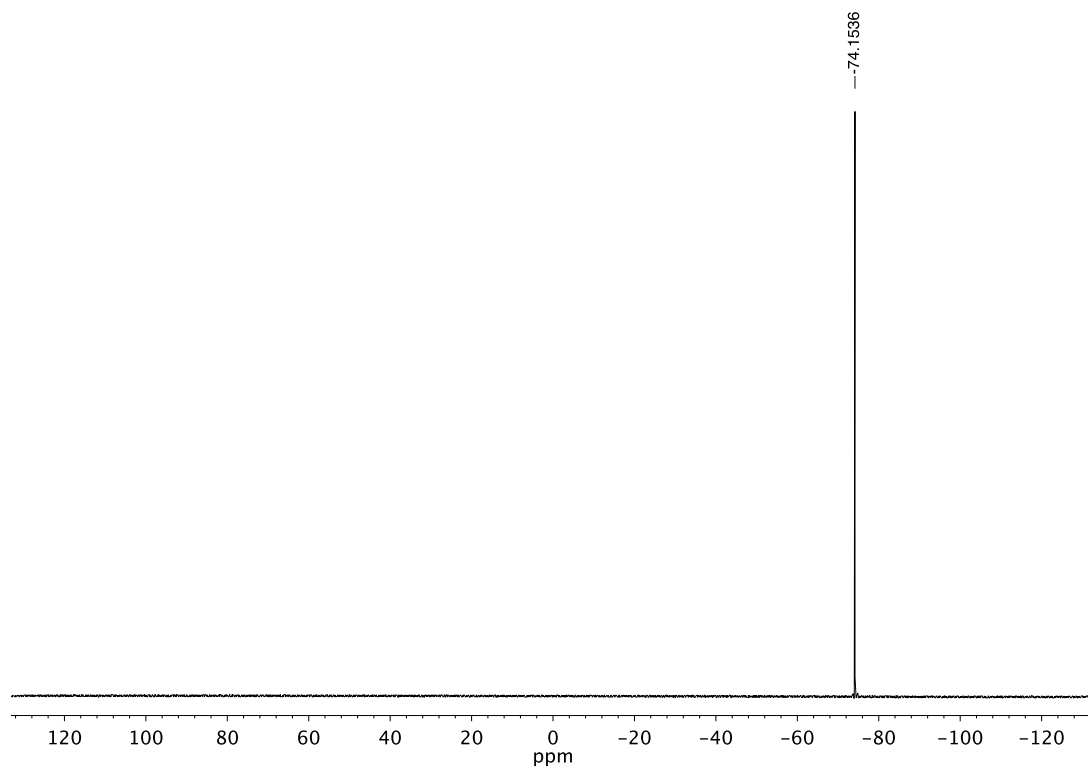


**Figure 4.20**  $^{19}\text{F}$  NMR (376 MHz,  $\text{CDCl}_3$ ) of compound **4.23**.

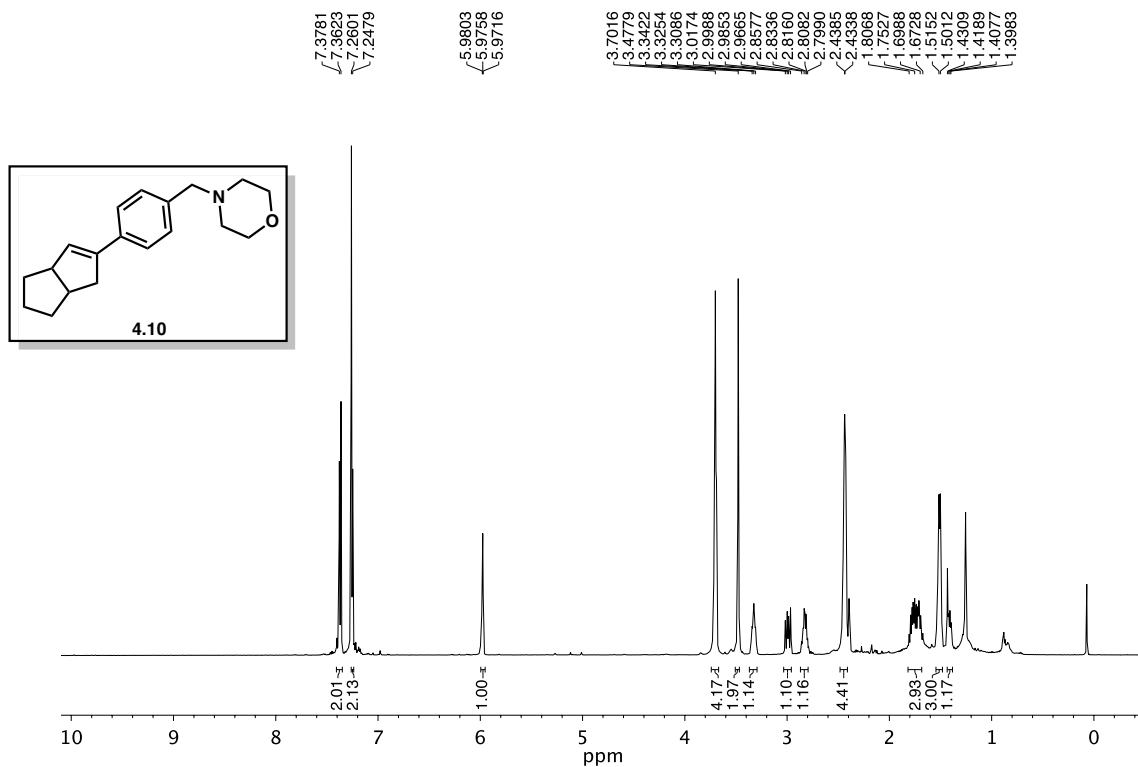


Figure 4.21 <sup>1</sup>H NMR (500 MHz, CDCl<sub>3</sub>) of compound 4.10.

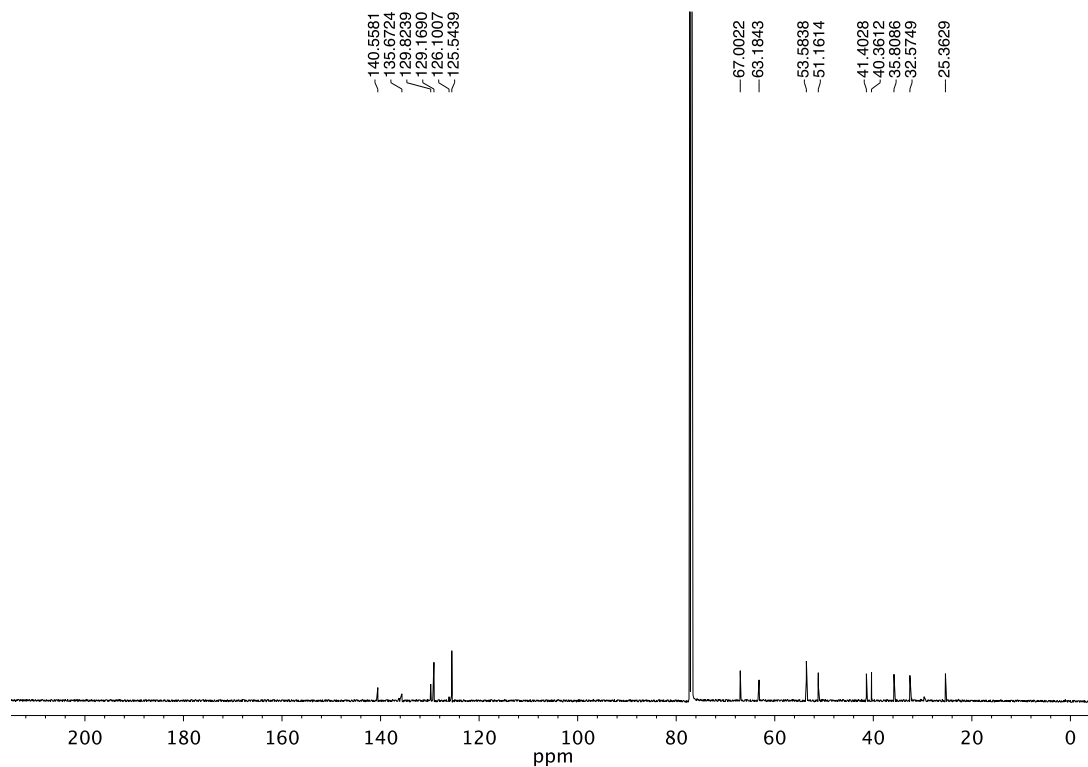
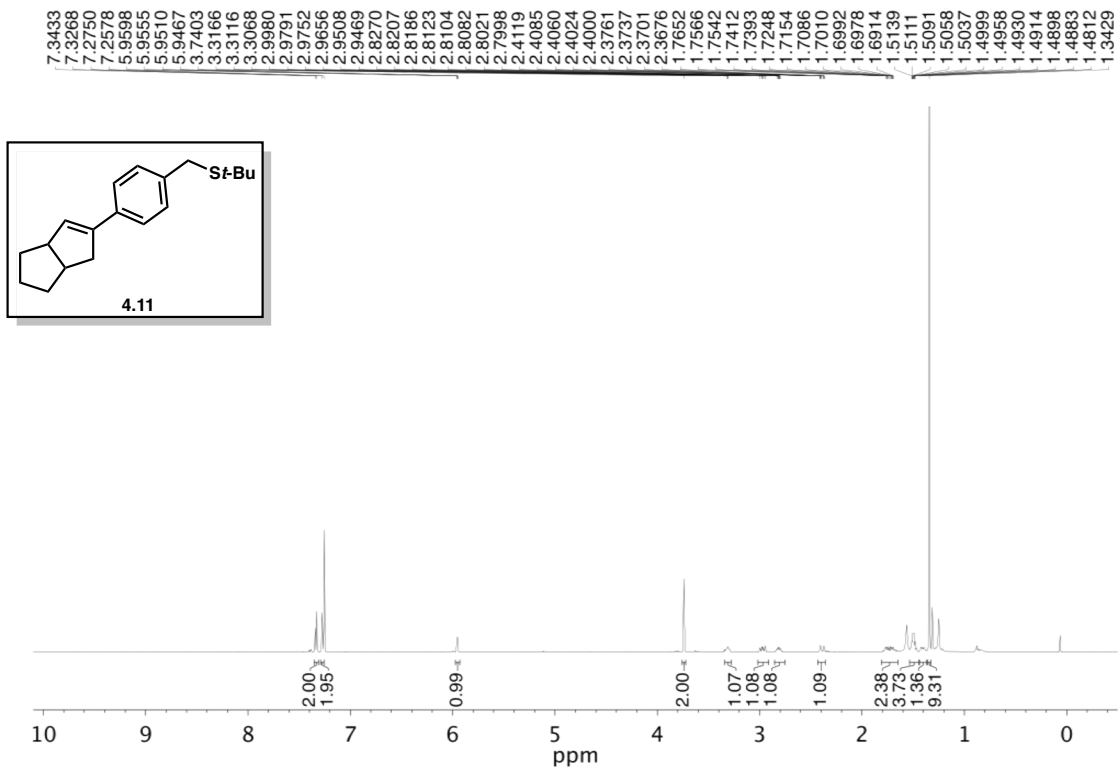
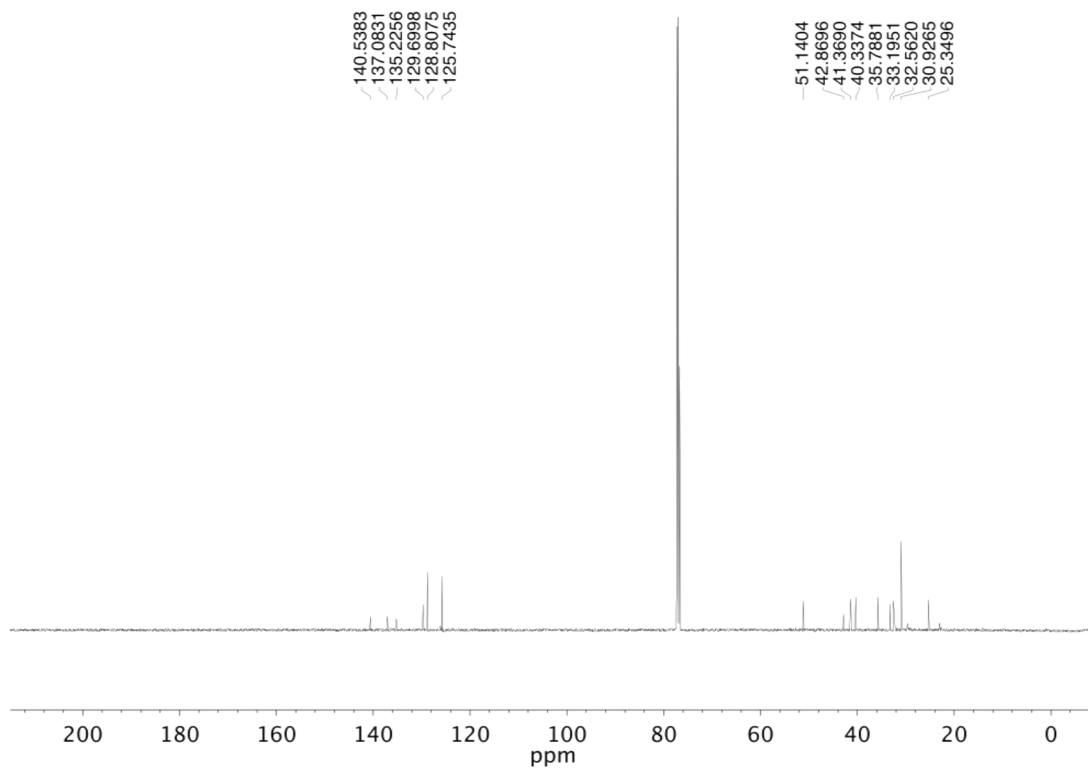


Figure 4.22 <sup>13</sup>C NMR (125 MHz, CDCl<sub>3</sub>) of compound 4.10.



**Figure 4.23**  $^1\text{H}$  NMR (500 MHz,  $\text{CDCl}_3$ ) of compound 4.11.



**Figure 4.24**  $^{13}\text{C}$  NMR (125 MHz,  $\text{CDCl}_3$ ) of compound 4.11.

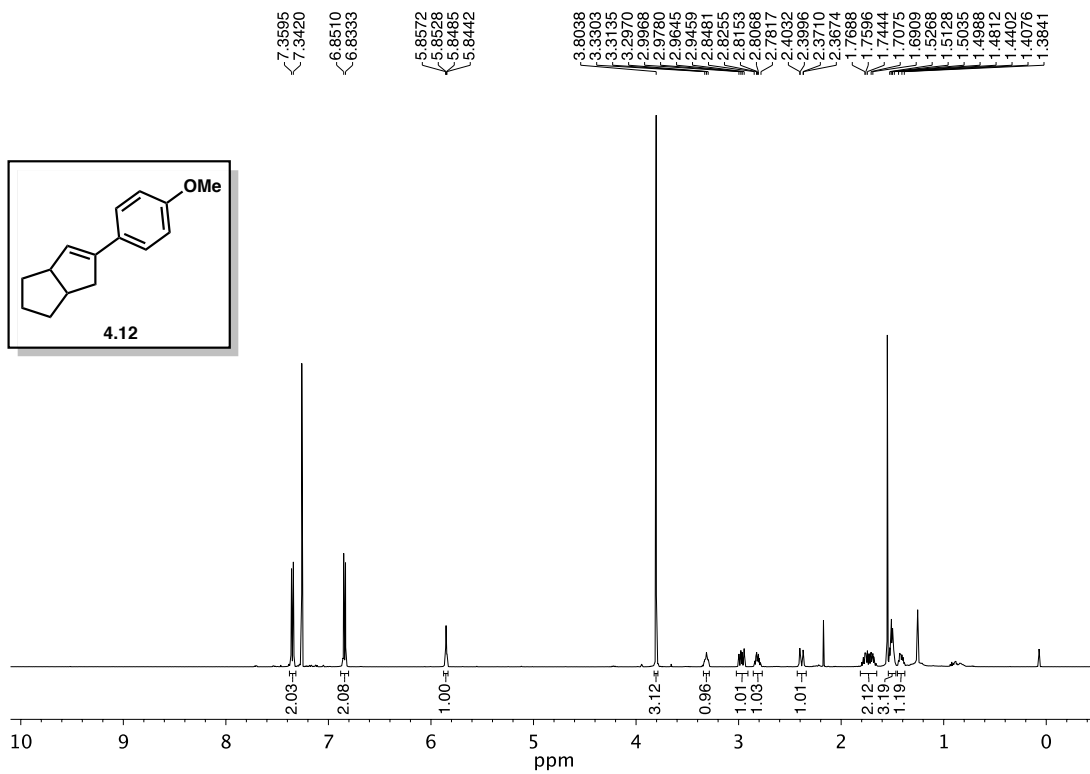


Figure 4.25 <sup>1</sup>H NMR (500 MHz, CDCl<sub>3</sub>) of compound 4.12.

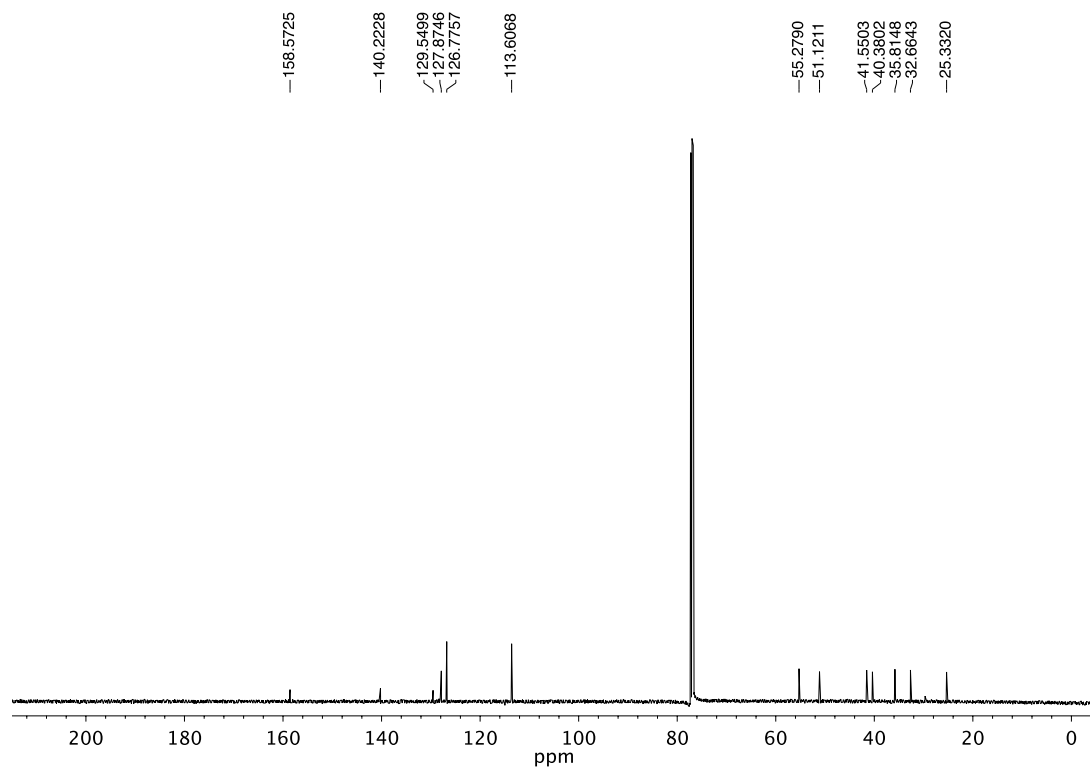


Figure 4.26 <sup>13</sup>C NMR (125 MHz, CDCl<sub>3</sub>) of compound 4.12.



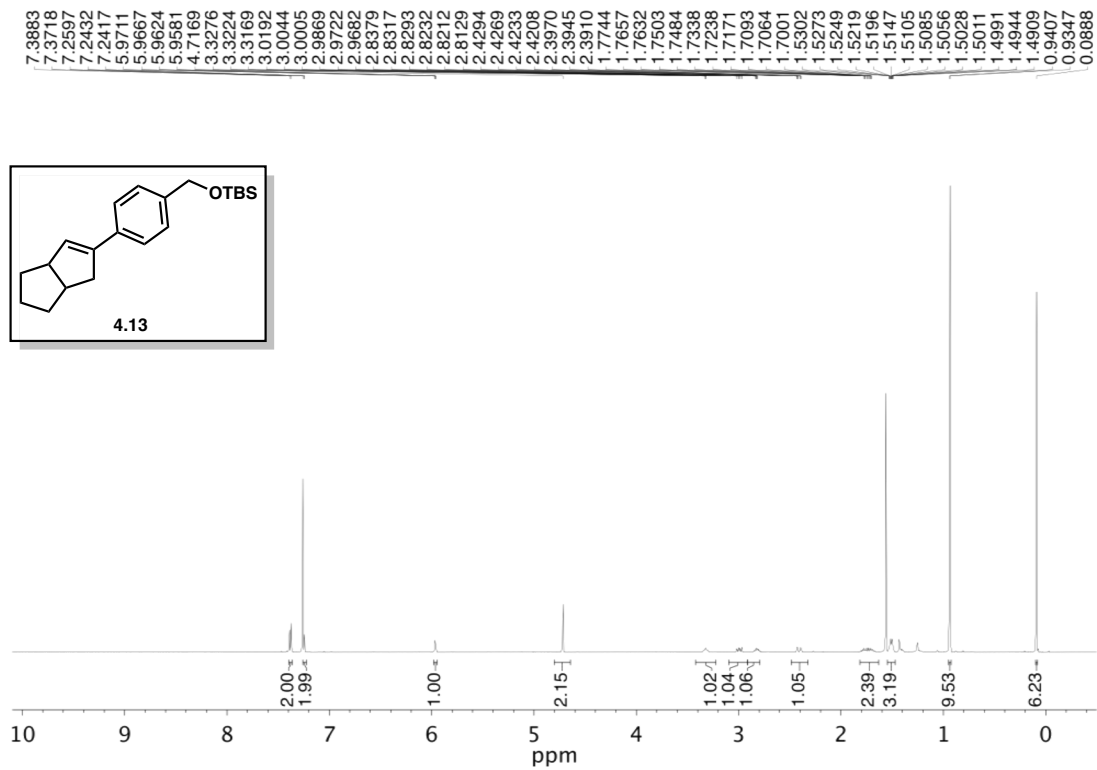


Figure 4.27 <sup>1</sup>H NMR (500 MHz, CDCl<sub>3</sub>) of compound 4.13.

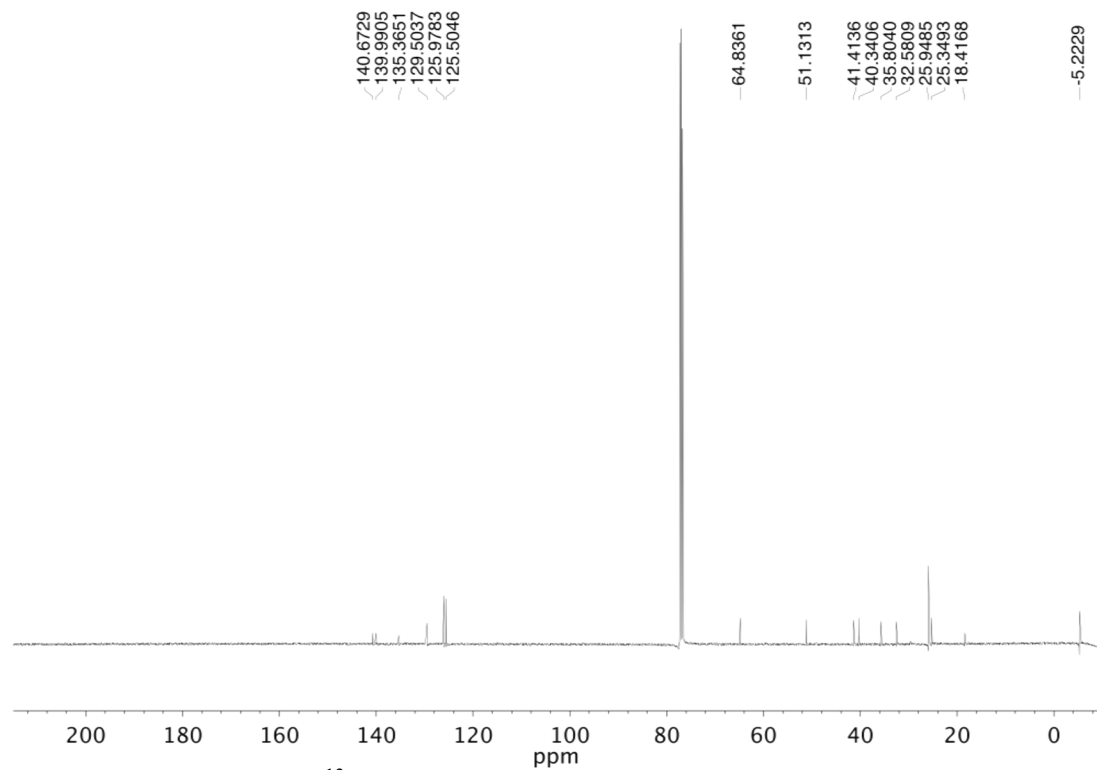


Figure 4.28 <sup>13</sup>C NMR (125 MHz, CDCl<sub>3</sub>) of compound 4.13.

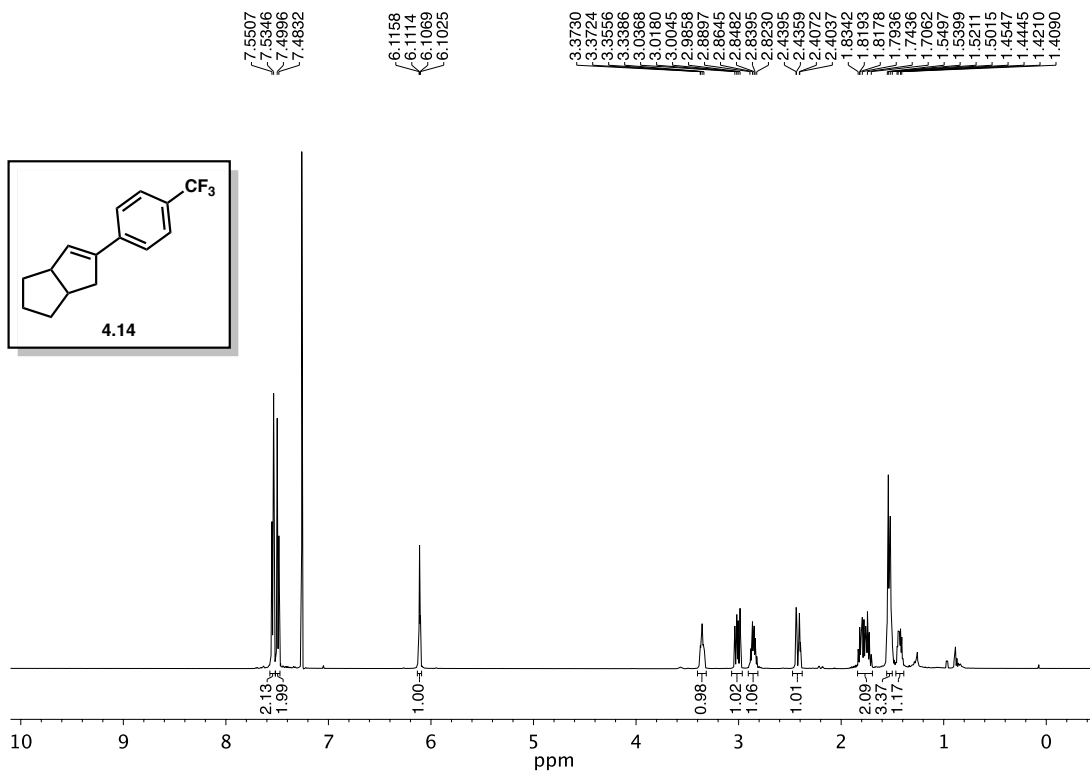


Figure 4.29 <sup>1</sup>H NMR (500 MHz, CDCl<sub>3</sub>) of compound 4.14.

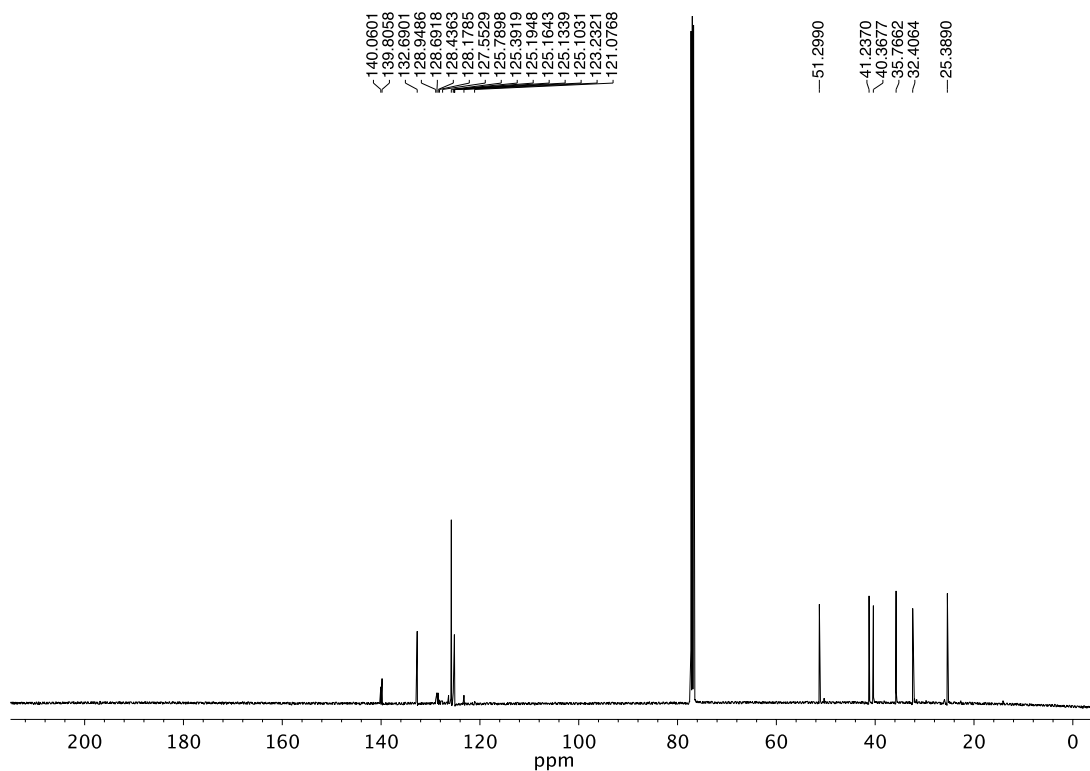


Figure 4.30 <sup>13</sup>C NMR (125 MHz, CDCl<sub>3</sub>) of compound 4.14.

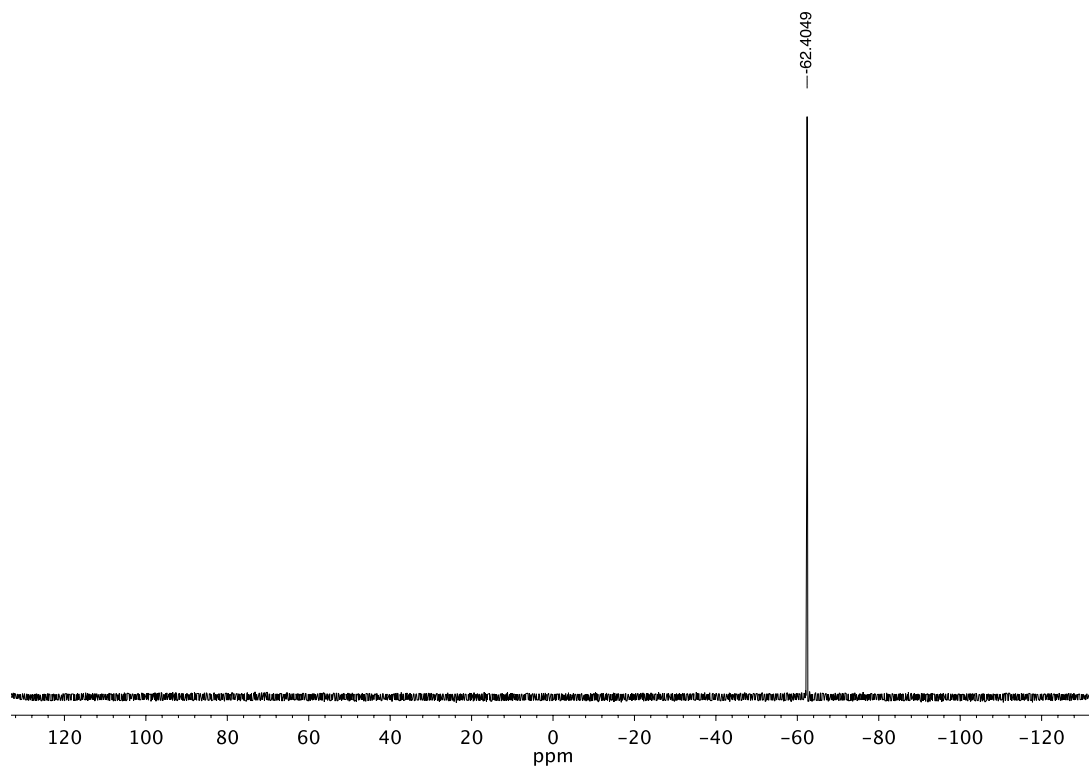


Figure 4.31  $^{19}\text{F}$  NMR (282 MHz,  $\text{CDCl}_3$ ) of compound 4.14.

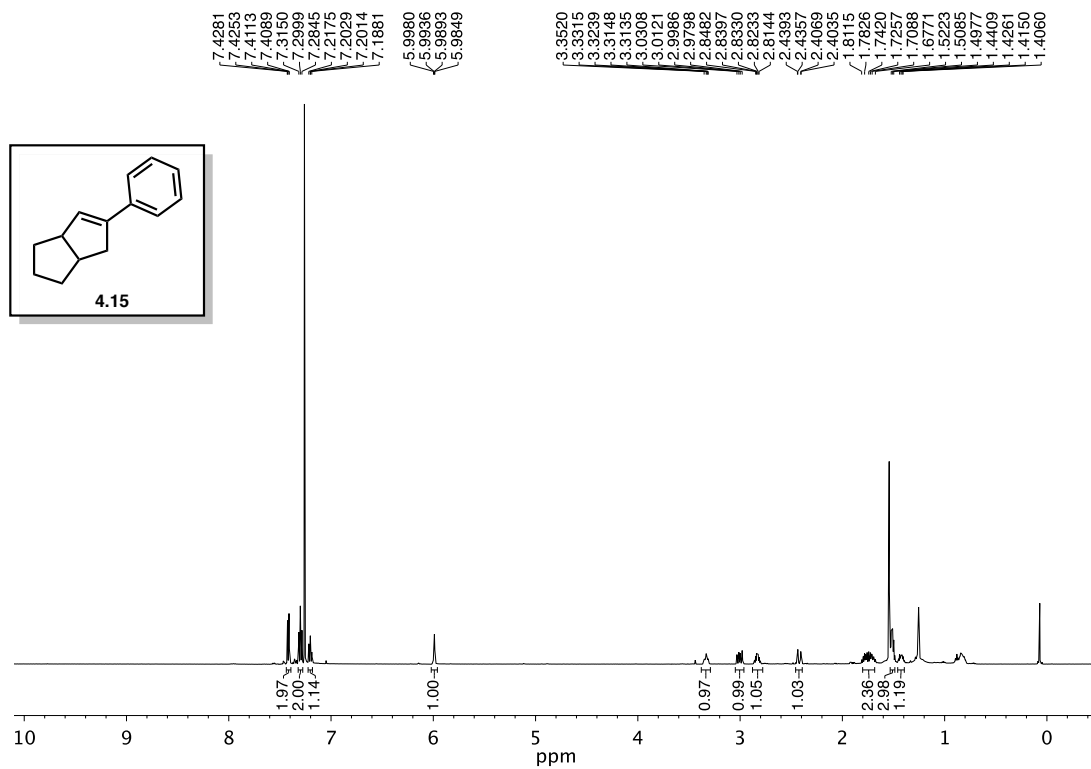
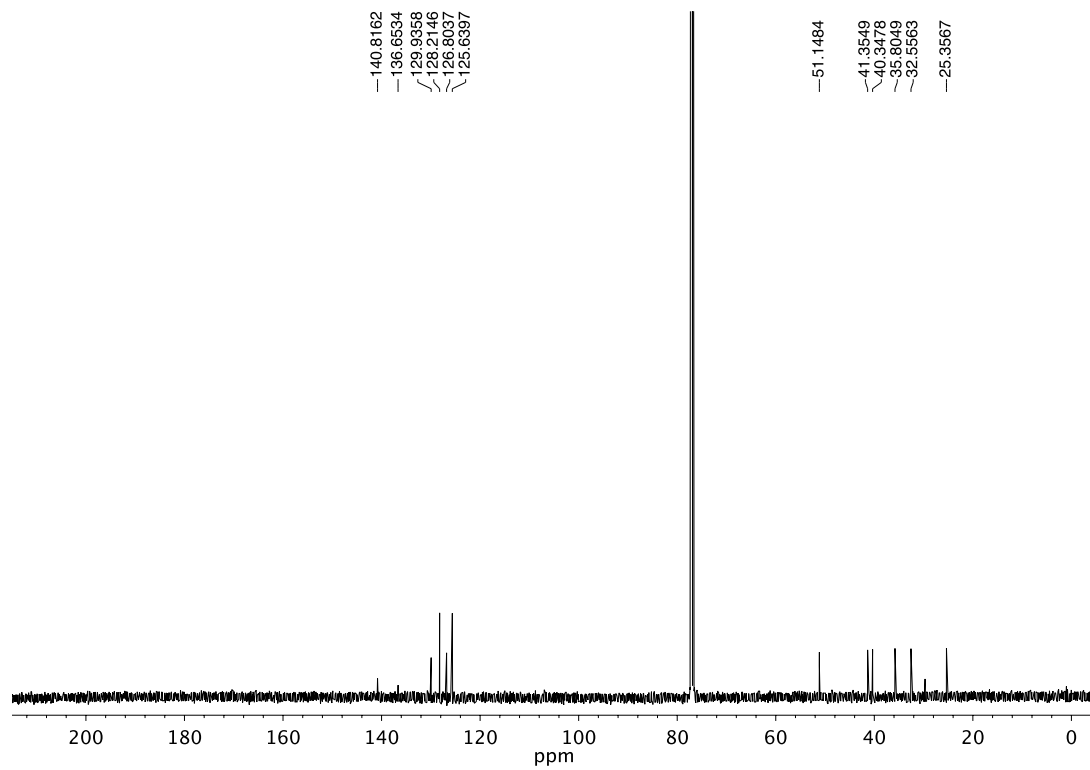


Figure 4.32  $^1\text{H}$  NMR (500 MHz,  $\text{CDCl}_3$ ) of compound 4.15.



**Figure 4.33**  $^{13}\text{C}$  NMR (125 MHz,  $\text{CDCl}_3$ ) of compound **4.15**.

## 4.8 Notes and References

- (1) (a) Shao, B.; Bagdasarian, A. L.; Popov, S.; Nelson, H. M. *Science* **2017**, *355*, 1403–1407.  
(b) Popov, S., et al. *Science* **2018**, *361*, 381–387.
- (2) Lühmann, N.; Panish, R.; Müller, T. A. *Appl. Organomet. Chem.* **2010**, *24*, 533–537.
- (3) Biermann, U.; Koch, R.; Metzger, J. O. *Angew. Chem. Int. Ed.* **2006**, *45*, 3076–3079.
- (4) Cleary, S. E.; Hensinger, M. J.; Brewer, M. *Chem. Sci.* **2017**, *8*, 6810–6814.
- (5) Vyakaranam, K.; Körbe, S.; Michl, J. *J. Am. Chem. Soc.* **2006**, *128*, 5680–5686.
- (6) Vyakaranam, K.; Barbour, J. B.; Michl, J. *J. Am. Chem. Soc.* **2006**, *128*, 5610–5611.
- (7) Kitazawa, Y., et al. *J. Org. Chem.* **2017**, *82*, 1931–1935.
- (8) McDonald, R. I.; Liu, G.; Stahl, S. S. *Chem. Rev.* **2011**, *111*, 2981–3019.
- (9) Beller, M.; Seayad, J.; Tillack, A.; Jiao, H. *Angew. Chem. Int. Ed.* **2004**, *43*, 3368–3398.
- (10) Sandmeyer, T. *Ber. Dtsch. Chem. Ges.* **1884**, *17*, 1633–1635.
- (11) Wigman, B., et al. *J. Am. Chem. Soc.* **2019**, *141*, 9140–9144.
- (12) Grundl, M. A.; Lehmann, M.; Schulz, A.; Villinger, A. *Org. Lett.* **2006**, *29*, 1421–1427.